



Norwegian University of Life Sciences
Faculty of Veterinary Medicine
Department of Paraclinical Sciences (PARAFAG)

Philosophiae Doctor (PhD)
Thesis 2021:49

Persistent infection of Piscine orthoreovirus-1 (PRV-1) in Atlantic salmon (*Salmo salar*)

Persistent infeksjon av
Piscine orthoreovirus-1 (PRV-1)
i atlantisk laks (*Salmo salar*)

Muhammad Salman Malik

Persistent infection of *Piscine orthoreovirus-1* (PRV-1) in Atlantic salmon (*Salmo salar*)

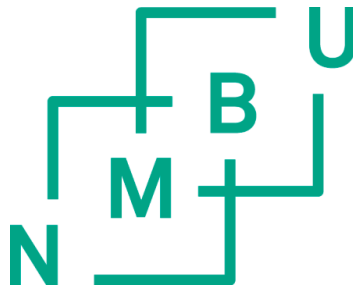
Persistent infeksjon av *Piscine orthoreovirus-1* (PRV-1) i atlantisk laks (*Salmo salar*)

Philosophiae Doctor (PhD) Thesis

Muhammad Salman Malik

Faculty of Veterinary Medicine
Department of Paraclinical Sciences (PARAFAG)
Norwegian University of Life Sciences

Campus Ås (2021)



Thesis number 2021:49
ISSN 1894-6402
ISBN 978-82-575-1820-2

"Persistence in scientific research leads to what I call instinct for truth"

Louis Pasteur

Table of contents

Acknowledgements.....	i
Abbreviations.....	iii
List of papers	v
Summary	vii
Sammendrag (Summary in Norwegian).....	xi
1. Introduction	1
1.1. Aquaculture of salmonids	1
1.2. Piscine orthoreovirus (PRV).....	3
1.2.1. Classification & taxonomy	3
1.2.2. Structure	4
1.2.3. Replication and transmission.....	6
1.3. PRV associated diseases	8
1.3.1. Heart and skeletal muscle inflammation (HSMI).....	9
1.3.2. Melanized focal changes in Atlantic salmon.....	11
1.3.3. Jaundice syndrome	12
1.3.4. Erythrocytic inclusion body syndrome (EIBS)	13
1.3.5. HSMI-like disease	13
1.3.6. Proliferative darkening syndrome (PDS)	14
1.4. PRV-1 target cell types	14
1.4.1. Erythrocytes.....	14
1.4.2. Cardiomyocytes.....	15
1.4.3. Myocytes	15
1.4.4. Macrophages and melano-macrophages.....	15
1.4.5. Hepatocytes	16
1.4.6. Enterocytes	16
1.5. Innate and adaptive immunity against PRV-1 infection.....	16
1.6. Macrophage response in inflammation.....	18
1.7. Persistent viral infections in salmonids.....	20
1.8. Vaccination against HSMI.....	22
2. Aims	23
3. Summary of papers	25
4. Results and general discussions.....	29
4.1. PRV-1 establishes a productive and persistent infection in Atlantic salmon	29
4.2. PRV-1 infects erythroid and macrophage lineage cell population	31

4.3.	PRV-1 is associated with macrophage polarization in melanized focal changes and HSML.....	34
4.4.	PRV-3 subtype cross-protects against PRV-1 infection in Atlantic salmon.....	37
4.5.	MHC-I and CD8 ⁺ cells presents specific immune response against PRV-1 infection in Atlantic salmon.....	38
5.	Methodological consideration	43
5.1.	Detection of PRV-1 genomic (dsRNA) and transcript (ssRNA) nucleic acids by qPCR.....	43
5.2.	Western blot.....	45
5.3.	<i>In situ</i> hybridization (ISH).....	46
5.3.1.	Chromogenic ISH detection (singleplex & duplex).....	47
5.3.2.	Multiplex fluorescent <i>in situ</i> hybridization (FISH).....	49
5.4.	Confocal microscopy.....	49
6.	Main conclusions	51
7.	Future perspectives	53
8.	References	57
9.	Scientific papers I-IV	71

Acknowledgements

This study was conducted at the Department of Paraclinical Sciences, Faculty of Veterinary Medicine at the Norwegian University of Life Sciences (Nov 2017-Feb 2021). The Norwegian Seafood Research Fund (FHF) (grant #901221, 901501) and Research Council of Norway (RCN) (grant #280847/E40 ViVaAct), supported this study financially.

There is a long list of people to whom I want to thank, but first I would like to express sincere gratitude to my main supervisor Prof. Espen Rimstad for having faith in me and introducing me in the world of fish and giving me all the support, guidance and enthusiasm. I am truly grateful to my co-supervisors Maria Krudtaa Dahle and Øystein Wessel for all philosophical discussions, ideas, and suggestions. You are an inspiration to me. I always admire the way you encourage, motivate and transfer leadership qualities to boost confidence in colleagues.

I consider myself fortunate to have the nice colleagues in our PRV group which I always considered as a family; Ida, Dharmotharan, Turhan, Ingrid and Nina, who supported me and gave me fruitful ideas when needed. Special thanks to Elisabeth, Ingvild and, Stine for teaching me laboratory methods and helping in the daily lab work. Moreover, I want to thank Prof. Erling Olaf Koppang and Håvard as you were always open to constructive ideas and criticism. I will always remember Prof. Koppang unmatched humor that eased out to navigate complexities and made a cheerful environment. My appreciation goes to all other colleagues at Lindern and Ås, Mette, Hege, Henning, Grethe, Kari, Erik, Stanislav, Ruchika, Özgün, Alex, Karla, John, Leif, Preben, Lena, Ane, Clementine and Cristopher.

I would like to acknowledge all the co-authors; together we have been able to move forward. Thanks to other neighboring students for sharing the floor with me at Lindern most of the time during my PhD. It was relaxing to share fun experiences, coffee, and cakes. Thanks to Stanislav and Dharmo for the swimming and badminton sessions.

I am extremely grateful to my parents, brothers and wife for the patience, care, and endless support. It would not have been possible for me to keep pursuing a research career. Thanks to all my dear friends who cheered for me during this journey.

Muhammad Salman Malik (Ås, 2021)

Abbreviations

A

ARV Avian orthoreovirus

B

BSA Bovine serum albumin

C

CCL19 Chemokine (C-C motif) ligand 19
CD8 Cluster of differentiation 8

E

EIBS Erythrocytic inclusion body syndrome
EPO Erythropoietin
EPOR Erythropoietic receptor

F

FAST Fusion associated small transmembrane
FFPE Formalin-fixed paraffin embedded
FISH Fluorescent *in situ* hybridization

G

GCRV Grass carp reovirus

H

HSMI Heart and skeletal muscle inflammation

I

i.p. intraperitoneal
ICTV International committee on taxonomy of viruses
IFN Interferon
IHC Immunohistochemistry
IHNV Infectious hematopoietic necrosis virus
IPNV Infectious pancreatic necrosis virus
ISAV Infectious salmon anemia virus
ISGs Interferon stimulated genes
ISH *In situ* hybridization
ISVP Infectious subviral particle

J

JAM-A Junctional adhesion molecule A

M

MCSF Macrophage colony stimulating factor
MCSFR Macrophage colony stimulating factor receptor
MDA5 Melanoma differentiation-associated gene 5
MHC-I Major histocompatibility complex I
MRV Mammalian reovirus

N

NOS2 Nitric oxide synthase 2

P

PCR Polymerase chain reaction
PD Pancreas disease
PKR Protein kinase RNA-activated
PRR Pattern recognition receptor
PRV Piscine orthoreovirus
PMCV Piscine myocarditis virus

R

RBCs Red blood cells
RIG-I Retinoic acid-inducible gene I
ROS Reactive oxygen species

S

SAV Salmonid alphavirus
SGPV Salmon gill poxvirus

T

TEM Transmission electron microscopy
Th1 T-helper 1
Th2 T-helper 2
TLR3 Toll-like receptor 3
TNF Tumor necrosis factor

V

VHSV Viral hemorrhagic septicemia virus
VLPs Virus-like particles

W

Wpc weeks post challenge

List of papers

Paper I:

Erythroid Progenitor Cells in Atlantic Salmon (*Salmo salar*) May Be Persistently and Productively Infected with *Piscine Orthoreovirus* (PRV)

Muhammad Salman Malik, Håvard Bjørgen, Kannimuthu Dhamotharan, Øystein Wessel, Erling Olaf Koppang, Emiliano Di Cicco, Elisabeth F. Hansen, Maria K. Dahle, Espen Rimstad

Paper II:

M1 polarized macrophages in red and black spots in white muscle of Atlantic salmon (*Salmo salar*) are PRV-1 infected and correlates with a pro-inflammatory environment.

Muhammad Salman Malik, Håvard Bjørgen, Ingvild B Nyman, Øystein Wessel, Erling O. Koppang, Maria K Dahle and Espen Rimstad

Paper III:

Dynamics of polarized macrophages and activated CD8⁺ cells in heart tissue of Atlantic salmon infected with *Piscine orthoreovirus*-1.

Muhammad Salman Malik, Øystein Wessel, Ingvild B Nyman, Maria K Dahle and Espen Rimstad

Paper IV:

***Piscine orthoreovirus* (PRV)-3, but not PRV-2, cross-protects against PRV-1 and heart and skeletal muscle inflammation (HSMI) in Atlantic salmon (*Salmo salar*)**

Muhammad Salman Malik, Lena H. Teige, Stine Braaen, Anne Berit Olsen, Monica Nordberg, Marit M. Amundsen, Kannimuthu Dhamotharan, Steingrim Svenning, Eva Stina Edholm, Tomokazu Takano, Jorunn B. Jørgensen, Øystein Wessel, Espen Rimstad, Maria K. Dahle

Summary

This thesis focuses on infection kinetics, infected cell types, viral shedding, and specific immune responses in persistently *Piscine orthoreovirus-1* (PRV-1) infected Atlantic salmon. The aim is to enhance the understanding of viral pathogenesis.

PRV is ubiquitous in Norwegian Atlantic salmon (*Salmo salar*) aquaculture. The currently identified subtypes of PRV include PRV-1 and PRV-2 and PRV-3 which have been associated with diseases in Atlantic salmon, coho salmon (*Oncorhynchus kisutch*) and rainbow trout (*O. mykiss*), respectively. PRV-1 causes an acute infection of erythrocytes of Atlantic salmon and thereafter the virus spreads to cardiomyocytes which may induce the disease of heart and skeletal muscle inflammation (HSMI). PRV-1 is also found to infect other organs and tissues, but the causal relationship to diseases or disorders apart from HSMI is vague. PRV-1 is not cleared by the Atlantic salmon immune system after acute infection and persists life-long in the host.

In Atlantic salmon focal melanized changes (black spots) of white skeletal muscle tissues, which histologically appear as granulomatous structures, are commonly observed in the fillet. The black spots presumably develop from red spots characterized by extravasal erythrocytes. Many of the inflammatory cells in the melanized spots are infected with PRV-1. Even if PRV-1 associates with the development of melanized focal changes, the causal relationship is questionable.

In the first study, reproduction of black spots in the Atlantic salmon was attempted by intramuscularly injection of PRV-1 infected blood in the same individual fish from which the blood was drawn. Although black spots could not be reproduced experimentally, PRV-1 genome and transcripts levels were explored in different tissues to understand viral activity and persistence. PRV-1 transcription level was high in blood cells in the acute phase and in the kidney during the persistent phase. PRV-1 caused plasma viremia that started in the acute phase and lasted for at least 18 weeks, i.e. the end of the experiment. *In situ* hybridization assays identified PRV-1 infection of Macrophage colony-stimulating factor receptor (MCSFR) positive macrophages in kidney and spleen and Erythropoietin receptor (EPOR) positive erythroid progenitor cells in the kidney, in

both acute and persistent phases. The infected erythroid progenitor cells may represent a possible reservoir for PRV-1 as a continuous source of new generated erythrocytes. In the persistent phase, PRV-1 is cleared from the cardiomyocytes but still present in the erythrocytes.

The macrophage polarization response in relation to PRV-1 infection in focal melanized changes of the white skeletal muscle and in cardiac tissue of fish with HSMI was evaluated in the second and third studies, using fluorescent *in situ* hybridization (FISH) and RT-qPCR. Macrophages polarize either into pro-inflammatory M1 or anti-inflammatory/regenerating M2 phenotypes. M1 macrophages were dominant in the red spots and almost all co-stained for PRV-1. In spots assessed as “late phase” of red spots melanized M2 melano-macrophages appeared, indicating a transition phase to melanized spots. In the melanized spots M2 macrophages were highly abundant. The M2 melano-macrophages of the black spot generally co-stained for PRV-1.

In the initial development of HSMI, macrophages were not abundant. Heart and skeletal muscle tissues with characteristic lesions of HSMI showed low numbers of M1 macrophages that only partly co-localized with PRV-1. M2 macrophages, on the other hand, dominated in the heart tissue and were abundant even at the peak in pathologic lesions, which is supportive of a good regenerating ability of the salmon heart. Specific cell mediated responses represented by CD8+, granzyme A (GzmA) and MHC-I expressing cells were identified in heart tissue of fish with HSMI. Massive staining of CD8+ cells with GzmA transcripts were detected in the heart compared to the skeletal muscle after the peak infection of PRV-1. PRV-1 was detected in multiple CD8+ and MHC-1 expressing cells in the heart. Skeletal muscle tissue had a relatively moderate immune response with low number of CD8+ and MHC-I cells and no co-localization with PRV-1. The FISH method revealed the close interplay between PRV-1 infected and cytotoxic cells.

A vaccination experiment was performed by immunizing Atlantic salmon with the PRV subtypes PRV-2 or PRV-3 to study the protection potential against consecutive PRV-1 infection. This approach was also compared with an inactivated PRV-1 vaccine. The PRV-3 subtype cross-protected fish against secondary PRV-1 infection, while only

partial protection was achieved by PRV-2 immunization and by the inactivated vaccine. Antibodies, cross reactive to PRV-1, were elevated in the PRV-3 immunized group, but low in PRV-2 immunized, and undetectable in the inactivated vaccine groups. Moreover, histopathological analysis showed no HSMI like heart lesions in the PRV-3 immunized group. The results provided sufficient evidence that PRV-3 can block the subsequent PRV-1 infection efficiently, at least for the ten-weeks period that the experiment lasted.

To conclude, our studies show that 1) PRV-1 establishes a productive and persistent infection with plasma viremia in Atlantic salmon. 2) Renal erythroid progenitor cells and macrophages could be long-term cellular reservoirs for PRV-1. 3) PRV-1 infection correlates with macrophage polarization in melanized focal changes of skeletal muscle. 4) M1 polarized macrophages do not correlate with initial development of HSMI however, M2 macrophages are associated with high level of PRV-1. 5) A strong activation of cellular immune response is triggered in heart, followed by a drop in PRV-1 levels. And finally, 6) we demonstrated that the PRV-3 subtype can cross-protect against PRV-1 infection in Atlantic salmon.

Sammendrag (Summary in Norwegian)

Piscine orthoreovirus (PRV) er en meget vanlig infeksjon i havbruk av norsk Atlantisk laks (*Salmo salar*). Tre varianter av PRV har vært beskrevet, PRV-1 og PRV-2 og PRV-3, som hovedsakelig har vært assosiert med sykdommer i henholdsvis Atlantisk laks, coholaks (*Oncorhynchus kisutch*) og regnbueørret (*O. mykiss*). PRV-1 gir en akutt infeksjon av erytrocytter i Atlantisk laks og spres deretter til kardiomyocytter. Dette kan utløse sykdommen i hjerte- og skjelettmuskulær betennelse (HSMB). PRV-1 er også funnet å infisere andre organer og vev, men forholdet til sykdommer eller lidelser bortsett fra HSMI er vagt. PRV-1 infeksjon er persistent i Atlantiske laks. Fokale melaniserte forandringer i hvit skjelettmuskulatur, forandringene kan histologisk fremstå som granulomer, utvikler seg fra røde flekker som inneholder ekstravasale erytrocytter. Mange av betennescellene i melaniserte flekker er infisert med PRV-1. Selv om PRV-1 kan assosieres med utviklingen av melaniserte fokale endringer, har vi ikke funnet at PRV-1 er årsaken til at flekkene oppstår. I artiklene i denne tesis ble det fokusert på infeksjonskinetikk, infiserte celletyper, og immunresponser i persistent PRV-1-infisert Atlantisk laks, for å gi en bedre forståelse av PRV-1 sin eventuelle rolle i utvikling av flekker.

I den første studien ble reproduksjon av svarte flekker i Atlantisk laks forsøkt ved injeksjon av PRV-1-infisert blod intramuskulært i det samme individ som blodprøven var tatt fra. Selv om svarte flekker ikke kunne reproduseres eksperimentelt, ble PRV-1 genom- og transkripsjonsnivåer utforsket i forskjellige vev for å forstå viral aktivitet og persistens. Transkripsjonsnivå av PRV-1 var høyt i blodceller i den akutte fasen og i nyrene under den persistente fasen. PRV-1 forårsaket plasmaviremi som startet i den akutte fasen og varte ut forsøket, det vil si minst 18 uker. *In situ* hybridiseringsanalyser identifiserte PRV-1-infeksjon i celler i nyre og milt med reseptor for makrofagkolonistimulerende faktor (MCSFR), det vil si makrofager, og i celler i nyrene positive for erythropoietinreseptor (EPOR) det vil si erytroide stamceller. De infiserte erytroide stamcellene kan representere et mulig reservoar for PRV-1 og en potensiell kontinuerlig kilde til nye genererte erytrocytter. I den persistente fasen blir PRV-1 fjernet fra kardiomyocytene, men vil fremdeles være i erytrocyttene.

Polarisering av makrofager i relasjon til PRV-1-infeksjon ble studert i fokale melaniserte forandringer av den hvite skjelettmuskelen og i hjertevev i fisk med HSMB forandringer og evaluert ved bruk av fluorescerende *in situ* hybridisering (FISH) og RT-qPCR. Makrofager kan polarisere enten til proinflammatoriske M1 fenotype eller antiinflammatoriske / regenererende M2 fenotype. Dette er en dynamisk prosess hvor cellene kan gå inn og ut av de ulike fenotypene. M1 makrofager var dominerende i de røde flekkene hvor nesten alle ble farget for PRV-1. I flekker vurdert som "sen fase" av røde flekker, det vi så at melaniserte M2 melanomakrofager begynte å opptre, noe som indikerer en overgangsfase til melaniserte flekker var det færre M1 makrofager. I de melaniserte flekkene (makroskopisk svart) var M2 makrofager den dominerende fenotypen. M2 melanomakrofager i svarte flekker ble vanligvis farget for PRV-1. I HSMI var makrofager ikke en vanlig celletype. Hjerte- og skjelettmuskulaturvev med karakteristiske HSMB lesjoner viste moderat antall M1-makrofager, som bare var delvis co-lokalisert med PRV-1. M2 makrofager dominerte i hjertevev sammenlignet med skjelettmuskulatur, noe som understøtter den regenererende evne til laksens hjerte.

Spesifikke cellulære responser representert av CD8⁺, granzyme A (GzmA) og MHC-I uttrykk ble identifisert i hjertevev av fisk med HSMI. Massiv farging av CD8⁺ -celler med GzmA-transkripsjoner ble funnet i hjertet sammenlignet med skjelettmuskulatur. PRV-1 ble påvist i flere CD8⁺ og MHC-1-uttrykkende celler i hjertet. Skjelettmuskulaturvev hadde en relativt moderat immunrespons med lavt antall CD8⁺ og MHC-I celler og ingen samlokalisering med PRV-1. FISH-metoden avslørte det tette samspillet mellom PRV-1-infiserte og cytotoksiske celler.

Et vaksinasjonseksperiment ble utført ved å immunisere atlantisk laks med PRV-variantene PRV-2 eller PRV-3 for å studere beskyttelsespotensialet mot påfølgende PRV-1-infeksjon. Denne tilnærmingen ble også sammenlignet med en inaktivert PRV-1-vaksine. PRV-3-varianten kryss-beskyttet fisk mot sekundær PRV-1-infeksjon, mens bare delvis beskyttelse ble oppnådd ved PRV-2-immunisering og ved den inaktiverede vaksinen. Antistoffer, kryssreaktive mot PRV-1, ble forhøyet i den PRV-3-immuniserte gruppen, men var lave i PRV-2-immuniserte, og knapt detekter bare i den inaktiverede

vaksinegruppen. Videre viste histopatologisk analyse ingen HSMB-lignende hjertesjoner i den PRV-3-immuniserte gruppen. Resultatene ga tilstrekkelig bevis for at PRV-3 kan blokkere den påfølgende PRV-1-infeksjonen effektivt, i minst i ti uker.

For å konkludere viser våre studier at 1) PRV-1 etablerer en produktiv og persistent infeksjon med plasmaviremi hos Atlantisk laks. 2) Renale erytroide stamceller og makrofager kan være langvarige cellulære reservoarer for PRV-1. 3) PRV-1-infeksjon korrelerer med makrofagpolarisering i melaniserte fokale endringer i skjelettmuskulaturen. 4) M1-polariserte makrofager korrelerer ikke med tidlig utvikling av HSMI, men M2-makrofager er assosiert med relativt høyt nivå av PRV-1 infeksjon. 5) En sterk aktivering av cellulær immunrespons utløses i hjertet ved HSMB, etterfulgt av et fall i PRV-1 nivåer. Og til slutt, 6) demonstrerte vi at PRV-3-varianten gir kryssbeskyttelse mot PRV-1-infeksjon i Atlantisk laks.

1. Introduction

1.1. Aquaculture of salmonids

Atlantic salmon (*Salmo salar*) is one of the most intensified farmed fish species, where the farming mainly takes place in Norway, Chile, Canada United Kingdom and Faroe Islands (Figure 1) (1). Norway is the dominant producer (2).

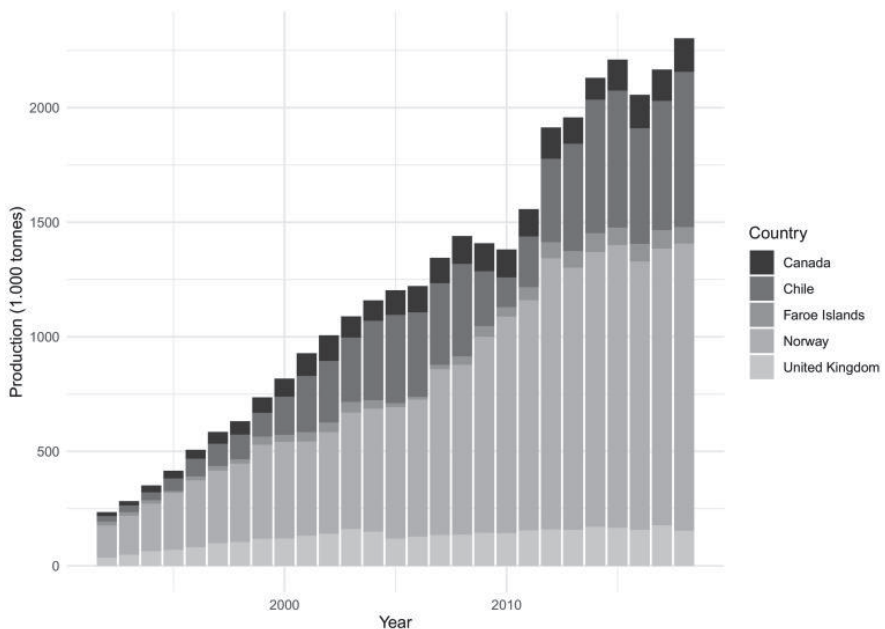


Figure 1. Atlantic salmon production in five largest producer countries (2003-2018) (Kontali Analyse AS).

Emerging infectious diseases are one of the biggest threats for the sustainability of Atlantic salmon aquaculture due to substantial problems related to fish health (3), economic costs, trade restrictions and effects on wild fauna (4). The industrial farming practices with large stocks of genetically relatively homogenous fish in a confined volume make farmed fish more susceptible to pathogens. High stock densities, lack of environment variation and delayed sexual maturation are the hallmarks of salmon farming (5, 6). Viruses spread efficiently when the abundance of hosts facilitating transmission is high (3). The seawater phase of the production is the phase where the farmed salmon are most prone to get infected by pathogens such as viruses (7). Strict

biosecurity measures are the major key to reduce the spread of infectious diseases, especially if prophylactic measures like vaccines are not available or genetic resistance not adequately efficient.

Viral diseases have a great influence on salmon farming. Norwegian aquaculture industry spends millions of NOK every year on vaccines. Large efforts are made to monitor, detect, and control infectious diseases and their etiological agents to keep the fish healthy (Table 1). As an exporting industry, salmon farming is dependent upon control of notifiable diseases to avoid trade restrictions. As a food producing industry its products should be safe for consumers and have low environmental impact. As an industry based on utilization of live animals, it should take ample consideration to the welfare of the fish, including keeping diseases under control and reducing risk of health challenges.

Table 1. Number of registered outbreaks for various viral diseases in farmed salmonids (8).

Viral Diseases	2015	2016	2017	2018	2019	2020
PD	137	138	176	163	152	158
HSMI*	135	101	93	104	79	161
CMS*	105	90	100	101	82	154
ISA	15	12	14	13	10	23
IPN*	30	27	23	19	23	22

(*) indicates minimum estimate due to non-notifiable diseases

Piscine orthoreovirus (PRV) is a widespread virus in the Norwegian Atlantic salmon aquaculture. The subtype PRV-1 is the etiological agent of heart and skeletal muscle inflammation (HSMI) (9), and it is also linked to the development, but probably not in the original etiology, of melanized focal changes in the white muscle of Atlantic salmon (10). HSMI as a disease was recognized in late 1990s in farmed Atlantic salmon, and the histopathology was reported a few years later (11). PRV is one of the top three disease causing viruses in Norway, according to the annual Fish Health Report (8).

In this work the identification of PRV infected cell types and local immune responses to the infection were mapped with the purpose to obtain a better understanding of the host-PRV cross talk and how the virus can replicate for long-term in Atlantic salmon.

1.2. Piscine orthoreovirus (PRV)

1.2.1. Classification & taxonomy

PRV was first described in 2010 in material from fish with acute HSMI, using high-throughput sequencing, a technique which was in its infancy at that time. PRV was immediately recognized as a novel reovirus (12). Based on the phylogenetic analysis and genomic structure organization, PRV was grouped in the *Orthoreovirus* genus in the *Reoviridae* family (12, 13).

“REOvirus was first attributed to a group of viruses in 1959 who were recovered from respiratory tract (R = respiratory) and gastrointestinal tracts (E = enteric) but without any association with the disease (O = Orphan)(14). Viruses belonging to *Reoviridae* family have key features including; double capsid; non-enveloped; spherical shape and a genome of 10-12 linear segments of double stranded RNA (dsRNA) (15). Reoviruses infect a diverse groups of hosts including mammals, reptiles, fish, mollusks, birds, insects and plants (16), and is the largest dsRNA virus family (17). *Reoviridae* family is divided into two subfamilies based on the presence of turret proteins (Figure 2) which are either present or absent on the icosahedral axis of the virion (18). “Turreted” sub-family i.e. *Spinoreovirinae* includes genus *Orthoreovirus* with seven other genera (Figure 3)(19).

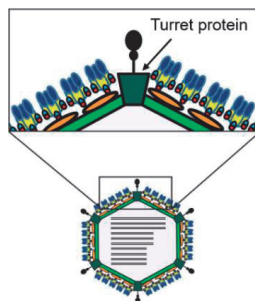


Figure 2. Schematic overview of turret protein in the outer capsid of reovirus virion (image modified from (20)).

Orthoreoviruses and Aquareoviruses have conserved core proteins, and evolutionary studies indicate that the two genera originate from a common ancestor (21). But there are key differences that place them in two different genera. Orthoreoviruses have 10 genomic segments and do not induce syncytia, whereas Aquareoviruses have 11

genomic segments and most of them induce syncytia (21). The viruses of the *Aquareovirus* genus have been isolated from poikilotherm finfish in marine- and freshwater and can replicate in mammalian and fish cell lines. These viruses have also been isolated from crustaceans (22). PRV with 10 dsRNA segments is more closely related to *Orthoreovirus* than to *Aquareovirus* and was the first orthoreovirus found to infect fish (12). International committee on taxonomy of viruses (ICTV) classification criteria based on nucleotide and amino acids similarities, and the non-fusogenic properties, confirms PRV in the *Orthoreovirus* genus (23, 24). PRV is genetically and functionally classified as related to the prototype MRV species as both lack the fusion associated small transmembrane (FAST) protein that enables cell-cell fusion. PRV encodes an integral membrane protein (p13), which makes it distinct among other orthoreoviruses (25). PRV has three identified subtypes i.e. PRV-1, PRV-2, and PRV-3. Phylogenetic analysis shows 90% nucleotide sequence homology between PRV-1 and PRV-3, whereas PRV-1 is 80% homologous with the PRV-2 subtype (26).

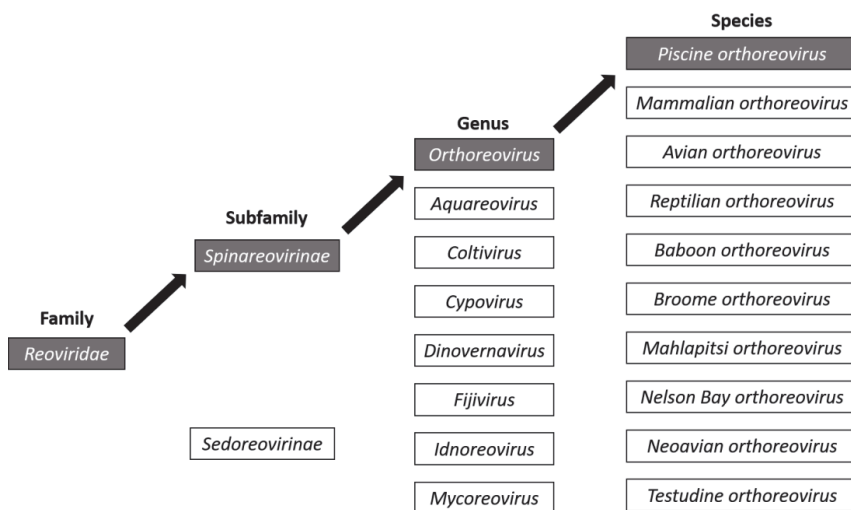


Figure 3. Taxonomical overview of *Piscine orthoreovirus*.

1.2.2. Structure

PRV is a non-enveloped virus and has an icosahedral double layered capsid with a diameter of 70-80 nm (Figure 4A). Total size of the PRV genome is 23320 nt (12, 13, 27). The genome consists of 10 linear dsRNA segments that clusters in three size groups:

Large (L1-L3), Medium (M1-M3) and Small (S1-S4), in line with other orthoreoviruses. The segment groups code for λ , μ and σ proteins as per size class, respectively, and some accessory proteins as well (13). Based on sequence analysis, there are nine structural proteins packed in inner and outer layer of the capsid (Figure 4B) and three non-structural proteins present in the infected cell. Functional properties for translated products have been assessed based on the sequence homology with other orthoreoviruses, including presence of conserved motifs (13). For some proteins, the functional properties has been shown experimentally (28-30).

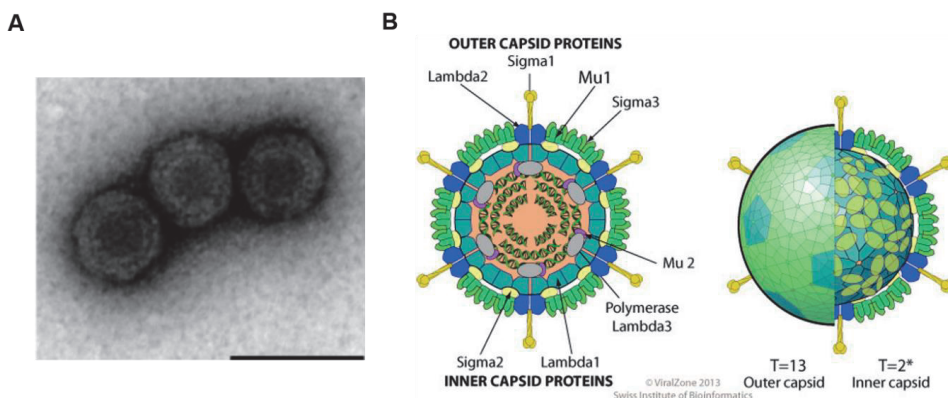


Figure 4. (A) TEM image showing PRV particle with outer diameter of 70nm and inner core of 39nm (image modified from (9)). (B) Orthoreovirus proteins and viral symmetry. *Source:* <https://viralzone.expasy.org/viralzone>, Swiss Institute of Bioinformatics (SIB).

Outer protein shells (outer capsid) of orthoreoviruses consist of μ_1 , σ_3 and the σ_1 (31, 32). Outer capsid proteins interact with host cells and deliver the viral core into the cytosol. The S4 genome segment of PRV encodes the σ_1 protein is assumed to be involved in cell attachment. It is one of the most variable proteins and a serotype determinant among orthoreoviruses (33). MRV serotypes grouping i.e. MRV type 1 Lang (T1L), type 2 langdon (T2L) and type 3 Dearing (T3D) is based on σ_1 neutralization. Such serotyping is not possible for PRV due to the virus' resistance to propagate in cell lines. PRV gene segment M2 codes for the μ_1 protein which is essential for endosomal membrane penetration. This protein undergoes myristoylation and proteolytic cleavages (μ_1N/μ_1C fragments) during viral entry (34, 35). For *Avian orthoreovirus* (ARV), the μ_1 homolog (μ_B) protein has been implicated in strain-specific differences in

macrophage infection (35). The S1 segment codes for the σ_3 protein which is present on the viral surface as a trimer of $\mu_1\sigma_3$ heterodimers. The σ_3 protein has a zinc finger motif which is conserved in orthoreoviruses, and it has the ability to bind dsRNA and may therefore moderate the cellular antiviral innate responses due to reduced stimulation of dsRNA receptors such as cytoplasmic retinoic acid inducible gene (RIG-I) (30). This second smallest S-class gene segment also encodes an additional nonstructural cytotoxic and integral membrane protein called p13 (13), but the primary function for this protein is yet to be characterized. The λ_2 protein encoded by the L2 segment, forms pentameric turrets at the fivefold axes in the viral particle, providing exit for nascent transcripts. In addition, the protein is responsible for mRNA capping at 5' end with guanylyltransferase and methyltransferase activity (34).

The inner capsid, "the core", consists of the λ_1 , λ_3 , σ_2 and μ_2 structural proteins. The core has an icosahedral symmetry (Figure. 4). Many of the motifs of the replication machinery made up by the λ proteins are conserved within the orthoreoviruses. The L3 segment codes for the λ_1 protein, which is a major structural protein and has helicase functions in the replication. The λ_3 protein encoded by the L1 segment is the RNA-dependent RNA polymerase (RdRp). The S2 gene segment encodes the σ_2 inner core protein (13, 36). The M1 segment encodes the μ_2 polymerase associated protein, which is present in low amounts compared to other core proteins (18).

The non-structural proteins σ_{NS} and μ_{NS} are coded by the S3 and M3 gene segments. Their main functions are formation of viral factories and recruitment of other PRV proteins to these neo-organelles (28).

1.2.3. Replication and transmission

Replication studies of PRV are cumbersome due the virus' resistance to propagation in cell lines, and it has consequently mostly been done by *ex vivo* experiments in cultured red blood cells. The well characterized replication of MRV is considered as a valid model to understand fundamental mechanisms.

The cellular receptors for PRV are not known, but sialic acid, JAM-A, NgoR or B-integrins are used by MRV (37-39). The cellular attachment protein $\sigma 1$ determines the cell and tissue tropism of the virus. After cellular attachment, the MRV virions are endocytosed via the clathrin or caveolin pathways, and are sorted into early and late endosomes (39, 40). The proteolytic cleavage of the $\mu 1$ outer capsid protein during virus entry enables endosomal membrane penetration and entrance of the core into the cytoplasm (41, 42). In this process $\sigma 3$ protein is freed from the viral particle, that has the dsRNA binding properties in the cytoplasm to make viral RNA less accessible to be recognized by cellular innate immune response. $\sigma 3$ modulates the interferon response by reducing the stimuli that activate viral RNA recognizing receptors of the innate immune response, such as RIG-1 and protein kinase R (PKR).

The virus particle will be in called infectious subviral particles (ISVP) during the process of crossing the endosomal membrane, and the ISVP are converted to transcriptionally active viral core particles in the cytoplasm (43). Alternatively, extracellular proteolysis can result in the formation of ISVPs, particularly in the intestinal mucosa (44). These extracellular ISVPs have the potential to internalize through the plasma membrane into the cell, i.e. they are infectious. The remaining disassembly and conversion to the viral core happens after translocation to the host cell cytoplasm (Figure 5).

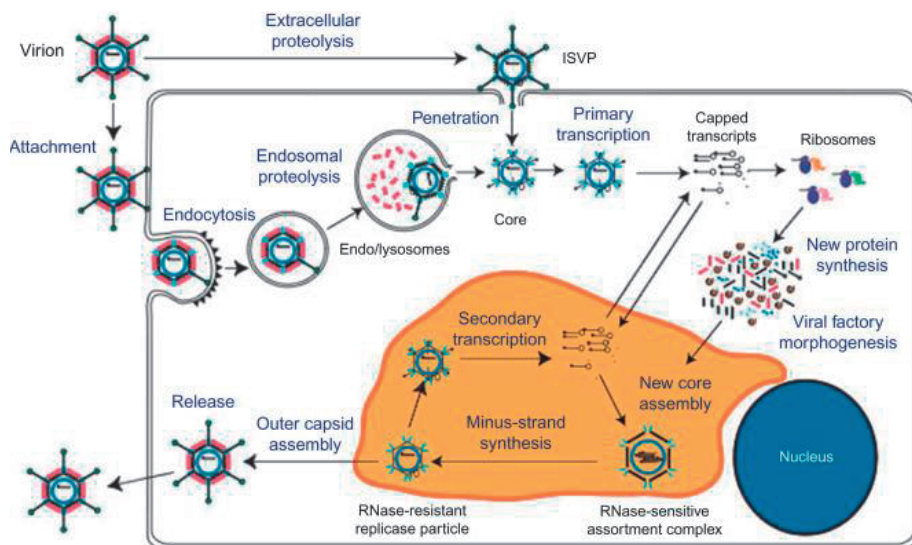


Figure 5. Schematic overview of reovirus replication cycle. (45)

The $\lambda 3$ RNA-dependent RNA polymerase enzyme initiates viral transcription of the dsRNA genome and mRNA is synthesized. It is capped in the 5' end but lacks polyadenylation in the 3' end. The mRNA is identical to the positive strand of the dsRNA genomic segments. $\lambda 2$ is responsible for the capping of the positive strand RNA transcripts, which are extruded through the $\lambda 2$ turrets (46). The turrets also hold the cell attachment protein $\sigma 1$, but the $\sigma 1$ is lost during the transition from ISVP to a core particle (32, 47). The ten genome segments are transcribed inside the core. During the replication cycle neither the viral genomic dsRNA nor the negative strand ssRNA are exposed to the cytoplasmic innate immune response receptors in the host-cell cytoplasm during the replication cycle (48). After initial translation, the non-structural μ NS protein organizes formation of viral factories where the core assembly, packaging and replication of the viral genome take place (49). The non-structural proteins are required for the viral replication but are not parts of the viral particles (50). μ NS has an important role in PRV viral factory formation (28). One copy of each 10 plus strand mRNA is encapsulated by inner capsid proteins to make an intermediate structure. The synthesis of the complementary negative strand RNA then generates a new dsRNA genome inside the newly formed core (51). Outer capsid proteins are added to make new PRV virions, which are released from the cell either by lysis or non-lytic egress (52) (still unknown).

In experimental settings in a tank PRV is spread from shedder fish to naive fish, i.e. through water. The route of shedding is largely unknown, but it is believed to spread the fecal-oral route to other fish. However, reoviruses are known to infect both through the respiratory as well as the alimentary tract, and this may be the case for PRV as well. Anal intubation of the virus showed efficient infection, indicating that uptake may occur through the intestinal wall and thus makes the fecal-oral route a possible way of transmission (53). There are no specific findings that indicate vertical spread, i.e. from broodfish to offspring in aquaculture settings.

1.3. PRV associated diseases

There are three registered subtypes of PRV i.e. PRV-1, PRV-2, and PRV-3, which causes different diseases in different salmonid species as described in the following.

1.3.1. Heart and skeletal muscle inflammation (HSMI)

HSMI is one of the most prevalent diseases in Atlantic salmon aquaculture in Norway (Figure 6). It was first recognized as a new disease in 1999 with characteristic histopathological lesions in the heart and skeletal muscle tissue (54, 55). HSMI was first spotted in Hitra/Frøya area (55). Continuous investigations were made to elucidate the etiological agent of this disease. HSMI was suggested as an infectious disease based on the initial experimental challenges, where injected tissue from the diseased fish induced similar cardiac and skeletal muscle lesions as in HSMI in both the injected and the cohabitant fish (56). Transmission electron microscopy revealed presence of various virus-like particles in HSMI affected fish and some of these particles showed close resemblance to those earlier described in EIBS (57). In 2010, high throughput sequencing identified a novel reovirus associated to HSMI and it was named *Piscine orthoreovirus* (12). Later, the causal relationship to HSMI was proven (9). But, while characteristic severe cardiac lesions are typical of HSMI in Atlantic salmon in Norway (9, 58), generally mild cardiac lesions (with occasionally severe lesions in some individuals) are reported from west-coast, Canada (59). A recent report demonstrated that some Norwegian PRV-1 isolates, but not all, are more virulent than Canadian isolates in terms of inducing histopathological lesions (60).

HSMI is considered as a serious disease problem in seawater farms, and it was originally added to the list of national notifiable diseases for the Norwegian Food Safety Authority to take specific actions to control the disease outbreaks. The number of outbreaks rose every year since after the disease became listed. HSMI was de-listed in 2014, at a time when it was clarified that PRV was widespread. In 2020, 161 outbreaks were recorded (Table 1), however, this possibly reflects an under-reporting due to removal of HSMI from the national notifiable disease list.

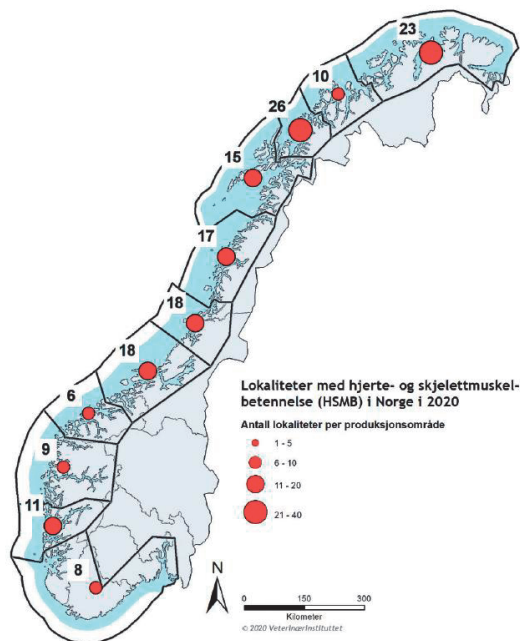


Figure 6. Distribution of HSMI outbreaks in 2020 in Norway (Modified from Fish Health Report 2020, Norwegian veterinary institute).

Clinical symptoms of HSMI are abnormal swimming patterns, loss of appetite, reduced weight gain, and increased mortality of the population (11). Macroscopic pathological changes include pale heart, yellowish liver, visceral ascites, and swollen spleen tissue (Figure 7). Histologic examination the heart tissue reveal severe inflammation in epi-, myo- and endocardium in both ventricle and atrium, especially in spongiosum and compactum layers (Figure 8) (54). Histopathological analysis of red skeletal muscle shows inflammation and necrosis seen as mild to moderate degeneration of myocytes, presence of infiltrating cells and vacuolization of muscle fibers (54).

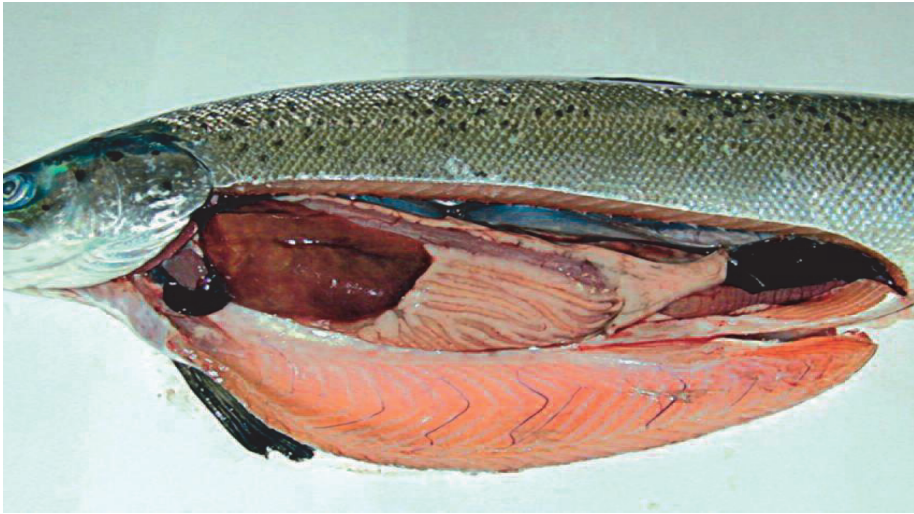


Figure 7. HSMI diseased Atlantic salmon with bloody fluid in the body cavity. Other visceral organs are also affected e.g. pale heart and fibrinous membrane over liver (Photo: A. Lyngøy, Fish Health Report 2019, Norwegian Veterinary Institute).

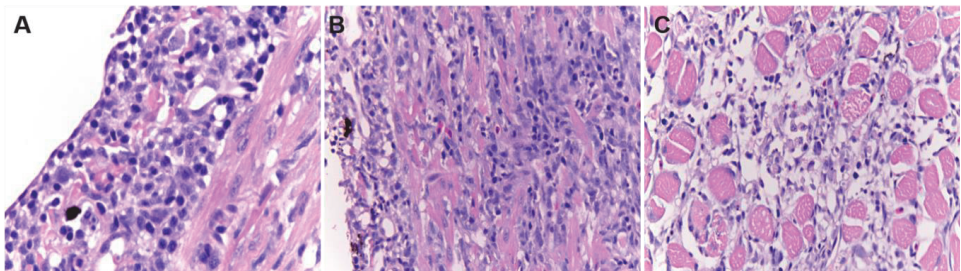


Figure 8. Histological overview of HSMI affected heart and skeletal muscle tissues in Atlantic salmon. (A) severe diffuse epicarditis in heart. (B) Compact ventricular myocardium with inflammatory infiltrate. (C) Red skeletal muscle with mild to moderate multifocal myositis. Source: FISH PATHOLOGY (<https://fishhistopathology.com>)

1.3.2. Melanized focal changes in Atlantic salmon

Melanized focal changes (black spots) is a common quality problem of the white muscle fillet in farmed Atlantic salmon. The condition is first observed at slaughter and mostly occurs in the cranio-ventral part but can be present elsewhere as well (61). The etiology of this condition has not been revealed, but the severity of the lesions is associated with PRV-1 infection as found in recent studies (10, 62). It is assumed that the spot development commences as red focal changes in the white muscle tissue where hemorrhages are central. The melanin synthesis, observed as black spots, is assumed to

be a result of protection against reactive oxygen species, induced as a consequence of a long-lasting inflammatory response. In short, the more severe the inflammation is, the more melanin is produced. In severe spots with granulomatous inflammation, PRV-1 is a constant finding (Figure 9). However, it has not been possible to reproduce the condition experimentally, and the eventual role of PRV-1 in the etiology of the condition is not clarified (63). Overall, 20-30% of fillets are affected with this condition as observed during processing, hence it causes huge economic losses every year for the salmon industry in Norway.

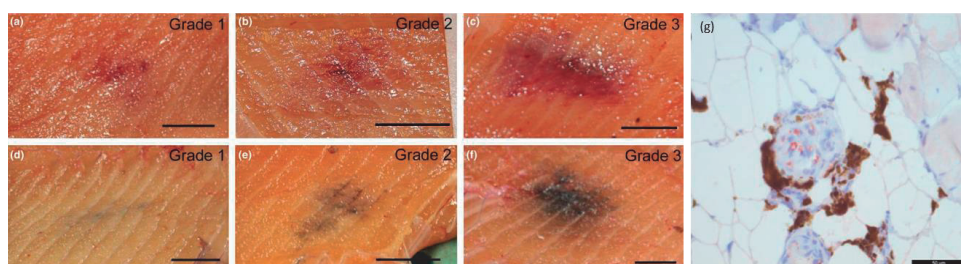


Figure 9. Red & Black spots in white muscle of Atlantic salmon. Macroscopically graded red spots from grade-1 to grade-3 (a-c) and black spots (d-f). (g) A granuloma containing PRV positive cells (red) which is surrounded by pigmented cells in the black spots. Pictures modified from (62).

1.3.3. Jaundice syndrome

Recently, a condition termed jaundice syndrome has been associated with PRV-1 infection in farmed Chinook salmon (*Oncorhynchus tshawytscha*) in British Columbia, Canada (59). The disease has some clinical symptoms resembling HSMI in Atlantic salmon, but in contrast to HSMI, fish with jaundice syndrome have anemia, yellowish liver and yellow discoloration of the abdomen ("jaundice"). The eventual etiological relationship with PRV-1 is not established experimentally (59). Similarly, farmed coho salmon (*Oncorhynchus kisutch*) in Chile have also been diagnosed with a similar jaundice syndrome that is associated with PRV-1 infection (Figure 10) (64).

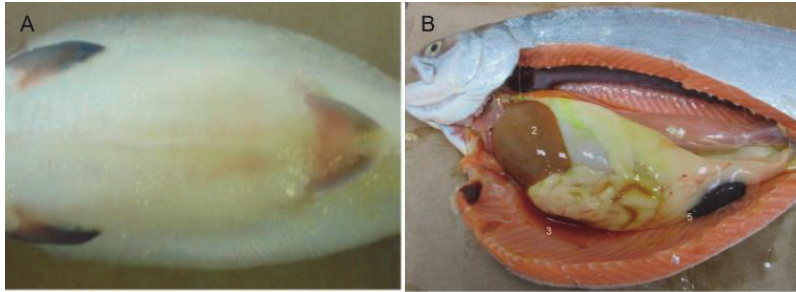


Figure 10. Coho salmon affected with jaundice syndrome characterized by (A) Yellowish abdominal part (B) pale, liver, yellow abdominal fat with bloody ascitic fluids. Modified images from (64).

1.3.4. Erythrocytic inclusion body syndrome (EIBS)

Erythrocytic inclusion bodies syndrome (EIBS) is a severe anemic disease that occurs frequently in coho salmon farms in Japan. Whole genome sequencing and experimental infection confirmed the causal relationship of PRV-2 with EIBS in coho salmon (65). The disease EIBS was first reported from yearling Chinook salmon at a fish hatchery in Washington, USA in 1982 (66). Import of eggs from the EIBS positive area has been suspected as the source of this disease in Japan (67), however, PRV-2 has never been reported from North-America. The expression EIBS has often been used to describe conditions where inclusions in erythrocytes is a prominent finding. Salmonid species differ in susceptibility for EIBS development, with rainbow trout being the least susceptible in the *Oncorhynchus* genus along with low affinity in the brook trout and brown trout, but Atlantic salmon showed a tendency to develop EIBS (68-70). High mortality is reported in farmed Atlantic salmon in Ireland (71), whereas EIBS like inclusions have been detected in wild Atlantic salmon in Scotland (72). Apart from low hematocrit level and inclusions, necrosis in the heart (ventricle and atrium) and yellow colored liver are observed in histopathological examination (73, 74).

1.3.5. HSMI-like disease

An HSMI like disease outbreak was reported in rainbow trout farms in Norway in 2013. Viral sequences related to PRV was identified. Phylogenetic analysis later confirmed a new PRV variant, which was named PRV-3 and shown to be the etiological agent of an HSMI-like disease in rainbow trout (75, 76). This disease shows resemblance with HSMI

regarding pathological changes, such as the heart lesions, necrosis of red skeletal muscle and liver. But infected rainbow trout also show anemia which is not a characteristic of HSMI.

1.3.6. Proliferative darkening syndrome (PDS)

Proliferative darkening syndrome (PDS) is a serious disease in brown trout (*Salmo trutta fario*) that can cause 100% mortality in affected geographical areas in Central Europe. It is also named as “black trout phenomenon” because the diseased fish develop a dark pigmentation. Besides the sub-cutaneous black spots, other clinical signs are apathy and elevated respiratory rates. Pathological lesions include hepatic hemorrhages, enlargement of spleen and ascites (77). PRV-3 was identified, by next generation sequencing, in the infected brown trout and was suggested as the causative agent for PDS (78). However, this has been refuted after detection of severely diseased fish without PRV-3 infection (79).

1.4. PRV-1 target cell types

1.4.1. Erythrocytes

Red blood cells (RBCs) comprise a large part (98-99%) of the blood cells in teleost fish (80). Mature teleost RBCs are ellipsoidal, nucleated and of different sizes (6.9-17.1 μm) with a life span of 13-500 days. The size of erythrocytes are inversely related to the aerobic swimming pattern in teleost fish species (81). The amount of erythrocytes is linked with age, nutrition, environmental and seasonal conditions such as temperature, amount of dissolved oxygen level in the water, pH and salinity (82-84). The vital function of RBCs is the gaseous exchange of oxygen and carbon dioxide (85). Additionally, it is speculated that piscine RBCs have an active role in the immune responses during infections (86). Head kidney is the main organ for the proliferation of erythroid precursor cells (erythropoiesis) which generate new erythrocytes. Spleen pulp can compensate with release of new erythrocytes during anemia (87). The major target cells for PRV-1 are erythrocytes, and the majority of erythrocytes can be infected with PRV-1 during peak of infection (88). The nucleated piscine erythrocytes are permissive for

viral replication. PRV has resisted any propagation in cell lines, but can be cultivated *ex vivo* in RBCs of Atlantic salmon (89).

1.4.2. Cardiomyocytes

The teleost fish heart is one of the earliest developed organs during embryogenesis in higher vertebrates (90). Classically, the piscine heart comprises of four chambers i.e. the sinus venosus, atrium, ventricle and conus arteriosus (also called bulbus arteriosus) (91). Ventricular chambers are divided into two layers i.e. the trabeculated (spongy) layer and an outer compact layer (compactum). Proliferation of cardiomyocytes is the main source of heart growth. Teleost fish have a relatively efficient regeneration mechanism associated with largely undiscovered molecular mechanisms (92, 93).

In addition to HSMI, various viral infections in Atlantic salmon result in heart diseases such as in cardiomyopathy syndrome (CMS) and pancreatic disease (PD).

1.4.3. Myocytes

Atlantic salmon skeletal muscle tissue is composed of striated, long sheets of myotomes. Intramuscular connective, adipose and vascular tissues are also constituents in addition to muscle fibers. Locomotor muscle fibers are categorized into red and white muscle fibers. Red muscle fibers make up for 10% of the myotomal musculature and are enriched with capillary supply and aerobic energy metabolism (94). These are also called “slow fibers” and work during sustained movement ability. Whereas white muscle fibers, that compose 70% of the skeletal muscle tissue, are called “fast fibers” for their fast start burst swimming pattern and are poorly vascularized (94). In HSMI, PRV-1 causes inflammation in the red skeletal muscle with moderate necrosis of the myocytes (11).

1.4.4. Macrophages and melano-macrophages

Macrophages have versatile roles in coping with infections and maintaining a homeostatic environment. Macrophages can rapidly phagocytose pathogens and inactivate them through production of substances such as reactive oxygen species (95). Polarization of macrophages into M1 type macrophages is linked to expression of pro-inflammatory cytokines (IL-1 β , IL-6, IL-12 and TNF- α) (96), lipid mediators and

chemokines for initiating the adaptive immune response, In contrast, M2 type macrophages express anti-inflammatory cytokines such as IL-10, inducing tissue healing and repair (97, 98). Melano-macrophages are cells characterized with high amounts of melanin, lipofuscin or hemosiderin, found in the poikilotherm species (99). In teleosts, these cells reside in the head kidney and spleen in clusters called melano-macrophage centers (MMC). These cells can also be found in inflamed tissues (100). Macrophages and melano-macrophages stain positive for PRV-1 in Atlantic salmon in chronic inflammatory white muscle tissue (10).

1.4.5. Hepatocytes

Liver is a multifunctional organ in teleost fish and is often a target for viral infections. HSMI affected fish from experimental challenge or field outbreaks show low numbers of PRV-1 infected hepatocytes, indicating that hepatocytes in Atlantic salmon, compared to other cell types, do not seem to be particularly permissive for PRV-1 (59, 101). On the other hand, PRV-1 is associated with jaundice syndrome in farmed Chinook and coho salmon, where virus positive hepatocytes can be found. However, hepatocytes are pivotal in detoxification, and virus positive cells could be a secondary effect of anemia due to destruction of erythrocytes and not a primary infection of hepatocytes as such (59).

1.4.6. Enterocytes

Enterocytes are the intestinal absorptive epithelial cells, lining the inner surface of the intestine. Cytoplasmic detection of PRV-1 positive enterocytes has been demonstrated in HSMI diseased fish (59). This supports the suggested oral-fecal as a route of transmission of PRV-1 (53).

1.5. Innate and adaptive immunity against PRV-1 infection

Teleost fish have an immune system to cope with the wide variety of infectious agents of the aquatic environment. PRV-1 is one of the most common virus-infection in sea-water reared Atlantic salmon. The mucosal surfaces are the first barrier that the virus must pass.

PRV-1 is thought to bind the target cell by $\sigma 1$ cell-attachment protein (13), followed by the internalization of the virus particle into the early endosomes as in MRV (40). Cellular sensing mechanisms are set up to detect pathogen specific molecular patterns (PAMPS), among which the dsRNA nucleic acid is the most important for viruses, by the endosomal pattern recognition receptors (PRRs) (102). In fish, PRRs such as toll-like receptor 3 (TLR3) in the endosomes, and cytoplasmic RIG-I and melanoma differentiation associated gene (MDA5) recognize viral nucleic acids, including dsRNA (103, 104). Stimulation of PRRs induces various cascade signaling pathways. For viruses, and RNA viruses in particular, the type I interferons (IFN) have a central organizing position in the innate antiviral response in vertebrates (105). IFNs induce an antiviral state by inducing signaling pathways via type I IFN receptor to regulate interferon stimulated genes (ISGs). ISGs are related to elimination of viral components, apoptosis and protection of non-infected cells (106). The complexity of the innate response is vast, but proteins with general antiviral activity such as Myxovirus protein (Mx), virus inhibitory protein (viperin) and protein kinase RNA-activated (PKR) are induced (107, 108). IFNs upregulate myriads of proteins including the antigen-presentation of MHC type I, which is followed by activation of macrophages, cytotoxic T cells and NK cells (109).

Piscine erythrocytes are nucleated, and sensing of pathogens cause induction of an innate antiviral response with elevated expression of antiviral effector genes (110). Transcriptomic analyses performed on purified erythrocytes infected with PRV-1 have demonstrated downregulation of erythrocyte cellular proteins but several genes that potentially are involved in translational shutoff and inhibition of reovirus replication are upregulated (PKR, Viperin, ISG-15) (111). Viral mRNA translation is maintained as compared to the blocked cellular translation due to the activation of PKR and phosphorylation of eukaryotic initiation factor eIF2 α (107, 112, 113). PRV-1 isolates from Canada are not able to induce innate antiviral responses in Atlantic and Sockeye salmon that indicates differences in hosts immune response or it could be due to differences in the viral virulence (114).

Orthoreoviruses, including PRV-1, evades the innate immune response by limited exposure of viral genomic dsRNA during the replication cycle. The transcription of viral mRNA occurs in the incoming core particle and the only viral RNA free in cytoplasm is viral mRNA, which initiates translation (115). Furthermore, the new plus strand of viral genomic RNA, which is identical to the viral mRNA, is packed in a capsid before the complementary negative strand is synthesized. This way, in a successful viral replication, viral dsRNA are never exposed in cytoplasm and the dsRNA recognizing PRRs in the cytoplasm i.e. RIG-1 or MDA5 are not induced (115). Furthermore, the PRV $\sigma 3$ protein that is released into the cytoplasm from the outer capsid layer during the fusion process with the endosomal membrane binds with dsRNA (30), and thus also contributes to inhibit the innate immune response.

Adaptive immune responses, both humoral and cellular, are mounted in Atlantic salmon against PRV-1 infection. IgM is the most dominant antibody isotype present in fish compared to the IgD and IgT class (116), and teleost fish lack isotype switching of immunoglobulins (117, 118). PRV-1 specific antibodies against $\mu 1C$, μNS and $\sigma 1$ have previously been detected in experimental challenge studies (119, 120). Peak specific IgM level in plasma corresponded in time with the decline in myocardial inflammation (119). Immunohistochemical detection shows a wide distribution of CD8⁺ cytotoxic T cells (CTLs) in HSMI affected heart (121). CTLs are involved in killing of virus-infected cells through detection of viral peptides presented in MHC-I on the infected cell surface (122, 123), followed by production of granzymes and perforins to induce apoptotic responses causing cell death (124, 125). Increased expressions of CD8 and granzyme are observed in spleen after PRV-1 infection (126). Transcriptomic analysis of heart tissue with HSMI also suggest presence of macrophages, T helper cells and B cells (121, 127). Upregulation of chemokine CCL19/MIP-3 β in spleen is detected after PRV-1 infection (126), that has a function to attract dendritic, T- and B cells.

1.6. Macrophage response in inflammation

Tissue macrophages originate during embryonic development and partly from circulating monocytes. (128). Macrophages are one of the first lines of cells involved during inflammatory responses. Type II interferon (interferon gamma) (IFN- γ) may

activate macrophages in teleost fish (129). Type I IFNs are mainly responsible for expression of ISGs while IFN- γ reinforce and coordinate antiviral mediated effects (129). Although IFN- γ can be expressed by various immune cells, the T lymphocytes subset T-helper 1 (Th1) cell population produce it to activate and polarize macrophages to the M1 type (Figure 11) (129, 130). M1 type macrophages can be induced by both stimulation of PRRs or by INF- γ (131). The inflammatory M1 macrophages induce iNOS2 expression and elevates antigen presentation. iNOS2 produce nitric oxide, which is a reactive free oxygen radical with antimicrobial activity. M1 polarized macrophages have the capacity to kill ingested pathogens while producing pro-inflammatory cytokines such as TNF- α , IL-1 β and IL-6 (98).

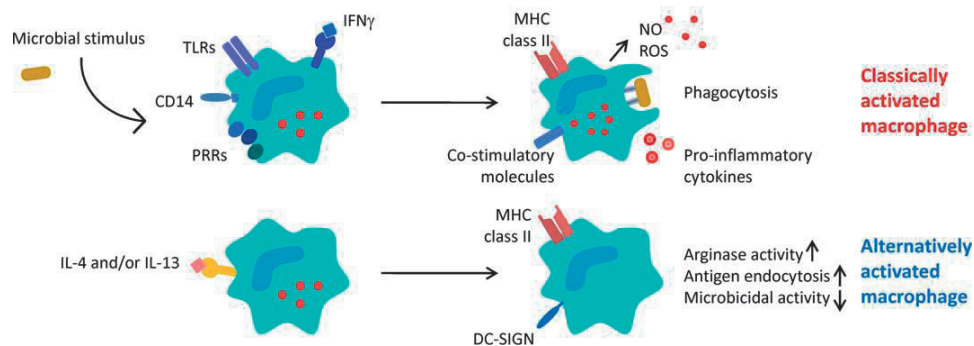


Figure 11. Polarization of macrophage phenotypes in fish. Illustration shows activation of classically activated (M1) and alternatively activated (M2) macrophage populations under microbial infection and inflammatory conditions. Picture modified from (131).

On the other hand, anti-inflammatory cytokine production from T-helper 2 (Th2) cells alters the phenotype of macrophages to the so called M2 type, with increased arginase (Arg2) activity and production of extracellular matrix and polyamines (130). The presence of M2 macrophages indicates an anti-inflammatory microenvironment and tissue repair process. It is worth noting that M2 macrophages can counter-balance the M1 macrophage activity by upregulating Arg2 that will convert the L-arginine to L-ornithine and urea, whereas L-arginine is the main substrate of iNOS2 enzyme which is converted into L-citrulline. M2 macrophages are further categorized, based upon the source of stimulation including other factors such as parasites infestation, CSF-1 or IL-10, but IL-4/-13 forms the best characterized M2 macrophages. Arg2 presence is

defined as a marker of M2 macrophages in teleost fish (98). The macrophage dichotomous paradigm is dependent on arginine metabolism, which is highly conserved in fish (132).

1.7. Persistent viral infections in salmonids

Persistent viral infection follows when the host is unable to clear an acute infection (Figure 12) (133). Virus-host interplay is largely dependent on specific immune responses after the acute phase. Persistent infections can be non-productive (latent infections), as they are for herpesviruses, or productive as they are for retroviruses (134). The pattern of persistence varies among viruses, but common features for maintaining the viral activity for long periods include infection of subsets of long lived cells to protect the viral genome, avoid induction of apoptotic pathways, bypass specific immune responses and modulation of the viral gene expression (134). Inefficient immune responses and viral evasion facilitates viral persistence.

Although teleost fish generates specific immunity against a foreign antigen such as a virus, lack of antibody class shift and increased affinity maturation limits the neutralization of viruses and hence provide partial protection (116). Fish is more dependent on innate responses than mammals are (135). Viral carrier states or persistence are not very well explored in fish, but persistence is a common outcome of virus infections of fish. PRV-1 infects macrophage-like cells in the Atlantic salmon, and chronic infections associated with melanized focal changes are reported (10). PRV-1 was reported to persist for at least 59 weeks post challenge in western north America but fails to produce HSMI disease in the sentinel fish (114). An IFN type I response is induced in the infected fish, but PRV is still produced at high levels (111). On the other hand, PRV-3 infects rainbow trout but gets cleared off (75), which indicates that the host-virus interplay is an important factor for persistent infections. IPNV replicates in the head kidney macrophages and persists in different salmonid species (136-138). Vaccination against IPNV did not hinder viral carrier states in the fish (139). Anti-inflammatory cytokines, e.g. IL-10, can indirectly promote persistence as it suppresses pro-inflammatory cytokines (140). IPNV infected tissues show a low number of apoptotic cells (141), indicating that differentiated macrophages are not prone to

apoptotic signaling which facilitates persistent infection. Viral clearance is not absolute in persistent infections, like SAV infection in Atlantic salmon. It is likely that an infected fish becomes long-time carrier. SAV persistence is reported after several months in the gills, heart and pancreas (142). Recurring outbreaks of salmon gill poxvirus (SGPV) in Atlantic salmon farms are also reported, suggesting a possible viral reservoir and reactivation of the virus after acute infection (143). Viral hemorrhagic septicemia virus (VHSV) and Infectious hematopoietic necrosis virus (IHNV) produce persistent infections in salmonids and infect macrophages and hemopoietic area comprising precursor cells in the head kidney respectively (144-147).

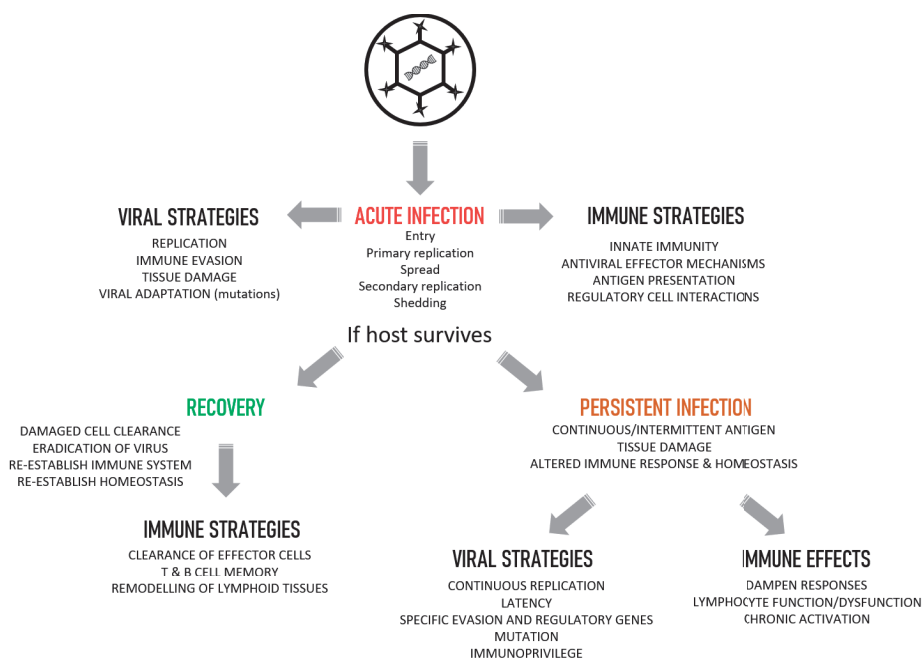


Figure 12. Illustration of a course of viral infection from acute to persistent phase. Acute phase is mostly dominated by viral replication, and cellular and tissue damage. Depending upon the immune response from host, either the host is recovered from the antigen by targeted elimination of the virus or acute infections develops into chronic/persistent infection with prolonged viral effects depending upon viral species. Picture modified from (148).

1.8. Vaccination against HSMI

Vaccination can be an efficient tool to control an infectious disease. For farmed Atlantic salmon, many bacterial diseases are controlled by vaccination, but viral diseases still pose a huge threat for the industry. For several vaccines against viral diseases in mammals, protection is correlated with the specific antibody level (149), but specific antibodies do not always indicate a protective response. Inactivated vaccines has induced neutralizing antibodies in other viral infections in salmonids, e.g. Salmonid alphavirus (SAV) (150). For SAV and Infectious pancreatic necrosis virus (IPNV) infections, it is observed that inactivated vaccines do not reduce the number of disease outbreaks (151, 152). The protective immune response against HSMI is not known. In a previous study, PRV-specific IgM appeared at about the same time as a significant drop in the myocardial inflammation (119). Partial protection against PRV was demonstrated by applying an inactivated vaccine based on purified virus particles. This vaccine protected only the vaccinated individuals when they were exposed to PRV by i.p. injection, and to a lesser degree when PRV were administrated through addition of infected shedder fish (153). A DNA vaccine expressing non-structural and structural proteins showed moderate protection against HSMI (154). The limited protection seen after cohabitant exposure using inactivated whole virus vaccination or DNA vaccination, suggest that alternatives such as attenuated live vaccines should be tested for protection against HSMI.

2. Aims

Main Objective

The **aim of the project** was to study viral and immunological mechanisms of PRV1 persistence in Atlantic salmon.

Sub-goals

1. Study PRV-1 kinetics and infected cell types in the persistent phase of infection in Atlantic salmon. The hypothesis was that the in-host reservoir of persistent PRV-1 is infection of long living cells.
2. Study the role of polarized macrophages and cell mediated immune response versus PRV-1 infection in HSMI and in black spot formation.
3. Study if a live attenuated virus vaccine could give effective protection against PRV-1 infection and HSMI. The hypothesis was that PRV-2 or PRV-3, which are naturally attenuated in Atlantic salmon, could provide protection.

3. Summary of papers

Paper I:

Erythroid progenitor cells in Atlantic salmon (*Salmo salar*) may be persistently and productively infected with Piscine orthoreovirus (PRV)

Muhammad Salman Malik, Håvard Bjørgen, Kannimuthu Dharmotharan, Øystein Wessel, Erling Olaf Koppang, Emiliano Di Cicco, Elisabeth F. Hansen, Maria K. Dahle, Espen Rimstad

In this study, PRV-1 was investigated in various organs and tissues from experimentally challenged Atlantic salmon for a period of 18 weeks. PRV-1 was found to be actively transcribing which contrasted the low level of viral proteins. Differential expression pattern of PRV-1 segments was not observed, as RNV levels indicated homogenous transcription of segments belonging to large (L), medium (M) and small (S) class. Comparison of genomic dsRNA and PRV-1 ssRNA transcripts was performed to understand viral activity in different organs. Detection of intact PRV-1 particles with genomic dsRNA in plasma showed viremia in the fish at all timepoints. The relative abundance of viral ssRNA showed that kidney is a more active site for the viral transcription in the persistent phase of the infection than blood cells are. *In situ* hybridization assays i.e. singleplex and duplex, confirmed that PRV-1 is capable of targeting erythrocytes, macrophage colony-stimulating factor receptor (MCSFR) positive macrophages and melano-macrophages along with long living erythropoietin receptor (EPOR) positive erythroid progenitor cells in the kidney. In addition, some uncharacterized cell populations which are positive for PRV-1 are yet to be mapped. Altogether, PRV-1 establishes a productive and persistent infection in Atlantic salmon.

Paper II:

M1 polarized macrophages in red and black spots in white muscle of Atlantic salmon (*Salmo salar*) are PRV-1 infected and cause a pro-inflammatory environment.

Muhammad Salman Malik, Håvard Bjørgen, Ingvild B Nyman, Øystein Wessel, Erling O Koppang, Maria K Dahle and Espen Rimstad

Melanin spots in white skeletal muscle represent a major problem in sea farmed Atlantic salmon. Piscine orthoreovirus-1 (PRV-1) is associated with the condition, but the etiology of the focal changes is unclear. There are indications that the spots start as muscle bleeding and muscle necrosis (red spots), which can develop into chronic granulomatous changes, which appear as melanized focal areas (black spots). In the granulomatous melanized changes, PRV infection and associated inflammation are important contributors to the changes, but both red and incipient black spots occur in PRV-1 negative fish as well. In this study, we looked at the relationship between PRV infection and the development of melanized focal changes. Fluorescent in situ hybridization (FISH) analysis showed co-localization in the same cells of iNOS2 mRNA, i.e. activated, pro-inflammatory macrophages (M1 phase) with PRV-1 in red spots. In black spots, we found co-localization with PRV-1 in both M1 and M2 macrophages and melano-macrophages. M2 is associated with wound healing and tissue repair, characterized by high levels of Arg2 transcripts. Melano-macrophages positive for Arg2 mRNA were found in the late phase of red spots, indicating the transformation of a red spot into black spot when melano-macrophages were abundant. There were very low levels of cells with M1- and M2-specific transcripts in spots in PRV-negative fish, indicating that inflammation caused by PRV infection in the spots is a driver of the melanization in the focal changes. Cells with transcripts specific for melanin production were found in early-stage non-melanized cells and in late-stage melano-macrophages. The function of the melanoma macrophages is disputed, and why the cells produce melanin are not fully understood. This study reveals new properties of the pathogenesis of focal melanized changes, as well as for the melano-macrophages.

Paper III:

Dynamics of polarized macrophages and activated CD8+ cells in heart tissue of Atlantic salmon infected with Piscine orthoreovirus-1.

Muhammad Salman Malik, Øystein Wessel, Ingvild B Nyman, Maria K Dahle and Espen Rimstad.

PRV-1 infection causes heart and skeletal muscle inflammation (HSMI) in Atlantic salmon. In this study the inflammatory microenvironment in heart and skeletal muscle during development of HSMI was characterized. Heart and skeletal muscle tissues with characteristic HSMI lesions showed presence of polarized M1 and M2 macrophages. M2 macrophages were prominently distributed in the heart, but to a lesser degree in skeletal muscle tissue. PRV-1 did not co-localized with widely distributed M2 macrophages surrounding the infected cardiomyocytes in the heart. M1 macrophages were low in number and moderately co-localized with PRV-1 in both heart and skeletal muscle. PRV-1 was confirmed in MHC-I expressing cells in the heart tissue, and interacted with CD8+ cells expressing granzyme A. Skeletal muscle tissue did not pose a strong MHC-I/CD8+ cellular response as compared to heart. MHC-I and CD8+ cells were dispersed in between myocytes but did not overlap with PRV-1 staining. Gene expression analysis validated the *in situ* findings of the immune markers and showed that PRV-1 levels dropped after the increase in the cell mediated immune response in heart and skeletal muscle tissues.

Paper IV:

Piscine orthoreovirus (PRV)-3, but not PRV-2, cross-protects against PRV-1 and heart and skeletal muscle inflammation (HSMI) in Atlantic salmon (*Salmo salar*)

Muhammad Salman Malik, Lena H. Teige*, Stine Braaen, Anne Berit Olsen, Monica Nordberg, Marit M. Amundsen, Kannimuthu Dhamocharan, Steingrim Svenning, Eva Stina Edholm, Tomokazu Takano, Jorunn B Jørgensen, Øystein Wessel, Espen Rimstad, Maria K Dahle*

Immunization strategies against HSMI, including an inactivated whole virus vaccine and a DNA vaccine, have been experimentally tested previously but only shown to provide partial protection. So far, no vaccine has induced full protection against PRV-1 infection and HSMI, and none are commercially available. PRV-3 has previously been shown to replicate in Atlantic salmon, but without causing cardiac pathology. In this study, we aimed to test whether infection with PRV-2 or PRV-3 could provide effective protection against subsequent PRV-1 infection and HSMI. During the immunization period, PRV-2 and PRV-3 viral kinetics and production of cross-reactive antibodies against the PRV-1 $\sigma 1$ protein were studied, as well as the ability of PRV-2 or PRV-3 infection to transmit to naïve Atlantic salmon. PRV-2 replicated for a limited time at low levels, while PRV-3 replicated more effectively in Atlantic salmon. None of the viruses gave pathological findings or infected cohabitant fish between 5 and 10 weeks after injection. PRV-3 infection yielded high levels of antibodies that bound to PRV-1 $\sigma 1$, while PRV-2 infection did not. Ten weeks after PRV-2 or PRV-3 immunization, fish were infected with PRV-1 through cohabitation with shedder fish. It was found that both inactivated PRV-1 vaccine and PRV-2 infection provided partial protection against PRV-1 and HSMI, while PRV-3 blocked secondary PRV-1 infection and HSMI development totally. Although the safety aspect of infecting Atlantic salmon with PRV variants that cause disease in other salmonids makes this type of immunization disputed, but this shows a clear potential for the use of attenuated viruses for vaccination. Such studies can also be used to uncover the mechanisms involved in protection.

4. Results and general discussions

4.1. PRV-1 establishes a productive and persistent infection in Atlantic salmon

Establishing the causal relationship between PRV and HSMI has led to a series of investigations and research exploring the infection kinetics in the host and primarily the acute phase that lasts for approximately 4-6 weeks after infection. PRV has the potential to infect piscine nucleated erythrocytes efficiently in the initial acute phase (88). In the first paper we performed an experimental challenge study by inoculating PRV-1 NOR2012 isolate in fish intraperitoneally (i.p.) and followed the infection for 18 weeks to study the infection kinetics both in the acute and persistent phase. The expression of PRV segments L, M and S classes were studied to see if significant differential expression of genomic segments were linked to the persistent phase. Results showed homogenous expression of all segments analyzed, i.e. L1, M2, M3, S1, S2 and S3. Almost identical patterns for each segment were detected both in the acute and persistent phase. A Canadian PRV-1 isolate has also shown resemblance with respect to similar segment expression with minor proportional variations among them (155). Spleen tissue showed higher PRV levels at the peak time point compared to the blood cells, indicating aggregation of damaged blood cells, and *in situ* hybridization of the red pulp of the tissue confirmed this (from paper I).

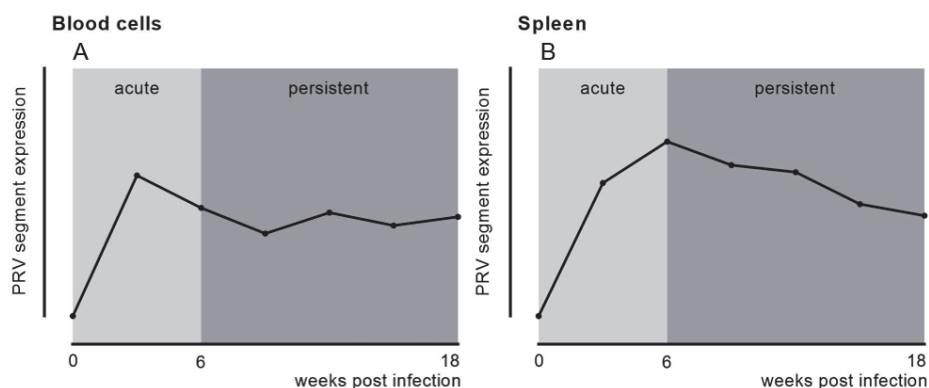


Figure 12. Homogenous segment expression of PRV-1 belonging to L, M and S class (mean trend line) in blood cells and spleen during experimental challenge study.

Double stranded genomic RNA (dsRNA) and single stranded viral transcripts (ssRNA) of PRV-1 were differentially detected by omitting the denaturation step in the RT-qPCR analysis. Different organs including blood cells and isolated plasma, spleen and kidney were screened for RNA levels of PRV-1. The results showed that ssRNA viral transcripts were higher in the kidney tissue compared to organs in the persistent phase and thus indicates kidney as the most active site for transcription to make a possible reservoir (Figure 13A). Moreover, PRV-1 viremia (virus particles in plasma), indicated by dsRNA in plasma, was detected at all timepoints (Figure 13B). ssRNA, i.e. viral mRNA, were detected in the plasma only at the peak of infection in the acute phase, i.e. the time with highest viral load and possible leakages from destroyed blood cells due to acute infection. dsRNA detection in plasma indicated that PRV-1 is continuously producing intact viral particles in the persistent phase, and that these are not immediately removed by the immunoglobulins produced by humoral response established after the acute infection. It cannot be disregarded that PRV-1 particles in the plasma could be present in extracellular vesicles that can shield the virus from antibody binding (156, 157). Fecal-oral route of transmission is suggested both in PRV-1 and MRV and other reoviruses such as rotaviruses which are also released from the cells in vesicles (53, 158, 159).

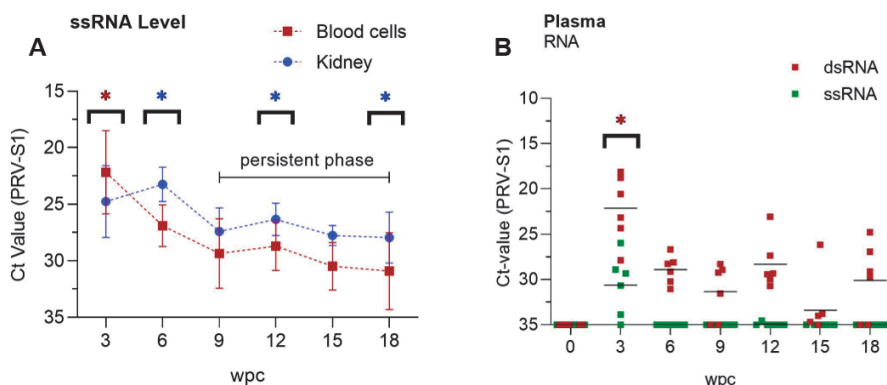


Figure 13. RT-qPCR analysis showed PRV-1 level in different organs during the acute and persistent phase. (A) PRV-1 is relatively higher in blood cells in acute phase but significantly higher in kidney from 9 wpc to 18 wpc (persistent phase). (B) PRV-1 dsRNA in plasma (red) indicating continuous production of viral particles. Asterisk sign (*) shows significant difference between fish groups at each time point (from paper I).

The PRV-NOR2012 isolate originated from an HSMI outbreak in Norway and has been used in other studies to reproduce HSMI experimentally (9). Viral shedding is often associated with the potential to transmit the virus to other hosts and spread the disease. PRV-1 virulence is linked to the evolutionary changes of the genome leading to the ability to cause HSMI (160). Canadian PRV-1 isolates do not produce HSMI related lesions to the same extent as many Norwegian isolates (155). Moreover, persistently infected fish (at least 41 weeks) do not cause viremia (it is still a possible technical issue about this) and have not the ability to spread the virus to cohabitant fish (114). High virulent strains of PRV-1 are associated with higher plasma viremia compared to non-virulent strains (60).

There is a contrast between PRV-1 transcriptional activity and detection of viral proteins during the persistent phase of infection. Outer capsid proteins $\sigma 1$ and $\sigma 3$ were detected in the blood cells until 3 weeks post challenge and not thereafter in this challenge study in line with previous studies (29). Cellular translational activity can be partly blocked that can halt the viral protein expression as described for mammalian reoviruses (161). Phosphorylation of eukaryotic translation initiation factor (eIF2 α) during innate immune response by the activated protein kinase (PKR) is considered a key factor for the inactive state of the cell (162, 163).

4.2. PRV-1 infects erythroid and macrophage lineage cell population

During the course of HSMI, PRV-1 infects blood cells and cardiomyocytes. However, PRV-1 has also been associated with the development of melanized focal changes in the Atlantic salmon, and is reported to infect mononuclear macrophage-like cells and pigmented melano-macrophages (10, 62).

The PRV-1 level is higher in the kidneys and spleen tissues compared to the heart tissue during the persistent phase. ISH assays showed PRV-1 in peritubular macrophage-like cells in the head kidney region (Figure 14A). This PRV-1 localization pattern was consistent from early time points until the end of the experimental trial, indicating that

these types of cells are prone to long-term infection with PRV-1. Similarly, the virus was also found in macrophage-like cells in the spleen (Figure 14B). The virus was heavily localized to the red pulp of the spleen during the acute phase which are special sites for antigen trapping (164, 165). Functional antibodies can form immune complexes in the blood plasma after binding to antigens that can be eliminated in the spleen (165). But a steady level of PRV-1 after the peak phase in blood indicates that PRV-1 is actively replicating and persists in cell populations without the host being able to clear it.

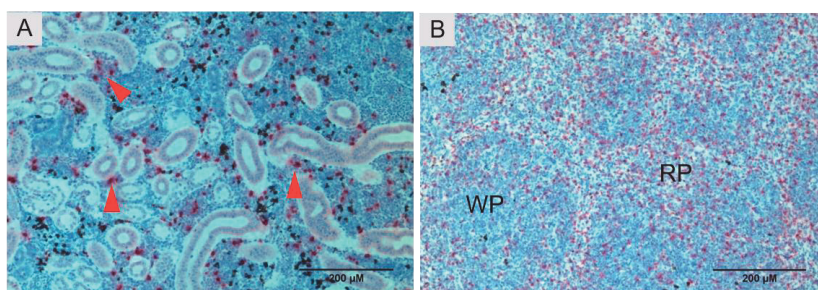


Figure 14. Localization of PRV-1 (red) in renal and splenic macrophage-like cells (*from paper 1*).

Cellular localization of PRV-1 was analyzed via duplex ISH detection, obtaining the identification of specific cell types infected by the virus. Localization of PRV-1 specific staining was noticed in MCSFR positive cells in kidney and spleen (Figure 15). Melanomacrophages were also sporadically positive for PRV-1 staining. MCSF is responsible for inducing proliferation and differentiation of macrophages in teleost fish through a transmembrane receptor known as macrophage colony stimulating factor receptor (MCSFR) (166). In higher vertebrates such as mammals, MCSFR is considered to be a marker for M2 polarized macrophages (167). In teleost fish, macrophage colony stimulating factor (MCSF) is also associated with a polarized macrophage population defined as M2c (98). They are also referred as regulatory macrophages with a main function to suppress Th1 immune response (98, 131). MCSFR positive cells represent an anti-inflammatory macrophage phenotype, but recent data suggests that arginase enzyme activity is a more specific marker of M2 polarized macrophages (98, 131). Continuation of the viral lifecycle is the utmost requirement to establish a persistent infection. Cells with properties of long life spans such as macrophages are attractive cells for viral reservoirs (168). ARV is also reported to replicate in macrophages for a

productive infection (169). High virulent strains have an increased tendency to replicate in macrophages (35).

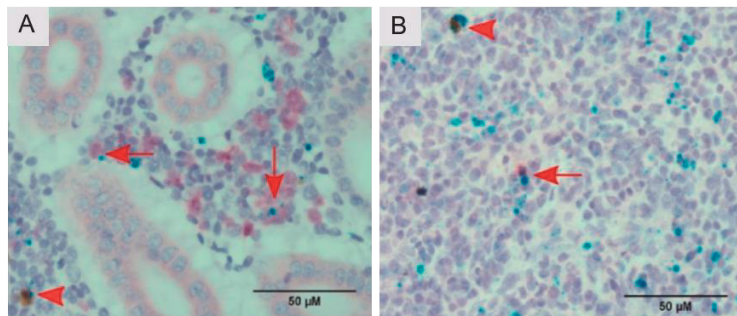


Figure 15. Co-localization of PRV-1 (green) in MCSFR (red) positive M2 macrophage phenotype (arrows) and some melano-macrophages (arrowheads) in (A) kidney and (B) spleen in the persistent phase (*modified from paper-1*).

Erythropoietin (EPO) protein is primarily responsible for proliferation and synthesis of circulatory erythrocytes to maintain enough oxygen supply to the tissues. Regulation of erythropoiesis is tightly controlled in hypoxic and anemic conditions via its cognate receptor i.e. EPOR. ISH was performed to identify EPOR positive erythroid progenitor cells in the head kidney (Figure 16). PRV-1 nucleic acid was detected in erythrocyte precursor cells sporadically in the hemopoietic tissue region, suggesting viral tropism in these long-lived cells. PRV-1 is not known for causing anemic conditions in Atlantic salmon, but permissiveness to EPOR positive cells points to the infection of newly synthesized young erythrocytes, which can be released to the circulation at any time. In the persistent phase, heart tissue shows significantly low number of PRV-1 positive cells or none at all, but it is worth noting that PRV-1 positive cells are still detected in the peripheral blood supply throughout the persistent phase. JAM-A is expressed both in endothelial and hematopoietic cells in mammals and MRV disseminates into the blood stream and cause viremia only after infection of JAM-A expressing endothelial cells, but not hematopoietic cells (170). Therefore, PRV-1 spread in the blood supply could be dependent on the distribution of specific receptors on cells involved in viral entry and infected erythroid progenitor cells could serve as long-term reservoir.

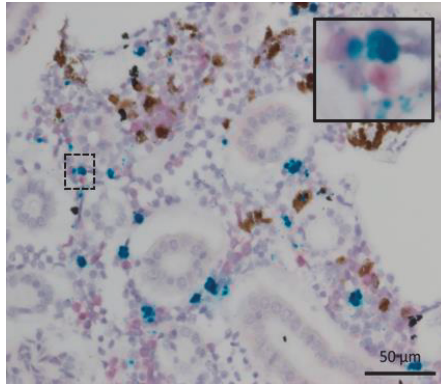


Figure 16. PRV-1 (green) is co-localized in erythroid progenitor cells (red) in the head kidney of Atlantic salmon.

4.3. PRV-1 is associated with macrophage polarization in melanized focal changes and HSMI.

HSMI is the consequence of an acute PRV-1 infection with high virus titers in blood preceding cardiac and skeletal muscle lesions (9). Thereafter, PRV-1 persists for a long period of time, perhaps life-long in surviving fish. PRV-1 is also present in the chronic pathological changes of melanized spots in Atlantic salmon. Ubiquitous presence of PRV-1 in sea water results in high prevalence of both these pathological conditions among farmed fish (171).

The macrophage response was characterized in paper II and III in chronically PRV-1 infected fish with red and black spots and in the peak phase of HSMI. The results showed that PRV-1 infection is associated with polarization from M1 to M2 in the process of black spot development (Figure 17). Red spots have a significant upregulation of iNOS2 expression and the iNOS2 expressing M1 macrophages were also positive for PRV-1 transcripts during early and intermediate phases as shown by FISH technique. This indicates involvement of these cells in the pathogenesis of the spots. Type II IFN (IFN- γ) can activate and polarize macrophages into the M1 phenotype, which phagocytose and inactivate pathogens by actions of nitric oxide (NO) and reactive oxygen species (ROS) (172, 173). Melanized focal changes or black spots, defined by their macroscopic presentation in white musculature of Atlantic salmon, have abundant melanin

containing cells (10). High expression of iNOS2 is linked with high melanin production in melanocytes in mammals (174), and therefore it is highly likely that activation of the classical M1 macrophage phenotype with high iNOS2 expression is linked to melanin production in Atlantic salmon. Whereas a clear contrast is observed to the old black spots, where the iNOS2 expression is reduced and there is a significantly higher arginase-2 (Arg2) level and presence of M2 type macrophages. Arginase-2 specific transcripts were spotted mostly in the melanized area in both melano-macrophages and non-melanized macrophages. IL-4 or IL-13 cytokines are involved in alternate activation of the M2 type phenotype. The M2 type macrophages are involved in resolution of tissue inflammation, regeneration and repair, i.e. healing process. Production of angiogenic substances and polyamines are some of the major functions of these cells (98, 175). Collagen expression with pro-fibrotic factors such as transforming growth factor (TGF- β), vascular endothelial growth factor A (VEGF-A) and insulin-like growth factors are reported for M2 macrophages to suppress inflammation and promote repair (175).

Presence of melano-macrophages at the infected site indicates their role in the tissue repair mechanism. Phagocytosed infected cells have been reported in macrophages and melano-macrophages in other viral infections in Atlantic salmon (176). This study shows that PRV-1 was associated with the pro-inflammatory microenvironment during red spot and early black spot formation and was consistently associated with melano-macrophage detection from the late phase of red spots and onwards.

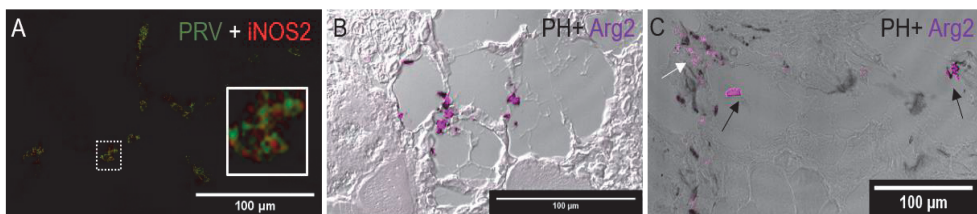


Figure 17. Macrophage polarization (M1/M2) in red and black spots. (A) Co-localization of PRV-1 in classically activated M1 macrophages in intermediate phase of red spot. (B) Detection of M2 macrophages in melanized area in late phase of red spots. (C) Dominance of M2 macrophages in melanized (black arrow) and non-melanized (white arrow) in the black spot (*modified from paper II*).

Pro-inflammatory cytokines generally predominate in acute viral infections (177, 178), but HSMI affected fish groups showed moderate level of M1 macrophages in the heart and skeletal muscle tissue and the M1 cells only partly co-localized with PRV-1 staining. On the other hand, heart tissue had many cells with a pronounced Arg2 expression (Figure 18). Fewer M2 macrophages were seen in the skeletal muscle tissue. The M2 macrophages were scattered in all cardiac layers but did not show co-localization with PRV-1. High Arg2 expression correlates well with the efficient regeneration function of the Atlantic salmon heart (101).

Polarization of M1 macrophages was a prominent finding of back spots formation, but not equally so in HSMI. Upregulated iNOS2 expression is associated with black spot formation, assumably through stimulation of melanin production in melanomacrophages. iNOS2 activity is involved in Grass carp reovirus (GCRV) induced hemorrhages, which is a characteristic pathological phenomenon for GCRV infection in Grass carp, as well as in the induction of apoptosis in vascular endothelial cells (179). We did not find indications that macrophage polarization was important during initial development of HSMI.

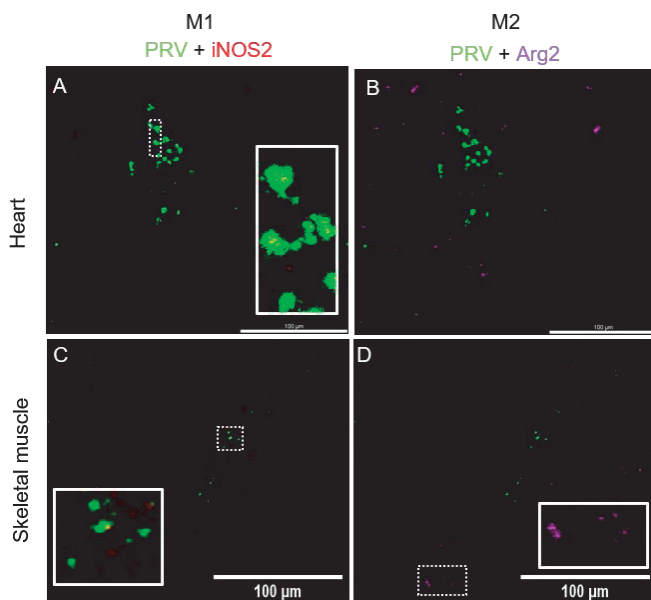


Figure 18. Macrophage polarization (M1/M2) in Heart and skeletal muscle inflammation in Heart (A-B) and skeletal muscle (C-D) (from paper III).

4.4. PRV-3 subtype cross-protects against PRV-1 infection in Atlantic salmon.

Farmed fish undergoes several life-stages and rearing procedures, including artificial sea-water adaptation, light regimes, handling and transportation activities. These potential stressful conditions make the fish more susceptible for opportunistic pathogens. Intensive farming of Atlantic salmon combined with the ubiquitous PRV-1 in seawater pose a threat to fish health. PRV has three identified subtypes i.e. PRV-1, PRV-2 and PRV-3, which produce different diseases in different salmonid species (9, 65, 76). A vaccine approach is tested in paper IV to study the cross protective potential of PRV subtypes i.e. PRV-2 and PRV-3 against PRV-1 infection (Figure 19A).

PRV-3 replicated efficiently in Atlantic salmon and produced high virus titers for 18 weeks of experimental challenge, while PRV-2 replicated less efficiently. During the vaccination trial, cohabitant fish were added to see if PRV-1, -2 and -3 were transmitted to the naïve fish. Only PRV-1 infected fish infected the naïve cohabitant fish. PRV-1 and PRV-3 has higher overall amino acid sequence similarity (90% identity) compared to their similarities to PRV-2 (80% identity) (26). Whereas the cell attachment protein ($\sigma 1$) amino acid sequence of PRV-1 has 82% identity with PRV-3, it has only 67% identity with PRV-2. Dissimilarity among PRVs could be linked to the difference in receptor binding efficiency in their target species, which could possibly be associated with PRV-2 and PRV-3 failure of transmission into the naïve fish. Although PRV-3 did not persist like PRV-1 in Atlantic salmon, the virus nevertheless replicated for at least 18 weeks. This differs from rainbow trout, in which PRV-3 infection is eliminated (76). The assumed natural host for PRV-3, brown trout (*Salmo trutta*), is much closer related to Atlantic salmon than what rainbow trout is. Bead-based immunoassay detected PRV-1 cross-binding antibodies in blood from PRV-3 infected fish, not at high levels, but higher than in PRV-2 infected fish, which is in line with the difference in protection between these two infections. Whereas an inactivated vaccine was used as a control, it did not lead to measurable production of specific antibodies against PRV-1 $\sigma 1$.

Blocking of PRV-1 infection by prior immunization with PRV-3 infection may involve a cell mediated immune response or antiviral immunity, however, this was not indicated

by expression analysis of the immune genes. The protective mechanism would possibly not be solely dependent on cross-binding antibodies. It is possible that protection was present already at the mucosal surfaces. PRVs are not well studied for their route of entrance apart from suggested fecal-oral route for PRV-1 and infection through intestinal wall (53). This indicates that mucosal immunity may have a role in obstructing PRV-1 infection. Live attenuated vaccines may induce mucosal immunity, especially if they are administered at the mucosal surfaces and could be very promising vaccines against PRV-1.

The heart is the main infected organ in acute PRV-1 infection (11) after a prior virus propagation in erythrocytes (9, 89). Histological evaluation showed that HSMI like lesions were completely absent in all fish immunized with PRV-3 (Figure 19B).

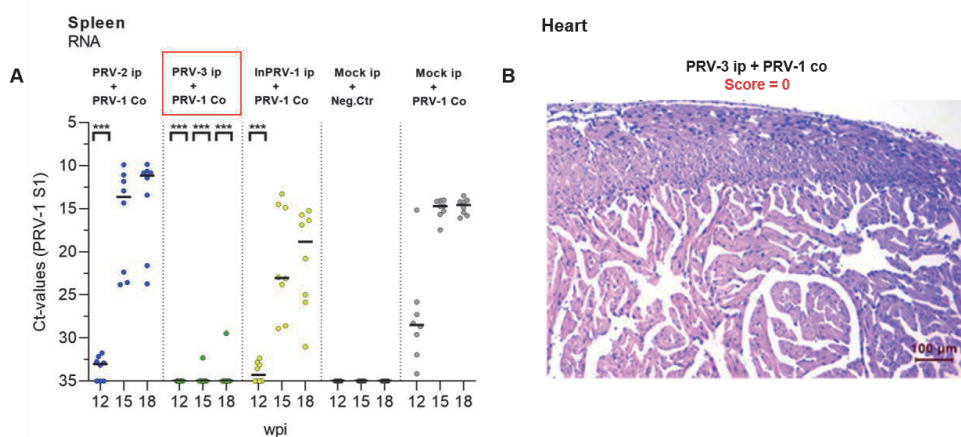


Figure 19. PRV-3 subtype protection potential against PRV-1 infection. (A) PRV-1 level in fish groups immunized with PRV-2, PRV-3, and inactivated PRV-1 vaccine. (B) Histopathological overview of PRV-3 immunized fish heart after PRV-1 shedder fish cohabitants (from paper IV).

4.5. MHC-I and CD8⁺ cells presents specific immune response against PRV-1 infection in Atlantic salmon.

The teleost fish immune system shows a diverse dynamics of innate and adaptive immune responses against viruses (118). Both antiviral and acquired immune responses against PRV-1 infection are explored in various studies to evaluate host-virus

interaction and its ability to eradicate the virus (111, 121, 180). The FISH method was performed to observe PRV-1 localization in MHC-I and CD8 expressing cells during acute infection, HSMI, and chronic inflammatory condition, i.e. red & black spots.

A strong activation of immune genes i.e. CD8 α , GzmA and MHC-I were observed in the HSMI affected heart after the peak phase of experimental PRV-1 infection, at the time of severe histopathological lesions. FISH results showed that PRV-1 co-localize with CD8 cells which were scattered massively in different cardiac layers, however, most frequent in *stratum spongiosum* (Figure 20). Although Granzyme A synthesis is induced in CD8 cells *in situ* analysis also revealed non-CD8 cells with GzmA expression, possibly other immune cells such as natural killer cells. Transcriptional or immunohistochemical analysis performed previously indicated recruitment of T cells in the heart (121, 127), but FISH method allowed us to map localization of the CD8 and MHC-I expressing cell populations to indicate antigen presentation and cytotoxic killing of PRV-1 infected cells. Skeletal muscle tissue showed a relatively low targeted response compared to heart, but the PRV-1 level declines after the cellular immune response in both tissues. The higher PRV-1 infection level in heart may be the reason for the relative difference in the immune response between heart and skeletal muscle tissue.

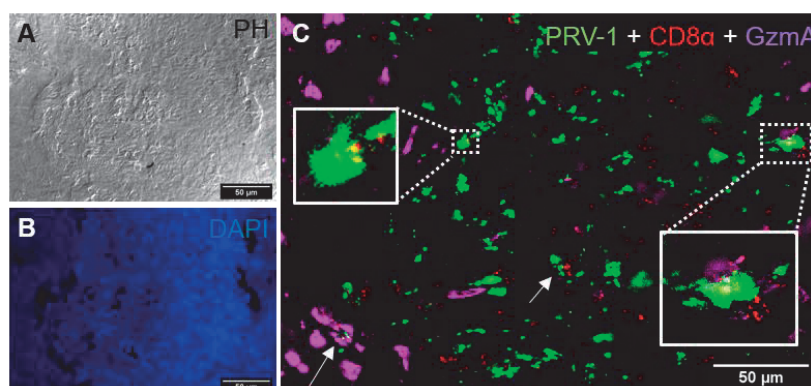


Figure 20. PRV-1 co-localization in CD8 positive cells in the heart tissue during experimental challenge study (from paper III).

Field samples of macroscopic red or black spots in the white muscle tissues showed moderate cellular inflammatory responses i.e. CD8⁺ and GzmA positive cells, but PRV-1 infected cells were nevertheless associated with, and thus possibly targeted by, CD8 positive cells both in red and black spots. PRV-1 partly co-localized in MHC-I cells present in melanized areas of black spots samples (Figure 21). With individual variation, RT-qPCR results showed that CD8 α expression is moderately higher in the red and black spots, but granzyme A and MHC-I expression level are significantly increased in both types of spots. One interesting finding is that no MHC-I positive cells were observed in this study, and neither were PRV-1 positive myocytes in skeletal muscle. Therefore, it can be assumed that infection of myocytes with PRV-1 may not be a relevant inducer of spot formation.

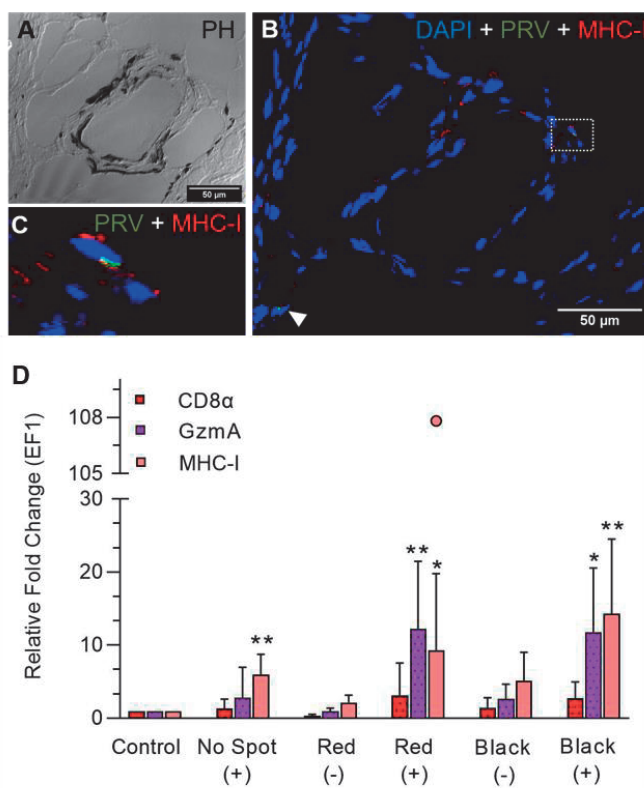


Figure 21. PRV-1 sporadic co-localization in MHC-I cells (A-C) in the black spots. (D) Gene expression analysis of CD8 α , GzmA and MHC-I in the red and black spots (*from paper II*).

Although this study did not prove that PRV-1 was the causal agent for melanized focal changes, all the infected fish had a significant inflammatory response during pathogenesis of this condition, based on the presence of M1 macrophages. Moreover, a specific cell mediated response is raised against PRV-1, but still, the Atlantic salmon is unable to clear the infection. Spot formation is most likely a long-lasting process where the host tries to control PRV-1 infection continuously.

PRV-1 persistence in long living renal erythroid progenitor cells or macrophages leads to a bypass from immune responses, and results in a continuous renewal of the infection (paper I), that may have consequences different from those observed during acute infection. In aquaculture, Atlantic salmon can be coinfecting with PRV-1, SAV, PMCV and calicivirus, and probably with many other viruses as well (181-183). PRV-1 induced innate immune responses can partly protect against other viruses such as SAV (184). It can be speculated that the innate antiviral response raised against the ubiquitous PRV-1 have the cross-protection effect against secondary viral infections.

5. Methodological consideration

5.1. Detection of PRV-1 genomic (dsRNA) and transcript (ssRNA) nucleic acids by qPCR.

PRV-1 nucleic acid detection was performed by extraction of RNA, reverse transcription to cDNA and real time PCR of the cDNA. It was used to assess the viral RNA load in samples from Atlantic salmon. In general, PCR is among the most efficient and sensitive methods for viral detection. PRV-1 genomic segment expression of the L, M and S classes was evaluated based upon 35 cycles of amplification. Comparable levels were found for all segments, which led us to distinguish between genomic dsRNA and ssRNA transcript in the same tissue sample.

Denaturation of the total RNA extracted is performed by heating to 95 °C for 5 min. This breaks the hydrogen bonds of the double stranded genomic RNA, and it separates into single strands that are accessible for primers. Omitting the denaturation step such that the dsRNA does not separate into ssRNA, will limit the primers of the PCR recognizing only the ssRNA PRV-1 transcripts (Figure 22A). The validity of the method has been verified earlier when the effect of heat denaturation was compared to the effect of using ssRNA and dsRNA specific RNAases (155). This method led to a consistent difference between dsRNA and ssRNA levels in all tested organs. However, since there is only one type of viral transcripts from reoviruses, the viral mRNA is identical to the positive strand of the viral genomic RNA, which implies that we could not distinguish between transcripts used for viral protein production or as templates for synthesis of new genomic RNA. The detection of viral ssRNA would, nevertheless, indicate viral transcriptional activity.

Plasma samples, being devoid of cells, showed a clear difference between genomic and transcript detection. Viral dsRNAs were detected in plasma throughout the experimental period of 18 weeks which indicates consistent presence of PRV-1 particles. In contrast, ssRNA transcripts were only detected at the peak phase of PRV-1 infection (Figure 22B), probably due to leakage of transcripts from infected cells such as erythrocytes at this time point of the infection. Both the continuous detection of

ssRNA, albeit at a very low level, and the continuous detection of dsRNA in plasma, support the conclusion that the persistence of PRV-1 in Atlantic salmon is a continuous productive infection.

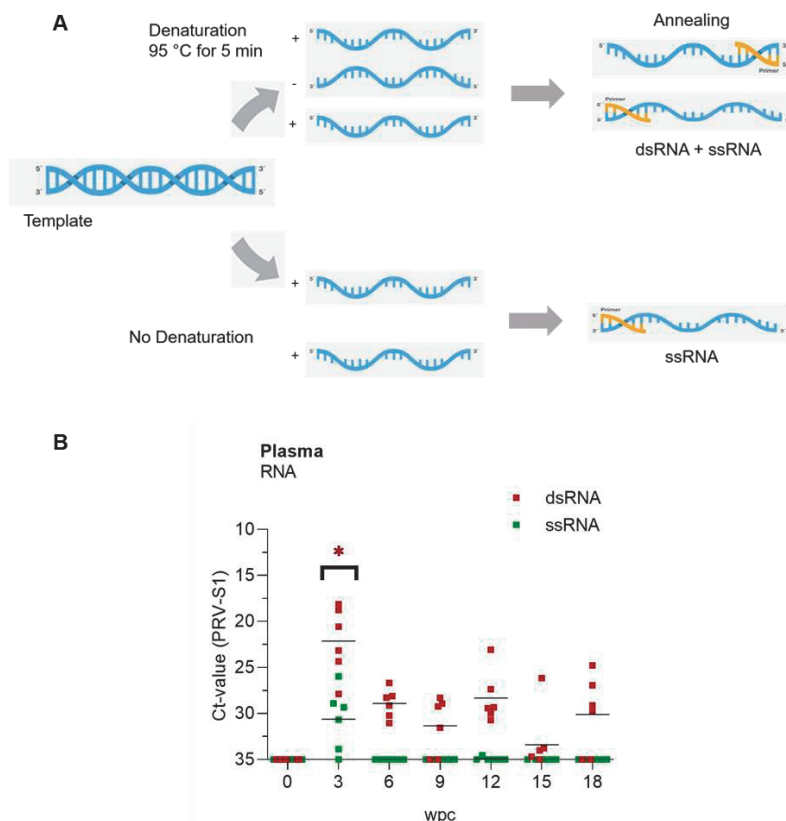


Figure 22. (A) Schematic overview of PRV-1 dsRNA and ssRNA nucleic acid detection. (B) PRV-1 transcripts (green) were detected in the plasma at peak phase by RT-qPCR method whereas dsRNA (red) were detected throughout the study period.

When the new synthesized ssRNAs are packed in new cores and capsids, then only one copy of each strand is packed, probably due to space constrictions (185). The viral ssRNA, identical to the positive strand of the viral genomic RNA, is capped in the 5' end and is not polyadenylated in the 3' end. However, when RNAs are packed, there must be a connection between the ten different transcripts packed to ensure that there is only one copy of each and that they are all different. There are no indications that the packing occurs arbitrarily for reoviruses. If this particular property was known, it could

theoretically be possible to distinguish between viral mRNA and viral genome templates.

5.2. Western blot

The Western blot method was used to detect expression of specific viral protein expression in blood homogenates. Key steps include sample preparation, gel electrophoresis, blotting and detection. Samples were prepared using NP-40 lysis buffer for cell lysis, supplemented with protease inhibitors. Proteins were denatured by heating, followed by gel electrophoresis, and blotting to membranes. Sample loading was customized by using β -actin as a control of amount loaded. Amongst various transfer systems for gel proteins to the PVDF or nitrocellulose membrane, semidry trans-blot turbo transfer system was chosen for its rapid blot transfer, high throughput, high efficiency, and reproducibility compared to other wet and dry methods. In every assay, positive and negative controls were included to judge the specificity of bands and to assess background noise due to cross-reactivity.

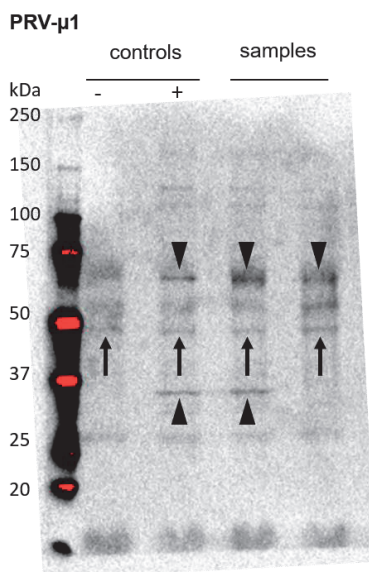


Figure 23. WB image showing specific (arrowheads) and unspecific (arrows) bands both in controls and samples.

During the blot development process, important steps were followed to reduce the background, “blocking”, due to cross reactive antibodies. The blots were incubated with 3% bovine serum albumin (BSA) solution in PBS to avoid non-specific protein detection, BSA is a small protein and often used for coating of surfaces in immune based solid phase techniques.

The in-lab produced polyclonal antibodies against PRV-1 proteins e.g. $\mu 1$ often gave unspecific bands in samples and thus demonstrating the necessity to use adequate controls for this work (Figure 23). Dilution of the samples were performed to reduce the background and unspecific binding, but this did not completely remove the background.

5.3. *In situ* hybridization (ISH)

Morphology-based detection methods allow specific detection of the cells of interest. The *in situ* hybridization (ISH) method spots specific DNA or RNA sequences by a labeled complementary nucleic acid strand that specifically bind to the target sequence and produce output signal after addition and reaction with a substrate. RNAscope ISH technology was used for the detection of mRNA sequences of the target cellular genes, and for PRV-1 this means any viral RNA. This technology is based on specific probes that can bind to 1000 bp of the target strand, which makes it very specific for target detection. The RNAscope ISH has enhanced the knowledge of PRV-1 localization in the tissues, by specific detection and characterization of infected cell types and cells in the vicinity of the infection. Being an expensive method compared to IHC, careful selection of the samples used for RNAscope ISH should be assured before staining.

Formalin fixed paraffin embedded (FFPE) tissue blocks were made for the mapping of PRV-1 infected cell types by *in situ* hybridization assays. The samples were originally fixed in formalin, but the formalin was exchanged with ethanol after approximately 24 h to avoid inaccessibility to RNA by too much formalin induced protein-protein cross binding. The whole procedure requires cautious handling and staining of tissue sections with approximate thickness of 5 μm . In general, pre-treatment of the section is performed before hybridizing specific probes on the slide sections. It includes

incubation with hydrogen peroxide, target antigen retrieval reagent and protease plus that is performed to reduce background noise, initial blocking and give better permeability of sections, respectively. It is critical that specific tissue samples from different species should be incubated for different time durations, ranging from 15-45 min variably, to get the optimum results. The Z structure of the probe is designed to bind the target strand in one end (Figure 24), whereas pre-amplifiers are attached to the upper end to enhance the signal amplification and make targets more visible under the microscope.

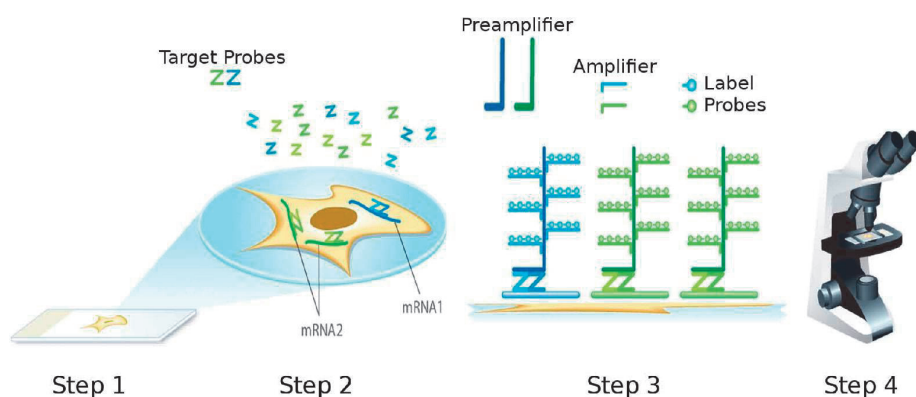


Figure 24. Schematic of the RNAscope workflow steps for *in situ* hybridization method. Image source (186)

5.3.1. Chromogenic ISH detection (singleplex & duplex)

In our studies, we used different ISH versions based on chromogenic dyes that gave high contrast in the tissues better distinguished the target from background. Chromogenic based singleplex and duplex ISH assays that can detect one or two target genes simultaneously, respectively, were performed to study PRV-1 co-localization in infected tissues. Different amplification steps are involved in singleplex (Amp1-Amp6) and duplex (Amp1-Amp10) after hybridization of the probes. ISH was demonstrated to specifically detect PRV-1 RNA, but with heating as a part of the ISH procedure it was not possible to distinguish viral transcripts (ssRNA) and viral genomic dsRNA. Ideal results of chromogenic dyes should be punctuated and dot-like. But it was observed that both in singleplex and duplex ISH, the alkaline phosphatase (AP) enzyme-based dyes can be

hazy, diffused or faint. Horseradish peroxidase (HRP) conjugated dye (green) showed relatively more punctuated pattern. This was observed in different organs with various types of target cell populations. Lymphoid organs, such as kidney and spleen, showed more hazy or diffused staining compared to the heart tissue (Figure 25).

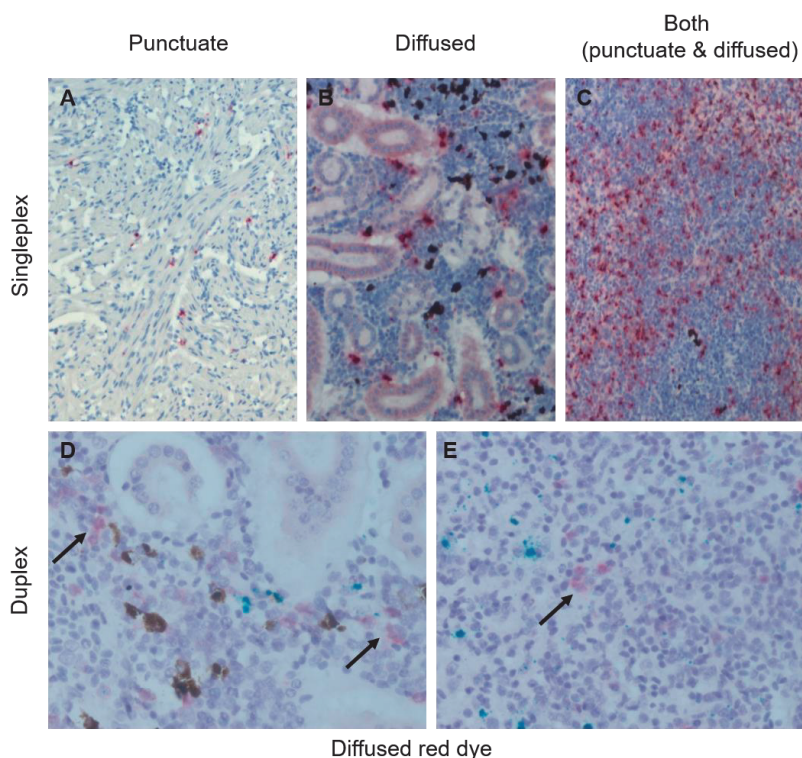


Figure 25. Chromogenic expression of ISH results. Singleplex ISH shows punctuated expression in (A) heart but more diffused in lymphoid organs of (B) kidney and (C) spleen. Duplex results showed diffused red dye staining compared to green dye both in (D) kidney and (E) spleen.

Homogenous gene expression was also associated with punctuate staining pattern as it was observed that denser patches of staining could mask the other target in duplex procedures. It is possible that tissues with high levels of endogenous peroxidases have interfered with the staining pattern of the dyes, although incubation with hydrogen peroxide was done to reduce this. Nevertheless, specific cells could easily be detected as there was almost no background or other unspecific staining.

5.3.2. Multiplex fluorescent *in situ* hybridization (FISH)

Fluorescent *in situ* hybridization assay was established at our lab to study colocalization of PRV-1 with various cell populations in FFPE tissue samples. Up to four target sequences can be detected simultaneously and distinguished by the method we used. RNAscope probes which are designed for chromogenic detection works equally well for FISH detection, however they are labeled differently. Different fluorophores with excitation and emission wavelengths that can be distinguished, were used. Dilutions of fluorophores can be different depending upon the intensity of the signal, and this should be optimized between 1:750 to 1:3000 dilution. The procedure for each probe was optimized and blocked by probe developer and blocker reagents that inhibits cross binding of different fluorophores to the same probe. In comparison to chromogen based ISH, FISH produced sharper punctuated expression and specific detection, and was able to detect four targets in the same section, compared to two using chromogens. The FISH method is useful for the study of colocalization of multiple RNA targets, but it may reduce the overview of individual gene expression in the same section. Therefore, it is recommended that the chosen assay, i.e. single-, multiple-, chromogenic, fluorescent etc. should be optimized to the experimental design and hypothesis of the study. Moreover, it is not possible to see or overlay the histopathological view of the slide that limits the simultaneous evaluation of the target sample.

5.4. Confocal microscopy

Laser scanning via confocal microscope is an optical imaging technique that produce high optical resolution and contrast by using spatial pinhole to block unfocused light in the image formation. Signals were recorded from all hybridized probes assigned with different colors to differentiate from each other. Overlapping signals indicated colocalization of PRV-1 in the targeted cell type. Different wavelengths in the light spectrum were assigned for each fluorophore used in FISH according to their excitation and emission ranges. For the removal of background generated by the excitation light, and to avoid coverslip reflection, gating was performed that defined the start and end of image acquisition in relation to the laser pulse.

6. Main conclusions

This study has shed light on the characteristics of PRV-1 persistence in Atlantic salmon and helped to better understand disease pathogenesis of HSMI and melanized focal changes.

PRV-1 establishes a productive and persistent infection in Atlantic salmon with plasma viremia. The plasma viraemia lasted throughout the experimental period of 18 weeks. The persistent phase is characterized by high viral transcription in erythrocytes but lack of detection of viral proteins. There was a homogenous expression of all genomic segments both in the acute and persistent phase. Infection kinetics in various visceral organs showed that kidney is the most active organ for viral transcription during persistent phase. MCSFR positive macrophages are one of the most frequently infected cells in kidney and spleen tissues. Moreover, PRV-1 also infects erythroid progenitor cells in the head kidney that could be a reservoir cell for persistent virus infection.

This study showed that polarization of macrophages is associated with PRV-1 infection. M1 macrophages dominated in red spots, i.e. the precursor to the melanized spots and co-localized with PRV-1 to a large extent. Late phase of red spots indicated the transformation of red spot into a black spot and it was found that melanized M2 macrophages entered the scene at this stage. The M2 phenotype was the dominating macrophage phenotype in black spots. There was no indication that a local PRV-1 infection was the initial causative agent for black spot formation, but PRV-1 is associated with the development of the melanization.

Macrophage polarization at peak phase of HSMI lesions was less prominent. There was a low level of M1 macrophages both in heart and skeletal muscle tissues, while a prominent presence of M2 macrophages in heart was evident. The latter could indicate high regeneration potential. Immune genes, e.g. MHC-1, CD8 α , GzmA, involved in cell mediated response (Figure 26) showed a significant upregulation and there was a drop in PRV-1 level at the same time both in melanized focal changes and HSMI.

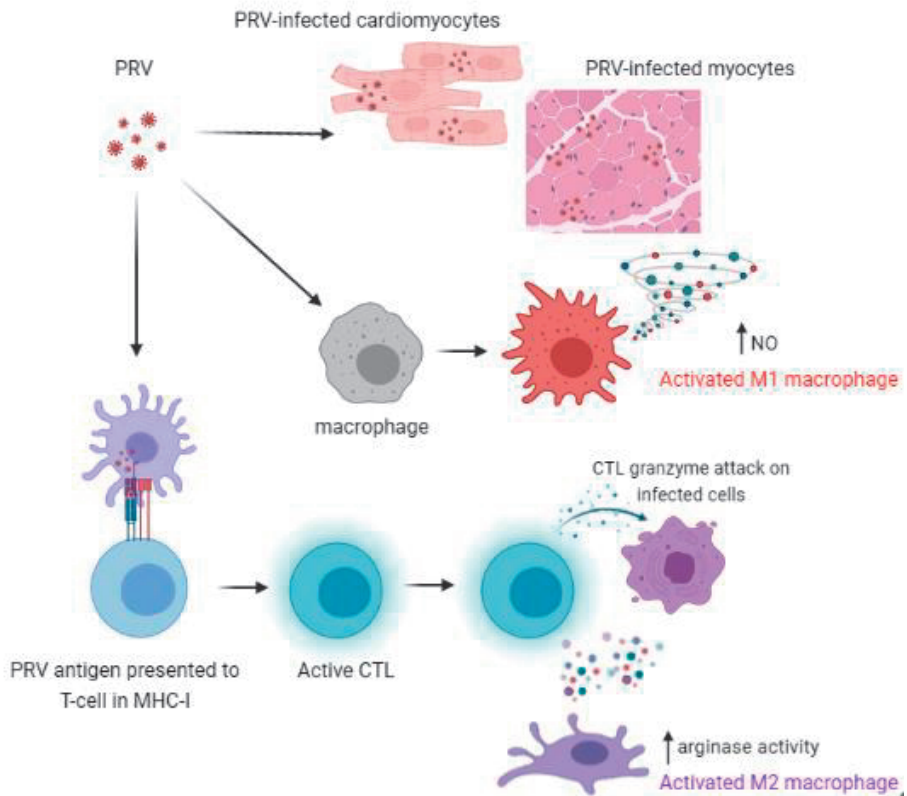


Figure 26. Illustration showing immunopathological responses initiated against PRV-1 infection.

A vaccination challenge showed the protective potential of prior immunization of Atlantic salmon with PRV-3 against a consecutive PRV-1 infection. PRV-3 induced production of antibodies cross-reactive with PRV-1 $\sigma 1$, and fully protected against HSMI lesions. This endorse a live attenuated vaccination approach.

7. Future perspectives

Viruses are selected to best fit the environment of the host and the transition between hosts. The crossroad between farming of fish and wild fish regarding transmission of pathogens will be a part of aquaculture in the foreseeable future. Although the future production facilities may be different from the present, it is unlikely that they can become virus proof. Therefore, information is required as a basis for a proper evaluation of the consequences of PRV-1 transmission from aquaculture to the wild fish species and vice versa. It is essential, in the future, to optimize management including better immunization to minimize the interaction between wild and farmed fish. A virus may survive in its host for a long time if it replicates in the host's cells in such a way that it is hidden from clearance by the immune response. In recent years, PRV-1 infection has been characterized to understand the pathogenesis of HSMI in Atlantic salmon. PRV-1 gives long-term presence in the host Atlantic salmon, which indicates inefficiency of clearance by the specific immune response. HSMI, which is caused by PRV-1, is not a notifiable disease anymore, but nevertheless several outbreaks are reported every year and it is ranked as a serious disease problem by the industry itself. Moreover, the PRV-1 association with development of black spots formation, may potentially signify another important economic aspect of PRV-1 in the Atlantic salmon farming industry.

At present, there are fundamental knowledge gaps regarding the PRV-1 entry-exit mechanisms, at both the level of transmission between fish and viral entry mechanisms at the cellular level. If these knowledge gaps are filled it would significantly increase the understanding of infection, transmission routes and enhance control and vaccine development. Entry of viruses into host cells require binding to specific receptor(s). It would be important to identify the cell surface receptor(s) which enables PRV-1 to infect erythrocytes, cardiomyocytes, macrophages, and renal erythroid progenitor cells.

PRV-1 causes plasma viremia in Atlantic salmon. This has been demonstrated in the present study by the findings of dsRNA genomic viral particles in plasma for at least 18 weeks after challenge. This is far beyond the time the host fish uses to raise a specific antibody response against PRV-1. The viruses found in plasma are shed from infected

cells and the presence of virus in plasma indicate that an exact timeline when the fish is no longer infectious cannot be drawn. Nevertheless, estimating the duration of the most infectious period of the fish would be of practical significance. Similarly, it would be of interest to study if a low level, persistent PRV-1 infection could be revived to produce enough virus for the fish to become infectious. A simple question like “Does stress exposure of a persistently PRV-1 infected population cause shedding?” cannot be answered adequately today.

PRV-1 does not cause anemia in Atlantic salmon, which indicates that the viral release from the infected erythrocyte include non-lytic egress pathways. However, the exit of naked viruses from a cell is generally known to be due to cell lysis. Moreover, viral protein detection is disappearing in plasma after the acute viral phase, as assessed by WB, indicating that the PRV-1 protein level in the persistent phase in the plasma was below the detection limit. Whether plasma PRV-1 is present as free viral particles or enclosed in extracellular vesicles or protected from specific antibodies by other mechanisms is not known. Further research is needed to study PRV-1 release mechanism and the nature of virus in plasma. It will be important to find out if there is a specific shutoff mechanism of viral protein translation, and eventually what these molecular mechanisms are.

PRV-1 chronic infection is associated with black spots in white muscle of Atlantic salmon. However, not all PRV-1 infected fish develop black spots. The spots are characterized by severe necrosis and melanin production. The condition has not been reproduced experimentally by PRV-1 challenge, suggesting that host and environmental factors such as rapid growth, feed, physical injury, or unknown environmental factors may be involved. It is specifically observed that PRV-1 infection is associated with macrophage polarization, and this precedes the melanin production that transforms a red spot into a black spot. But it does not define PRV-1 as the initial cause, because non-infected fish may also have macroscopic red and black spots. These spots, however, are histologically different from those of infected fish, i.e. the expressions “red” and “black” spots do not express specific entities. Melanin production are assessed as being a biological response to the macrophage inflammatory response against viral infections,

i.e. it can represent a protective wall against oxygen radicals. The present study showed a moderate cell mediated immune response in red and black spots as compared to the overwhelming CD8⁺ cell cytotoxic response in the HSMI diseased heart. Several hypotheses can be brought forward to explain this discrepancy in immune responses; it could be linked to differences between organs i.e. heart versus white skeletal muscle; it could be due to acute versus chronic infection; it could be due to different PRV-1 variants involved in HSMI and spot formation.

In the vaccination study, a successful immunization strategy using a live PRV-3 vaccine was tested out for Atlantic salmon. Although immunization with PRV-3 significantly blocked PRV-1 infection, there are many questions needed to be addressed before such an approach can be used in commercial farming. Will it be accepted to introduce the PRV-3 subtype to Atlantic salmon aquaculture as it can infect and replicate in Atlantic salmon for relatively long period of time? Furthermore, PRV-3 has been found to be pathogenic to rainbow trout and possibly to brown trout, and due to lack of cultivation in cell cultures the source for PRV-3 today is blood from an infected fish. Theoretically, immunization would be a huge benefit and save big economic losses for the industry if it can reduce the prevalence of severe melanized focal changes and HSMI. But on the other hand, such a procedure would impose a risk for rainbow trout farming and introduce an unknown risk for wild salmonids. PRV-3 is a virus naturally occurring in brown trout and the sea ranging form, sea trout, along the Norwegian coast. Therefore PRV-3 is not an exotic virus. Low virulent PRV-1 variants should also be tested out as live vaccines, at least against HSMI. However, this would require that the low virulent variants are not involved in the spot formation. Other vaccination approaches based on reverse genetics and subsequent production of variants with lack of pathogenic functions, recombinant vaccines or viral like particles (VLPs) should also be considered in the future. Vaccination may not be the only tool to reduce infection load. The use of selective breeding may be an alternative for increased host resistance, although such benefits could be of limited duration.

8. References

1. Iversen A, Asche F, Hermansen Ø, Nystøyl R. Production cost and competitiveness in major salmon farming countries 2003–2018. *Aquaculture*. 2020;522:735089.
2. Moffitt CM, Cajas-Cano L. Blue Growth: The 2014 FAO State of the World Fisheries and Aquaculture. *Fisheries*. 2014;39(11):552-3.
3. Rimstad E. Examples of emerging virus diseases in salmonid aquaculture. *Aquaculture Research*. 2011;42:86-9.
4. Lafferty KD, Harvell CD, Conrad JM, Friedman CS, Kent ML, Kuris AM, et al. Infectious diseases affect marine fisheries and aquaculture economics. 2015.
5. Einum S, Fleming I. Implications of stocking: ecological interactions between wild and released salmonids. *Nordic Journal of Freshwater Research*. 2001;75:56-70.
6. Glover KA, Otterå H, Olsen RE, Slinde E, Taranger GL, Skaala Ø. A comparison of farmed, wild and hybrid Atlantic salmon (*Salmo salar* L.) reared under farming conditions. *Aquaculture*. 2009;286(3-4):203-10.
7. Lillehaug A, Santi N, Østvik A. Practical Biosecurity in Atlantic Salmon Production. *Journal of Applied Aquaculture*. 2015;27(3):249-62.
8. Sommerset I WCS, Bang Jensen B, Bornø G, Haukaas A and Brun E. Fiskehelserapporten 2020. 2020. Report No.: 1890-3290.
9. Wessel Ø, Braaen S, Alarcon M, Haatveit H, Roos N, Markussen T, et al. Infection with purified Piscine orthoreovirus demonstrates a causal relationship with heart and skeletal muscle inflammation in Atlantic salmon. *PloS one*. 2017;12(8):e0183781.
10. Bjørgen H, Wessel Ø, Fjellidal PG, Hansen T, Sveier H, Sæbø HR, et al. Piscine orthoreovirus (PRV) in red and melanised foci in white muscle of Atlantic salmon (*Salmo salar*). *Veterinary Research*. 2015;46(1):89.
11. Kongtorp R, Taksdal T, Lyngøy A. Pathology of heart and skeletal muscle inflammation (HSMI) in farmed Atlantic salmon *Salmo salar*. *Diseases of aquatic organisms*. 2004;59(3):217-24.
12. Palacios G, Lovoll M, Tengs T, Hornig M, Hutchison S, Hui J, et al. Heart and skeletal muscle inflammation of farmed salmon is associated with infection with a novel reovirus. *PloS one*. 2010;5(7):e11487.
13. Markussen T, Dahle MK, Tengs T, Lovoll M, Finstad OW, Wiik-Nielsen CR, et al. Sequence analysis of the genome of piscine orthoreovirus (PRV) associated with heart and skeletal muscle inflammation (HSMI) in Atlantic salmon (*Salmo salar*). *PloS one*. 2013;8(7):e70075.
14. Sabin AB. Reoviruses. *Science*. 1959;130(3386):1387.
15. Kapikian AZ, Shope RE. Rotaviruses, reoviruses, coltivirus, and orbiviruses. *Medical Microbiology 4th edition: University of Texas Medical Branch at Galveston*; 1996.

16. Day JM. The diversity of the orthoreoviruses: molecular taxonomy and phylogenetic divides. *Infection, Genetics and Evolution*. 2009;9(4):390-400.
17. Mertens P. The dsRNA viruses. *Virus research*. 2004;101(1):3-13.
18. Schiff L, Nibert ML, Tyler KL. Orthoreoviruses and their replication. *Fields virology*. 2007;5:1853-915.
19. Lefkowitz EJ, Dempsey DM, Hendrickson RC, Orton RJ, Siddell SG, Smith DB. Virus taxonomy: the database of the International Committee on Taxonomy of Viruses (ICTV). *Nucleic Acids Research*. 2017;46(D1):D708-D17.
20. Gummersheimer SL, Danthi P. Reovirus core proteins $\lambda 1$ and $\sigma 2$ promote stability of disassembly intermediates and influence early replication events. *Journal of Virology*. 2020;94(17).
21. Attoui H, Fang Q, Jaafar FM, Cantaloube J-F, Biagini P, de Micco P, et al. Common evolutionary origin of aquareoviruses and orthoreoviruses revealed by genome characterization of Golden shiner reovirus, Grass carp reovirus, Striped bass reovirus and golden ide reovirus (genus Aquareovirus, family Reoviridae) The accession numbers of sequences reported in this paper are AF450318–AF450324, AF403390–AF4034141 and AF418294–AF418304. *Journal of General Virology*. 2002;83(8):1941-51.
22. Crane MSJ, Carlile G. Aquareoviruses. In: Mahy BWJ, Van Regenmortel MHV, editors. *Encyclopedia of Virology (Third Edition)*. Oxford: Academic Press; 2008. p. 163-9.
23. King AM, Lefkowitz E, Adams MJ, Carstens EB. *Virus taxonomy: ninth report of the International Committee on Taxonomy of Viruses*: Elsevier; 2011.
24. Nibert ML, Duncan R. Bioinformatics of recent aqua-and orthoreovirus isolates from fish: evolutionary gain or loss of FAST and fiber proteins and taxonomic implications. *PLoS one*. 2013;8(7):e68607.
25. Key T, Read J, Nibert ML, Duncan R. Piscine reovirus encodes a cytotoxic, non-fusogenic, integral membrane protein and previously unrecognized virion outer-capsid proteins. *Journal of General Virology*. 2013;94(5):1039-50.
26. Dhamotharan K, Vendramin N, Markussen T, Wessel Ø, Cuenca A, Nyman IB, et al. Molecular and antigenic characterization of piscine orthoreovirus (PRV) from rainbow trout (*Oncorhynchus mykiss*). *Viruses*. 2018;10(4):170.
27. Kibenge MJ, Iwamoto T, Wang Y, Morton A, Godoy MG, Kibenge FS. Whole-genome analysis of piscine reovirus (PRV) shows PRV represents a new genus in family Reoviridae and its genome segment S1 sequences group it into two separate sub-genotypes. *Virology journal*. 2013;10(1):230.
28. Haatveit HM, Nyman IB, Markussen T, Wessel Ø, Dahle MK, Rimstad E. The non-structural protein μ NS of piscine orthoreovirus (PRV) forms viral factory-like structures. *Veterinary research*. 2016;47(1):1-11.

29. Haatveit HM, Wessel Ø, Markussen T, Lund M, Thiede B, Nyman IB, et al. Viral protein kinetics of piscine orthoreovirus infection in atlantic salmon blood cells. *Viruses*. 2017;9(3):49.
30. Wessel Ø, Nyman IB, Markussen T, Dahle MK, Rimstad E. Piscine orthoreovirus (PRV) $\sigma 3$ protein binds dsRNA. *Virus research*. 2015;198:22-9.
31. Weiner HL, Powers ML, Fields BN. Absolute linkage of virulence and central nervous system cell tropism of reoviruses to viral hemagglutinin. *Journal of infectious diseases*. 1980;141(5):609-16.
32. Dryden KA, Wang G, Yeager M, Nibert ML, Coombs KM, Furlong DB, et al. Early steps in reovirus infection are associated with dramatic changes in supramolecular structure and protein conformation: analysis of virions and subviral particles by cryoelectron microscopy and image reconstruction. *J Cell Biol*. 1993;122(5):1023-41.
33. Weiner HL, Ramig RF, Mustoe TA, Fields BN. Identification of the gene coding for the hemagglutinin of reovirus. *Virology*. 1978;86(2):581-4.
34. Reinisch KM, Nibert ML, Harrison SC. Structure of the reovirus core at 3.6 Å resolution. *Nature*. 2000;404(6781):960-7.
35. O'Hara D, Patrick M, Cepica D, Coombs KM, Duncan R. Avian reovirus major μ -class outer capsid protein influences efficiency of productive macrophage infection in a virus strain-specific manner. *Journal of virology*. 2001;75(11):5027-35.
36. Dermody T, Schiff L, Nibert M, Coombs K, Fields B. The S2 gene nucleotide sequences of prototype strains of the three reovirus serotypes: characterization of reovirus core protein sigma 2. *Journal of virology*. 1991;65(11):5721-31.
37. Barton ES, Forrest JC, Connolly JL, Chappell JD, Liu Y, Schnell FJ, et al. Junction adhesion molecule is a receptor for reovirus. *Cell*. 2001;104(3):441-51.
38. Chappell JD, Gunn VL, Wetzel JD, Baer GS, Dermody TS. Mutations in type 3 reovirus that determine binding to sialic acid are contained in the fibrous tail domain of viral attachment protein sigma1. *Journal of virology*. 1997;71(3):1834-41.
39. Lemay G. Synthesis and Translation of Viral mRNA in Reovirus-Infected Cells: Progress and Remaining Questions. *Viruses*. 2018;10(12).
40. Mainou BA, Dermody TS. Transport to late endosomes is required for efficient reovirus infection. *Journal of virology*. 2012;86(16):8346-58.
41. Gummersheimer SL, Snyder AJ, Danthi P. Control of Capsid Transformations during Reovirus Entry. *Viruses*. 2021;13(2):153.
42. Guglielmi K, Johnson E, Stehle T, Dermody T. Attachment and cell entry of mammalian orthoreovirus. *Reoviruses: Entry, Assembly and Morphogenesis*. 2006:1-38.
43. Nibert M, Furlong D, Fields B. Mechanisms of viral pathogenesis. Distinct forms of reoviruses and their roles during replication in cells and host. *The Journal of clinical investigation*. 1991;88(3):727-34.

44. Schulz WL, Haj AK, Schiff LA. Reovirus uses multiple endocytic pathways for cell entry. *Journal of virology*. 2012;86(23):12665-75.
45. Kibenge F, Godoy M. Reoviruses of aquatic organisms. *Aquaculture virology*: Elsevier; 2016. p. 205-36.
46. Bartlett NM, Gillies SC, Bullivant S, Bellamy A. Electron microscopy study of reovirus reaction cores. *Journal of Virology*. 1974;14(2):315-26.
47. Zhang X, Ji Y, Zhang L, Harrison SC, Marinescu DC, Nibert ML, et al. Features of reovirus outer capsid protein $\mu 1$ revealed by electron cryomicroscopy and image reconstruction of the virion at 7.0 Å resolution. *Structure*. 2005;13(10):1545-57.
48. Tytell A, Lampson G, Field A, Hilleman M. Inducers of interferon and host resistance. 3. Double-stranded RNA from reovirus type 3 virions (reo 3-RNA). *Proceedings of the National Academy of Sciences of the United States of America*. 1967;58(4):1719.
49. Novoa RR, Calderita G, Arranz R, Fontana J, Granzow H, Risco C. Virus factories: associations of cell organelles for viral replication and morphogenesis. *Biology of the Cell*. 2005;97(2):147-72.
50. Becker MM, Peters TR, Dermody TS. Reovirus σ NS and μ NS proteins form cytoplasmic inclusion structures in the absence of viral infection. *Journal of virology*. 2003;77(10):5948-63.
51. Dermody T, Parker J, Sherry B. *Orthoreoviruses*. *Fields virology*. 2: Lippincott Williams & Wilkins Philadelphia; 2013. p. 1304-46.
52. Fernández de Castro I, Tenorio R, Ortega-González P, Knowlton JJ, Zamora PF, Lee CH, et al. A modified lysosomal organelle mediates nonlytic egress of reovirus. *Journal of Cell Biology*. 2020;219(7).
53. Hauge H, Dahle M, Moldal T, Thoen E, Gjevne A-G, Weli S, et al. Piscine orthoreovirus can infect and shed through the intestine in experimentally challenged Atlantic salmon (*Salmo salar* L.). *Veterinary research*. 2016;47(1):1-12.
54. Kongtorp R, Kjerstad A, Taksdal T, Guttvik A, Falk K. Heart and skeletal muscle inflammation in Atlantic salmon, *Salmo salar* L.: a new infectious disease. *Journal of fish diseases*. 2004;27(6):351-8.
55. Watanabe K, Devold M, Myhr E, Lyngøy A, Isdal E, Fridell F, et al. Heart and skeletal muscle inflammation (HSMI): a new viral disease. *Fiskehelse*. 2003;5:23-30.
56. Kongtorp R, Taksdal T. Studies with experimental transmission of heart and skeletal muscle inflammation in Atlantic salmon, *Salmo salar* L. *Journal of fish diseases*. 2009;32(3):253-62.
57. Watanabe K, Karlsen M, Devold M, Isdal E, Litlabø A, Nylund A. Virus-like particles associated with heart and skeletal muscle inflammation (HSMI). *Diseases of Aquatic Organisms*. 2006;70(3):183-92.
58. Yousaf MN, Koppang EO, Skjødt K, Hordvik I, Zou J, Secombes C, et al. Comparative cardiac pathological changes of Atlantic salmon (*Salmo salar* L.) affected with heart and skeletal muscle inflammation (HSMI), cardiomyopathy

- syndrome (CMS) and pancreas disease (PD). *Veterinary immunology and immunopathology*. 2013;151(1-2):49-62.
59. Di Cicco E, Ferguson HW, Kaukinen KH, Schulze AD, Li S, Tabata A, et al. The same strain of Piscine orthoreovirus (PRV-1) is involved in the development of different, but related, diseases in Atlantic and Pacific Salmon in British Columbia. *Facets*. 2018;3(1):599-641.
 60. Wessel Ø, Hansen EF, Dahle MK, Alarcon M, Vatne NA, Nyman IB, et al. Piscine Orthoreovirus-1 Isolates Differ in Their Ability to Induce Heart and Skeletal Muscle Inflammation in Atlantic Salmon (*Salmo salar*). *Pathogens*. 2020;9(12).
 61. Mørkøre T, Heia K. Black spots in salmon fillet-extent and methods of measurement. *Norsk fiskeoppdrett*. 2012;3:50-3.
 62. Bjørgen H, Haldorsen R, Oaland Ø, Kvellestad A, Kannimuthu D, Rimstad E, et al. Melanized focal changes in skeletal muscle in farmed Atlantic salmon after natural infection with Piscine orthoreovirus (PRV). *Journal of fish diseases*. 2019;42(6):935-45.
 63. Malik MS, Bjørgen H, Dhamotharan K, Wessel Ø, Koppang EO, Di Cicco E, et al. Erythroid progenitor cells in Atlantic salmon (*Salmo salar*) may be persistently and productively infected with Piscine Orthoreovirus (PRV). *Viruses*. 2019;11(9):824.
 64. Cartagena J, Jiménez C, Spencer E. Detection of Piscine orthoreoviruses (PRV-1b AND PRV-3a) in farmed Coho salmon with jaundice syndrome from Chile. *Aquaculture*. 2020;528:735480.
 65. Takano T, Nawata A, Sakai T, Matsuyama T, Ito T, Kurita J, et al. Full-Genome Sequencing and Confirmation of the Causative Agent of Erythrocytic Inclusion Body Syndrome in Coho Salmon Identifies a New Type of Piscine Orthoreovirus. *PLoS One*. 2016;11(10):e0165424.
 66. Leek SL. Viral erythrocytic inclusion body syndrome (EIBS) occurring in juvenile spring chinook salmon (*Oncorhynchus tshawytscha*) reared in freshwater. *Canadian Journal of Fisheries and Aquatic Sciences*. 1987;44(3):685-8.
 67. Takahashi K, Okamoto N, Kumagai A, Maita M, Ikeda Y, Rohovec J. Epizootics of erythrocytic inclusion body syndrome in coho salmon cultured in seawater in Japan. *Journal of Aquatic Animal Health*. 1992;4(3):174-81.
 68. Piacentini S, Rohovec J, Fryer J. Epizootiology of erythrocytic inclusion body syndrome. *Journal of Aquatic Animal Health*. 1989;1(3):173-9.
 69. Shanks CA. Erythrocytic inclusion body syndrome: salmonid stock susceptibility, secondary diseases, and vitamin therapy. 1991.
 70. Okamoto N, Takahashi K, Maita M, Rohovec JS, Ikeda Y. Erythrocytic inclusion body syndrome: Susceptibility of selected sizes of coho salmon and of several other species of salmonid fish. *Fish Pathology*. 1992;27(3):153-6.
 71. Graham D, Curran W, Rowley H, Cox D, Cockerill D, Campbell S, et al. Observation of virus particles in the spleen, kidney, gills and erythrocytes of Atlantic salmon,

- Salmo salar* L., during a disease outbreak with high mortality. *Journal of fish diseases*. 2002;25(4):227-34.
72. Rodger H. Erythrocytic inclusion body syndrome virus in wild Atlantic salmon, *Salmo salar* L. *Journal of fish diseases*. 2007;30(7):411-8.
 73. Hayakawa Y, Harada T, Yamamoto M, Hatai K, Kubota SS, Bunya T, et al. Histopathological studies on viral anemia in sea-cultured coho salmon (*Oncorhynchus kisutch*). *Fish Pathology*. 1989;24(4):203-10.
 74. Sakai T, Murata H, Yamauchi K, Takahashi K, Okamoto N, Kihira K, et al. Hyperbilirubinemia of coho salmon *Oncorhynchus kisutch* infected with erythrocytic inclusion body syndrome (EIBS) virus. *Fisheries science*. 1994;60(5):519-21.
 75. Hauge H, Vendramin N, Taksdal T, Olsen AB, Wessel Ø, Mikkelsen SS, et al. Infection experiments with novel Piscine orthoreovirus from rainbow trout (*Oncorhynchus mykiss*) in salmonids. *PloS one*. 2017;12(7):e0180293.
 76. Vendramin N, Kannimuthu D, Olsen AB, Cuenca A, Teige LH, Wessel Ø, et al. Piscine orthoreovirus subtype 3 (PRV-3) causes heart inflammation in rainbow trout (*Oncorhynchus mykiss*). *Veterinary research*. 2019;50(1):1-13.
 77. Schwaiger J, Ferling H, Dembek G, Gerst M, Scholz K. Bachforellensterben in Bayern-Auf den Spuren eines ungeklärten Phänomens. *Proceedings of the Bachforellensterben in Bayern*(Jul 12). 2003.
 78. Kuehn R, Stoeckle BC, Young M, Popp L, Taeubert J-E, Pfaffl MW, et al. Identification of a piscine reovirus-related pathogen in proliferative darkening syndrome (PDS) infected brown trout (*Salmo trutta fario*) using a next-generation technology detection pipeline. *PloS one*. 2018;13(10):e0206164.
 79. Fux R, Arndt D, Langenmayer MC, Schwaiger J, Ferling H, Fischer N, et al. Piscine orthoreovirus 3 is not the causative pathogen of proliferative darkening syndrome (pds) of brown trout (*salmo trutta fario*). *Viruses*. 2019;11(2):112.
 80. Fänge R. Blood cells, haemopoiesis and lymphomyeloid tissues in fish. *Fish & Shellfish Immunology*. 1994;4(6):405-11.
 81. Lay PA, Baldwin J. What determines the size of teleost erythrocytes? Correlations with oxygen transport and nuclear volume. *Fish Physiology and Biochemistry*. 1999;20(1):31-5.
 82. Luskova V. Determination of normal values in fish hematology. *ACTA-Universitatis Carolinae Biologica*. 1995;39:191-200.
 83. Witeska M. Erythrocytes in teleost fishes: a review. *Zoology and Ecology*. 2013;23(4):275-81.
 84. Ghanbari M, Jami M, Domig KJ, Kneifel W. Long-term effects of water pH changes on hematological parameters in the common carp (*Cyprinus carpio* L.). *African Journal of Biotechnology*. 2012;11(13):3153-9.
 85. Nikinmaa M. Haemoglobin function in vertebrates: evolutionary changes in cellular regulation in hypoxia. *Respiration physiology*. 2001;128(3):317-29.

86. Puente-Marin S, Thwaite R, Mercado L, Coll J, Roher N, Ortega-Villaizan MDM. Fish Red Blood Cells Modulate Immune Genes in Response to Bacterial Inclusion Bodies Made of TNF α and a G-VHSV Fragment. *Frontiers in Immunology*. 2019;10(1055).
87. Wlasow T. Erythrocyte system of rainbow trout, *Salmo gairdneri* Rich. affected by prolonged subacute phenol intoxication. *Acta Ichthyologica et Piscatoria*. 1984;14(1-2).
88. Finstad ØW, Dahle MK, Lindholm TH, Nyman IB, Løvoll M, Wallace C, et al. Piscine orthoreovirus (PRV) infects Atlantic salmon erythrocytes. *Veterinary Research*. 2014;45(1):35.
89. Wessel Ø, Olsen CM, Rimstad E, Dahle MK. Piscine orthoreovirus (PRV) replicates in Atlantic salmon (*Salmo salar* L.) erythrocytes ex vivo. *Veterinary research*. 2015;46:26-.
90. Stainier DY. Zebrafish genetics and vertebrate heart formation. *Nature Reviews Genetics*. 2001;2(1):39-48.
91. Icardo JM. 1 - Heart Morphology and Anatomy. In: Gamperl AK, Gillis TE, Farrell AP, Brauner CJ, editors. *Fish Physiology*. 36: Academic Press; 2017. p. 1-54.
92. Jaźwińska A, Blanchoud S. Towards deciphering variations of heart regeneration in fish. *Current Opinion in Physiology*. 2020;14:21-6.
93. Matrone G, Tucker CS, Denvir MA. Cardiomyocyte proliferation in zebrafish and mammals: lessons for human disease. *Cell Mol Life Sci*. 2017;74(8):1367-78.
94. Kiessling A, Ruohonen K, Bjørnevik M. Muscle fibre growth and quality in fish. 2006.
95. Hodgkinson JW, Grayfer L, Belosevic M. Biology of bony fish macrophages. *Biology*. 2015;4(4):881-906.
96. Wang T, Secombes CJ. The cytokine networks of adaptive immunity in fish. *Fish & shellfish immunology*. 2013;35(6):1703-18.
97. Joerink M, Savelkoul HF, Wiegertjes GF. Evolutionary conservation of alternative activation of macrophages: structural and functional characterization of arginase 1 and 2 in carp (*Cyprinus carpio* L.). *Molecular immunology*. 2006;43(8):1116-28.
98. Wiegertjes GF, Wentzel AS, Spaink HP, Elks PM, Fink IR. Polarization of immune responses in fish: The 'macrophages first' point of view. *Molecular immunology*. 2016;69:146-56.
99. Stosik MP, Tokarz-Deptuła B, Deptuła W. Melanomacrophages and melanomacrophage centres in Osteichthyes. *Central European Journal of Immunology*. 2019;44(2):201-5.
100. Agius C, Roberts R. Melano-macrophage centres and their role in fish pathology. *Journal of fish diseases*. 2003;26(9):499-509.
101. Dhamotharan K, Bjørgen H, Malik MS, Nyman IB, Markussen T, Dahle MK, et al. Dissemination of Piscine orthoreovirus-1 (PRV-1) in Atlantic Salmon (*Salmo salar*)

- during the Early and Regenerating Phases of Infection. *Pathogens* (Basel, Switzerland). 2020;9(2):143.
102. DeWitte-Orr SJ, Mossman KL. dsRNA and the innate antiviral immune response. *Future Virology*. 2010;5(3):325-41.
 103. Chen SN, Zou PF, Nie P. Retinoic acid-inducible gene I (RIG-I)-like receptors (RLRs) in fish: current knowledge and future perspectives. *Immunology*. 2017;151(1):16-25.
 104. Strandskog G, Skjæveland I, Ellingsen T, Jørgensen JB. Double-stranded RNA-and CpG DNA-induced immune responses in Atlantic salmon: comparison and synergies. *Vaccine*. 2008;26(36):4704-15.
 105. Robertsen B. The role of type I interferons in innate and adaptive immunity against viruses in Atlantic salmon. *Developmental & Comparative Immunology*. 2018;80:41-52.
 106. Takeuchi O, Akira S. Innate immunity to virus infection. *Immunological reviews*. 2009;227(1):75-86.
 107. Samuel CE. Antiviral actions of interferons. *Clinical microbiology reviews*. 2001;14(4):778-809.
 108. Heim MH. The Jak-STAT pathway: cytokine signalling from the receptor to the nucleus. *Journal of Receptors and Signal Transduction*. 1999;19(1-4):75-120.
 109. Paun A, Pitha PM. The innate antiviral response: new insights into a continuing story. *Advances in virus research*. 2006;69:1-66.
 110. Wessel Ø, Krasnov A, Timmerhaus G, Rimstad E, Dahle MK. Antiviral responses and biological consequences of piscine orthoreovirus infection in salmonid erythrocytes. *Frontiers in immunology*. 2019;9:3182.
 111. Dahle MK, Wessel Ø, Timmerhaus G, Nyman IB, Jørgensen SM, Rimstad E, et al. Transcriptome analyses of Atlantic salmon (*Salmo salar* L.) erythrocytes infected with piscine orthoreovirus (PRV). *Fish & shellfish immunology*. 2015;45(2):780-90.
 112. Skup D, Millward S. Reovirus-induced modification of cap-dependent translation in infected L cells. *Proceedings of the National Academy of Sciences*. 1980;77(1):152-6.
 113. Sharpe AH, Fields BN. Reovirus inhibition of cellular RNA and protein synthesis: role of the S4 gene. *Virology*. 1982;122(2):381-91.
 114. Garver KA, Johnson SC, Polinski MP, Bradshaw JC, Marty GD, Snyman HN, et al. Piscine orthoreovirus from western North America is transmissible to Atlantic salmon and sockeye salmon but fails to cause heart and skeletal muscle inflammation. *PLoS One*. 2016;11(1):e0146229.
 115. Zinzula L, Tramontano E. Strategies of highly pathogenic RNA viruses to block dsRNA detection by RIG-I-like receptors: hide, mask, hit. *Antiviral research*. 2013;100(3):615-35.

116. Hordvik I. Immunoglobulin isotypes in Atlantic salmon, *Salmo salar*. *Biomolecules*. 2015;5(1):166-77.
117. Mutoloki S, Jørgensen JB, Evensen Ø. The adaptive immune response in fish. *Fish vaccination*. 2014;9:104-15.
118. Workenhe ST, Rise ML, Kibenge MJ, Kibenge FS. The fight between the teleost fish immune response and aquatic viruses. *Molecular immunology*. 2010;47(16):2525-36.
119. Teige LH, Lund M, Haatveit HM, Røsæg MV, Wessel Ø, Dahle MK, et al. A bead based multiplex immunoassay detects Piscine orthoreovirus specific antibodies in Atlantic salmon (*Salmo salar*). *Fish & shellfish immunology*. 2017;63:491-9.
120. Teige LH, Kumar S, Johansen GM, Wessel Ø, Vendramin N, Lund M, et al. Detection of salmonid IgM specific to the Piscine orthoreovirus outer capsid spike protein sigma 1 using lipid-modified antigens in a bead-based antibody detection assay. *Frontiers in immunology*. 2019;10:2119.
121. Mikalsen AB, Haugland O, Rode M, Solbakk IT, Evensen O. Atlantic salmon reovirus infection causes a CD8 T cell myocarditis in Atlantic salmon (*Salmo salar* L.). *PLoS one*. 2012;7(6):e37269.
122. Barber LD, Parham P. Peptide binding to major histocompatibility complex molecules. *Annual review of cell biology*. 1993;9(1):163-206.
123. Wilson AB. MHC and adaptive immunity in teleost fishes. *Immunogenetics*. 2017;69(8):521-8.
124. Nakanishi T, Fischer U, Dijkstra J, Hasegawa S, Somamoto T, Okamoto N, et al. Cytotoxic T cell function in fish. *Developmental & Comparative Immunology*. 2002;26(2):131-9.
125. Trapani JA, Smyth MJ. Functional significance of the perforin/granzyme cell death pathway. *Nature Reviews Immunology*. 2002;2(10):735-47.
126. Johansen L-H, Dahle MK, Wessel Ø, Timmerhaus G, Løvoll M, Røsæg M, et al. Differences in gene expression in Atlantic salmon parr and smolt after challenge with Piscine orthoreovirus (PRV). *Molecular immunology*. 2016;73:138-50.
127. Johansen L-H, Thim HL, Jørgensen SM, Afanasyev S, Strandkog G, Taksdal T, et al. Comparison of transcriptomic responses to pancreas disease (PD) and heart and skeletal muscle inflammation (HSMI) in heart of Atlantic salmon (*Salmo salar* L.). *Fish & shellfish immunology*. 2015;46(2):612-23.
128. Geissmann F, Manz MG, Jung S, Sieweke MH, Merad M, Ley K. Development of monocytes, macrophages, and dendritic cells. *Science*. 2010;327(5966):656-61.
129. Pereiro P, Figueras A, Novoa B. Insights into teleost interferon-gamma biology: An update. *Fish & shellfish immunology*. 2019;90:150-64.
130. Martinez FO, Gordon S. The M1 and M2 paradigm of macrophage activation: time for reassessment. *F1000prime reports*. 2014;6.
131. Forlenza M, Fink IR, Raes G, Wiegertjes GF. Heterogeneity of macrophage activation in fish. *Developmental & Comparative Immunology*. 2011;35(12):1246-55.

132. Wentzel AS, Petit J, van Veen WG, Fink IR, Scheer MH, Piazzon MC, et al. Transcriptome sequencing supports a conservation of macrophage polarization in fish. *Scientific reports*. 2020;10(1):1-15.
133. Boldogh I, Albrecht T, Porter DD. *Persistent viral infections*. Medical Microbiology 4th edition. 1996.
134. Kane M, Golovkina T. Common threads in persistent viral infections. *Journal of virology*. 2010;84(9):4116-23.
135. Riera Romo M, Pérez-Martínez D, Castillo Ferrer C. Innate immunity in vertebrates: an overview. *Immunology*. 2016;148(2):125-39.
136. Johansen LH, Sommer AI. Multiplication of infectious pancreatic necrosis virus (IPNV) in head kidney and blood leucocytes isolated from Atlantic salmon, *Salmo salar* L. *Journal of fish diseases*. 1995;18(2):147-56.
137. Murray AG. Persistence of infectious pancreatic necrosis virus (IPNV) in Scottish salmon (*Salmo salar* L.) farms. *Preventive veterinary medicine*. 2006;76(1-2):97-108.
138. Knott RM, Munro A. The persistence of infectious pancreatic necrosis virus in Atlantic salmon. *Veterinary immunology and immunopathology*. 1986;12(1-4):359-64.
139. Munang'andu HM, Fredriksen BN, Mutoloki S, Brudeseth B, Kuo T-Y, Marjara IS, et al. Comparison of vaccine efficacy for different antigen delivery systems for infectious pancreatic necrosis virus vaccines in Atlantic salmon (*Salmo salar* L.) in a cohabitation challenge model. *Vaccine*. 2012;30(27):4007-16.
140. Reyes-Cerpa S, Reyes-López FE, Toro-Ascuy D, Ibañez J, Maisey K, Sandino AM, et al. IPNV modulation of pro and anti-inflammatory cytokine expression in Atlantic salmon might help the establishment of infection and persistence. *Fish & shellfish immunology*. 2012;32(2):291-300.
141. Ellis A, Cavaco A, Petrie A, Lockhart K, Snow M, Collet B. Histology, immunocytochemistry and qRT-PCR analysis of Atlantic salmon, *Salmo salar* L., post-smolts following infection with infectious pancreatic necrosis virus (IPNV). *Journal of fish diseases*. 2010;33(10):803-18.
142. Graham D, Fringuelli E, Wilson C, Rowley H, Brown A, Rodger H, et al. Prospective longitudinal studies of salmonid alphavirus infections on two Atlantic salmon farms in Ireland; evidence for viral persistence. *Journal of fish diseases*. 2010;33(2):123-35.
143. Gulla S, Tengs T, Mohammad SN, Gjessing M, Garseth ÅH, Sveinsson K, et al. Genotyping of salmon gill poxvirus reveals one main predominant lineage in Europe, featuring fjord- and fish farm-specific sub-lineages. *Frontiers in microbiology*. 2020;11:1071.
144. Tafalla C, Figueras A, Novoa B. Role of nitric oxide on the replication of viral haemorrhagic septicemia virus (VHSV), a fish rhabdovirus. *Veterinary immunology and immunopathology*. 1999;72(3-4):249-56.

145. Scott CJW, Morris PC, Austin B. Cellulat, Molecular, Genomics, And Biomedical Approaches | Molecular Fish Pathology. In: Farrell AP, editor. Encyclopedia of Fish Physiology. San Diego: Academic Press; 2011. p. 2032-45.
146. Müller A, Sutherland BJ, Koop BF, Johnson SC, Garver KA. Infectious hematopoietic necrosis virus (IHNV) persistence in Sockeye Salmon: influence on brain transcriptome and subsequent response to the viral mimic poly (I: C). *BMC Genomics*. 2015;16(1):1-19.
147. Neukirch M. Demonstration of persistent viral haemorrhagic septicaemia (VHS) virus in rainbow trout after experimental waterborne infection. *Journal of Veterinary Medicine, Series B*. 1986;33(1-10):471-6.
148. Virgin HW, Wherry EJ, Ahmed R. Redefining chronic viral infection. *Cell*. 2009;138(1):30-50.
149. Plotkin SA. Correlates of protection induced by vaccination. *Clinical and vaccine immunology*. 2010;17(7):1055-65.
150. Xu C, Mutoloki S, Evensen Ø. Superior protection conferred by inactivated whole virus vaccine over subunit and DNA vaccines against salmonid alphavirus infection in Atlantic salmon (*Salmo salar* L.). *Vaccine*. 2012;30(26):3918-28.
151. Evensen Ø, Leong J-AC. DNA vaccines against viral diseases of farmed fish. *Fish & shellfish immunology*. 2013;35(6):1751-8.
152. Jensen BB, Kristoffersen AB, Myr C, Brun E. Cohort study of effect of vaccination on pancreas disease in Norwegian salmon aquaculture. *Diseases of aquatic organisms*. 2012;102(1):23-31.
153. Wessel Ø, Haugland Ø, Rode M, Fredriksen BN, Dahle MK, Rimstad E. Inactivated Piscine orthoreovirus vaccine protects against heart and skeletal muscle inflammation in Atlantic salmon. *Journal of fish diseases*. 2018;41(9):1411-9.
154. Haatveit HM, Hodneland K, Braaen S, Hansen EF, Nyman IB, Dahle MK, et al. DNA vaccine expressing the non-structural proteins of Piscine orthoreovirus delay the kinetics of PRV infection and induces moderate protection against heart-and skeletal muscle inflammation in Atlantic salmon (*Salmo salar*). *Vaccine*. 2018;36(50):7599-608.
155. Polinski MP, Marty GD, Snyman HN, Garver KA. Piscine orthoreovirus demonstrates high infectivity but low virulence in Atlantic salmon of Pacific Canada. *Scientific reports*. 2019;9(1):1-22.
156. Miller KD, Schnell MJ, Rall GF. Keeping it in check: chronic viral infection and antiviral immunity in the brain. *Nature Reviews Neuroscience*. 2016;17(12):766.
157. Patton J, Silvestri L, Tortorici M, Vasquez-Del Carpio R, Taraporewala Z, Roy P. *Reoviruses: Entry, Assembly and Morphogenesis*. Springer; 2006.
158. Tyler K, Virgin H, Fields B. Sites of Action of Immune-Mediated Protection Against Neurotropic Reoviruses: 1: 30 PM 1. *Neurology*. 1989;39(3).

159. Santiana M, Ghosh S, Ho BA, Rajasekaran V, Du W-L, Mutsafi Y, et al. Vesicle-cloaked virus clusters are optimal units for inter-organismal viral transmission. *Cell host & microbe*. 2018;24(2):208-20. e8.
160. Dharmotharan K, Tengs T, Wessel Ø, Braaen S, Nyman IB, Hansen EF, et al. Evolution of the piscine orthoreovirus genome linked to emergence of heart and skeletal muscle inflammation in farmed atlantic salmon (*salmo salar*). *Viruses*. 2019;11(5):465.
161. Smith JA, Schmechel SC, Williams BR, Silverman RH, Schiff LA. Involvement of the interferon-regulated antiviral proteins PKR and RNase L in reovirus-induced shutoff of cellular translation. *Journal of virology*. 2005;79(4):2240-50.
162. Chang YH, Lau KS, Kuo RL, Horng JT. dsRNA Binding Domain of PKR Is Proteolytically Released by Enterovirus A71 to Facilitate Viral Replication. *Front Cell Infect Microbiol*. 2017;7:284.
163. Samuel CE, Duncan R, Knutson GS, Hershey J. Mechanism of interferon action. Increased phosphorylation of protein synthesis initiation factor eIF-2 alpha in interferon-treated, reovirus-infected mouse L929 fibroblasts in vitro and in vivo. *Journal of Biological Chemistry*. 1984;259(21):13451-7.
164. Press CM, Evensen Ø. The morphology of the immune system in teleost fishes. *Fish & shellfish immunology*. 1999;9(4):309-18.
165. Ellis A. Antigen-trapping in the spleen and kidney of the plaice *Pleuronectes platessa* L. *Journal of fish diseases*. 1980;3(5):413-26.
166. Wang T, Hanington PC, Belosevic M, Secombes CJ. Two macrophage colony-stimulating factor genes exist in fish that differ in gene organization and are differentially expressed. *The Journal of Immunology*. 2008;181(5):3310-22.
167. Hume DA, MacDonald K. Therapeutic applications of macrophage colony-stimulating factor-1 (CSF-1) and antagonists of CSF-1 receptor (CSF-1R) signaling. *Blood*. 2012;119(8):1810-20.
168. Nikitina E, Larionova I, Choinzonov E, Kzhyshkowska J. Monocytes and macrophages as viral targets and reservoirs. *Int J Mol Sci*. 2018;19(9):2821.
169. Bülow Vv, Klasen A. Effects of avian viruses on cultured chicken bone-marrow-derived macrophages. *Avian Pathology*. 1983;12(2):179-98.
170. Lai CM, Boehme KW, Pruijssers AJ, Parekh VV, Van Kaer L, Parkos CA, et al. Endothelial JAM-A promotes reovirus viremia and bloodstream dissemination. *The Journal of infectious diseases*. 2015;211(3):383-93.
171. Garseth Å, Fritsvold C, Opheim M, Skjerve E, Biering E. Piscine reovirus (PRV) in wild Atlantic salmon, *Salmo salar* L., and sea-trout, *Salmo trutta* L., in Norway. *Journal of fish diseases*. 2013;36(5):483-93.
172. Gordon S. The macrophage: past, present and future. *European journal of immunology*. 2007;37(S1):S9-S17.
173. Gordon S, Taylor PR. Monocyte and macrophage heterogeneity. *Nature Reviews Immunology*. 2005;5(12):953-64.




174. Lassalle MW, Igarashi S, Sasaki M, Wakamatsu K, Ito S, Horikoshi T. Effects of melanogenesis-inducing nitric oxide and histamine on the production of eumelanin and pheomelanin in cultured human melanocytes. *Pigment cell research*. 2003;16(1):81-4.
175. Viola A, Munari F, Sánchez-Rodríguez R, Scolaro T, Castegna A. The metabolic signature of macrophage responses. *Frontiers in immunology*. 2019;10:1462.
176. Falk K, Press CM, Landsverk T, Dannevig BH. Spleen and kidney of Atlantic salmon (*Salmo salar* L.) show histochemical changes early in the course of experimentally induced infectious salmon anaemia (ISA). *Veterinary immunology and immunopathology*. 1995;49(1-2):115-26.
177. Grayfer L, Kerimoglu B, Yaparla A, Hodgkinson JW, Xie J, Belosevic M. Mechanisms of fish macrophage antimicrobial immunity. *Frontiers in immunology*. 2018;9:1105.
178. Gama L, Abreu C, Shirk EN, Queen SE, Beck SE, Pate KAM, et al. SIV latency in macrophages in the CNS. *HIV-1 Latency*. 2018:111-30.
179. Liang B, Su J. Inducible nitric oxide synthase (iNOS) mediates vascular endothelial cell apoptosis in grass carp reovirus (GCRV)-induced hemorrhage. *Int J Mol Sci*. 2019;20(24):6335.
180. Dahle MK, Jørgensen JB. Antiviral defense in salmonids—Mission made possible? *Fish & shellfish immunology*. 2019;87:421-37.
181. Wiik-Nielsen J, Alarcón M, Jensen BB, Haugland Ø, Mikalsen A. Viral co-infections in farmed Atlantic salmon, *Salmo salar* L., displaying myocarditis. *Journal of fish diseases*. 2016;39(12):1495-507.
182. Madhun AS, Karlsbakk E, Isachsen CH, Omdal LM, Eide Sørvik A, Skaala Ø, et al. Potential disease interaction reinforced: double-virus-infected escaped farmed Atlantic salmon, *Salmo salar* L., recaptured in a nearby river. *Journal of fish diseases*. 2015;38(2):209-19.
183. Løvoll M, Wiik-Nielsen J, Grove S, Wiik-Nielsen CR, Kristoffersen AB, Faller R, et al. A novel totivirus and piscine reovirus (PRV) in Atlantic salmon (*Salmo salar*) with cardiomyopathy syndrome (CMS). *Virology Journal*. 2010;7(1):1-7.
184. Røsæg MV, Lund M, Nyman IB, Markussen T, Aspehaug V, Sindre H, et al. Immunological interactions between Piscine orthoreovirus and Salmonid alphavirus infections in Atlantic salmon. *Fish & shellfish immunology*. 2017;64:308-19.
185. Tenorio R, Fernández de Castro I, Knowlton JJ, Zamora PF, Sutherland DM, Risco C, et al. Function, architecture, and biogenesis of reovirus replication neorganelles. *Viruses*. 2019;11(3):288.
186. Wang F, Flanagan J, Su N, Wang L-C, Bui S, Nielson A, et al. RNAscope: a novel in situ RNA analysis platform for formalin-fixed, paraffin-embedded tissues. *The Journal of molecular diagnostics*. 2012;14(1):22-9.

9. Scientific papers I-IV

I

Article

Erythroid Progenitor Cells in Atlantic Salmon (*Salmo salar*) May Be Persistently and Productively Infected with Piscine Orthoreovirus (PRV)

Muhammad Salman Malik¹, Håvard Bjørgen², Kannimuthu Dhamotharan¹, Øystein Wessel¹ , Erling Olaf Koppang², Emiliano Di Cicco³, Elisabeth F. Hansen¹, Maria K. Dahle⁴ , and Espen Rimstad^{1,*} 

¹ Department of Food Safety and Infection Biology, Faculty of Veterinary Medicine, Norwegian University of Life Sciences, 0454 Oslo, Norway

² Department of Basic Science and Aquatic Medicine, Faculty of Veterinary Medicine, Norwegian University of Life Sciences, 0454 Oslo, Norway

³ Pacific Biological Station, Fisheries and Oceans Canada, Nanaimo, BC V9T 6N7, Canada

⁴ Department of Fish Health, Norwegian Veterinary Institute, 0454 Oslo, Norway

* Correspondence: espen.rimstad@nmbu.no; Tel.: +47-672-32-227

Received: 1 July 2019; Accepted: 3 September 2019; Published: 5 September 2019



Abstract: Piscine orthoreovirus (PRV-1) can cause heart and skeletal muscle inflammation (HSMI) in farmed Atlantic salmon (*Salmo salar*). The virus targets erythrocytes in the acute peak phase, followed by cardiomyocytes, before the infection subsides into persistence. The persistent phase is characterized by high level of viral RNA, but low level of viral protein. The origin and nature of persistent PRV-1 are not clear. Here, we analyzed for viral persistence and activity in various tissues and cell types in experimentally infected Atlantic salmon. Plasma contained PRV-1 genomic dsRNA throughout an 18-week long infection trial, indicating that viral particles are continuously produced and released. The highest level of PRV-1 RNA in the persistent phase was found in kidney. The level of PRV-1 ssRNA transcripts in kidney was significantly higher than that of blood cells in the persistent phase. In-situ hybridization assays confirmed that PRV-1 RNA was present in erythroid progenitor cells, erythrocytes, macrophages, melano-macrophages and in some additional un-characterized cells in kidney. These results show that PRV-1 establishes a productive, persistent infection in Atlantic salmon and that erythrocyte progenitor cells are PRV target cells.

Keywords: PRV-1; piscine orthoreovirus; persistence; erythroid progenitor cells

1. Introduction

Marine farming of Atlantic salmon (*Salmo salar*) has become a major industry. Infectious diseases pose a significant threat for intensive aquaculture, and pathogens produced in dense farmed populations may be extensively released and be a threat for wild fauna [1]. Piscine orthoreovirus (PRV) is a virus with ubiquitous presence in farmed Atlantic salmon in the final half of the marine grow out phase [2]. PRV can induce heart and skeletal muscle inflammation (HSMI) in Atlantic salmon [3,4], where the major pathological changes are moderate to severe endo-, myo- and epicarditis and red skeletal myositis and myonecrosis [5]. However, PRV can be present in Atlantic salmon without HSMI lesions, indicating that factors related to virus strains, host, and environment including management influence the outcome of the infection [5–8]. HSMI causes low to moderate mortality (0–20%), but the number of HSMI outbreaks is high in some areas, leading to a significant effect on the Atlantic salmon aquaculture industry.

PRV belongs to the family Reoviridae, genus Orthoreovirus, which has a 10-segmented double stranded RNA (dsRNA) genome enclosed in a double-layered protein capsid [9]. The genomic segments are divided into three groups; long (L1-L3), medium (M1-M3) and small (S1-S4). Currently there are three identified genotypes of PRV; some forms of PRV-1 causes HSMI in Atlantic salmon [4]; PRV-2 causes erythrocytic inclusion body syndrome (EIBS) in coho salmon (*Oncorhynchus kisutch*) [10], and PRV-3 causes heart inflammation in Rainbow trout (*Oncorhynchus mykiss*) [11].

A number of studies addressing of PRV-1 have focused on the acute phase of infection, which is characterized by infection of erythrocytes and cardiomyocytes, leading to the development of HSMI [12]. Piscine erythrocytes are nucleated and particularly young salmonid erythrocytes contain the transcriptional and translational machinery enabling virus replication [13]. In an experimental challenge study of EIBS in coho salmon, inclusions appeared only in immature erythrocytes at an early stage in the disease development [14]. The acute phase of PRV-1 infection in Atlantic salmon erythrocytes occurs 4-6 weeks after virus exposure and lasts for approximately 1-2 weeks, after which the virus protein load falls radically in blood cells, and the virus infection transfers into persistence [15]. The PRV structural and non-structural proteins, apart from a fragment of the structural protein $\mu 1$, are below detection level after the acute phase [15]. On the other hand, the level of viral RNA in blood cells does not drop accordingly; which indicates continuous viral transcription with partial arrest of viral translation. Generally, farmed Atlantic salmon do not eliminate PRV-1, since viral RNA can be detected in different tissues for at least 36 week post infection in experimental trials (end of experiment) [2], and in blood for more than a year after challenge [16]. PRV-1 strains that cause HSMI induce an innate antiviral immune response in erythrocytes in the acute phase of the infection [17], while infection with PRV-1 strains from BC, Canada associated with lack of or mild clinical signs and no elevated mortality and only a low antiviral transcriptional response in the host [8,18]. However, establishment of persistent infection, requires viral evasion of the innate immune response, i.e., viral dsRNA must be shielded from dsRNA recognizing receptors [19]. Studies of the mammalian orthoreovirus (MRV) have shown that genomic dsRNA is not exposed in the cytoplasm, as viral mRNA transcription occurs within core particles [20]. New positive ssRNA strands are encapsidated before they template the synthesis of negative strands to form the dsRNA genome [21]. Less information is available for PRV replication, since all genotypes have resisted cultivation in fish cell lines, and most studies have been performed in experimentally infected fish.

Persistent infections of PRV-1 in farmed Atlantic salmon represent a formidable reservoir of virus, with estimated more than 400 million infected individuals per year in Norway alone. An experimental trial indicated that fish persistently infected with PRV-1 do not continuously shed the virus, since PRV-1 was not transmitted to sentinel fish from persistently infected shedders at 59 weeks post challenge [16]. On the other hand, farmed fish may be immunosuppressed due to crowding, transportation, handling and various treatments, possibly allowing the virus production to proceed. For example, fish persistently infected with infectious pancreatic necrosis virus (IPNV), another dsRNA virus, have been found to be intermittent virus shedders [22]. However, a recent study found that the prevalence of PRV in farmed escapees (86%) was significantly higher than in wild salmon (8%), and did not find association between salmon farming and prevalence of PRV infection in wild salmon [23].

In this study, we characterized the viral kinetics during the acute and persistent phase of PRV-1 infection in Atlantic salmon. PRV-1 establishes a persistent, low-activity, but productive infection in Atlantic salmon. Using *in situ* hybridization techniques for cell-specific detection of PRV, PRV-1 persistence was mapped to the erythropoietic tissue of kidney, particularly to erythroid progenitor cells, macrophages, melano-macrophages, and erythrocytes.

2. Materials and Methods

2.1. Experimental Challenge

Atlantic salmon smolts, approximately of 200 g size at onset of experiment, were reared in tanks at 40 kg/m³, supplied with particle filtered and UV treated seawater at 12 °C ± 1 °C, 34 ‰ salinity and 24-hour daylight regime. The fish originated from broodstock found negative by RT-qPCR for infectious salmon anemia virus (ISAV), salmonid alphavirus (SAV), infectious pancreatic necrosis virus (IPNV) and PRV. The study population was tested and found negative for these agents before recruitment to the experiment. The PRV-1 NOR2012 isolate was used as challenge material, an isolate that originated from an HSMI outbreak in 2012 and that has been repeatedly used in experimental infections reproducing HSMI [4]. The inoculum consisted of pelleted blood cells diluted in PBS. It was administered by intraperitoneal (i.p.) injection using 0.1 mL per fish to ensure a defined time point of infection ($n = 42$). Control group of uninfected fish ($n = 42$) were kept in a separate tank. The fish were anesthetized by bath immersion in benzocaine chloride (2–5 min, 0.5 g/10 L) prior to handling, and euthanized using overdose of benzocaine chloride (1 g/5 L). Sampling ($n = 6$) was done every third week by harvesting heart, spleen, kidney, skeletal muscle and blood cells in RNeasy Lysis Buffer (Thermo Fischer Scientific, Waltham, MA, USA) and in formalin until termination of the study at 18 weeks post challenge (wpc). Plasma was collected from the blood samples. The sampling intervals reflect a focus on the persistent phase and not the viral peak or eventual development of histopathological lesions typical of HSMI.

2.2. Ethics Statement

An experimental challenge with PRV-1 was performed at the VESO Vikan research facility (Namsos, Norway), in compliance with the regulatory requirements by Norwegian Food Safety Authority, EU Council Directive 2004/10/EC and Guidelines to Good Manufacturing Practice by European Commission Directives 2003/94/EC and 91/412/EC. The Norwegian Food Safety Authority (NFSA) according to the European Union Directive 2010/63/EU for animal experiments approved the experiment (use protocol V3740).

2.3. RNA Isolation

Total RNA was isolated from pelleted blood cells (20 µL), spleen and kidney samples (25 mg) by using QIAzol Lysis Reagent (Qiagen, Hilden, Germany), TissueLyser II (Qiagen) with 5 mm steel beads for 2 × 5 min at 25 Hz followed by chloroform addition and collection of the aqueous phase. RNeasy QIAcube Kit (Qiagen) was used for automated RNA isolation of the aqueous phase as described by manufacturer. RNA was quantified in a NanoDrop ND-100 spectrophotometer (Thermo Fisher Scientific, Waltham, MA, USA). For cell free samples (plasma), 10 µL plasma was diluted in 130 µL PBS and QIAamp Viral RNA Mini QIAcube Kit (Qiagen) used according to the manufacturer instructions. Isolated RNA was eluted in 60 µL RNase-free water and stored at –80 °C until further use.

2.4. RT-qPCR

For transcription analysis of the individual PRV segments, cDNA was synthesized from 1 µg RNA of spleen tissue and blood cells using Quantitect Reverse Transcription Kit (Qiagen) with genomic DNA elimination (Qiagen) following the manufacturer's instructions with prior denaturation of RNA at 95 °C for 5 min. Quantitative PCR was performed using 15 ng cDNA input in a total reaction volume of 12 µL and Maxima SYBR Green/ROX qPCR Master Mix (2X)-K0253. qPCRs were run with initial denaturation for 10 min/95 °C and 40 cycles of 15 sec/95 °C, 30 sec/60 °C and 30 sec/72 °C. Cut-off value was set to Ct 34. Specificity of assays were confirmed by melting point analysis, and all samples were run on the same plate with positive and no template controls (NTC). Elongation factor (EF1α) was used as reference gene and its expression in spleen and blood cells for the individual fish is showed in Figure S1.

For PRV S1 segment, one-step RT-qPCR assay was performed for blood cells and kidney samples using Qiagen OneStep kit (Qiagen) with 100 ng (5 μ L of 20 ng/ μ L) RNA per reaction, or purified RNA from 5 μ L plasma, in duplicates of 12.5 μ L total reaction volume. RNA was used both with and without a prior denaturation step, i.e. pre-heating at 95 $^{\circ}$ C of the template to evaluate ratio between genomic dsRNA and single stranded transcripts [8]. Cycling parameters were 30 min/50 $^{\circ}$ C, 15 min/95 $^{\circ}$ C, 40 cycles of 15 sec/94 $^{\circ}$ C, 30 sec/60 $^{\circ}$ C and 30 sec/72 $^{\circ}$ C. Samples were run in duplicates and cut off value was set to Ct 35 [3]. Analyses were based on mean Ct-value of six fish per group per sampling. Sequences of probes and primers, and specific concentrations are listed in Table 1. Primer sequences were designed by software MEGA version 7.0 and open source primer-3 applications.

Table 1. Primer and probe sequences (5'-3') for various PRV gene segments.

Target (PRV)	Primer/Probe	Concentration	Sequence (5'-3')
L1	Fwd	400 nM	CGCACTCCCACAGATACAGTTC
	Rev		CGCGAGGTGTACGTATTGTGA
M2	Fwd	400 nM	AGACTGGGAAGATCGTTGCTTT
	Rev		ATGCGTCTTGTGAGTGTAGGT
M3	Fwd	400 nM	GGCCTGCATTGTGTCAACGT
	Rev		TGCGTTCAAGGTCGTCTCA
S1 [12]	Fwd	400 nM	TGCGTCTGCGTATGGCACC
	Rev	300 nM	GGCTGGCATGCCGAATAGCA
	Probe (FAM)	300 nM	ATCACAACGCCTACTCT
S2	Fwd	400 nM	ATCAATGGCTTCGCTCTTCTCTCT
	Rev		TCTATATCCATTGCCGCAITTTCCAGC
S3	Fwd	300 nM	AGCATCTCACCAITTTCCAAGCACTT
	Rev		AGAGGCACGATACACTAGAGCTTGA
EF1 α [24]	Fwd	300 nM	TGCCCTCCAGGATGTCTAC
	Rev		CACGGCCACAGGACTGTG

2.5. Data Analysis

RT-qPCR data was analyzed and graphically laid out with Graphpad Prism version 8.1.1 (Graphpad Software Inc., La Jolla, CA, USA). Statistical analysis was performed to measure PRV genomic segment expression, ratio of PRV genomic segments and viral transcripts in tissue and ratio of ssRNA viral transcripts level in blood cells and kidney by applying Wilcoxon matched-pairs signed rank test, and *p*-values of *p* \leq 0.05 were considered as significant.

2.6. Western Blotting

Heparinized blood cell pellets from the experimental PRV-1 challenged Atlantic salmon were used for virus protein expression analysis in western blotting (WB). Heparinized blood from PRV-1 infected and uninfected fish from a previous challenge trial were used as positive and negative controls, respectively [3]. For each sample, 15 μ L blood pellet was added to Nonidet-P40 lysis buffer containing complete ultra mini protease inhibitor cocktail (1:5) (Roche, Mannheim, Germany) and incubated for 30 min on ice. After centrifugation at 5000 \times *g* for 5 min, the supernatant was diluted with DEPC treated water (1:5) and mixed with XT sample buffer and XT reducing agent (Bio-Rad, Hercules, CA, USA) and boiled at 95 $^{\circ}$ C for 5 min. PRV proteins were separated by sodium dodecyl sulfate-polyacrylamide gel electrophoresis (SDS-PAGE), using 4–12% criterion XT bis-tris gel. TransBlot Turbo (Bio-Rad) for 20 min at 15 V transferred proteins to polyvinylidene fluoride (PVDF) membranes (Bio-Rad). The membranes were incubated at 4 $^{\circ}$ C overnight using polyclonal rabbit sera anti- σ 1 and anti- μ 1C diluted 1:500; [24]. Rabbit anti-actin (Sigma-Aldrich, St. Louis, MO, USA) was used to standardize the amount of protein added to the blots. Horseradish peroxidase (HRP)-conjugated anti-rabbit IgG (1:20,000) (Amersham, GE Healthcare, Buckinghamshire, UK) was used as secondary antibody. For immune detection, Clarity Western ECL Substrate kit (Bio-Rad) was used along with Precision Plus Protein™ (Bio-Rad)

as molecular weight ladder. Images were developed by ChemiDoc XRS+ System and ImageOne software (Bio-Rad).

2.7. In-Situ Hybridization (ISH)

RNAscope® (RED) 2.5 HD Detection Kit (Advanced Cell Diagnostic, Newark, CA, USA) was used for RNA-ISH, following the instructions of the manufacturer. Paraffin embedded tissue sections (5 µm) of spleen, kidney and heart from PRV-challenged fish with lowest Ct values from each sampling were dewaxed at 60 °C for 90 min in ACD HybEZ™ II followed by hydrogen peroxide for 10 min incubation at room temperature. Samples were boiled in RNAscope target antigen retrieval reagent for 15 min and each section was incubated with RNAscope protease plus at 40 °C for 15min in HybEZ™ oven. Each section was hybridized by RNAscope probe (Table 2) designed against PRV-1 genome segment L3 (Advanced Cell Diagnostics catalog number-537451), that encodes inner capsid protein (helicase) for 2 hrs at room temperature. Probe targeting Peptidylpropyl Isomerase B (PPIB) in Atlantic salmon (Advanced Cell Diagnostics, catalog number-494421) was used reference target gene expression to test for RNA integrity in the samples. As negative control, probe-DapB (Advanced Cell Diagnostics catalog number-310043) were used to evaluate cross reactivity (Figure S2). Fast Red chromogenic substrate was used for detection of signals amplified following manufacturer's instructions. Counterstaining was done with 50% Gill's hematoxylin solution and mounted with EcoMount (BioCare Medical, Pacheco, CA, USA). Imaging was performed by bright field microscopy (Carl Zeiss Light Microscopy System with Axio Imager 2 (Carl Zeiss AG, Oberkochen, Germany). Fish injected i.m. ($n = 42$) with heat inactivated (85 °C, 20 min) PRV-1 infected erythrocytes were used as control fish (Figure S5).

Table 2. Target and control probes for *in situ* hybridization.

	Probe	Channel **	Accession no.	Target Region (bp)
Target	PRV-L3	C1	KY429945	415–1379
	MCSFR	C2	NM_001140235	434–1425
	EPOR	C2	NM_001140235	764–1754
Control	PPIB *	C1	NM_001140870	20–934
	DapB *	C1	EF191515	414–862
	DapB *	C2	EF191515	414–862

* Controls shown in Figure S3 ** Channel is a spectral attribution of the probes, which gives specific output with different amplification and detection systems.

2.8. Duplex In-Situ Hybridization

RNAscope® 2.5 HD Duplex Detection Kit-Chromogenic for simultaneous detection of two RNA targets (Advanced Cell Diagnostics) was used for kidney and spleen samples. Probes for PRV-1 segment L3 was combined with probes for macrophage colony stimulating factor (MCSFR) (Advanced Cell Diagnostics catalog number-557811) or erythropoietin receptor (EPOR) (Advanced Cell Diagnostics catalog number-561741) (Table 2). Additional amplification steps were applied (Amp1-Amp10) for the duplex assay according to manufacturer's instructions. Signals were detected by using Green substrate specific for HRP conjugated probes and Fast Red for Alkaline phosphatase (AP) conjugated probes. Each slide was counter stained with 50% Gill's hematoxylin staining solution and mounted with VectaMount (Cat. No: H-5000, Vector Labs, Burlingame, CA, USA).

3. Results

3.1. PRV-1 Segments Have Similar Expression Pattern

The segment expression levels, judged through Ct values, were very similar as assessed in a time course study of PRV-1 infection (0–18 weeks). RNA levels of various PRV-1 segments in blood and spleen were mapped in order to investigate potential differential expression pattern of the segments in the acute and persistent phases of infection. The analysis targeted the genomic segments L1, M2,

M3, S1, S2 and S3; and individual fish with a low number of L and M segment copies, also had low number of S segment copies (Figure 1). In blood cells, the amount of PRV-1 RNA levelled out from 6 wpc towards the end of the study (18 wpc) (Figure 1A,B). In spleen, peak PRV RNA load for all segments was reached at 6 wpc, followed by a gradual reduction in viral RNA (Figure 1C,D). Figure 1E shows the difference in the PRV-1 RNA loads in blood, i.e., levelling out from 6 wpc, versus that of spleen, i.e., a more gradual reduction. PRV segment expression levels were not significantly different. PRV-1 was not cleared from any of the sampled fish, but at 18 weeks the PRV RNA level varied more between individual fish compared to the preceding samplings (Figure 1).

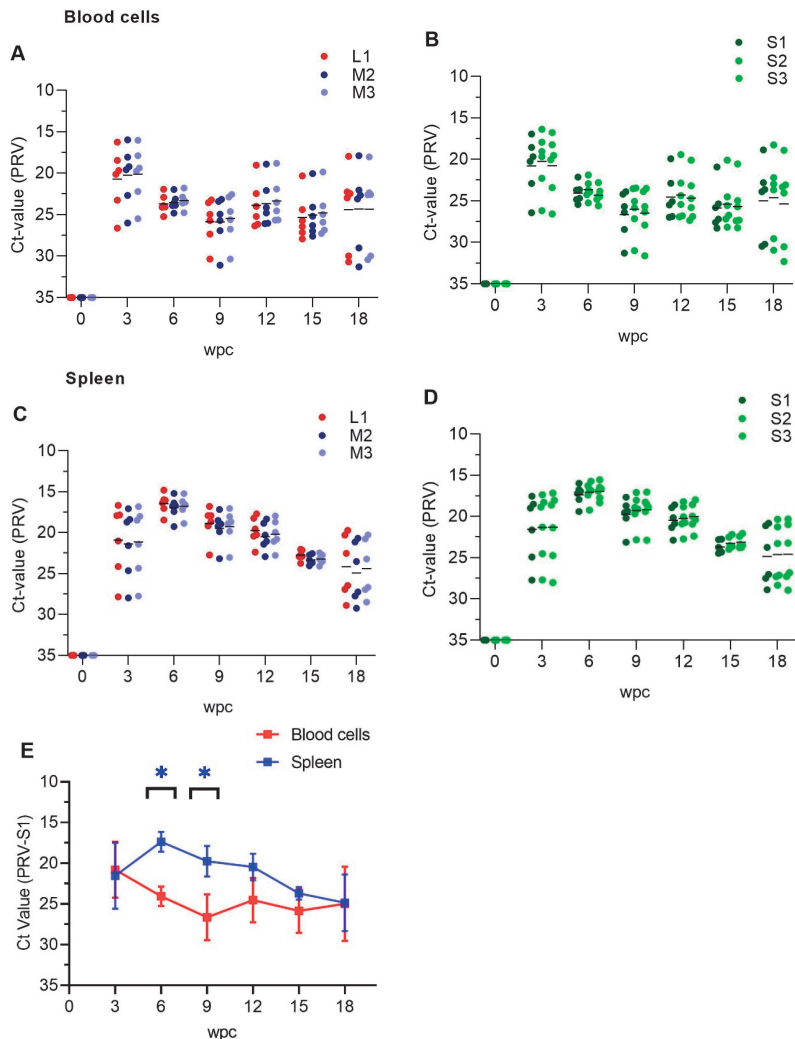


Figure 1. Expression analysis of PRV-1 segments and transcripts. qPCR detection of segment L1, M2, M3, S1-S3 and corresponding transcripts in blood cells (A,B) and spleen (C,D) from Atlantic salmon. Individual fish shown as dots, and mean Ct value-PRV as lines. $n = 6$ for each point. (E) S1 as a representative for PRV genomic segments expression between blood cells and spleen. Paired analysis was performed by non-parametric Wilcoxon matched pairs signed rank test ($p < 0.05$), asterisk (*) indicates significantly different group. wpc = weeks post challenge.

3.2. Viral Genomic RNA Versus Viral Transcripts

Genomic dsRNA levels were higher in both blood cells and kidney than PRV transcripts at each time point of the experiment (Figure 2A,B). Isolated RNA with or without prior denaturation before cDNA synthesis was used in qPCR to estimate the ratio between viral genomic dsRNA and ssRNA transcripts, where the dsRNA will make up the difference between denatured and non-denatured RNA (Table S1). At the peak of infection at 3 wpc, ssRNA viral transcripts levels were high in blood cells and Δ Ct value between denatured and non-denatured was 1, i.e., ssRNA made up approximately 50% of the viral RNA (Figure 2A). For the samples from 6 wpc onward the Δ Ct between denatured and non-denatured RNA was on average -4 for blood cells. It indicated that the viral genomic dsRNA level was approximately 16 fold higher, or that ssRNA made up approximately 6% of the viral RNA in blood cells (Figure 2A, Table S1A). Paired data analysis showed significantly high levels of ssRNA PRV transcripts in blood cells during acute phase i.e 3wpc, and in kidney during persistent phase (9 wpc–18 wpc) of infection, when compared to each other (Figure 2D). The ssRNA level in kidney was higher during persistent phase indicating active transcription and viral activity in this organ. In plasma, viral ssRNA transcripts were detectable at the viral peak at 3 wpc, but not thereafter (Figure 2C, Table S1C), while PRV-1 genomic dsRNA was present in plasma throughout experiment (Figure 2C). However, at 9, 15 and 18 wpc the dsRNA could not be detected in 2-3 out of six fish.

3.3. Low Level of PRV-1 Protein Synthesis in the Persistent Phase

Western blotting did not detect expression of PRV σ 1 and σ 3 proteins in blood cells in the persistent phase. Samples from fish with high loads of viral RNA, collected from the acute phase of infection at 3 wpc and 6 wpc, were compared to samples from the persistent phase of infection at 15 wpc and 18 wpc (two fish per time point). σ 1 specific bands (34.6 kDa) were only detected in samples from 3 wpc. Similarly σ 3 specific bands (approximately 35 kDa) were also observed, but bands were not stronger than negative control thereafter (Figure 3).

3.4. Tissue Localization of PRV-1 in the Acute Phase

In situ hybridization targeting PRV was performed on 3 samples from individual fish from each time point, 3 wpc and 6 wpc representing the acute and early persistent phase, respectively, and 9 wpc and 18 wpc representing the persistent phase. PRV demonstrated of tissue specific localization in heart, spleen and kidney.

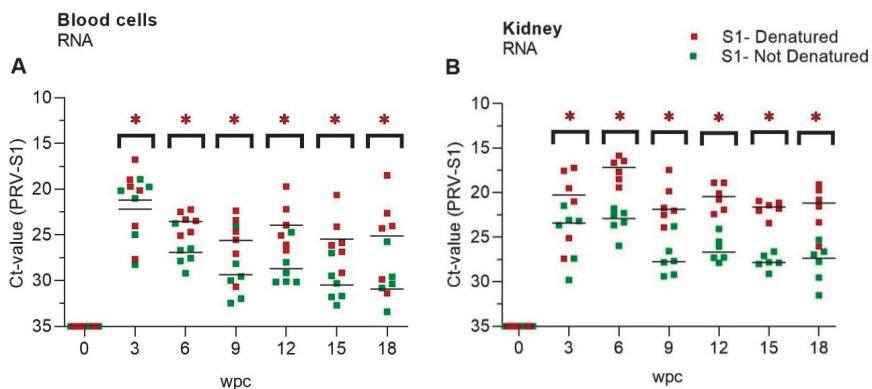


Figure 2. Cont.

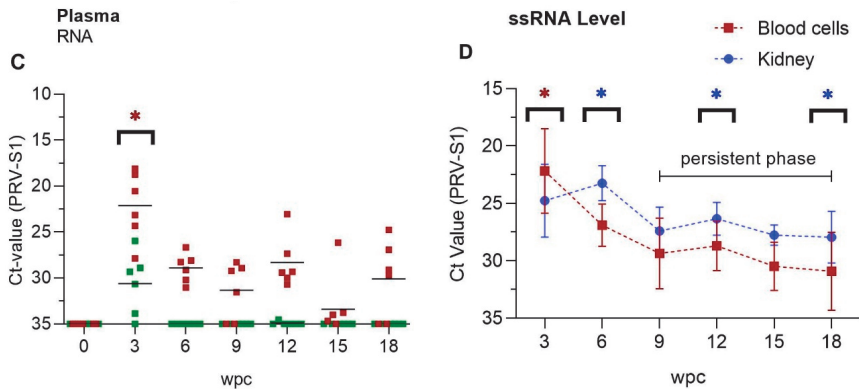


Figure 2. PRV-1 dsRNA and ssRNA levels. Mean Ct-values of RT-qPCR (PRV-S1) for (A) Blood cells, (B) Kidney and (C) Plasma was pre-heated (red dots) or not (green dots), indicating presence of viral dsRNA plus ssRNA transcripts or ssRNA PRV transcripts only, respectively. $n = 6$ for each time point. Statistical analysis between denaturated and not-denaturated samples from the same RNA was performed by non-parametric, Wilcoxon matched pairs signed rank test. Asterisk shows significantly high level ($* p < 0.05$) (D) Paired analysis of ssRNA Ct-values (Table S1) of kidney compared to blood cells in persistent phase (9 wpc–18 wpc). Each dot shows mean Ct-value at each time point. Statistical analysis was performed by non-parametric, Wilcoxon matched pairs signed rank test ($p < 0.05$), asterisk (red/blue) indicates significantly different group.). wpc = weeks post challenge.

In heart, PRV-1 was not detected at 3 wpc (Figure 4A). At 6 wpc, numerous cardiomyocytes in the spongy layer (*stratum spongiosum*) of the heart ventricle showed abundant viral staining, whereas a few positive cells in the inner part of compact layer (*stratum compactum*) (Figure 4B) and a few positive erythrocyte-like cells or infiltrating macrophage-like cells were present in the epicardium.

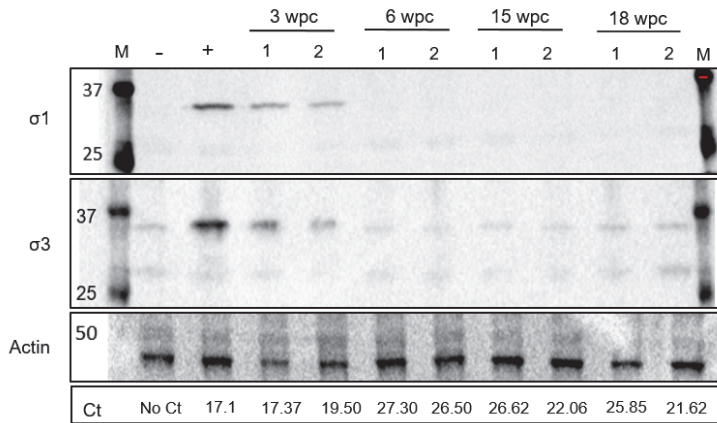


Figure 3. Low levels of PRV proteins in the persistent phase. Detection of outer PRV-1 capsid proteins $\sigma 1$ and $\sigma 3$ in blood cells from 3–18 weeks post challenge (wpc) by western blotting. Ct values in lower row. Actin (42 kDa) was used as a protein load control. Blood cells from uninfected fish used as negative control. Positive control sample from a fish having Ct value of 17.1 and significant $\sigma 1$ protein level [15].

In spleen at 3 wpc, some erythrocytes, melano-macrophages and cells with macrophage-like morphology (“macrophage-like cells”) were positively stained (Figure 4C). At 6 wpc PRV-1 was localized in large number of erythrocyte-like cells in the spleen. These cells had aberrant shape or signs

of damage. Red pulp contained primarily PRV-1 positive cells. Clusters of PRV-1 positive macrophage- and erythrocyte-like cells were scattered throughout the tissue (Figure 4D).

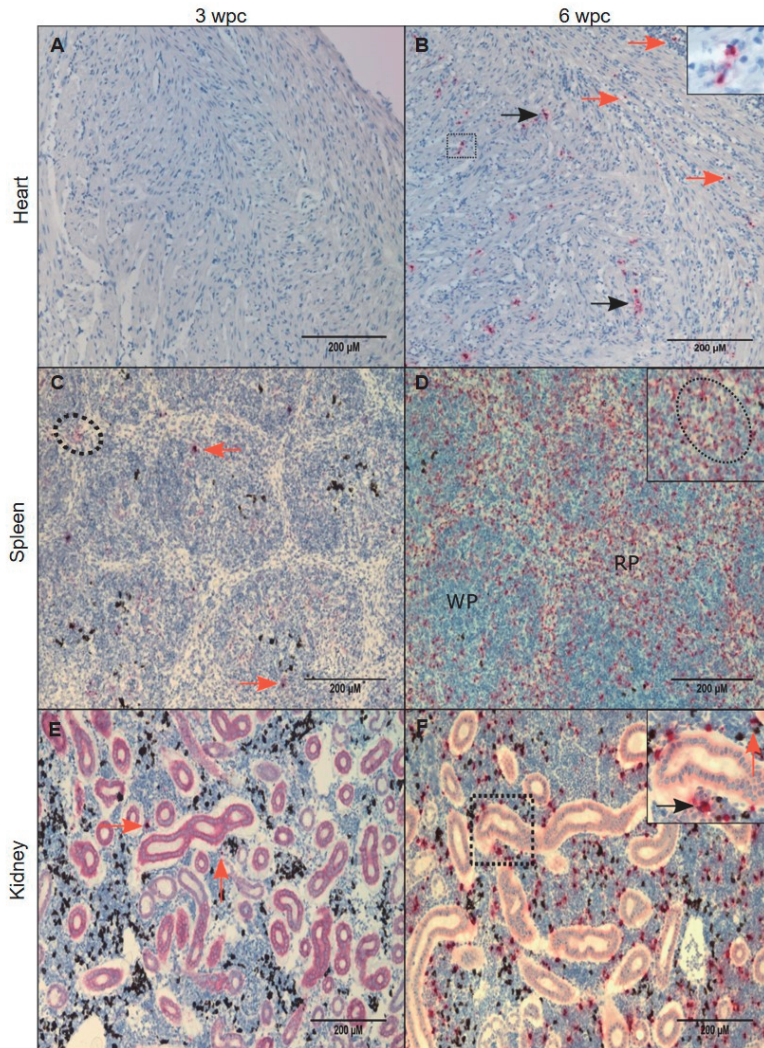


Figure 4. PRV-1 localization in the acute phase. PRV-1 localization shown by *in situ* hybridization (red) at 3 and 6 wpc. Heart (A,B): A, (3 wpc), no PRV detection. B, (6 wpc), PRV positive cardiomyocytes in compact layer (orange arrows) and a few positive erythrocytes or infiltrating macrophage-like cells were present in the epicardium and scattered PRV staining in the spongy layer of the heart ventricle (black arrows). Spleen (C,D): C, (3 wpc), few PRV-1 positive RBCs (dotted circle) and macrophage-like cells (orange arrows). D (6 wpc) shows a large number of positively stained cells in the red pulp (RP) area. Dotted circle in magnified version in upper right corner shows cluster of cells with erythrocyte- and macrophage-like morphology. Kidney (E,F): E, (3 wpc) shows a few PRV-1 positive cells (orange arrow), primarily macrophage-like cells. F, (6 wpc), a high number of PRV-1 positive macrophage-like cells (black arrow) along with melano-macrophages (orange arrow) were found in peritubular regions of the kidney. Scale bar = 200 μ m.

In kidney, primarily cells morphologically assessed as macrophage-like and in melano-macrophages stained PRV-1 positive. At 3 wpc, only a few positive cells were identified (Figure 4E). At 6 wpc, several PRV-1 positive macrophage-like cells and melano-macrophages were found in the peritubular regions of the kidney (Figure 4F).

3.5. Tissue Localization of PRV-1 in the Persistent Phase

PRV-1 gradually cleared from the heart in the persistent phase. Few PRV-1 positive cells were visible in the *stratum compactum* at 9 wpc and 12 wpc, as some positive cardiomyocytes were still detected (Figure 5A and Figure S4).

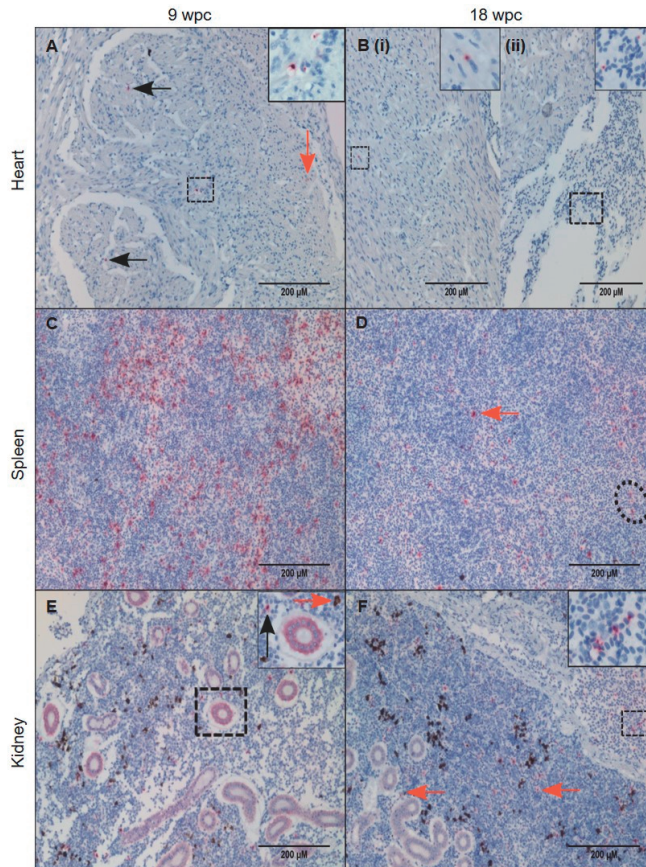


Figure 5. PRV-1 localization during the persistent phase. PRV-1 localization shown by *in situ* hybridization (red) at 9 and 18 wpc. Heart (**A,B**): **A**, (9 wpc) A small number of cells in the compact layer stained positive for PRV-1 (orange arrow), and similarly faintly in a few macrophage-like cells in the in the luminal space of the spongy layer (black arrows) and some circulatory cells, near blood vessel (dotted square and magnified image). **B**, (18 wpc) Very few cells were positive for PRV-1 with the exception of (i) some positive cardiomyocytes in the spongy layer (dotted square) or (ii) peripheral blood in the heart (dotted square). Spleen (**C,D**): **C**, (9 wpc) numerous PRV-1 positive cells in red pulp. **D**, (18 wpc) A few PRV-1 positive macrophage-like cells (orange arrow) and erythrocyte like cells (dotted circle). Kidney (**E,F**): **E**, (9 wpc) PRV-1 present in macrophage-like cells (black arrow) and melano-macrophages (orange arrow). **F**, (18 wpc) PRV-1 positive erythrocytes and macrophage-like cells throughout the section (orange arrows) and in blood vessels (magnified picture). Scale bar = 200 µm.

Moreover, peripheral blood in the heart contained PRV-1 positive circulatory cells (Figure 5B). Putative PRV staining was very low in the heart at 18 wpc compared to spleen and kidney. In spleen, the number of PRV-1 positive cells gradually dropped during persistence. At 9 wpc there were still a large number of positive cells in the red pulp, while at 18 wpc the number of positive cells, i.e., macrophage-like cells and damaged erythrocytes, was moderate (Figure 5C,D). In kidney, there was also a decrease in virus positive cells over time, but positive macrophage-like cells and erythrocytes in the blood vessels was consistent during the persistent phase (Figure 5E,F). Many PRV-1 positive cells were present in the hematopoietic portion of the kidney (Figure 5E,F).

3.6. Characterization of the PRV-1 Infected Cell Populations in Kidney and Spleen

In situ hybridization against macrophage colony stimulating factor (MCSFR) defined macrophages in the PRV-1 infected population. Co-localization of PRV-1 and MCSFR transcripts in kidney and spleen revealed a few double stained macrophages and melano-macrophages in both the peak phase (6 wpc) and persistent phase of infection (15 wpc and 18 wpc) (Figure 6).

The red dye defining MCSFR mRNA expression, presented as diffuse staining, which was different from the punctuated staining of green dye. However, the background (Figure 6C,E), was free of the diffuse staining, demonstrating the specificity of the MCSFR staining. Similar diffuse staining with the red dye when applied no kidney and spleen tissue of Atlantic salmon has been observed earlier [25]. PRV-1 localized to some MCSFR positive macrophages; however, this was not the dominating cell type that stained positive for virus. In spleen, the expression of MCSFR dropped after the peak phase, but a few MCSFR positive macrophages, melano-macrophages, erythrocytes and other cells were PRV-1 positive.

In situ hybridization against erythropoietin receptor (EPOR) defined erythroid progenitor cells in the PRV-1 infected population. Co-staining of EPOR transcripts and PRV-1 in kidney detected some double positive cells (Figure 7). The red dye designating EPOR also gave a diffuse staining, but there was no diffuse staining of the background, demonstrating the specificity of the EPOR staining (Figure 7, inserts). These cells were mainly located in the haematopoietic tissue of the kidney in both the acute and persistent phase. Although both MCSFR and EPOR positive cells were PRV infected, they were not the only infected cell types, as other cell types in kidney and spleen, morphologically resembles macrophage-like, but not staining positive for MCSFR or EPOR, also stained positive for PRV-1.

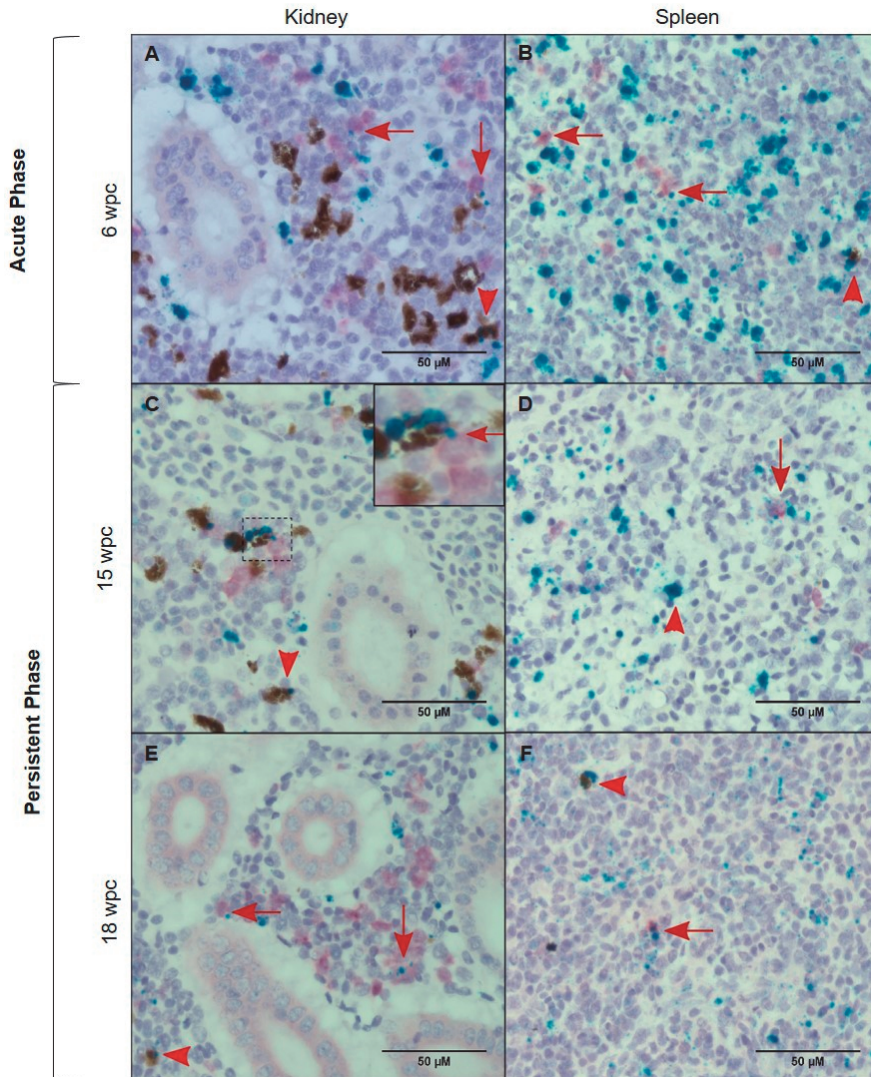


Figure 6. PRV-1 (green) localization in macrophages and melano-macrophages. Duplex *in situ* hybridization against PRV-1 and macrophage colony stimulating factor (MCSFR) (red). Kidney (A,C,E) and Spleen (B,D,F), showing PRV positive macrophages (red arrows) and melano-macrophages (red arrowhead) at 6 wpc, 15 wpc and 18 wpc. The use of red dye in salmon kidney sections in duplex *in situ* gave diffuse staining of positive cells (no background staining). The diffuse staining was different from the punctate staining seen in single *in situ*, or the use of green dye in duplex *in situ*. PRV-1 is also positive in other cell types in the sections. Scale bar = 50 μm.

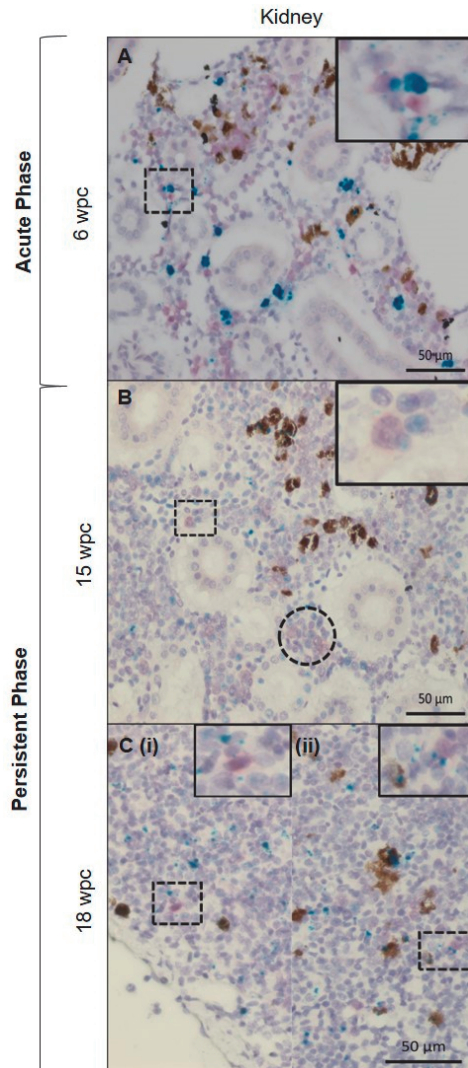


Figure 7. PRV-1 localization in hematopoietic cells. Duplex *in situ* hybridization against PRV-1 (green) and erythropoietin receptor (EPOR) (red). Kidney (A) Acute phase, dually stained PRV/EPOR positive cells in hematopoietic tissue in the magnified picture. (B,C) Persistent phase, dually stained EPOR-PRV1 positive cells in hematopoietic tissue scattered around in the kidney (magnified pictures). Cluster of partially stained positive erythroid cells at 15 wpc (dotted circle). The use of red dye in salmon kidney sections in duplex *in situ* gave diffuse staining of positive cells (no background staining). The diffuse staining was different from the punctate staining seen in single *in situ*, or the use of green dye in duplex *in situ*. Scale bar = 50 µm.

4. Discussion

PRV-1 causes an acute infection of Atlantic salmon erythrocytes, and during the peak of the infection, the virus also infects cardiomyocytes [18,26]. A few weeks later, the pathological changes characteristic for HSMI develop in the myocardium, and subsequently heal. After the heart lesions

have healed, PRV infection becomes persistent. In this study, we focused on the kinetics and cell tropism of PRV-1 in the persistent phase of the infection. Since PRV-1 infects erythrocytes also during persistence [16], the virus can be detected by RT-qPCR in any vascularized organ. However, the kidney consistently contained proportionally high levels of PRV transcripts compared to blood cells in the persistent phase, and thus represent the major reservoir of infected cells and potential site of virus production during persistence.

The PRV-1 RNA level in the blood cells stayed moderately stable in the persistent phase while the PRV-1 RNA level gradually dropped in spleen. It was only minor differences in the expression level of the different genomic segments. In the persistent phase, the dominating target was genomic dsRNA and the viral ssRNA transcripts only made up approximately 6% of total RNA. In a recent study of a Canadian PRV-1 isolate, the viral ssRNA represented 0.1–0.7% of the total PRV-1 RNA load in the persistent phase [8]. In the acute phase, i.e., at 3 wpc, the ssRNA fraction constituted approximately 50% of total viral RNA in blood cells, indicating a highly active viral transcription during early infection.

In contrast to PRV-1 RNA, PRV-1 proteins were detectable in blood cells only in the acute phase, in line with earlier findings [15]. The limited virus protein expression after the primary acute infection phase contrasts the continuous high level of PRV-1 RNA. For mammalian reoviruses, the virus protein expression is halted as a result of a partial block in the translational activity of the cell [27]. This effect is caused by the innate antiviral response, and linked to phosphorylation of the alpha subunit of eukaryotic translation initiation factor 2 (eIF2 α), executed by the viral dsRNA activated protein kinase (PKR) [28,29]. This can lead to a translationally inactive state of the cell [30].

Viral dsRNA, i.e., genomic viral RNA indicating the presence of intact viral particles, was detected in plasma at all phases of infection. Although the dsRNA level of some individual plasma samples at 9, 15 and 18 wpc were below the detection limit, the average level of viral dsRNA in plasma of the sampled groups was remarkably stable at 9 wpc and 18 wpc. This indicates a continuous virus production and shedding into the circulation. Previously, PRV-1 has been found at high levels in plasma in the acute phase, simultaneous with high viral loads in the blood cells [12]. Our findings of virus in plasma, both in the acute phase and in the persistent phase oppose the previous results from an experiment where two PRV-1 isolates from Canada were administered to Atlantic salmon. In that particular study, virus was not detected in plasma at any sampling point [8]. However, there is a marked phenotypic difference between the PRV-1 strains used in these experiments. In our experiment, we used the PRV-1 NOR-2012 isolate, which originates from a field HSMI outbreak, and has repeatedly been used in experimental infections that reproduce HSMI [4,17,31,32]. On the other hand, in laboratory-based studies in farmed Atlantic salmon with Canadian PRV-1 isolates are not associated with HSMI-like lesions [16], while in field, cardiac inflammation and mild clinical signs have been reported in one farm [18]. This could suggest a relationship between the ability to produce plasma viremia and induction of HSMI. For the Canadian PRV-1 isolates, the lack of detectable virus in plasma [8] could indicate that the PRV-1 infection of erythrocytes does not primarily take place in blood. If erythroid progenitor cells continuously generate new PRV-1 infected erythrocytes, this would be an ideal long-term reservoir for PRV. Salmonid erythrocytes, like all non-mammalian vertebrate erythrocytes, are cells with nucleus and organelles, and young salmonid erythrocytes are more transcriptionally active than older cells [13]. In line with this, an experimental challenge with EIBS in coho salmon, performed two decades before PRV-2 was described as the etiological cause of EIBS in coho [10], found viral inclusions preferably in young erythrocytes early in the course of the disease [14]. However, in *ex vivo* systems erythrocytes are susceptible to infection with PRV-1, or at least the HSMI inducing variants of PRV-1 [12].

The salmon immune response is not able to clear the PRV-1 infection, and does not stop PRV-1 from circulating in plasma. However, this does not imply a continuous shedding of infectious virus to the external environment. For the Canadian PRV-1 isolates that do not induce plasma viremia; sentinel

fish were not infected when placed in the tank with persistently infected fish, 41 weeks after initial exposure [16].

IgM is the dominating Ig class in salmonid plasma, and virus neutralizing activities of plasma, designated to IgM, has been demonstrated for several viruses [33]. Formation of PRV-specific plasma IgM after infection has been demonstrated, and the peak antibody production corresponded in time with a decrease in myocardial inflammation [34]. Lack of functional antibodies has been reported for infectious pancreatic necrotic virus (IPNV) both in acute and persistent infections, with moderate presence of neutralizing antibodies only in fish with low degree of clinical signs [35]. Splenic ellipsoids are specialized to remove any immune complexes from salmon plasma [36], but the low level of virus in spleen in this phase, indicate that eventual virus-IgM complexes are not readily removed in the persistent phase. Just after the peak phase of infection in blood cells, PRV-1 RNA loads in spleen exceeded levels in blood cells, in line with earlier findings [12]. This corresponded to the *in situ* observations that most of the PRV-1 positive cells were trapped in red pulp of the spleen in the acute phase. Viral RNA loads in spleen gradually dropped after the peak infection phase as demonstrated by both RT-qPCR and *in situ* hybridization.

It could be speculated that PRV-1 in plasma is present as free viral particles or carried by extracellular vesicles, which are increasingly recognized for both intra- and inter-organism transmission for viruses [37,38]. Vesicle coating of rotaviruses are found to increase fecal-oral transmission [38]. Rotaviruses also belong to the family Reoviridae, and the fecal-oral route is considered a transmission pathway for PRV-1 [39] as well as for mammalian orthoreovirus [40]. If RNA viruses bud through cell membranes in extracellular vesicles, this could shelter the virus from antibody detection [41,42].

PRV-1 RNA levels in the persistent phase, as assessed by qPCR, were higher in kidney and spleen compared to blood and plasma. This was reflected by *in situ* staining of PRV in macrophage-like cells, in melano-macrophages, as well as in erythrocytes present in kidney and spleen. PRV-1 has been suggested earlier to infect macrophage-like cells in kidney and spleen based on a Canadian study of a field outbreak of HSMI [25]. Our data could indicate that PRV specifically target these long living immune cells, however, macrophage-like cells may stain because they actually phagocytize infected erythrocytes, as usually occurs in the spleen. Numerous macrophages and melano-macrophages are present at antigen trapping sites in kidney and spleen [36,43]. Melano-macrophages have earlier been demonstrated to be PRV target cells in Atlantic salmon [44]. Similar to all vertebrates, the survival, proliferation, differentiation, and functionality of bony fish macrophages are governed by macrophage-colony-stimulating factor, MCSF [45]. MCSF mediates its effects through a high affinity transmembrane receptor, the MCSF receptor (MCSFR) [46], which served as the macrophage identification marker in this study. The MCSFR expressed as reported both on myeloid precursors and derivative macrophage population in teleost fish [45], while other reports have claimed that MCSFR is specific to the macrophage population [47]. The MCSFR has been used to characterize monocytes/macrophages in Atlantic salmon [48], and stimulation with MCSFR has been found to enhance antimicrobial and phagocytic responses of macrophages in fish [45,49]. In mammals, MCSFR positive cells have been associated with an anti-inflammatory or immunosuppressive M2 macrophage population [50,51]. Duplex *in situ* hybridization demonstrated that some MCSFR positive cells in kidney and spleen are target cells for PRV-1. In an earlier study, using an antiserum against the non-structural viral protein μ NS present only during viral replication [52], macrophage-like cells were associated with PRV replication [53]. Avian orthoreovirus (ARV), which also belongs to the Orthoreovirus genus, replicates in macrophages, and virulent ARV strains have shown enhanced ability to replicate in such cells [54].

Our study revealed that a number of additional so far un-characterized cell types, particularly in the erythropoietic tissue in the kidney, also stained positive for PRV-1. This encouraged us to use duplex *in situ* hybridization staining for the erythroid precursor cells together with PRV-1. Erythropoietin (EPO) plays a pivotal role in erythropoiesis by signaling through the specific erythropoietin receptor (EPOR) [55]. We found many EPOR positive cells in kidney stained positive also for PRV-1, suggesting

there might be co-localization. This could indicate that the erythropoietic precursor cells were permissive to PRV-1, but future studies are required to elucidate this further. In fish, EPO is primarily produced in heart and transported to erythropoietic sites through blood [56], and triggers erythroid precursor cells to differentiate and proliferate into erythrocytes [57]. Despite of distinct differences between mammalian and teleost red blood cells, these functions are quite conserved [58]. Zebrafish (*Danio rerio*), have erythroid progenitor cells only in kidney [59], while in rainbow trout (*Oncorhynchus mykiss*) and European perch (*Perca fluviatilis*), spleen acts as additional organ for erythropoiesis [60]. In Atlantic salmon, an elevated level of EPOR expression in spleen suggests mobilization of early progenitors to cope with an anemic condition [61]. We found cells staining positive for PRV-1 in the tubular part of the kidney, but the dually stained EPOR and PRV-1 interstitial cells were primarily found in the hematopoietic centers. It could be speculated that these cells are involved in long-term infection of the host and contribute to generation of new PRV-1 infected erythrocytes.

Notably, *in situ* localization of PRV-1 RNA in different tissues illustrates a change in infection pattern when the infection moves into the persistent phase. Although high loads of PRV in heart is a hallmark of HSMI, PRV-1 levels in heart drops significantly during the persistent phase. On the other hand, viral RNA load is particularly high in kidney in the late persistent phase, indicating a shift in viral tissue tropism as the infection proceeds. This is in line with previous reports where tissue tropism was explored with qPCR methodology [4,12].

5. Conclusions

Taken together, this study describes the persistent phase of PRV-1 infection in Atlantic salmon and identifies cell types functioning as viral reservoirs. This work also identifies possible mechanisms of importance for PRV-1 persistence that can aid the understanding of PRV infection, possible viral recurrence and potential long-term effects of the infection.

Supplementary Materials: The following are available online at <http://www.mdpi.com/1999-4915/11/9/824/s1>, Figure S1: Elongation Factor-1 α expression, Figure S2: Positive and negative probes in singleplex *in situ* hybridization assays, Figure S3: Positive and negative probes in duplex *in situ* hybridization assays. Figure S4: PRV localization in persistent phase. Figure S5: Negative control fish tissue for *in situ* hybridization. Table S1: RT-qPCR results from RNA isolated from blood cells, kidney and plasma with and without prior heating RNA at 95 °C for 5 min.

Author Contributions: M.S.M., Ø.W. and E.R. launched the project idea and participated in the overall design and coordination of the study and interpretation of data. MSM and ER drafted the manuscript. H.B., E.D.C., M.S.M. and K.D. helped to establish and analyze results from the *in situ* hybridization. E.F.H. and M.S.M. performed sample preparation, RT-qPCR and revised the manuscript. M.S.M. performed western blot and statistical analyses. E.O.K. performed morphological analyses and revised the manuscript. M.K.D. and Ø.W. participated in the coordination of the study, interpretation of data, and revised the manuscript. All authors approved the final manuscript.

Funding: The Norwegian Seafood Research Fund (FHF), Grant #901221, and Research Council of Norway, Grant #280847, supported this study financially.

Acknowledgments: We would like to thank Turhan Markussen and Stine Braaen, Norwegian University of Life Sciences for technical and scientific assistance.

Conflicts of Interest: The authors declare no conflict of interest.

References

1. Taranger, G.L.; Karlsen, O.; Bannister, R.J.; Glover, K.A.; Husa, V.; Karlsbakk, E.; Kvamme, B.O.; Boxaspen, K.K.; Bjorn, P.A.; Finstad, B.; et al. Risk assessment of the environmental impact of norwegian atlantic salmon farming. *ICES J. Mar. Sci.* **2015**, *72*, 997–1021. [[CrossRef](#)]
2. Lovoll, M.; Wiik-Nielsen, J.; Grove, S.; Wiik-Nielsen, C.R.; Kristoffersen, A.B.; Faller, R.; Poppe, T.; Jung, J.; Pedamallu, C.S.; Nederbragt, A.J.; et al. A novel totivirus and piscine reovirus (prv) in atlantic salmon (*salmo salar*) with cardiomyopathy syndrome (cms). *Virol. J.* **2010**, *7*, 309. [[CrossRef](#)]
3. Palacios, G.; Lovoll, M.; Tengs, T.; Hornig, M.; Hutchison, S.; Hui, J.; Kongtorp, R.T.; Savji, N.; Bussetti, A.V.; Solovyov, A.; et al. Heart and skeletal muscle inflammation of farmed salmon is associated with infection with a novel reovirus. *PLoS ONE* **2010**, *5*, e11487. [[CrossRef](#)]

4. Wessel, O.; Braaen, S.; Alarcon, M.; Haatveit, H.; Roos, N.; Markussen, T.; Tengs, T.; Dahle, M.K.; Rimstad, E. Infection with purified piscine orthoreovirus demonstrates a causal relationship with heart and skeletal muscle inflammation in atlantic salmon. *PLoS ONE* **2017**, *12*, e0183781. [[CrossRef](#)]
5. Kongtorp, R.T.; Taksdal, T.; Lyngoy, A. Pathology of heart and skeletal muscle inflammation (hsmi) in farmed atlantic salmon *salmo salar*. *Dis. Aquat. Org.* **2004**, *59*, 217–224. [[CrossRef](#)]
6. Dharmotharan, K.; Tengs, T.; Wessel, O.; Braaen, S.; Nyman, I.B.; Hansen, E.F.; Christiansen, D.H.; Dahle, M.K.; Rimstad, E.; Markussen, T. Evolution of the piscine orthoreovirus genome linked to emergence of heart and skeletal muscle inflammation in farmed atlantic salmon (*salmo salar*). *Viruses* **2019**, *11*, 465. [[CrossRef](#)]
7. Lund, M.; Krudtaa Dahle, M.; Timmerhaus, G.; Alarcon, M.; Powell, M.; Aspehaug, V.; Rimstad, E.; Jorgensen, S.M. Hypoxia tolerance and responses to hypoxic stress during heart and skeletal muscle inflammation in atlantic salmon (*salmo salar*). *PLoS ONE* **2017**, *12*, e0181109. [[CrossRef](#)]
8. Polinski, M.P.; Marty, G.D.; Snyman, H.N.; Garver, K.A. Piscine orthoreovirus demonstrates high infectivity but low virulence in atlantic salmon of pacific canada. *Sci. Rep.* **2019**, *9*, 3297. [[CrossRef](#)]
9. Coombs, K.M. Reovirus structure and morphogenesis. In *Reoviruses: Entry, Assembly and Morphogenesis*; Roy, P., Ed.; Springer: Berlin/Heidelberg, Germany, 2006; pp. 117–167.
10. Takano, T.; Nawata, A.; Sakai, T.; Matsuyama, T.; Ito, T.; Kurita, J.; Terashima, S.; Yasuike, M.; Nakamura, Y.; Fujiwara, A.; et al. Full-genome sequencing and confirmation of the causative agent of erythrocytic inclusion body syndrome in coho salmon identifies a new type of piscine orthoreovirus. *PLoS ONE* **2016**, *11*, e0165424. [[CrossRef](#)]
11. Hauge, H.; Vendramin, N.; Taksdal, T.; Olsen, A.B.; Wessel, O.; Mikkelsen, S.S.; Alencar, A.L.F.; Olesen, N.J.; Dahle, M.K. Infection experiments with novel piscine orthoreovirus from rainbow trout (*oncorhynchus mykiss*) in salmonids. *PLoS ONE* **2017**, *12*, e0180293. [[CrossRef](#)]
12. Finstad, O.W.; Dahle, M.K.; Lindholm, T.H.; Nyman, I.B.; Lovoll, M.; Wallace, C.; Olsen, C.M.; Storset, A.K.; Rimstad, E. Piscine orthoreovirus (prv) infects atlantic salmon erythrocytes. *Vet. Res.* **2014**, *45*, 35. [[CrossRef](#)]
13. Gotting, M.; Nikinmaa, M.J. Transcriptomic analysis of young and old erythrocytes of fish. *Front. Physiol.* **2017**, *8*, 1046. [[CrossRef](#)]
14. Takahashi, K.; Okamoto, N.; Maita, M.; Rohovec, J.S.; Ikeda, Y. Progression of erythrocytic inclusion body syndrome in artificially infected coho salmon. *Fish Pathol.* **1992**, *27*, 89–95. [[CrossRef](#)]
15. Haatveit, H.M.; Wessel, O.; Markussen, T.; Lund, M.; Thiede, B.; Nyman, I.B.; Braaen, S.; Dahle, M.K.; Rimstad, E. Viral protein kinetics of piscine orthoreovirus infection in atlantic salmon blood cells. *Viruses* **2017**, *9*, 49. [[CrossRef](#)]
16. Garver, K.A.; Johnson, S.C.; Polinski, M.P.; Bradshaw, J.C.; Marty, G.D.; Snyman, H.N.; Morrison, D.B.; Richard, J. Piscine orthoreovirus from western north america is transmissible to atlantic salmon and sockeye salmon but fails to cause heart and skeletal muscle inflammation. *PLoS ONE* **2016**, *11*, e0146229. [[CrossRef](#)]
17. Dahle, M.K.; Wessel, O.; Timmerhaus, G.; Nyman, I.B.; Jorgensen, S.M.; Rimstad, E.; Krasnov, A. Transcriptome analyses of atlantic salmon (*salmo salar* l.) erythrocytes infected with piscine orthoreovirus (prv). *Fish Shellfish Immunol.* **2015**, *45*, 780–790. [[CrossRef](#)]
18. Di Cicco, E.; Ferguson, H.W.; Schulze, A.D.; Kaukinen, K.H.; Li, S.; Vanderstichel, R.; Wessel, O.; Rimstad, E.; Gardner, I.A.; Hammell, K.L.; et al. Heart and skeletal muscle inflammation (hsmi) disease diagnosed on a british columbia salmon farm through a longitudinal farm study. *PLoS ONE* **2017**, *12*, e0171471. [[CrossRef](#)]
19. Zuniga, E.I.; Macal, M.; Lewis, G.M.; Harker, J.A. Innate and adaptive immune regulation during chronic viral infections. *Annu. Rev. Virol.* **2015**, *2*, 573–597. [[CrossRef](#)]
20. Lemay, G. Synthesis and translation of viral mrna in reovirus-infected cells: Progress and remaining questions. *Viruses* **2018**, *10*, 671. [[CrossRef](#)]
21. Patton, J.T.; Vasquez-Del Carpio, R.; Tortorici, M.A.; Taraporewala, Z.F. Coupling of rotavirus genome replication and capsid assembly. In *Advances in Virus Research*; Academic Press: Cambridge, MA, USA, 2006; Volume 69, pp. 167–201.
22. Urquhart, K.; Murray, A.G.; Gregory, A.; O’Dea, M.; Munro, L.A.; Smail, D.A.; Shanks, A.M.; Raynard, R.S. Estimation of infectious dose and viral shedding rates for infectious pancreatic necrosis virus in atlantic salmon, *salmo salar* l., post-smolts. *J. Fish Dis.* **2008**, *31*, 879–887. [[CrossRef](#)]
23. Madhun, A.S.; Isachsen, C.H.; Omdal, L.M.; Einen, A.C.B.; Maehle, S.; Wennevik, V.; Niemela, E.; Svasand, T.; Karlsbakk, E. Prevalence of piscine orthoreovirus and salmonid alphavirus in sea-caught returning adult atlantic salmon (*salmo salar* l.) in northern norway. *J. Fish Dis.* **2018**, *41*, 797–803. [[CrossRef](#)]

24. Lovoll, M.; Austbo, L.; Jorgensen, J.B.; Rimstad, E.; Frost, P. Transcription of reference genes used for quantitative rt-pcr in atlantic salmon is affected by viral infection. *Vet. Res.* **2011**, *42*, 8. [[CrossRef](#)]
25. Di Cicco, E.; Ferguson, H.W.; Kaukinen, K.H.; Schulze, A.D.; Li, S.; Tabata, A.; Guenther, O.P.; Mordecai, G.; Suttle, C.A.; Miller, K.M. The same strain of piscine orthoreovirus (prv-1) is involved in the development of different, but related, diseases in atlantic and pacific salmon in british columbia. *Facets* **2018**, *3*, 599–641. [[CrossRef](#)]
26. Finstad, O.W.; Falk, K.; Lovoll, M.; Evensen, O.; Rimstad, E. Immunohistochemical detection of piscine reovirus (prv) in hearts of atlantic salmon coincide with the course of heart and skeletal muscle inflammation (hsmi). *Vet. Res.* **2012**, *43*, 27. [[CrossRef](#)]
27. Smith, J.A.; Schmechel, S.C.; Williams, B.R.; Silverman, R.H.; Schiff, L.A. Involvement of the interferon-regulated antiviral proteins pkr and rnae 1 in reovirus-induced shutoff of cellular translation. *J. Virol.* **2005**, *79*, 2240–2250. [[CrossRef](#)]
28. Chang, Y.H.; Lau, K.S.; Kuo, R.L.; Horng, J.T. Dsrna binding domain of pkr is proteolytically released by enterovirus a71 to facilitate viral replication. *Front. Cell. Infect. Microbiol.* **2017**, *7*, 284. [[CrossRef](#)]
29. Samuel, C.E.; Duncan, R.; Knutson, G.S.; Hershey, J.W. Mechanism of interferon action. Increased phosphorylation of protein synthesis initiation factor eif-2 alpha in interferon-treated, reovirus-infected mouse 1929 fibroblasts in vitro and in vivo. *J. Biol. Chem.* **1984**, *259*, 13451–13457.
30. Li, M.M.; MacDonald, M.R.; Rice, C.M. To translate, or not to translate: Viral and host mrna regulation by interferon-stimulated genes. *Trends Cell Biol.* **2015**, *25*, 320–329. [[CrossRef](#)]
31. Lund, M.; Rosaeg, M.V.; Krasnov, A.; Timmerhaus, G.; Nyman, I.B.; Aspehaug, V.; Rimstad, E.; Dahle, M.K. Experimental piscine orthoreovirus infection mediates protection against pancreas disease in atlantic salmon (*salmo salar*). *Vet. Res.* **2016**, *47*, 107. [[CrossRef](#)]
32. Wessel, O.; Haugland, O.; Rode, M.; Fredriksen, B.N.; Dahle, M.K.; Rimstad, E. Inactivated piscine orthoreovirus vaccine protects against heart and skeletal muscle inflammation in atlantic salmon. *J. Fish Dis.* **2018**, *41*, 1411–1419. [[CrossRef](#)]
33. Diaz-Rosales, P.; Munoz-Atienza, E.; Tafalla, C. Role of teleost b cells in viral immunity. *Fish Shellfish Immunol.* **2019**, *86*, 135–142. [[CrossRef](#)]
34. Teige, L.H.; Lund, M.; Haatveit, H.M.; Rosaeg, M.V.; Wessel, O.; Dahle, M.K.; Storset, A.K. A bead based multiplex immunoassay detects piscine orthoreovirus specific antibodies in atlantic salmon (*salmo salar*). *Fish Shellfish Immunol.* **2017**, *63*, 491–499. [[CrossRef](#)]
35. Reyes-Cerpa, S.; Reyes-Lopez, F.; Toro-Ascuy, D.; Montero, R.; Maisey, K.; Acuna-Castillo, C.; Sunyer, J.O.; Parra, D.; Sandino, A.M.; Imarai, M. Induction of anti-inflammatory cytokine expression by ipnv in persistent infection. *Fish Shellfish Immunol.* **2014**, *41*, 172–182. [[CrossRef](#)]
36. Press, C.M.; Evensen, O. The morphology of the immune system in teleost fishes. *Fish Shellfish Immunol.* **1999**, *9*, 309–318. [[CrossRef](#)]
37. Bautista, D.; Rodriguez, L.S.; Franco, M.A.; Angel, J.; Barreto, A. Caco-2 cells infected with rotavirus release extracellular vesicles that express markers of apoptotic bodies and exosomes. *Cell Stress Chaperones* **2015**, *20*, 697–708. [[CrossRef](#)]
38. Santiana, M.; Ghosh, S.; Ho, B.A.; Rajasekaran, V.; Du, W.L.; Mutsafi, Y.; De Jesus-Diaz, D.A.; Sosnovtsev, S.V.; Levenson, E.A.; Parra, G.I.; et al. Vesicle-cloaked virus clusters are optimal units for inter-organismal viral transmission. *Cell Host Microbe* **2018**, *24*, 208–220.e8. [[CrossRef](#)]
39. Hauge, H.; Dahle, M.; Moldal, T.; Thoen, E.; Gjevre, A.G.; Weli, S.; Alarcon, M.; Grove, S. Piscine orthoreovirus can infect and shed through the intestine in experimentally challenged atlantic salmon (*salmo salar* l.). *Vet. Res.* **2016**, *47*, 57. [[CrossRef](#)]
40. Tyler, K.L.; Virgin, H.W.; Fields, B.N.J.N. Sites of action of immune-mediated protection against neurotropic reoviruses. *Neurology* **1989**, *39*, 268.
41. Miller, K.D.; Schnell, M.J.; Rall, G.F. Keeping it in check: Chronic viral infection and antiviral immunity in the brain. *Nat. Rev. Neurosci.* **2016**, *17*, 766. [[CrossRef](#)]
42. Patton, J.; Silvestri, L.; Tortorici, M.; Vasquez-Del Carpio, R.; Taraporewala, Z. Rotavirus genome replication and morphogenesis: Role of the viroplasm. In *Reoviruses: Entry, Assembly and Morphogenesis*; Springer: Berlin/Heidelberg, Germany, 2006; pp. 169–187.
43. Ellis, A. Antigen-trapping in the spleen and kidney of the plaice *pleuronectes platessa* L. *J. Fish Dis.* **1980**, *3*, 413–426. [[CrossRef](#)]

44. Bjorgen, H.; Wessel, O.; Fjellidal, P.G.; Hansen, T.; Sveier, H.; Saebo, H.R.; Enger, K.B.; Monsen, E.; Kvellestad, A.; Rimstad, E.; et al. Piscine orthoreovirus (prv) in red and melanised foci in white muscle of atlantic salmon (*salmo salar*). *Vet. Res.* **2015**, *46*, 89. [[CrossRef](#)]
45. Hodgkinson, J.W.; Grayfer, L.; Belosevic, M. Biology of bony fish macrophages. *Biology* **2015**, *4*, 881–906. [[CrossRef](#)]
46. Wang, T.H.; Hanington, P.C.; Belosevic, M.; Secombes, C.J. Two macrophage colony-stimulating factor genes exist in fish that differ in gene organization and are differentially expressed. *J. Immunol.* **2008**, *181*, 3310–3322. [[CrossRef](#)]
47. Mulero, I.; Sepulcre, M.P.; Roca, F.J.; Meseguer, J.; Garcia-Ayala, A.; Mulero, V. Characterization of macrophages from the bony fish gilthead seabream using an antibody against the macrophage colony-stimulating factor receptor. *Dev. Comp. Immunol.* **2008**, *32*, 1151–1159. [[CrossRef](#)]
48. Haugland, G.T.; Jordal, A.E.O.; Wergeland, H.I. Characterization of small, mononuclear blood cells from salmon having high phagocytic capacity and ability to differentiate into dendritic like cells. *PLoS ONE* **2012**, *7*, e49260. [[CrossRef](#)]
49. Grayfer, L.; Hanington, P.C.; Belosevic, M. Macrophage colony-stimulating factor (*csf-1*) induces pro-inflammatory gene expression and enhances antimicrobial responses of goldfish (*Carassius auratus* L.) macrophages. *Fish Shellfish Immunol.* **2009**, *26*, 406–413. [[CrossRef](#)]
50. Hume, D.A.; MacDonald, K.P.A. Therapeutic applications of macrophage colony-stimulating factor-1 (*csf-1*) and antagonists of *csf-1* receptor (*csf-1r*) signaling. *Blood* **2012**, *119*, 1810–1820. [[CrossRef](#)]
51. Svensson, J.; Jenmalm, M.C.; Matussek, A.; Geffers, R.; Berg, G.; Ernerudh, J. Macrophages at the fetal-maternal interface express markers of alternative activation and are induced by *m-csf* and *il-10*. *J. Immunol.* **2011**, *187*, 3671–3682. [[CrossRef](#)]
52. Haatveit, H.M.; Hodneland, K.; Braaen, S.; Hansen, E.F.; Nyman, I.B.; Dahle, M.K.; Frost, P.; Rimstad, E. DNA vaccine expressing the non-structural proteins of piscine orthoreovirus delay the kinetics of prv infection and induces moderate protection against heart -and skeletal muscle inflammation in atlantic salmon (*salmo salar*). *Vaccine* **2018**, *36*, 7599–7608. [[CrossRef](#)]
53. Bjorgen, H.; Haldorsen, R.; Oaland, O.; Kvellestad, A.; Kannimuthu, D.; Rimstad, E.; Koppang, E.O. Melanized focal changes in skeletal muscle in farmed atlantic salmon after natural infection with piscine orthoreovirus (prv). *J. Fish Dis.* **2019**, *42*, 935–945. [[CrossRef](#)]
54. O'Hara, D.; Patrick, M.; Cepica, D.; Coombs, K.M.; Duncan, R. Avian reovirus major μ -class outer capsid protein influences efficiency of productive macrophage infection in a virus strain-specific manner. *J. Virol.* **2001**, *75*, 5027–5035. [[CrossRef](#)]
55. Paffett-Lugassy, N.; Hsia, N.; Fraenkel, P.G.; Paw, B.; Leshinsky, I.; Barut, B.; Bahary, N.; Caro, J.; Handin, R.; Zon, L.I. Functional conservation of erythropoietin signaling in zebrafish. *Blood* **2007**, *110*, 2718–2726. [[CrossRef](#)]
56. Lai, J.C.C.; Kakuta, I.; Mok, H.O.L.; Rummer, J.L.; Randall, D. Effects of moderate and substantial hypoxia on erythropoietin levels in rainbow trout kidney and spleen. *J. Exp. Biol.* **2006**, *209*, 2734–2738. [[CrossRef](#)]
57. Morceau, F.; Dicato, M.; Diederich, M. Pro-inflammatory cytokine-mediated anemia: Regarding molecular mechanisms of erythropoiesis. *Mediat. Inflamm.* **2009**, *2009*, 405016. [[CrossRef](#)]
58. Kulkeaw, K.; Sugiyama, D. Zebrafish erythropoiesis and the utility of fish as models of anemia. *Stem Cell Res. Ther.* **2012**, *3*, 55. [[CrossRef](#)]
59. Davidson, A.J.; Zon, L.I. The 'definitive' (and 'primitive') guide to zebrafish hematopoiesis. *Oncogene* **2004**, *23*, 7233–7246. [[CrossRef](#)]
60. Catton, W.T. Blood cell formation in certain teleost fishes. *Blood* **1951**, *6*, 39–60.
61. Krasnov, A.; Timmerhaus, G.; Afanasyev, S.; Takle, H.; Jørgensen, S.M.J.G.; Endocrinology, C. Induced erythropoiesis during acute anemia in atlantic salmon: A transcriptomic survey. *Gen. Comp. Endocrinol.* **2013**, *192*, 181–190. [[CrossRef](#)]



II



PRV-1 Infected Macrophages in Melanized Focal Changes in White Muscle of Atlantic Salmon (*Salmo salar*) Correlates With a Pro-Inflammatory Environment

Muhammad Salman Malik¹, Håvard Bjørgen², Ingvild Berg Nyman¹, Øystein Wessel¹, Erling Olaf Koppang², Maria K. Dahle³ and Espen Rimstad^{1*}

¹ Section of Virology, Faculty of Veterinary Medicine, Norwegian University of Life Sciences, Ås, Norway, ² Section of Anatomy, Faculty of Veterinary Medicine, Norwegian University of Life Sciences, Ås, Norway, ³ Department of Fish Health, Norwegian Veterinary Institute, Oslo, Norway

OPEN ACCESS

Edited by:

Verónica Chico Gras,
Universidad Miguel Hernández de
Elche, Spain

Reviewed by:

Kim Dawn Thompson,
Moredun Research Institute,
United Kingdom
Sebastian Boltana,
University of Concepcion, Chile

*Correspondence:

Espen Rimstad
espen.rimstad@nmbu.no

Specialty section:

This article was submitted to
Comparative Immunology,
a section of the journal
Frontiers in Immunology

Received: 05 February 2021

Accepted: 13 April 2021

Published: 29 April 2021

Citation:

Malik MS, Bjørgen H, Nyman IB, Wessel Ø, Koppang EO, Dahle MK and Rimstad E (2021) PRV-1 Infected Macrophages in Melanized Focal Changes in White Muscle of Atlantic Salmon (*Salmo salar*) Correlates With a Pro-Inflammatory Environment. *Front. Immunol.* 12:664624. doi: 10.3389/fimmu.2021.664624

Melanized focal changes in white skeletal muscle of farmed Atlantic salmon, “black spots”, is a quality problem affecting on average 20% of slaughtered fish. The spots appear initially as “red spots” characterized by hemorrhages and acute inflammation and progress into black spots characterized by chronic inflammation and abundant pigmented cells. *Piscine orthoreovirus* 1 (PRV-1) was previously found to be associated with macrophages and melano-macrophages in red and black spots. Here we have addressed the inflammatory microenvironment of red and black spots by studying the polarization status of the macrophages and cell mediated immune responses in spots, in both PRV-1 infected and non-infected fish. Samples that had been collected at regular intervals through the seawater production phase in a commercial farm were analyzed by multiplex fluorescent *in situ* hybridization (FISH) and RT-qPCR methods. Detection of abundant inducible nitric oxide synthase (iNOS2) expressing M1-polarized macrophages in red spots demonstrated a pro-inflammatory microenvironment. There was an almost perfect co-localization with the iNOS2 expression and PRV-1 infection. Black spots, on the other side, had few iNOS2 expressing cells, but a relatively high number of arginase-2 expressing anti-inflammatory M2-polarized macrophages containing melanin. The numerous M2-polarized melano-macrophages in black spots indicate an ongoing healing phase. Co-localization of PRV-1 and cells expressing CD8⁺ and MHC-I suggests a targeted immune response taking place in the spots. Altogether, this study indicates that PRV-1 induces a pro-inflammatory environment that is important for the pathogenesis of the spots. We do not have indication that infection of PRV-1 is the initial causative agent of this condition.

Keywords: Atlantic salmon, black spots, macrophage polarization, *Piscine orthoreovirus*, red spots

INTRODUCTION

Melanized focal changes in the white skeletal muscle of farmed Atlantic salmon (*Salmo salar*), “black spots”, has emerged as a phenomenon that is found on average in 20% of the Atlantic salmon slaughtered at Norwegian processing plants (1). Fish affected with spots appear clinically healthy, and the condition is therefore regarded as a quality problem rather than associated with a disease state. Most melanized changes locate to the cranio-ventral and mid-ventral parts of the fillet, which could indicate an anatomical and physiological disposition for the condition (2). However, the etiological cause of the focal melanization remains unknown.

The black spots are primarily observed at slaughter of seawater farmed Atlantic salmon (3), and there are no reports that such spots are common in wild fish. Histologically, black spots appear heterogenous. The more severe black spots are classically characterized as chronic inflammatory reactions of granulomatous character, where macrophages are the dominating cell type, and the presence of melano-macrophages gives the black discoloration (3). In a longitudinal study where the presence of spots was followed through the seawater production phase in a commercial farmed salmon population, it was concluded that red spots preceded the formation of black spots (2). The term red spots refer to foci in the white muscle assumed to be intramuscular hemorrhages. The red spots were found to have a stable low prevalence in the production period, while the black spots accumulated over time in the fish population in seawater (2). Histopathological classification of the melanized spots show that they develop over the time the fish population has spent in sea water, and the most serious granulomatous inflammatory changes appear a few months before slaughter and are associated with *Piscine orthoreovirus 1* (PRV-1) (2). Aggregation of macrophages and other immune cells forming granulomatous structures in the black spots indicate a long-term activation of the immune response (4).

Both immunohistochemistry and *in situ* hybridization methods have demonstrated presence of PRV-1 in melanized foci (2, 4). PRV-1 is a very common infection in farmed Atlantic salmon in the marine phase (5). The presence of PRV-1 in the black spots has been associated with the severity of the spots (2, 4). However, due to the increasing prevalence of PRV-1 infection in farmed Atlantic salmon with time spent in seawater, an alternative hypothesis would be that the presence of melanized changes is coincidental and not caused by PRV-1 infection. In line with this, some macroscopic dark spots are found in fish without detectable PRV-1 infection, but histologically these spots do not show the same chronic inflammatory and granulomatous reactions (2). In black spots with histopathological changes, classified as granulomatous changes, PRV-1 seems to be a consistent finding (2).

PRV virions are naked particles of 70 nm-large icosahedral capsids encompassing the genome of ten double stranded (ds) RNA segments, categorized into long (L1-L3), medium (M1-M3) and small (S1-S4) segments. There are three recognized subtypes of PRV. PRV-1 is mainly found in Atlantic salmon where it may cause heart and skeletal muscle inflammation (HSMI) (6). Following infection of PRV-1 in Atlantic salmon, the virus

replicates to high titers in its main target cell, the erythrocyte (7, 8), and subsequently high virulent variants of PRV-1 infect cardiomyocytes leading to the cardiac inflammation observed during heart and skeletal muscle inflammation (HSMI) (9).

Previous studies have indicated that Atlantic salmon does not clear the PRV-1 infection, and the acute infection develops into a persistent, low productive infection (10). In the persistent phase, PRV-1 infection can be found in circulating erythrocytes and renal erythroid progenitor cells, but also in macrophages and melano-macrophages in kidney and spleen (11). In the melanized spots and in the granulomatous reactions of the more severe black spots in particular, PRV-1 is found in macrophage-like cells, melano-macrophages and erythrocytes (2, 12). This could indicate that the infected cells have a role in the pathogenesis of the melanized changes. Melano-macrophages primarily reside in the spleen and head kidney of teleost fish, where they can cluster to form so-called melano-macrophage centers, but they may also migrate to inflamed tissues (13).

Macrophages are often classified according to their polarization rather than their tissue location. The M1 type macrophages are classically activated and polarized by IFN- γ signaling. They produce a pro-inflammatory microenvironment by secreting inflammatory cytokines, and have the capacity to inactivate intracellular pathogens through, among other factors, the action of nitric oxide (NO) and reactive oxygen species (ROS) (14, 15). Presence of M1 macrophages in an area with infection suggests that macrophage polarization have occurred through sensing of danger signals (16, 17). M1 macrophages are a common phenotype of phagocytes during a cell mediated immune response (18).

The M2 macrophages, on the other hand, are anti-inflammatory and are central in wound healing and tissue repair (19, 20). M2 macrophages can be activated by anti-inflammatory cytokines (IL-4 or IL-13) (21) and their main functions are to generate extracellular matrix and polyamines for cell growth and division, in addition to protein synthesis necessary for the healing process (22). There are many indications that the polarized macrophage phenotypes exist also in teleost fish (23, 24), and the presence of inducible nitric oxide synthase (iNOS2) and arginase-2 (Arg2) have been defined as M1 and M2 specific markers, respectively (22).

Interaction between cytotoxic T-lymphocytes (CTLs) and the antigen presenting complex MHC-I on the target cell surface can initiate the killing of target cells by the actions of granzymes and perforins produced by CTLs (25, 26). Involvement of CTLs in the host defense mechanism against PRV-1 infected cells is indicated in HSMI (27) and spots development (12). The specific colocalization pattern of PRV-1 and the targeted response of these immune cells can be exposed through multiplex *in situ* hybridization method.

This study aimed to characterize the polarization of macrophages in red and black spots by multiplex fluorescent *in situ* hybridization (FISH) method and to study the correlation of markers of macrophage polarization, MHC-I and CD8 expressing cells with PRV-1 infection. The reduction of the relative number of PRV-1 infected cells through the spots' stages indicated an elimination of PRV-1 infected cells in the melanized focal spots

in Atlantic salmon. Transformation of red spots into black spots is associated with the emergence of melano-macrophages of M2 phenotype in the white skeletal muscle.

MATERIAL AND METHODS

Samples From Field Trial

Atlantic salmon smolts with an average weight of 110 g were transferred to sea in a commercial setting at Svåsand, Hardanger, Norway, as earlier described (2). The fish were sampled regularly throughout the seawater period and screened visually for presence of red and black spots in the white muscle (2). Formalin fixed samples of red and black spots had been categorized and graded based on macroscopic appearance and the PRV-1 infection status of the population had been monitored by RT-qPCR of gill, spleen and muscle samples by PatoGen Analyse, Ålesund, Norway as earlier described (2). The population was PRV negative upon transfer to sea and the first PRV positive fish were detected at 23 weeks post transfer. At 48 weeks post transfer about 98% of the sampled fish were PRV-1 positive. The samples used in the present study were collected at 4 and 52 weeks post sea transfer, i.e. prior to PRV-1 infection and after the population was near completely infected with PRV-1, in this context referred to as PRV negative and positive, respectively. The seawater temperature was 11–11.5°C at samplings.

The samples were collected from white muscle of the cranio-ventral part of the fillet and were no spots (normal tissue), macroscopic red spots and black spots (Table 1). Macroscopically the spots were graded 1–3 where grade 1 was very faint discoloration, 2 was a distinct but not severe discoloration and 3 was a prominent and severe discoloration (2).

RNA Extraction and RT-qPCR

Total RNA was extracted from a 25 mg sample of the tissues from all fish from each group as shown in Table 1 using 0.65 ml QIAzol Lysis reagent (Qiagen, Hilden, Germany). Tissues were homogenized using 5 mm steel beads in a TissueLyzer II (Qiagen) for 2 x 5 min at 25 Hz. Chloroform was added and the aqueous phase collected for automatic RNA isolation using a RNeasy Mini QIAcube Kit (Qiagen), eluting RNA in 50 µl RNase

free water. RNA concentrations were determined in a Nanodrop ND-100 spectrophotometer (Thermo Fisher Scientific, Waltham, MA, USA). Thereafter, RNA was stored at -80°C until further use.

cDNA was synthesized from 1 µg total RNA by using Quantitect Reverse Transcription Kit (Qiagen) according to the manufacturer's guidelines. In short, the procedure included elimination of genomic DNA and incubation at 42°C for 30 min with RT mastermix including reverse transcriptase enzyme and RNase inhibitor. Quantitative PCR was performed in duplicates in 96-well plates, using a reaction volume of 12 µl with 15 ng cDNA input per well, and the Maxima SYBR Green/ROX qPCR Master Mix-2x (Thermo Fisher Scientific). Thermal conditions were set for an initial denaturation at 10 min/95°C and 40 cycles of amplification at 15 sec/95°C, 30 sec/60°C and 30 sec/72°C. Melting curve analysis were included to ensure assay specificity. Elongation factor (EF1ab) was used as reference gene (28). No-template control (NTC) were run on the same plate as negative control. The cut off value was set to Ct 35, and fold induction of genes of interest was determined against the reference gene and control samples (29). Primers (Table 2) were designed using Vector NTI Advance™ 11 software (Thermo Fisher Scientific), and AlignX application (Vector NTI Advance™ 11 Package, Invitrogen Dynal AS) was used for sequence alignments. (Table 2)

Statistical Analysis

Fold change (2- $\Delta\Delta Ct$ formula) medians for genes of interest were compared in all groups, using non-parametric Mann-Whitney test due to small sample number, to display differences among the groups. GraphPad Prism version 9.0 (GraphPad Software Inc., La Jolla, CA, USA) was used for statistical analysis and graphical layouts. $p \leq 0.05$ was considered as significantly different.

Histology

Samples for histological examination were selected from PRV-1 infected and uninfected fish populations with or without macroscopic red and black spots (Table 1). Selection criteria for the uninfected population with red and black spots was spot grade level 2 (n = 1) because no uninfected fish had grade 3 level black spots. Samples from PRV-1 infected fish with red and black spots had grade 3 (n = 2). Samples from uninfected fish without macroscopic lesion were selected randomly and used as negative control, whereas samples from infected fish without spot were selected based on highest PRV-1 level (Table S1). Formalin fixed paraffin embedded (FFPE) tissue section (2 µm thickness) was dehydrated by gradual ethanol baths followed by xylene washing for paraffin clearance. Rehydration of the sections were performed for subsequent staining with hematoxylin and eosin (H&E staining). Standard procedures were followed (32). Bright field microscopy (Carl Zeiss Light Microscopy System with Axio Imager 2 - Carl Zeiss AG, Oberkochen, Germany) was performed for imaging.

Fluorescent *In Situ* Hybridization (FISH)

Sample Pretreatment

FFPE sections were sliced with 5 µm thickness from tissue samples and mounted on Superfrost plus (Thermo Fisher Scientific) slides. Slides were baked at 60°C for 2 h in a HybEZ™ II oven (Advanced Cell Diagnostics, catalog #321720)

TABLE 1 | Samples selected from red and black spots.

Category	PRV status	Grading	Sampling time (weeks after transfer to sea)
Black spot	Positive (n = 6)	Grade 1-3 black spots	52
	Negative (n = 6)	Grade 1-2 black spots	4
Red spot	Positive (n = 5)	Grade 1-3 red spots	52
	Negative (n = 6)	Grade 1-3 red spots	4
No spot	Positive (n = 6)	No macroscopic lesion	52
	Negative (n = 4)	No macroscopic lesion	4

TABLE 2 | List of specific primers for genes of interest.

Genes	Primer	Conc.	Sequence (5'-3')	Amplicon (bp)	Accession No.
iNOS2*	F	400 nM	CATCGGCAGGATTCAAGTGGTCCAAT	135	XM_014214975.1
	R		GGTAATCGCAGACCTTAGGTTTCCTC		
Arg2*	F	400 nM	CCTGAAGGACTTGGGTGTCCAGTA	109	XM_014190234.1
	R		CCGCTGCTTCTTGACAAAGAGGT		
MHC Class I (30)	F	400 nM	CTGCATTGAGTGGCTGAAGA	175	AF504022
	R		GGTGATCTTGTCCGTCTTTC		
CD8α (31)	F	400 nM	CACTGAGAGAGACGGGAAGACG	174	AY693393
	R		TTCAAAAACCTGCCATAAAGC		
Granzyme A (31)	F	400 nM	GACATCATGCTGCTGAAGTTG	81	BT048013
	R		TGCCACAGGGACAGGTAACG		
EF1αb (28)	F	500 nM	TGCCCTCCAGGATGTCTAC	57	BG933897
	R		CACGGCCACAGGACTAGT		

*Amplification efficiency (E) of newly designed primers were calculated for iNOS2 (E = 0.98) and Arg2 (E = 1.02).

followed by deparaffinization with 100% ethanol and fresh xylene baths. Samples were pretreated with hydrogen peroxide for 10 min at RT, boiled with RNAscope antigen retrieval reagent (Advanced Cell Diagnostics, catalog #322000) for 15 min at 99°C, and then incubated with RNAscope protease plus reagent for 15 min at 40°C in the HybEZTM II oven. Hydrophobic barrier was made around the tissue section using Immedge hydrophobic barrier pen (Vector Laboratories, Burlingame, CA).

Multiplex *In Situ* Probe Hybridization

RNAscope[®] Multiplex fluorescent V2 assay kit (Advanced Cell Diagnostics catalog #323100) was used for simultaneous detection of up to three different RNA targets. Probes (**Table 3**) were designed against; PRV-1 L3 segment (Advanced Cell Diagnostics catalog #537451) iNOS2 (Advanced Cell Diagnostics catalog #548391); Arg2 (Advanced Cell Diagnostics catalog #548381) CD8 α (Advanced Cell Diagnostics catalog #836821); Granzyme A (Advanced Cell Diagnostics catalog #836841) and MHC-I (Advanced Cell Diagnostics catalog #836831). Probes against Peptidylpropyl Isomerase B (PIIB) (Advanced Cell Diagnostics, catalog #494421) was used as reference gene for RNA integrity of the target samples. Dihydrodipicolinate reductase (DapB), a bacterial gene from *Bacillus subtilis* (Advanced Cell Diagnostics catalog #310043) was used as negative control gene to assess cross-reactivity and background noise. Probes were mixed and hybridized for 2 hrs at 40°C in the HybEZTM II oven. Amplification steps (Amp1-Amp3) were performed according to the manufacturer's protocol. Opal fluorophores (**Table 2**) (Akoya Biosciences, CA,

United States) were prepared and diluted (1:1500) using tyramide signal amplification (TSA) buffer (Advanced Cell Diagnostics catalog #322809) provided in the kit. Each probe was assigned a fluorophore, having a different emission and excitation range to distinguish each output signal (**Table 3**). Also, every probe was developed, labeled, and blocked separately by incubating with RNAscope[®] multiplex Fluorescent Detection Reagents v2 (catalog #323110) and diluted Opal fluorophores in a sequential order as per manufacturer recommendations. Each section was counter stained by adding DAPI (fluorescent DNA stain) for 30 sec at room temperature. Mounting was performed by adding 1-2 drops of Prolong Gold antifade mounting reagent (Thermo Fisher Scientific). Imaging was performed in a TCS SP8 gSTED confocal microscope (Leica microsystems GmbH, Mannheim, Germany).

RESULTS

Histology of Red and Black Focal Changes

In samples from white muscle from non-infected fish without visible spots, unaltered and intact myocytes were seen (**Figure 1A**). In samples of non-spot tissue from PRV-1 infected fish, mild myocyte degeneration was observed to some extent along with presence of infiltrating leukocytes (**Figure 1B**).

In red spots the white skeletal muscle tissue showed moderate to severe bleedings, and mild degeneration to moderate myocyte necrosis was observed in uninfected and infected fish, respectively (**Figures 1C, D**). The red spots from PRV-1

TABLE 3 | List of probes and corresponding fluorophores used in FISH.

	Probe	Target Region (bp)	Fluorophores	Emission/Excitation Wavelength (nm)	Channel*	
Target	PRV-L3	415–1379	Opal 520 (FP1487001KT)	494/525	C1	
	iNOS2	2–949	Opal 620 (FP1495001KT)	588/616	C2	
	Arg2	1332–2053	Opal 690 (FP1497001KT)	676/694	C3	
	CD8 α	8–1033	Opal 620 (FP1495001KT)	588/616	C2	
	Gzma	3–1088	Opal 690 (FP1497001KT)	676/694	C3	
	MHC-I	2–2321	Opal 620 (FP1495001KT)	588/616	C2	
	Control	PIIB	20–934	Opal 520 (FP1487001KT)	494/525	C1
		DapB	414–862	Opal 520 (FP1487001KT)	494/525	C1

*Channels signify the specific labeling of each fluorophore separately for their excitation and emission properties.

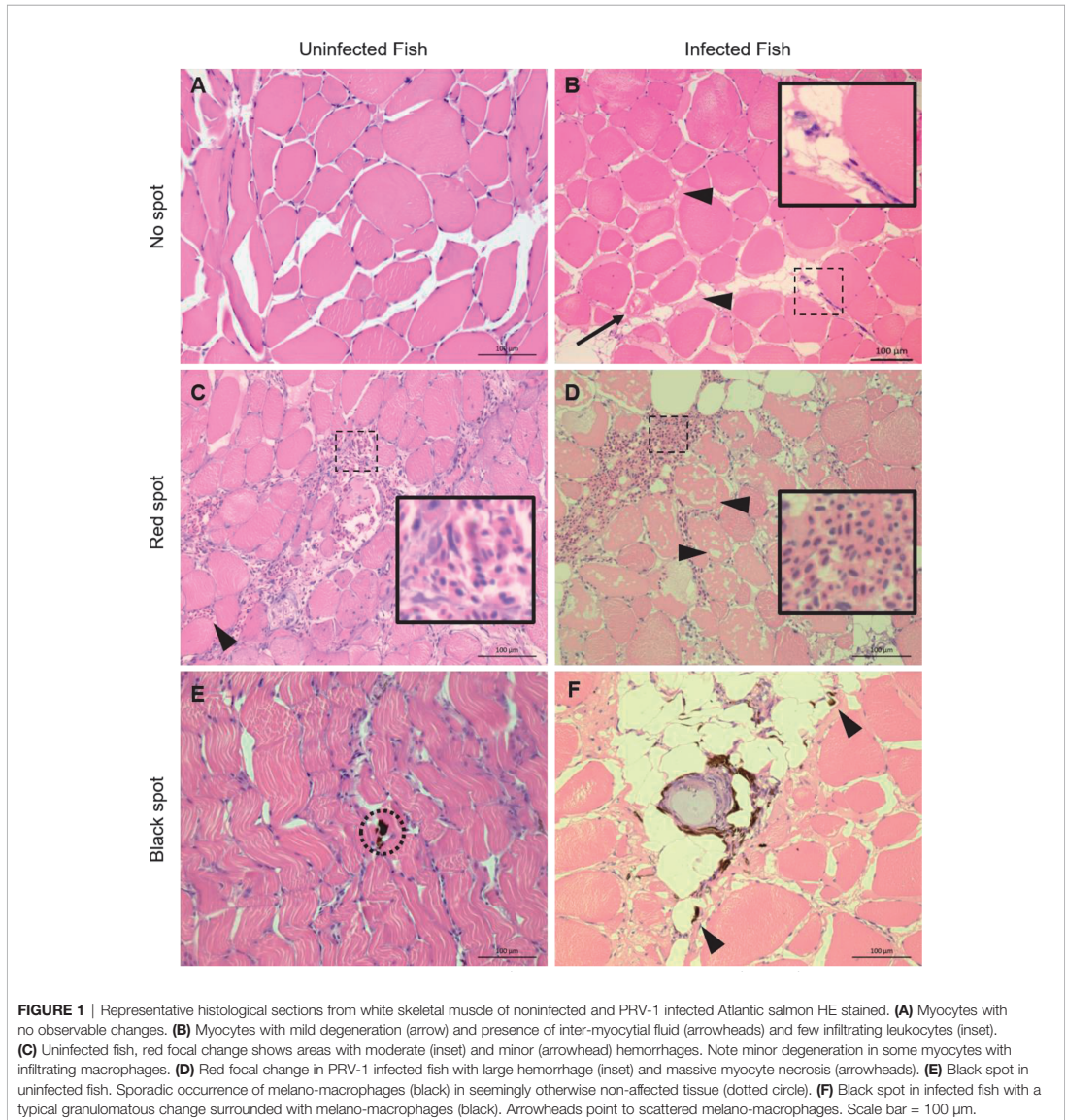
Accession numbers; PRV-L3- KY429945; PIIB- NM_001140870; DapB- EF191515, for the other genes the acc. nos. are listed in **Table 2**.

infected fish differed from the noninfected fish by infiltration of leukocytes and scattered appearance of adipocytes. In black spots, melanin was found in both groups (Figures 1E, F), however, the presence of macrophage-like cells with histologically observable melanin content, referred to as a melano-macrophages, in the samples of the infected fish were more prominent and widespread. Moreover, granulomatous changes in the black spots were observed in PRV-1 positive fish (Figure 1F) and never in the uninfected fish.

***In Situ* Localization of Differentiated, Polarized Macrophages and PRV-1 in Focal Changes**

a. Uninfected fish

The positive and negative controls, i.e. using the PPIB and DapB probes, are shown in Figures S1, S2, respectively. Tissues with macroscopic appearance of red focal changes from uninfected fish showed no iNOS2 specific staining, but some Arg2 positive



cells (**Figure S3**). Similarly, sections with the macroscopic appearance of black spots from uninfected fish showed low number of iNOS2 or Arg2 positive cells (**Figure S4**). No staining was seen in areas without spots from uninfected fish (**Figure S5**). No PRV-1 signal was detected from noninfected fish groups having spots or no spots (**Figures S3–S5**).

b. Red spot. Early phase. PRV-1 infected.

In red focal changes there were hemorrhages (**Figure 2A**) containing a large number of nucleated cells (**Figure 2B**). Hemorrhages analyzed by FISH showed PRV-1 in a few erythrocytes (**Figure 2C**). Numerous iNOS2 positive macrophages, i.e. M1 type polarized macrophages, were surrounding the hemorrhage (**Figure 2D**), but co-localization of PRV-1 and iNOS2 were not seen (**Figure 2E**). There was no staining for Arg2, i.e. M2 type polarized macrophages (**Figure 2F**). Due to the low presence of M1 activated macrophages and lack of organization of the hemorrhages, this appearance was assessed as being an early phase of the red spots.

c. Red spot. Intermediate phase. PRV-1 infected.

In red focal changes from infected fish, where the changes were assessed as more advanced and infiltrating cells were seen between the myocytes (**Figure 3A**). The large number of extravascular erythrocytes of the early phase was not present (**Figure 3B**). Co-localization of PRV-1 and iNOS2 was observed among infiltrating cells found between myocytes (**Figures 3C, D**). There was no staining with Arg2 (**Figure 3F**). Due to the high presence of M1 activated macrophages and the organized appearance of the hemorrhages, but lack of melano-macrophages, this was assessed as being an intermediate phase of the red spots.

d. Red spot. Late phase (transition between red and black spots). PRV-1 infected.

In another region from the same red spot sample, as displayed in **Figure 3**, there were some scattered deposits of melanin (**Figure 4A**). In these areas, there was a modest number of

PRV-1 positive cells (**Figure 4B**). Here, Arg2 specific transcripts were detected (**Figure 4C**), with co-localized PRV-1 staining (**Figure 4D**). Detection of Arg2 was only observed in melano-macrophages found in the sporadic melanin deposits (**Figure 4E**). The commencement of M2 type melano-macrophage detection was assessed as an indication of transition from red to black spots.

e. Black spots. PRV-1 infected

In macroscopic black spots, larger deposits of melanin were seen (**Figure 5A**), and there was a moderate density of cells (**Figure 5B**). PRV-1 stained cells were mainly seen in the area of melanization (**Figures 5C, D**). Scattered areas of iNOS2 positive cell populations were detected in the melanized focal changes (**Figure 5E**), but these only partly co-localized with PRV-1 staining (**Figure 5F**). Arg2 positive cells were also seen in the PRV-1 infected area together with melanin presence (**Figure 5G**), showing some co-localization of PRV-1 and Arg2 (**Figure 5H**). A number of melano-macrophages with PRV-1 were detected. Arg2 positive transcripts were primarily detected in melano-macrophages, but were also present in non-melanized M2 macrophages (**Figure 5I**).

f. No focal changes, PRV-1 infected

In PRV-1 infected fish, samples from areas in white muscle without spots showed co-localization of iNOS2 and PRV-1 (**Figures 6A–D**), while Arg2 and PRV-1 only partly overlapped (**Figures 6E, F**). The staining of iNOS2 and Arg2 did not overlap.

Presence of CD8⁺ and MHC-1 Positive Cells

a. Red Focal Changes, PRV-1 infected

In situ labeling revealed a mild influx of CD8⁺ cytotoxic T lymphocytes (CTLs) in the bleeding area of red focal changes in PRV-1 infected fish (**Figure 7A**). Some of the CD8⁺ cells were also positive for PRV-1 staining, whereas

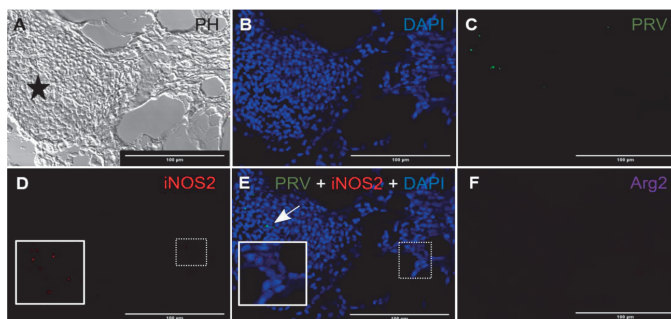


FIGURE 2 | Fluorescent *in situ* hybridization of PRV-1, iNOS2 and Arg2 in red focal changes (early phase). **(A)** Phase contrast image showing a large hemorrhage (star). **(B)** DNA staining of the cells by DAPI (blue). **(C)** Presence of a few PRV-1 (green) positive cells in the hemorrhage. **(D)** iNOS2 (red) specific transcripts detected in a limited number of cells surrounding a peripheral blood vessel. **(E)** Merged image showing presence of PRV-1 (arrow) but no co-localizing in the M1 macrophage (inset). **(F)** Arg2 (purple) specific transcripts (M2 type macrophages) were undetected. Scale bar = 100µm.

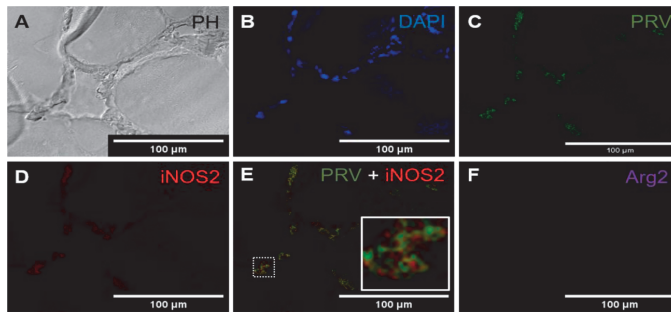


FIGURE 3 | *Fluorescent in situ hybridization of PRV-1, iNOS2 and Arg2 in red focal changes (intermediate phase).* (A) Phase contrast image showing infiltrating cells between myocytes. (B) Nuclei DNA staining of the cells with DAPI (blue). (C) Presence of PRV-1 (green) in infiltrating cells in between myocytes. (D) Presence of iNOS2 (red) in infiltrating cells between myocytes. (E) Merged image showing co-localization (inset) of PRV-1 and iNOS2 (yellow). (F) Arg2 transcripts (purple) were not detected. Scale bar = 100µm.

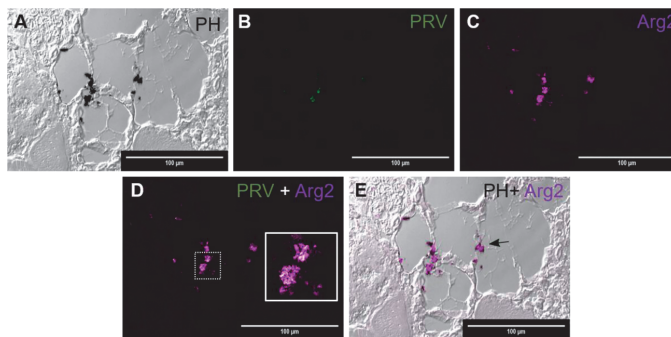


FIGURE 4 | *Fluorescent in situ hybridization of PRV-1 and Arg2 in red focal changes (late phase).* (A) Phase contrast image showing structure of the analyzed area and melanin deposit. (B) Sporadic presence of PRV-1 (green) in melanized area. (C) Arg2 (purple) positive cells (D) Merged image showing PRV-1 and Arg2 co-localization (white in the inset). (E) Merged image showing Arg2 positive staining of melano-macrophages (arrow). Scale bar = 100µm.

other CD8-positive cells were present around infected cells (Figures 7A, B). Granzyme A transcripts were detected in both CD8⁺ (Figures 7A–C) and other cell populations in the infected area (Figures 7A, B). Numerous MHC-I positive cells were present at the bleeding site (Figures 8A–C), with a limited number also being PRV-1 infected. PRV-1 did not appear to co-localize with MHC-I (Figures 8B, C).

b. Black Focal Changes, PRV-1 infected

CD8⁺ cells were detected in the areas with melanin deposits. Some PRV-1 infected cells were also detected in this area, but the staining did not co-localize (Figure 9). Granzyme A specific transcripts were co-localized with CD8⁺ (Figures 9C, D) but also found in other cell subsets (Figure 9B). Numerous MHC-I positive cells were detected around a vacuolar area surrounded by melano-macrophages and some PRV-1 infected cells, showing high melanin deposits

(Figures 10A, B). PRV-1 did co-localize with some MHC-I stained cells (Figure 10C).

Gene Expression in Red and Black Spots

a. iNOS2 and Arg2

iNOS2 expression was low in PRV positive (median Ct 30.7), non-spot samples (2 folds) while it was significantly increased (approximately 10 folds, MWU value = 0, n1 = 4, n2 = 5, p-value = 0.0079) in PRV positive (median 27) red focal changes (Figures 11A, S6). In contrast, iNOS2 was not upregulated in the samples from red focal changes of uninfected fish. In the black focal changes, iNOS2 expression was at the same level as in non-spot samples. Arg2 expression was significantly upregulated in all of the target groups, especially in PRV-1

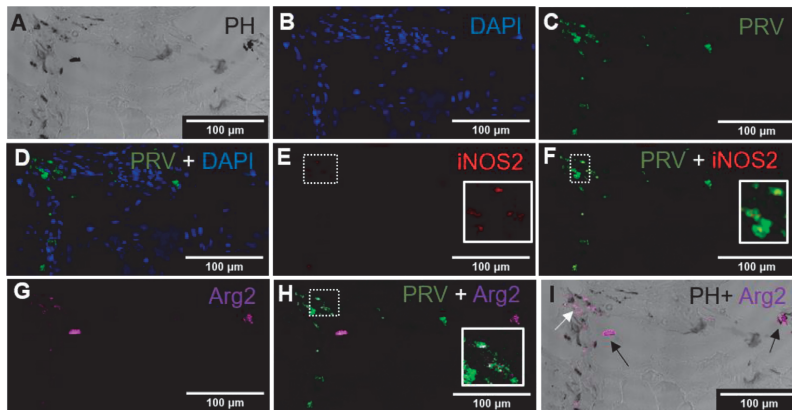


FIGURE 5 | Fluorescent in situ hybridization of PRV-1, iNOS2 and Arg2 in black focal changes (late phase). **(A)** Phase contrast image presence of melanin in the infected area. **(B)** Nuclei DNA stained with DAPI (blue). **(C)** PRV-1 (green) detected in severe melanized area **(D)** Merged PRV-1 and DAPI. Number of PRV-1 positive cells compared to total number of cells were low. **(E)** Few iNOS2 (red) positive cells detected at the infected area **(F)** Merged image showing co-localization (yellow in inset) of PRV-1 and iNOS2. **(G)** Presence of Arg2 (purple) positive cells. **(H)** Co-localization of PRV-1 and Arg2 positive cells (white in inset). **(I)** Localization of Arg2 specific transcripts in melanized M2 melano-macrophages (black arrows) and non-melanized M2 macrophages (white arrow). Scale bar = 100 μm.

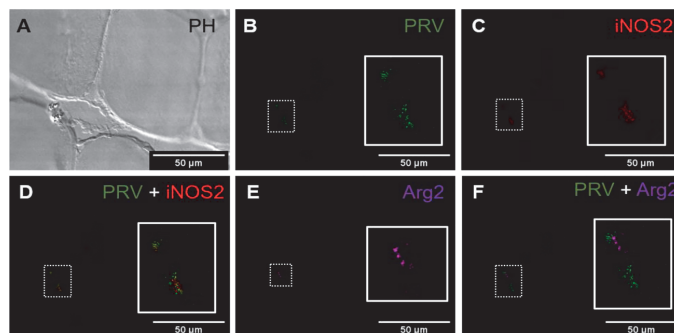


FIGURE 6 | Fluorescent in situ hybridization of PRV-1, iNOS2 and Arg2 in areas without spots, from PRV-1 infected fish. **(A)** Phase contrast image showing cells structure. **(B)** PRV-1 (green) specific transcripts detected between muscle cells. **(C)** iNOS2 (red) positive cells in the same area as PRV-1. **(D)** Merged image showing co-localization of PRV-1 and iNOS2 (yellow, inset). **(E)** Arg2 (purple) positive cells were detected partly in same area as PRV-1. **(F)** Merged image of PRV-1 and Arg2 show Arg2 positive cells surrounding PRV-1 infected cells (inset). Scale bar = 50 μm.

infected groups. Arg2 was upregulated both in infected, no spot samples (6.5 folds, MWU value = 0, n1 = 4, n2 = 6, p-value = 0.0048) and in red focal changes without PRV infection (4.7 folds, MWU value = 1, n1 = 4, n2 = 6, p-value = 0.0095), compared to the uninfected, no-spot control. Both iNOS2 and Arg2 expression were at the highest level in the PRV infected fish with red focal changes. But in black focal changes only Arg2 expression, in contrast to iNOS2, was significantly upregulated (MWU value = 0, n1 = 4, n2 = 6, p-value = 0.0048) in PRV-1 infected group (median 27.7) (Figures 11A, S6).

b. CD8α, GzmA and MHC-I

There was a trend towards upregulation of the CD8α gene in the red and black focal changes (Figure 11B) but this was not statistically significant. Granzyme A expression level was significantly upregulated in PRV-infected groups with red (16.5 folds, MWU value = 0, n1 = 4, n2 = 5, p-value = 0.0079) and black focal changes (approx. 15 folds, MWU value = 2, n1 = 4, n2 = 5, p-value = 0.0489). Non-infected groups showed no significant induction of CD8α and granzyme A. Increased expression of MHC-1 was spotted in all fish groups infected with PRV-1, compared to non-infected groups, and

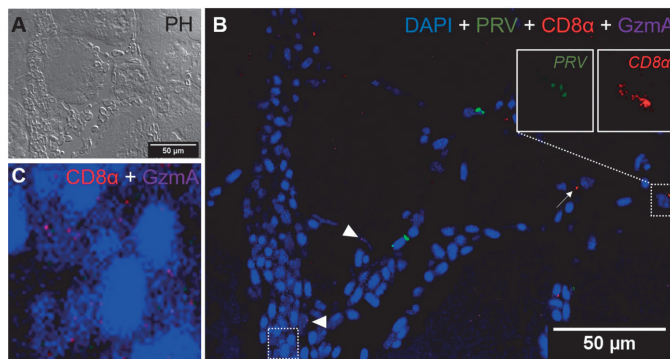


FIGURE 7 | Fluorescent *in situ* hybridization of PRV-1, CD8 α and GzmA in red focal changes. **(A)** Phase contrast image showing a bleeding area with a large aggregation of blood cells. **(B)** Merged image of PRV (green), CD8 α (red) and GzmA (purple). Localization of PRV-1 in CD8 α cell (dotted rectangle at right top) and co-expression of granzyme A in CD8 α T cells (dotted rectangle in left bottom). Individual T cells detected expressing granzyme A specific transcripts (arrowhead) along with other CD8 cells (arrow). Nuclei DNA stained with DAPI (blue) **(C)** Magnified image of CD8 α and GzmA co-expression from dotted square in image **(B)** Scale Bar = 50 μ m.

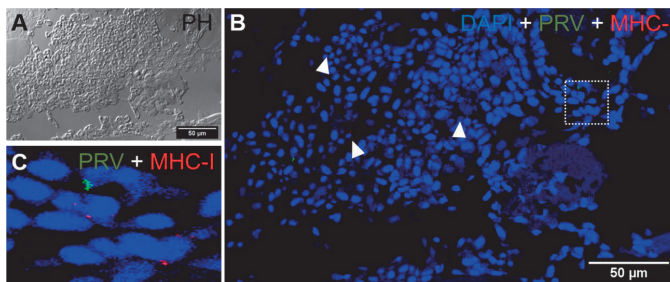


FIGURE 8 | Fluorescent *in situ* hybridization of PRV-1, and MHC-I in areas of red focal changes. **(A)** Phase contrast image showing a large hemorrhage. **(B)** Merged image of PRV-1 and MHC-I showed no co-expression of PRV-1 in MHC-I cells, but a few cells were detected in the bleeding area (arrowhead). **(C)** Magnified image from image B (dotted rectangle) showing PRV-1 infected cells along with MHC-I cells. Scale Bar = 50 μ m.

the MHC-I expression level was relatively higher in black focal changes (14 folds, MWU value = 0, n1 = 4, n2 = 6, p-value = 0.0048) than in red focal changes (9 folds, MWU value = 2, n1 = 4, n2 = 5, p-value = 0.0317) (**Figure 11B**).

DISCUSSION

This study aimed to clarify the role of PRV-1 infection and the immune mechanisms involved in the development of melanized foci in white muscle of Atlantic salmon, using immune cell gene markers representing the macrophage polarization pattern, and the cytotoxic immune response.

Macrophages respond to their environment by differentiating into the functional pro-inflammatory phenotypes M1 macrophages,

implicated in initiating and sustaining inflammation, or the anti-inflammatory M2 macrophages, implicated in tissue repair (33). In samples from red and black focal changes from non-infected fish there were no obvious detection of macrophage polarization apart from minimal occurrence of M2 macrophages, based on Arg2 transcript detection. Unaffected muscle areas of non-infected fish showed no presence of polarized macrophage markers. These findings were also reflected in the qPCR transcript analysis, which mirrored the *in situ* findings.

On the other hand, our results indicate that in the PRV-1 infected fish, the initial phase of the progress of the red and black spot formation were tightly connected to macrophage polarization and linked to the presence of PRV-1. The development of melanized focal changes is considered to be multifactorial. Viral diseases such as pancreas disease (PD) may affect the white muscle, but

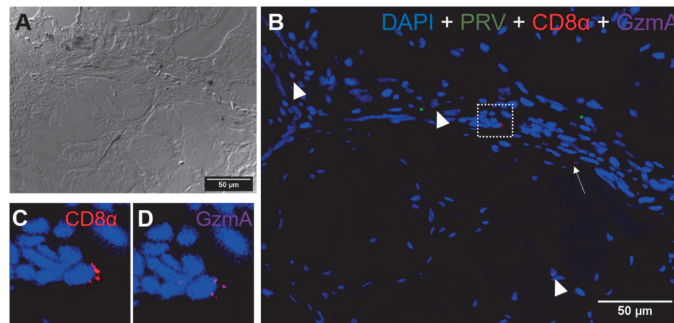


FIGURE 9 | Fluorescent in situ hybridization of PRV-1, CD8 α and GzmA in black focal changes. **(A)** phase contrast image showing cell structures with melanin accumulation. **(B)** Merged image showing presence of PRV-1 (green) infected cells with CD8 $^+$ cells (red) (arrows) and granzyme A (purple) in another cell population (arrowhead). Dotted rectangle showing co-expression of CD8 and GrzmA split in **(C, D)**. Nuclei DNA stained with DAPI (blue) Scale Bar = 50 μ m.

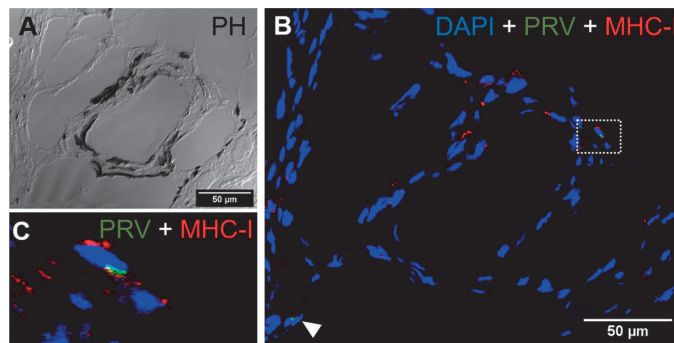
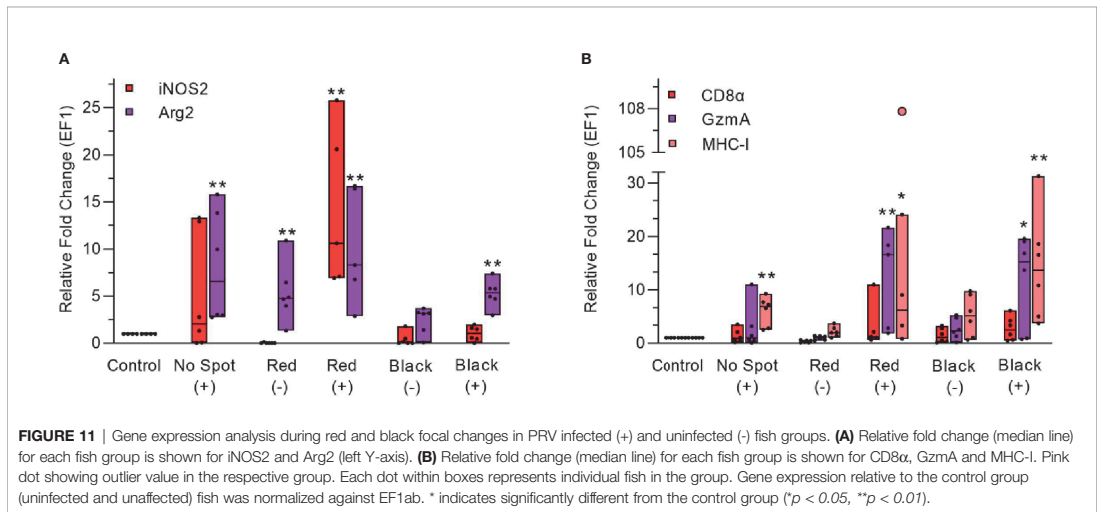


FIGURE 10 | Fluorescent in situ hybridization of PRV-1 and MHC-I in black focal changes. **(A)** phase contrast image showing vacuolar area surrounded by melano-macrophages and other immune cells. **(B)** Merged image showing presence of numerous MHC-I positive cells (red) where some are co-staining with PRV-1 (green) (dotted rectangle and arrowhead). **(C)** Magnified area from image B showing co-localization of PRV-1 in some MHC-I cells. Scale Bar = 50 μ m.

widespread presence of melanized changes in areas being free from PD historically suggest no etiological role for this disease in the development of melanized focal changes (34). Furthermore, melanized changes have not been found to be influenced by bacterial components (2). We found that local PRV-1 infection was associated with the M1 polarized cell marker iNOS2 in the early developmental phases of melanized foci. PRV-1 was detected in a limited number of erythrocytes in hemorrhages, and only a few M1 macrophages were detected in the initial phase of red spots. Erythrocytes are a primary cell target of PRV-1 both in the acute and persistent phases of infection (7), and infected cells can be detected in any vascularized tissue. We have not found evidence here indicating that the PRV-1 infection initiated these hemorrhages as in previous studies (2, 4). However, for the close PRV relative, Grass carp reovirus (GCRV), it is suggested that iNOS2 activity is implicated in apoptosis of the vascular endothelial

cells in hemorrhages characteristic for GCRV infection of Grass carp (*Ctenopharyngodon idella*) (35).

In PRV-1 infected fish, the M1 type macrophages were modestly detected in the early phase of red focal changes. However, in the more developed, intermediate phase of red spots the M1 macrophages were a dominating feature and were almost uniformly positive for PRV-1 specific staining, i.e. PRV-1 infected. The expression analysis by RT-qPCR also demonstrated elevated expression of iNOS2 in this phase. The dominating presence of PRV-1 infected, M1 polarized macrophages in this phase indicates a pro-inflammatory environment, which may be driven by the PRV-1 infection. In an earlier study, a significant downregulation of the anti-inflammatory cytokine IL10 was found associated with red changes (12), which indirectly indicates a pro-inflammatory environment.



Red spots with sporadic appearance of melano-macrophages were categorized as late red spot phase. This phase is considered to reflect the transition phase between red and black spots. Upregulation of iNOS2 level during red spots could be an indicator for commencement of melanogenesis. It is noteworthy that iNOS2 contributes to the melanogenesis in mammalian melanocytes (36). Based on the expression of the M2 marker Arg2, we found that the melano-macrophages at the site displayed the properties of anti-inflammatory M2 macrophages. We also found M2 macrophages without melanin. Co-localization pattern revealed PRV-1 abundance in melanized cells. The melano-macrophages of teleost fish are phagocytic cells (37) and they accumulate at long-term antigen retention sites in salmonids (13, 38). Phagocytosis of virus infected cells by macrophage and melano-macrophages have been reported earlier in Atlantic salmon (39). M2 macrophages are cells normally involved in tissue repair, and here they appeared first when melanin started to accumulate in the spots in skeletal muscle tissue.

Our findings indicate that PRV-1 infected macrophages are not innocent bystanders but represent M1 polarized macrophages important in the development of the pro-inflammatory microenvironment of red spots. The melanin accumulation starts in the late phase of red focal changes and

will ultimately progress into black focal changes. It therefore seems as if melano-macrophages do not infiltrate the changes as such, but rather as non-pigmented macrophages capable of accumulating melanin over time. Melanogenesis has previously been demonstrated in advanced black spots (3). This putative progression could also be an explanation for the low prevalence of red spots but an increasing prevalence of black spots through the production period in seawater (2).

The black spots demonstrated a more heterogenous macrophage populations, i.e. both M1 and M2 macrophages were present. In advanced melanized areas, few M1 macrophages were positive for PRV-1, whereas PRV-1 co-localization was detected both in melanized (melano-macrophages) and non-melanized M2 type macrophages. In mammals, Arg2 is shown to downregulate the nitric oxide production of the M1 macrophages (40). Our findings indicate that Arg2 specific transcripts are mostly linked to the melanized area and associate with melano-macrophages. Presence of melano-macrophages (M2) was consistent from the late phase of red spots into black spots transformation (Table 4).

The correlated upregulation of Arg2 transcripts with the stage of development of the spots in the PRV-1 infected fish indicated a gradual shift from an inflammatory to a healing response

TABLE 4 | Consolidated summary of results.

Type of spot		Key <i>In situ</i> findings	Characteristic gene expression level
Red spot	Early	Few M1 macrophages in PRV-1 positive hemorrhages.	Significant upregulation of <i>iNOS2</i> expression
	Intermediate	High co-localization of PRV-1 in M1 macrophages.	Significant upregulation of <i>MHC-I</i> and <i>GzmA</i> expression
	Late	Detection of few M2 melano-macrophages.	
Black spot		Domination of M2 melano-macrophages and co-localization with PRV-1.	Significant upregulation of <i>Arg2</i> transcription.

during the transition from red to black macroscopic appearance of the spots. The spots of the non-infected fish with lack of detection of M1 macrophage marker and only a few detected M2 polarized macrophages, strongly indicated that PRV-1 is driving macrophage polarization in the spots of infected fish.

The initial etiological cause(s) of the red spots is unknown. The outcome of the spots in uninfected fish groups is also unknown due to the ubiquitous presence of PRV-1 in farmed Atlantic salmon, and the lack of an experimental model for spot formation (11). However, it could be speculated if the lack of inflammation in spots in non-infected fish argues for a shorter longevity and lower severity of the spots.

To further characterize the inflammatory microenvironment in the spots, the presence of CD8, Granzyme A and MHC-I positive cells was characterized during spot development. There were substantial variations in the presence of these markers among the individual fish, but *in situ* visualization indicated that MHC-I positive, PRV-1 infected cells were targeted by CD8 positive T cells both in red and black spots. The relative low number of CD8 positive cells evenly observed both in red and black focal changes was in line with the RT-qPCR expression analysis. However, a moderate, but not statistically significant up-regulation of CD8 α expression in black focal changes compared to red focal changes was observed, and has been reported earlier (12). Mature cytotoxic T cells can use granzyme A for killing of target cells containing intracellular pathogens. Here, granzyme A specific transcripts were observed in cells that were not expressing CD8. By RT-qPCR, expression of Granzyme A was found to be significantly increased in both red and black spots compared to control samples, while CD8 was not. Granzyme A is also synthesized by natural killer cells (NK-cells) (41) or other immune and non-immune cells in the teleost fish (42).

Mammalian myopathies are often marked by up-regulation of MHC-I (43, 44). By immunolabelling, MHC-I positive cells have earlier been demonstrated to be abundant in red spots (12), and in the present *in situ* study MHC-I cells were common, but perhaps not abundant. In both studies an absence of MHC-I positive myocytes was observed in the affected area, combined with lack of observation of PRV-1. The present study did not indicate that infection of the skeletal muscle cells is an important factor of the spot formation. As for Granzyme A, the MHC-I expression was significantly increased in both PRV-1 infected red and black spots compared to control samples, and colocalization of MHC-I and PRV-1 were seen in some cells especially in the melanized areas. Taken together, the targeted cell mediated immune response by the host tries to resolve and eradicate PRV-1 infection during red and black spots formation.

CONCLUSION

A possible course of events in the pathogenesis of black spots, is that PRV-1 infected erythrocytes in the hemorrhages infect tissue macrophages through phagocytosis. The myocyte degeneration in red muscle caused by PRV-1 (6), could be an additional driver for influx of macrophages, but is probably not the initial cause of red

spots, as these are found at similar prevalence prior to PRV infection (2). The iNOS2 expressing M1-polarized non-melanized macrophages are mainly present in the period of the red focal changes, i.e. the time of inflammation, which suggests local production of NO and other oxygen radicals by the M1 macrophages. Melanin is a protector against free oxygen radicals (45), and its accumulation could be a consequence of the pro-inflammatory environment. Melanogenesis has previously been demonstrated in a salmon macrophage-like cell line (46, 47). The increased prevalence and severity of the black spots over time, indicates that the spot forming process is long lasting. The numerous M2-polarized melano-macrophages in black spots indicate that this is a healing phase of the process. Moreover, the presence of cytotoxic T cells and MHC-I positive cells in the focal changes represents the host's ability to target and eliminate PRV-1 infected cells. This suggests a role of PRV-1 infection in driving the development of black spots in white muscle of Atlantic salmon.

DATA AVAILABILITY STATEMENT

The raw data supporting the conclusions of this article will be made available by the authors, without undue reservation.

ETHICS STATEMENT

Ethical review and approval was not required for the animal study because the material was achieved from commercial production.

AUTHOR CONTRIBUTIONS

Conceptualization, MM, HB and ER. Methodology, MM, IN and HB. Software, MM. Validation, MM, ØW and MD. Formal analysis, MM, HB, ØW and ER. Investigation, MM, HB, ØW and ER. Resources, ER and EK. Data curation, MM, IN. Writing—original draft preparation, MM and ER. Writing—review and editing, ØW, MM, MD, HB, EK and ER. Visualization, MM, IN and HB. Supervision, ER, EK, MD and ØW. Project administration, ER. Funding acquisition, ER and EK. All authors contributed to the article and approved the submitted version.

FUNDING

The study was supported by the Norwegian Seafood Research Fund (FHF) grant 901501, and by the Research Council of Norway, grant 280847/E40 (ViVaAct).

SUPPLEMENTARY MATERIAL

The Supplementary Material for this article can be found online at: <https://www.frontiersin.org/articles/10.3389/fimmu.2021.664624/full#supplementary-material>

REFERENCES

- Färber F. *Melanin Spots in Atlantic Salmon Fillets: An Investigation of the General Problem, the Frequency and the Economic Implication Based on an Online Survey*. Ås, Norway: Norwegian University of Life Sciences (2017).
- Bjorgen H, Haldorsen R, Oaland O, Kvellstad A, Kannimuthu D, Rimstad E, et al. Melanized Focal Changes in Skeletal Muscle in Farmed Atlantic Salmon After Natural Infection With Piscine Orthoreovirus (PRV). *J Fish Dis* (2019) 42:935–45. doi: 10.1111/jfd.12995
- Larsen HA, Austbø L, Mørkøre T, Thorsen J, Hordvik I, Fischer U, et al. Pigment-Producing Granulomatous Myopathy in Atlantic Salmon: A Novel Inflammatory Response. *Fish Shellfish Immunol* (2012) 33:277–85. doi: 10.1016/j.fsi.2012.05.012
- Bjorgen H, Wessel O, Fjellidal PG, Hansen T, Sveier H, Saebø HR, et al. Piscine Orthoreovirus (PRV) in Red and Melanized Foci in White Muscle of Atlantic Salmon (*Salmo Salar*). *Vet Res* (2015) 46:89. doi: 10.1186/s13567-015-0244-6
- Kongtorp R, Taksdal T, Lyngøy A. Pathology of Heart and Skeletal Muscle Inflammation (Hsmi) in Farmed Atlantic Salmon *Salmo Salar*. *Dis Aquat Org* (2004) 59:217–24. doi: 10.3354/dao059217
- Wessel Ø, Braaen S, Alarcon M, Haatveit H, Roos N, Markussen T, et al. Infection With Purified Piscine Orthoreovirus Demonstrates a Causal Relationship With Heart and Skeletal Muscle Inflammation in Atlantic Salmon. *PLoS One* (2017) 12:e0183781. doi: 10.1371/journal.pone.0183781
- Finstad ØW, Dahle MK, Lindholm TH, Nyman IB, Lovoll M, Wallace C, et al. Piscine Orthoreovirus (PRV) Infects Atlantic Salmon Erythrocytes. *Vet Res* (2014) 45:35. doi: 10.1186/1297-9716-45-35
- Wessel Ø, Olsen CM, Rimstad E, Dahle MK. Piscine Orthoreovirus (PRV) Replicates in Atlantic Salmon (*Salmo Salar* L.) Erythrocytes Ex Vivo. *Vet Res* (2015) 46:26–6. doi: 10.1186/s13567-015-0154-7
- Wessel Ø, Hansen EF, Dahle MK, Alarcon M, Vatne NA, Nyman IB, et al. Piscine Orthoreovirus-1 Isolates Differ in Their Ability to Induce Heart and Skeletal Muscle Inflammation in Atlantic Salmon (*Salmo Salar*). *Pathogens (Basel Switzerland)* (2020) 9:1050. doi: 10.3390/pathogens9121050
- Garver KA, Johnson SC, Polinski MP, Bradshaw JC, Marty GD, Snyman HN, et al. Piscine Orthoreovirus From Western North America is Transmissible to Atlantic Salmon and Sockeye Salmon But Fails to Cause Heart and Skeletal Muscle Inflammation. *PLoS One* (2016) 11:e0146229. doi: 10.1371/journal.pone.0146229
- Malik MS, Bjorgen H, Dharmotharan K, Wessel Ø, Koppang EO, Di Cicco E, et al. Erythroid Progenitor Cells in Atlantic Salmon (*Salmo Salar*) may be Persistently and Productively Infected With Piscine Orthoreovirus (PRV). *Viruses* (2019) 11:824. doi: 10.3390/v11090824
- Bjorgen H, Kumar S, Gunnes G, Press CM, Rimstad E, Koppang EO. Immunopathological Characterization of Red Focal Changes in Atlantic Salmon (*Salmo Salar*) White Muscle. *Vet Immunol Immunopathol* (2020) 222:110035. doi: 10.1016/j.vetimm.2020.110035
- Agius C, Roberts R. Melano-Macrophage Centres and Their Role in Fish Pathology. *J Fish Dis* (2003) 26:499–509. doi: 10.1046/j.1365-2761.2003.00485.x
- Gordon S. The Macrophage: Past, Present and Future. *Eur J Immunol* (2007) 37:S9–S17. doi: 10.1002/eji.200737638
- Gordon S, Taylor PR. Monocyte and Macrophage Heterogeneity. *Nat Rev Immunol* (2005) 5:953–64. doi: 10.1038/nri1733
- Kanwal Z, Wiegertjes GF, Veneman WJ, Meijer AH, Spaik HP. Comparative Studies of Toll-Like Receptor Signalling Using Zebrafish. *Dev Comp Immunol* (2014) 46:35–52. doi: 10.1016/j.dci.2014.02.003
- Aoki T, Hikima J-i, Hwang SD, Jung TS. Innate Immunity of Finfish: Primordial Conservation and Function of Viral RNA Sensors in Teleosts. *Fish Shellfish Immunol* (2013) 35:1689–702. doi: 10.1016/j.fsi.2013.02.005
- Gordon S. Alternative Activation of Macrophages. *Nat Rev Immunol* (2003) 3:23–35. doi: 10.1038/nri978
- Martinez FO, Helming L, Gordon S. Alternative Activation of Macrophages: An Immunologic Functional Perspective. *Annu Rev Immunol* (2009) 27:451–83. doi: 10.1146/annurev.immunol.021908.132532
- Mills CD, Ley K. M1 and M2 Macrophages: The Chicken and the Egg of Immunity. *J Innate Immun* (2014) 6:716–26. doi: 10.1159/000364945
- Martinez FO, Gordon S. The M1 and M2 Paradigm of Macrophage Activation: Time for Reassessment. *F1000prime Rep* (2014) 6. doi: 10.12703/P6-13
- Wiegertjes GF, Wentzel AS, Spaik HP, Elks PM, Fink IR. Polarization of Immune Responses in Fish: The 'Macrophages First' point of View. *Mol Immunol* (2016) 69:146–56. doi: 10.1016/j.molimm.2015.09.026
- Wentzel AS, Janssen JJE, de Boer VCJ, van Veen WG, Forlenza M, Wiegertjes GF. Fish Macrophages Show Distinct Metabolic Signatures Upon Polarization. *Front Immunol* (2020) 11:152. doi: 10.3389/fimmu.2020.00152
- Wentzel AS, Petit J, van Veen WG, Fink IR, Scheer MH, Piazzon MC, et al. Transcriptome Sequencing Supports a Conservation of Macrophage Polarization in Fish. *Sci Rep* (2020) 10:13470. doi: 10.1038/s41598-020-70248-y
- Nakanishi T, Shibasaki Y, Matsuura YT. Cells in Fish. *Biology* (2015) 4:640–63. doi: 10.3390/biology4040640
- Trapani JA, Smyth MJ. Functional Significance of the Perforin/Granzyme Cell Death Pathway. *Nat Rev Immunol* (2002) 2:735–47. doi: 10.1038/nri911
- Mikalsen AB, Haugland O, Rode M, Solbakk IT, Evensen O. Atlantic Salmon Reovirus Infection Causes a Cd8 T Cell Myocarditis in Atlantic Salmon (*Salmo Salar* L.). *PLoS One* (2012) 7:e37269. doi: 10.1371/journal.pone.0037269
- Løvoll M, Austbø L, Jørgensen JB, Rimstad E, Frost P. Transcription of Reference Genes Used for Quantitative RT-PCR in Atlantic Salmon is Affected by Viral Infection. *Vet Res* (2011) 42:8. doi: 10.1186/1297-9716-42-8
- Pfaffl MW. Relative Quantification. *Real-time PCR* (2006) 63:63–82.
- Jørgensen SM, Lyng-Syvertsen B, Lukacs M, Grimholt U, Gjøen T. Expression of Mhc Class I Pathway Genes in Response to Infectious Salmon Anaemia Virus in Atlantic Salmon (*Salmo Salar* L.) Cells. *Fish Shellfish Immunol* (2006) 21:548–60. doi: 10.1016/j.fsi.2006.03.004
- Munang'andu HM, Fredriksen BN, Mutoloki S, Dalmo RA, Evensen Ø. The Kinetics of Cd4+ and Cd8+ T-Cell Gene Expression Correlate With Protection in Atlantic Salmon (*Salmo Salar* L.) Vaccinated Against Infectious Pancreatic Necrosis. *Vaccine* (2013) 31:1956–63. doi: 10.1016/j.vaccine.2013.02.008
- Bancroft J, Gamble M. *Theory and Practice of Histological Techniques*. Churchill Livingstone, London, United Kingdom: Elsevier Health Sciences (2008).
- Mills CD, Kincaid K, Alt JM, Heilman MJ, Hill AM. M-1/m-2 Macrophages and the th1/th2 Paradigm. *J Immunol* (2000) 164:6166–73. doi: 10.4049/jimmunol.164.12.6166
- Mørkøre T, Taksdal T, Birkeland S. Betydningen Av Pankreas Sykdom (Pd) For Filetkvalitet Av Oppdrettslaks. *Nofima Rapportserie* (2011).
- Liang B, Su J. Inducible Nitric Oxide Synthase (Inos) Mediates Vascular Endothelial Cell Apoptosis in Grass Carp Reovirus (Grcv)-Induced Hemorrhage. *Int J Mol Sci* (2019) 20:6335. doi: 10.3390/ijms20246335
- Lassalle MW, Igarashi S, Sasaki M, Wakamatsu K, Ito S, Horikoshi T. Effects of Melanogenesis-Inducing Nitric Oxide and Histamine on the Production of Eumelanin and Pheomelanin in Cultured Human Melanocytes. *Pigment Cell Res* (2003) 16:81–4. doi: 10.1034/j.1600-0749.2003.00004.x
- Stosik MP, Tokarz-Deptuła B, Deptuła W. Melanomacrophages and Melanomacrophage Centres in Osteichthyes. *Cent Eur J Immunol* (2019) 44:201. doi: 10.5114/cej.2019.87072
- Koppang E, Haugravoll E, Hordvik I, Aune L, Poppe T. Vaccine-Associated Granulomatous Inflammation and Melanin Accumulation in Atlantic Salmon, *Salmo Salar* L., White Muscle. *J Fish Dis* (2005) 28:13–22. doi: 10.1111/j.1365-2761.2004.00583.x
- Falk K, Press CM, Landsverk T, Dannevig BH. Spleen and Kidney of Atlantic Salmon (*Salmo Salar* L.) Show Histochemical Changes Early in the Course of Experimentally Induced Infectious Salmon Anaemia (Isa). *Vet Immunol Immunopathol* (1995) 49:115–26. doi: 10.1016/0165-2427(95)05427-8
- Gotoh T, Mori M. Arginase II Downregulates Nitric Oxide (No) Production and Prevents No-Mediated Apoptosis in Murine Macrophage-Derived Raw 264.7 Cells. *J Cell Biol* (1999) 144:427–34. doi: 10.1083/jcb.144.3.427
- Bratke K, Kuepper M, Bade B, Virchow JC Jr, Luttmann W. Differential Expression of Human Granzymes A, B, and K in Natural Killer Cells and During cd8+ T Cell Differentiation in Peripheral Blood. *Eur J Immunol* (2005) 35:2608–16. doi: 10.1002/eji.200526122
- Chaves-Pozo E, Valero Y, Lozano MT, Rodriguez-Cerezo P, Miao L, Campo V, et al. Fish Granzyme a Shows a Greater Role Than Granzyme B in Fish Innate Cell-Mediated Cytotoxicity. *Front Immunol* (2019) 10:2579. doi: 10.3389/fimmu.2019.02579

43. Pavlath GK. Regulation of Class I Mhc Expression in Skeletal Muscle: Deleterious Effect of Aberrant Expression on Myogenesis. *J Neuroimmunol* (2002) 125:42–50. doi: 10.1016/S0165-5728(02)00026-7
 44. Singh P, Kohr D, Kaps M, Blaes F. Skeletal Muscle Cell Mhc I Expression: Implications for Statin-Induced Myopathy. *Muscle Nerve* (2010) 41:179–84. doi: 10.1002/mus.21479
 45. Sarna T. Free Radical Scavenging Properties of Melanin. Interaction of Eu and Pheo Melanin Models With Reducing and Oxidizing Agents. *Free Radic Biol Med* (1999) 26:518–25. doi: 10.1016/S0891-5849(98)00234-2
 46. Thorsen J, Høyheim B, Koppang EO. Isolation of the Atlantic Salmon Tyrosinase Gene Family Reveals Heterogenous Transcripts in a Leukocyte Cell Line. *Pigment Cell Res* (2006) 19:327–36. doi: 10.1111/j.1600-0749.2006.00319.x
 47. Haugarvoll E, Thorsen J, Laane M, Huang Q, Koppang EO. Melanogenesis and Evidence for Melanosome Transport to the Plasma Membrane in a cd83+ Teleost Leukocyte Cell Line. *Pigment Cell Res* (2006) 19:214–25. doi: 10.1111/j.1600-0749.2006.00297.x
- Conflict of Interest:** The authors declare that the research was conducted in the absence of any commercial or financial relationships that could be construed as a potential conflict of interest.
- Copyright © 2021 Malik, Bjørgen, Nyman, Wessel, Koppang, Dahle and Rimstad. This is an open-access article distributed under the terms of the Creative Commons Attribution License (CC BY). The use, distribution or reproduction in other forums is permitted, provided the original author(s) and the copyright owner(s) are credited and that the original publication in this journal is cited, in accordance with accepted academic practice. No use, distribution or reproduction is permitted which does not comply with these terms.

III

Dynamics of polarized macrophages and activated CD8⁺ cells in heart tissue of Atlantic salmon infected with *Piscine orthoreovirus-1*.

Muhammad Salman Malik¹, Ingvild Berg Nyman¹, Øystein Wessel¹, Maria K. Dahle², Espen Rimstad^{1*}

¹ Section of Virology, Faculty of Veterinary Medicine, Norwegian University of Life Sciences, 1433 Ås, Norway

² Department of Fish Health, Norwegian Veterinary Institute, Ås, Norway

* Correspondence: espen.rimstad@nmbu.no (ER)

Manuscript

Abstract

Piscine orthoreovirus (PRV-1) infection causes heart and skeletal muscle inflammation (HSMI) in farmed Atlantic salmon (*Salmo salar*). PRV-1 is also associated with focal melanized changes in white skeletal muscle where infection of macrophages appears to be important. In this study, we studied the macrophage polarization into M1 (pro-inflammatory) and M2 (anti-inflammatory) phenotypes during experimentally induced HSMI. The immune response in heart with typical HSMI lesions was characterized by CD8⁺ and MHC-I expressing cells and not by polarized macrophages. Fluorescent *in situ* hybridization (FISH) assays revealed localization of PRV-1 in a few M1 macrophages in both heart and skeletal muscle. M2 type macrophages were widely scattered in the heart and were more abundant in heart compared to the skeletal muscle. However, M2 macrophages did not co-stain for PRV-1. There was a strong cellular immune response to the infection in the heart compared that of the skeletal muscle, with increased MHC-1 expression and partial colocalization with PRV-1 and high numbers of cytotoxic CD8⁺ granzyme producing cells that targeted PRV-1. In skeletal muscle, MHC-I and CD8⁺ cells were dispersed between myocytes, but these cells did not stain for PRV-1. Gene expression analysis by RT-qPCR agreed with the FISH results and confirmed a drop in the PRV-1 level following onset of the cell mediated immune response. Overall, the results indicated that M1 macrophages do not contribute to the initial development of HSMI however, large numbers of M2 macrophages reside in the heart and may contribute to the subsequent fast recovery following clearance of PRV-1 infection.

Keywords: Atlantic salmon, cell mediated immunity, heart and skeletal muscle inflammation macrophage polarization, Piscine orthoreovirus-1.

1. Introduction

Piscine orthoreovirus (PRV) infects salmonid fish and is linked to several diseases in different salmonid species [1]. The subtype PRV-1 is widespread in farmed Atlantic salmon (*Salmo salar*) and is found to be the etiological cause of heart and skeletal muscle inflammation (HSMI) [2]. This subtype is also associated with focal melanized changes in white skeletal muscle, commonly seen after slaughter [3]. PRV-1 infection of macrophages appears to be important for the development of the melanized changes. Comparative aspects of the pathogenesis and development of melanized changes and HSMI, including the role of macrophages, has not been explored.

HSMI is a common viral disease in the marine production phase of Atlantic salmon farming in Norway, and mortality has in some cases been reported to reach 20% [4,5]. The disease is also prevalent in other Atlantic salmon farming countries including Chile [6] and Scotland [7], but with few reported outbreaks in Canada [8]. Histopathological findings include moderate to severe inflammation of the epi-, myo- and endocardium layers of the heart and moderate necrosis in the red muscle tissue [9]. Experimentally it has been shown that the histopathological lesions of HSMI peaks about 2 weeks after the peak of the viral load during an acute PRV-1 infection [2].

In contrast, the melanized focal changes in white skeletal muscle have not been associated with clinical symptoms of disease or mortality. The condition is a rather common cause of reduced quality and declassification of the fillets. In contrast to HSMI, the focal melanized changes are only found in the skeletal muscle, and not in the heart. The histological appearance is different from HSMI and characterized as a chronic granulomatous inflammatory reaction. The melanized focal changes appear to increase in number and severity with time after transfer of the fish from fresh to sea water [10]. The chronicity of the condition indicates that it is not due to an acute PRV-1 infection, but possibly to the persistent infection phase.

PRV belongs to the *Reoviridae* family and has a ten-segmented, double stranded RNA (dsRNA) genome packed in double layered capsid. The virus initially infects and replicates in erythrocytes, which are considered as the major target cell population [11,12], implying that the virus can be found in any visceral organ [8,13]. In the acute phase when there is high viremia, the virus infects cardiomyocytes and several other cell types, while in the persistent phase PRV-1 establishes a

productive infection in long lived renal erythroid progenitor cells and in macrophages of Atlantic salmon [13].

The pathogenesis of HSMI is characterized by PRV-1 infection of cardiomyocytes and induction of a classic antiviral immune response that recruits CD8⁺ cytotoxic T cells [14-18]. Activated cytotoxic T cells use granzymes and perforins to kill pathogen infected cells through recognition of antigen presented by major histocompatibility complex I (MHC-I) [19]. Histological mapping of activated cytotoxic T cells and MHC-I positive cells and their correlation to PRV-1 infected cells could enhance the understanding of virus-specific cytotoxicity in HSMI. A transcriptomic analysis of HSMI affected heart tissue has indicated that CD4⁺T helper cells are also present [20].

In the focal melanized changes in white skeletal muscle, PRV-1 is not found in myocytes, but in macrophages and melano-macrophages [21,22]. The macrophage responses associated with PRV-1 infection seem to be central for the pathogenesis of these melanized spots [23], i.e. the PRV-1 infection is associated with the polarization of M1 and M2 macrophage phenotypes in the pathological changes. PRV-1 infected, pro-inflammatory M1 macrophages are found in the early stages of the spot formation, while PRV-1 infected melano-macrophages of the anti-inflammatory M2 phenotype, associated with tissue repair and regeneration, are found late in the spot development [23]. M1 polarized macrophages have a role in inactivation of pathogens through release of nitric oxide produced by the inducible nitric oxide synthase enzyme (iNOS2), whereas arginase-2 (Arg2) is considered as a marker for M2 type macrophages in teleost fish species [24,25].

In the present work we studied if the PRV-1 associated macrophage polarization seen in melanized changes in white skeletal muscle, also occurred in HSMI affected heart and skeletal muscle tissue. We used material from a well characterized experimental PRV-1 challenge [2], focusing on samples collected at the time of peak virus load and at the time of maximum histopathological changes. The samples were analyzed by multiplex fluorescent *in situ* hybridization (FISH) assays in combination with gene expression by RT-qPCR. In addition, the cellular immune response was mapped by targeting MHC-I, IL-17A and CD8 positive cells.

2. Results

2.1. *Localization of M1 and M2 polarized macrophage populations*

Heart and skeletal muscle tissues from an experimental PRV-1 challenge with samples selected from the key time points were used, i.e. peak virus load (4wpc), and maximum histopathological changes (6 wpc) (Fig. S3). Overall, PRV-1 infected cells were widely scattered in the layers of epicardium, compactum and spongiosum in infected fish at both sampling points (Fig 1F, Fig S2F), while only modest staining of PRV infected cells were seen in skeletal muscle (Fig 2D).

In the heart, a few iNOS2 positive M1 macrophages were spotted in the spongiosum layer both at the peak in viremia (Fig. S2A) and at the peak in HSMI associated pathological changes (Fig. 1A) and were localized particularly in aggregations of blood cells. iNOS2 stained cells were not found in the epi and compactum layers (Figs S2B, E). Several of the iNOS2 positive macrophages co-stained with PRV-1 (Fig 1B). Numerous Arg2 specific M2 type macrophages were detected in heart at both time points (Fig 1C, Fig. S2C), but with a more abundant appearance at 6 wpc. There was no staining of PRV-1 in Arg2 positive M2 macrophages (Fig. 1D, Fig S2D). In general, heart tissue from both time points had a lower number of M1 polarized macrophages compared to M2 polarized macrophages, as estimated through FISH (Fig. 1, Fig S2). The FISH results were in accordance with the transcript expression levels observed by RT-qPCR where the iNOS2 expression was low, while Arg2 expression was upregulated (approximately 11 folds, $p < 0.01$) in heart tissue at 6 wpc (Fig. 1G).

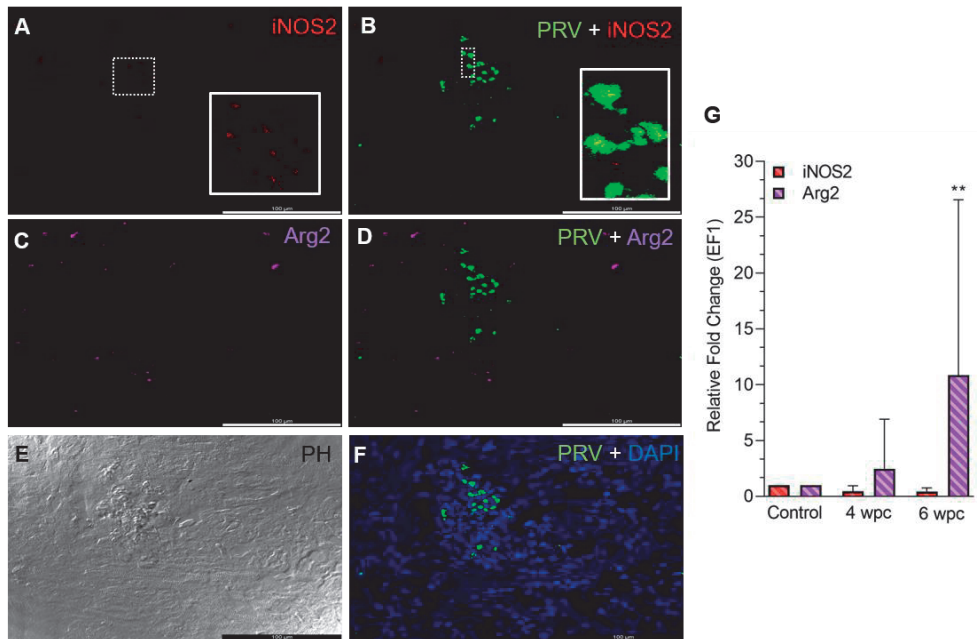


Figure 1. Fluorescent *in situ* hybridization (FISH) of *iNOS2*, *Arg2* and *PRV-1* (A-F) in heart tissue at the peak of HSMI (6 wpc). (A) A limited number of *iNOS2* (red) positive M1 macrophages were detected. (B) Merged image showing modest co-localization of *PRV-1* and *iNOS2* (inset). (C) Widely distributed *Arg2* (purple) positive M2 macrophages. (D) Merged image does not show co-localization of *PRV-1* and *Arg2*-positive M2 macrophages. (E) Phase contrast image showing aggregated blood cells in the stratum spongiosum layer. (F) *PRV-1* (green) infected cells amongst clustered blood cells. Cellular nuclei stained with DAPI (blue) (Scale Bar = 100 μ m). (G) Relative fold change expression (medians) of *iNOS2* and *Arg2* at 4 wpc and 6 wpc normalized against *EF1 α* expression. (*) shows significant difference from the control (** $p < 0.01$).

In skeletal muscle tissue at 4 wpc, dispersed M1 and M2 macrophage populations were observed (Fig. S3). At 6 wpc there were few *iNOS2* positive M1 macrophages detected around infected blood cells, but the majority of the M1 macrophages were negative for *PRV-1* (Fig. 2B). A similar pattern was observed for *Arg2* specific staining, with no co-localization of *PRV-1* and *Arg2* (Fig. 2D). There was a low level of *iNOS2* expression, however, the *Arg2* level was upregulated at 4 wpc (approximately 8 folds) but significantly upregulated at 6 wpc (6 folds, $p < 0.01$) (Fig. 2G).

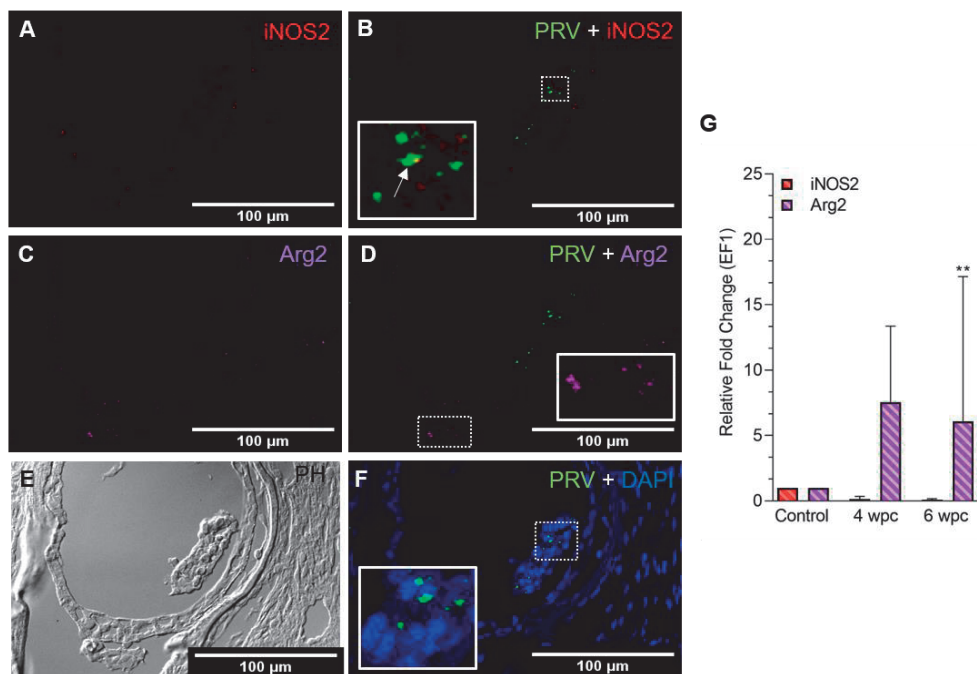


Figure 2. Fluorescent in situ hybridization (FISH) of iNOS2, Arg2 and PRV-1 (A-F) in skeletal muscle at the peak of HSMI (6 wpc). (A) Few iNOS2 (red) positive M1 macrophages were detected. (B) Merged image showing co-localization (yellow in inset) of PRV-1 and iNOS2-positive M1 macrophages. (C) Sporadic presence of Arg2 (purple) positive M2 macrophages (D) Merged image does not show co-localization of PRV-1 and Arg2 (E) Phase contrast image showing aggregated blood cells in a vessel in the center. (F) A limited number of PRV-1 infected cells (green) were found (Scale Bar = 100 μm). (G) Relative fold change expression (medians) of iNOS2 and Arg2 at 4 wpc and 6 wpc normalized against EF1α. (*) show significant difference from the control (** $p < 0.01$).

In non-infected control fish, Arg2 positive M2 macrophages were present in heart tissue but not found in skeletal muscle (Figs. S4, S5). No iNOS2 positive M1 macrophages were seen in neither heart nor skeletal muscle of these fish.

2.2. Localization of CD8⁺ cells in heart

A moderate level of CD8⁺ cells in the heart were detected at 4 wpc (Fig. S6) compared to very high numbers at 6 wpc (Fig. 3). CD8⁺ cells were abundant in the *stratum spongiosum* compared to epicardium and compactum layer. At 4 wpc, CD8⁺ cells localized around PRV-1 infected cardiomyocytes. No co-localization in the same cells was seen, but PRV-1 infected cardiomyocytes co-localizing with CD8⁺ cells was a typical feature. CD8⁺ cells were found widely distributed in the different heart regions at 6 wpc but were particularly abundant in areas with

dense PRV-1 staining and co-localized with the virus infected cells (Fig. 3C). CD8 α gene expression showed a minor increase at 4 wpc (1.2 fold) but was significantly increased at 6 wpc (67 fold, $p < 0.01$) (Fig 3D). Upregulation of CD8 α in heart at 6 wpc correlated in time with a moderate decline in PRV-1 RNA levels (Figs. S15A, 3D).

Granzyme A (GzmA) positive cells were prominent in heart tissue in areas with dense PRV-1 staining (Fig 3C). GzmA transcripts were highly increased at 6 wpc (approximately 5000 folds, $p < 0.01$), indicating increased cytotoxic activity (Fig 3E).

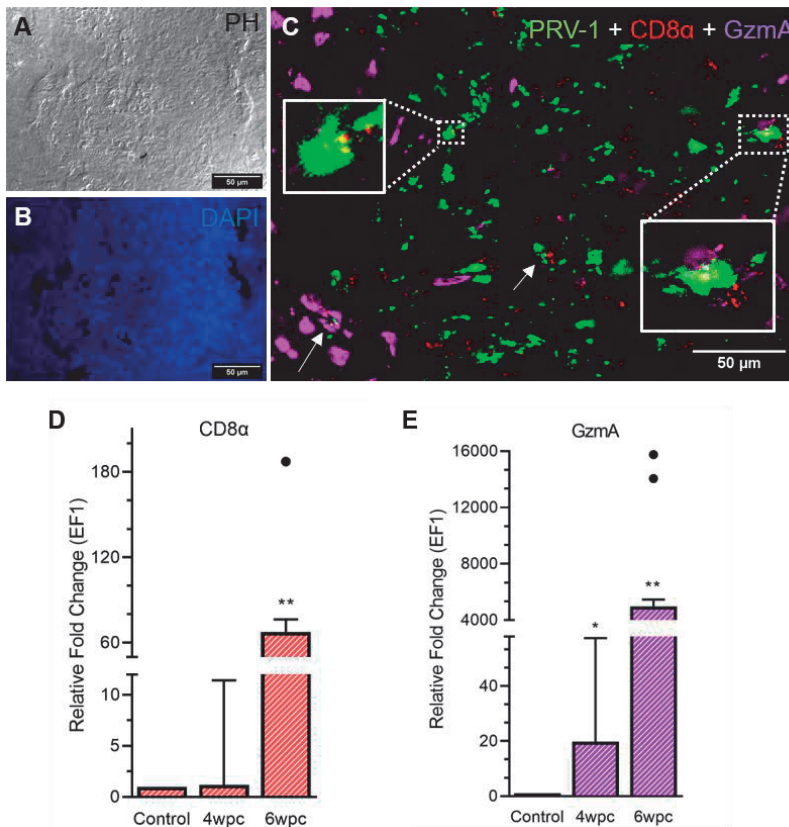


Figure 3. Fluorescent *in situ* hybridization (FISH) of PRV-1, CD8 α and GzmA in heart tissue at peak of HSMI associated histopathological changes (6 wpc). **(A)** Phase contrast image showing blood cells in the spongiosum. **(B)** Nuclei stained with DAPI (Blue). **(C)** Merged image showing co-localization of PRV-1 (green) with CD8 α (red) cells and cells expressing GzmA (purple) (arrows, yellow in inserts). GzmA stained cells were prominent in areas with dense PRV-1 staining (Scale Bar = 50 μ m). **(D-E)** Relative fold change expression (medians) of CD8 α and GzmA at 4 wpc and 6 wpc normalized against EF1 α . Dots show outlier values in the respective group of fish. (*) shows significant difference from the control (* $p < 0.05$, ** $p < 0.01$).

In the skeletal muscle tissue, the number of CD8⁺ cells were almost negligible at 4 wpc (Fig. S7) and cells were sporadically present at 6 wpc (Fig. 4). No co-localization of PRV-1 in CD8⁺ cells was detected (Fig 4C). Expression analysis showed a significant downregulation of CD8 α expression level at 4 wpc ($p < 0.05$) but a slight upregulated expression level at 6 wpc (3-folds, not statistically significant) (Fig 4D). GzmA positive cells were sporadically present in skeletal muscle at 6 wpc, but no co-localization with PRV-1 was seen (Fig. 4C). Gene expression of GzmA showed significant upregulation at 6 wpc (15 folds, $p < 0.01$) (Fig. 4E).

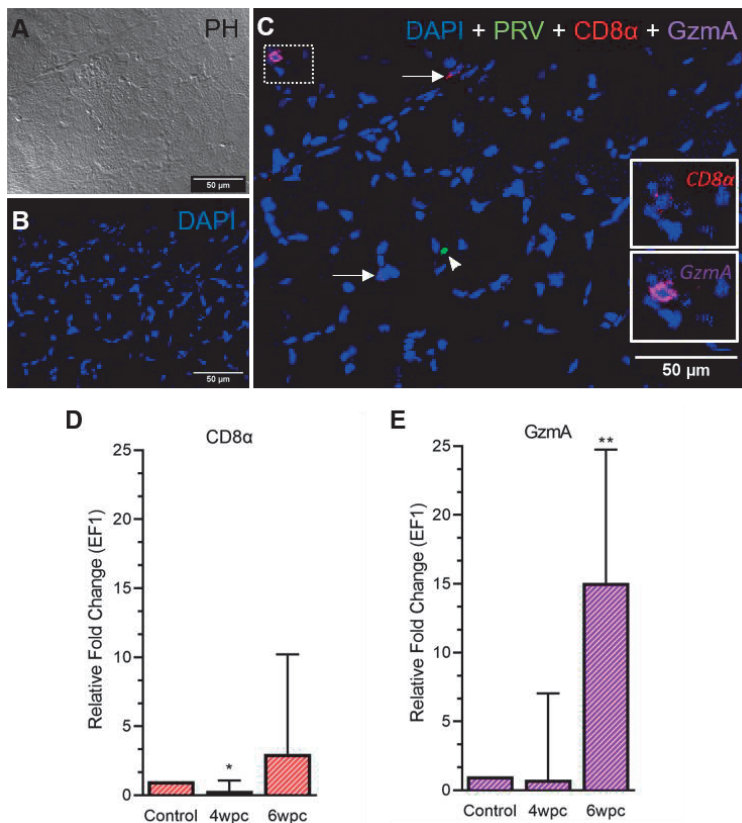


Figure 4. Fluorescent in situ hybridization (FISH) of CD8 α , GzmA and PRV-1 in skeletal muscle at the peak of HSMI (6 wpc). (A) Phase contrast image showing structures of myocytes. (B) Nuclei stained with DAPI (Blue). (C) Merged image showing presence of PRV-1 (green) infected cell (arrowhead), and CD8⁺ cells (insets). Some cells were stained positive only for CD8 α and GzmA specific transcripts (arrows) (Scale Bar = 50 μ m). (D-E) Relative fold expression (medians) of CD8 α and GzmA at 4 wpc and 6 wpc normalized against EF1 α . (*) shows significant difference from the control (* $p < 0.05$, ** $p < 0.01$).

2.3. PRV-1 in MHC-I positive and Th17 cells

In heart, modest co-staining of PRV-1 and MHC-I expressing cells was observed throughout the tissue at both peak of infection (Fig. S8) and peak HSMI changes (Fig. 5). Within aggregated blood cells, PRV-1 partially co-localized in MHC-I positive cells both at 4 wpc (Fig. S8) and 6 wpc (Fig. 5B). However, some MHC-I expressing cells in the aggregated blood did not stain for PRV-1. Significant upregulation of MHC-I was detected at both 4 wpc (72 folds, $p < 0.01$) and 6 wpc (93-folds, $p < 0.01$).

The Th17 T-helper cells of Atlantic salmon produce the proinflammatory cytokine IL-17A [26-29]. In heart, specific staining showed the presence of a few IL17A-positive cells at both samplings, however, no co-localization pattern with PRV-1 was observed (Fig 5B), and gene expression analysis showed a slight downregulation (not statistically significant) in expression of IL-17A in heart after PRV-1 infection (Fig S14).

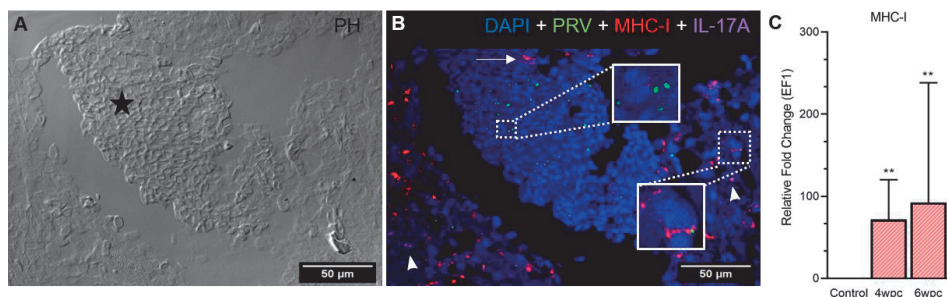


Figure 5. Fluorescent *in situ* hybridization (FISH) of PRV-1, MHC-I and IL-17A in heart tissue at peak of HSMI (6 wpc). **(A)** Phase contrast image showing an area with aggregated blood cells (star) in the spongiosum layer. **(B)** Merged image showing presence of PRV-1 (green) in cardiomyocytes and clotted blood cells, partially co-localizing with MHC-I (red) positive cells (insets). Some MHC-I positive cells in the aggregated blood did not co-stain for PRV-1 (arrow). IL-17A (purple) positive cells were sporadically scattered in the tissue (arrowhead). Nuclei stained with DAPI (Blue) (Scale Bar = 50 μ m). **(C)** Relative fold change expression (medians) of MHC-I at 4 wpc and 6 wpc normalized against EF1 α . Asterisk (*) shows significantly difference from the control (** $p < 0.01$).

In skeletal muscle tissue MHC-I positive cells were dispersed between myocytes at 4 wpc (Fig. S9B) and 6 wpc (Fig. 6B). A few PRV-1 positive cells were also present, but none of these co-localized with MHC-I positive cells. Expression analysis showed significant upregulation of MHC-I at 6 wpc (27-folds, $p < 0.01$) and correlated with a drop in the PRV-1 level. In contrast to the heart

tissue, no IL-17A specific transcripts could be detected in the skeletal muscle by FISH and RT-qPCR.

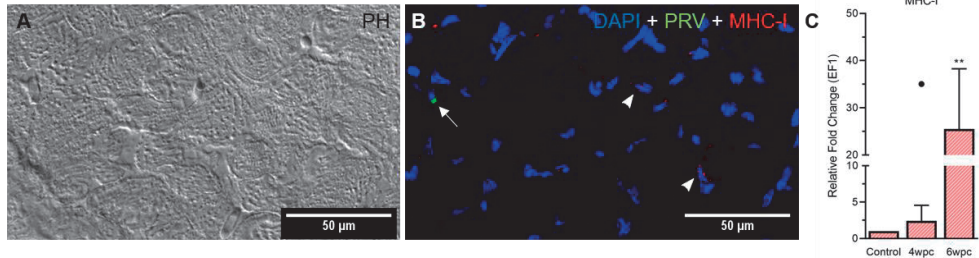


Figure 6. Fluorescent in situ hybridization (FISH) of PRV-1 and MHC-I in skeletal muscle at peak of HSMI associated histopathological changes (6 wpc). **(A)** Phase contrast image showing myocyte structure **(B)** Merged image showing MHC-I (red) positive cells (arrowheads) and PRV-1 (green) infected cells (arrow). Nuclei stained with DAPI (Blue) (Scale Bar = 50 µm). **(C)** Relative fold change expression (medians) of MHC-I at 4 wpc and 6 wpc normalized against EF1 α . Dot sign shows outlier value from the respective fish group. (*) shows significantly difference from the control (* $p < 0.05$, ** $p < 0.01$).

3. Discussion

The aim of this study was to map the cellular immune responses in heart and skeletal muscle tissues from PRV-1 infected fish by using FISH, targeting iNOS2 and Arg2 for M1 and M2 polarized macrophages respectively, with additional detection of MHC-I, and IL-17A, CD8, and GzmA positive cells. The focus was put on the peak of virus load (4 wpc) and the peak of histopathological changes in heart (6 wpc), using material from a previously performed PRV-1 experimental challenge. In accordance with the relative limited pathological changes of the skeletal muscle, the findings were in general more pronounced in heart, however the findings in the two organs were in accordance with each other.

We found that the Arg2-positive, tissue repair associated M2 type macrophages were the dominant type of macrophages in heart tissue both at 4 wpc and at 6 wpc. On the other hand, HSMI affected heart tissue showed a low presence of the classically activated M1 macrophage phenotype, based on iNOS2 staining. These results were corroborated by mRNA expression analyses by RT-qPCR. We did not observe presence of PRV-1 in M2 macrophages, and only a limited number of the M1 macrophages stained for PRV-1.

Contrasting these findings is the dominance of PRV-1 infected, pro-inflammatory M1 polarized macrophages recently reported from the early stages of melanized focal changes in skeletal muscle of Atlantic salmon [23]. In the later stages of the melanized focal changes the anti-inflammatory M2 phenotype dominates, but still many of these M2 cells are PRV-1 infected [23]. In the present study, many tissue repair associated M2 macrophages were found in heart tissue both at 4 wpc and 6 wpc. At 4 wpc the histopathological changes had not yet developed in the heart, and FISH of hearts from naive fish showed that they also harbored M2 positive cells. That heart tissues harbor a large number of M2 macrophages is in line with previous findings [13], and indicate the potential of the heart for healing via macrophage mediated repair mechanism [30]. The presence of self-renewing tissue macrophages, seeded during embryonic hematopoiesis, makes the repair of heart tissue in fish a well-organized process [31]. The macrophage M1 and M2 polarization is a dynamic process [32], and in line with this the pro-inflammatory M1 phenotype dominates early in the pathogenesis of melanized focal changes in skeletal muscle while the M2 phenotype dominates in the late stages [23]. Both macrophage phenotypes can be infected by PRV-1 [23]. The M1 macrophages with their high production of iNOS2 enzyme are inducers of melanin production [33], and in HSMI hearts there are only sporadic tiny patches of melanin present. The M2 macrophages found in heart were not stained for PRV-1 RNA, i.e. there was no indication of PRV-1 infection of this cell type in HSMI. Together this indicate a lack of a prominent role of M1 and M2 macrophages in the heart pathogenesis in HSMI. It is speculative whether the differences in pathogenesis of HSMI and melanized spots are caused by properties of the virus strain, i.e. different strains of orthoreovirus has been shown to vary in their ability to productively infect macrophages [34]; or of the tissue, i.e. heart tissue versus white skeletal muscle have differences in resident and recruited macrophage population; or of this is a difference associated with acute versus persistent infection.

The co-localization of PRV-1 infected cells with CD8⁺ cells and co-staining of PRV-1 with MHC-I positive cells by FISH assays enhanced the understanding of the pathogenesis of HSMI. Expression analysis supported the *in situ* expression of CD8⁺ cell marker and highly upregulated CD8 α expression was detected in heart, as in line with earlier studies [35]. Specific targeting of the infected cells by cells producing GzmA was seen by co-localization with PRV-1 infected cells.

GzmA specific transcripts are primarily produced by CD8⁺ T-cells, but can also be detected in natural killer cells [36]. In contrast to heart, skeletal muscle tissue exhibited moderate recruitment of CD8⁺ cells and these did also not co-localize with PRV-1 infected cells.

Atlantic salmon erythrocytes show high expression of MHC-I after PRV-infection [37]. MHC-I expressing cells also positive for PRV-1 were abundant and found associated with high numbers of GzmA positive cells. This finding suggests that antigen presentation to cytotoxic T cells is important for the elimination of PRV-1 from the heart. The high number of M2 macrophages indicates a rapid recovery of the heart tissue. The PRV-1 level correlated inversely with high CD8⁺ cell activity and MHC-I expression in heart.

4. Conclusion

The combination of FISH and RT-qPCR analysis confirmed that a strong CD8⁺ mediated immune response is important in the pathogenesis of HSMI, and demonstrated the co-localization of PRV-1 infected, MHC-I positive cells with CD8 and Granzyme A-positive cells in heart. The results did not indicate a prominent role of M1 polarized macrophages in the initial development of HSMI in Atlantic salmon, however the large population of M2 polarized macrophages resident in heart tissue indicates a prominent role of these cells in the rapid recovery of this organ after HSMI.

5. Materials and methods

5.1. Selection of the material

Material from a previously published PRV-1 challenge experiment were used in the present study [2]. In the previous study Atlantic salmon smolts had been injected with purified PRV-1 particles (2.3×10^6 copies/fish). PRV-1 level had been monitored by RT-qPCR previously for each individual fish as described earlier [2]. The fish reached peak viral load 4 weeks post challenge (wpc) and peak histopathological lesions at 6 wpc were consistent with HSMI. Tissue samples from heart (n = 6) and skeletal muscle (n = 6) were selected from 4 wpc and at 6 wpc for gene expression analysis. Non-infected fish at 4 wpc (n = 3) and 6 wpc (n = 3) were included as negative controls. Samples for fluorescent *in situ* hybridization analysis included heart and skeletal muscle samples from one fish at 4 wpc representing peak virus load with low cardiac score (cardiac score of 0.1, scale 0-3) and one fish at 6 wpc representing peak histopathological score (cardiac score of 2.6, scale 0-3). Tissue from a non-infected fish of the control group was used as negative control.

5.2. RNA isolation and RT-PCR

Total RNA had been extracted from the heart and skeletal muscle tissues (n = 6) as previously described [2]. For the present study, cDNA was synthesized from 1 µg total RNA from each tissue by using Quantitect Reverse Transcription Kit (Qiagen). Manufacturer's guidelines were followed for the elimination of genomic DNA by adding Wipeout buffer (7x) and for the incubation at 42 °C for 30 min with RT master-mix that includes reverse transcriptase enzyme and RNase inhibitor. A 12 µl reaction volume (15 ng cDNA input) was used for quantitative PCR using Maxima SYBR Green/ROX qPCR Master Mix (2x)-K0253 (Thermo Fisher Scientific). Thermal cycling conditions were set with initial denaturation for 10 min/95°C and 40 cycles of amplification with 15 sec/95 °C, 30 sec/60 °C and 30 sec/72 °C. The PRV-1 load had been examined in the previous study [2]. Melting curve analysis were performed to determine assay specificity. No template control (NTC) was run as a negative control on each plate. Elongation factor (EF1α) was run as a reference gene [38]. Cut off value was set at Ct 35 [39]. Relative fold change was measured for the genes of interest against the reference gene (EF1α) and the non-infected group (control). Specific primers targeting different genes were used for their amplification (Table 1).

Table 1. List of primers used in quantitative PCR analysis

Genes of interest	Primer	Concentration	Sequence (5'-3')	Product Size (bp)	Accession No.
<i>iNOS2</i> ^[23]	Fwd	400 nM	CATCGGCAGGATTCAAGTGGTCCAAT	135	XM_014214975.1
	Rev		GGTAATCGCAGACCTTAGGTTTCCTC		
<i>Arg2</i> ^[23]	Fwd	400 nM	CCTGAAGGACTTGGGTGTCCAGTA	109	XM_014190234.1
	Rev		CCGCTGCTTCCTTGACAAGAGGT		
<i>MHC Class I</i> ^[40]	Fwd	400 nM	CTGCATTGAGTGGCTGAAGA	175	AF504022
	Rev		GGTGATCTTGCCGTCTTTC		
<i>CD8α</i> ^[41]	Fwd	400 nM	CACTGAGAGAGACGGAAGACG	174	AY693393
	Rev		TTCAAAAACCTGCCATAAAGC		
<i>GzmA</i> ^[41]	Fwd	400 nM	GACATCATGCTGCTGAAGTTG	81	BT048013
	Rev		TGCCACAGGGACAGGTAACG		
<i>IL-17A</i> ^[28]	Fwd	400 nM	TGTTGTGTGCTGTGTGTCTATGC	136	XM_014211192
	Rev		TTCCCTCTGATTCTCTGTGGG		
<i>EF1α</i> ^[38]	Fwd	500 nM	TGCCCTCCAGGATGTCTAC	57	BG933897
	Rev		CACGGCCACAGGTAAGT		

5.3. Statistical analysis

Relative fold change (2- $\Delta\Delta$ Ct formula) medians of gene expression level was compared between control and infected groups of fish. Nonparametric Mann-Whitney test was applied to a low sample size in each group. Graphpad Prism version 9.0 (Graphpad Software Inc., La Jolla, CA, USA) was used for data analysis and graph layouts. A p-value ≤ 0.05 was considered as significantly different from the control.

5.4. Histopathological examination

Histopathological examination of heart and skeletal muscle tissues was performed to ensure that the selection criteria mentioned above were followed [2]. Imaging was performed using bright field microscope system (Carl Zeiss Light Microscopy System with Axio Imager 2 - Carl Zeiss AG, Oberkochen, Germany).

5.5. Multiplex-Fluorescent *in situ* hybridization (FISH)

Pretreatment of samples

Formalin fixed, paraffin embedded (FFPE) tissue sections (5 µm thickness) from heart and skeletal muscles tissues as selected earlier from fish with HSMI, were mounted using Superfrost plus (Thermo Fisher Scientific) slides. Sections were baked at 60 °C for 2 hrs in HybEZ™ II oven (Advanced Cell Diagnostics, catalog #321720) prior to deparaffinization with absolute ethanol (100 %) and fresh xylene. Initial blocking was done with hydrogen peroxide for 10 min at room temperature (RT). RNAscope antigen retrieval reagent (Advanced Cell Diagnostics, catalog #322000) was used for sections boiling for 15 min at 99 °C and further incubated with RNAscope protease plus reagent for 15 min at 40 °C in the HybEZ™ II oven as per manufacturer guidelines. Immedge hydrophobic barrier pen (Vector Laboratories, Burlingame, CA) was used to make hydrophobic barrier around tissue areas over slides for further probe hybridization procedures.

Multiplex *in situ* probes hybridization

Simultaneous detection multiple RNA targets were performed using RNAscope® Multiplex fluorescent V2 assay kit (Advanced Cell Diagnostics catalog #323100). Individual specific RNAscope probes (Listed in Table 2) were designed against PRV-1 L3 segment (Advanced Cell Diagnostics catalog #537451); iNOS2 (Advanced Cell Diagnostics catalog #548391); Arg2 (Advanced Cell Diagnostics catalog #548381) CD8α (Advanced Cell Diagnostics catalog #836821); Granzyme A (Advanced Cell Diagnostics catalog #836841); MHC-I (Advanced Cell Diagnostics catalog #836831) and IL-17A (Advanced Cell Diagnostics catalog #836861). Peptidylpropyl Isomerase B- (PPIB) (Advanced Cell Diagnostics, catalog #494421) was taken as a positive control for RNA integrity of the samples and dihydrodipicolinate reductase (DapB) from *Bacillus subtilis* (Advanced Cell Diagnostics catalog #310043) was taken as a negative control for cross-reactivity and background.

As per manufacturer's instructions, all probes were mixed and hybridized to each section for 2 hrs at 40 °C in the HybEZ™ II oven. Signal amplification was done by applying series of amplifier reagents (Amp1-Amp3) included in the kit. A 1:1500 diluted Opal fluorophores (Akoya Biosciences, CA, United States) in tyramide signal amplification (TSA) buffer (Advanced Cell

Diagnostics catalog #322809) were assigned separately to each probe with different excitation and emission spectrum to produce a specific output signal. RNAscope® multiplex Fluorescent Detection Reagents v2 (catalog #323110) were used to develop and block each probe sequentially. DAPI (fluorescent DNA stain) was used as a counter stain for 30 sec at RT. About 1-2 drops of Prolong Gold antifade mounting reagent (Thermo Fisher Scientific) were used to mount cover slides. Confocal microscopy was performed using TCS SP8 gSTED confocal microscope (Leica microsystems GmbH, Mannheim, Germany).

Table 2. List of probes used in FISH assays.

Probe		Target Region (bp)	Fluorophores	Emission/Excitation Wavelength (nm)	Channel*
Target	<i>PRV-L3</i>	415–1379	Opal 520 (FP1487001KT)	494/525	C1
	<i>iNOS2</i>	2–949	Opal 620 (FP1495001KT)	588/616	C2
	<i>Arg2</i>	1332–2053	Opal 690 (FP1497001KT)	676/694	C3
	<i>CD8α</i>	8-1033	Opal 620 (FP1495001KT)	588/616	C2
	<i>GzmA</i>	3-1088	Opal 690 (FP1497001KT)	676/694	C3
	<i>MHC-I</i>	2-2321	Opal 620 (FP1495001KT)	588/616	C2
	<i>IL-17A</i>	86-486	Opal 690 (FP1497001KT)	676/694	C3
Control	<i>PPIB</i>	20–934	Opal 520 (FP1487001KT)	494/525	C1
	<i>DapB</i>	414–862	Opal 520 (FP1487001KT)	494/525	C1

*Channel indicates excitation and emission properties for the specific fluorophores. Accession numbers: PRV-L3- KY429945; PPIB- NM_001140870; DapB- EF191515. For the other genes the acc. nos. are listed in Table 1.

References

1. Polinski, M.P.; Vendramin, N.; Cuenca, A.; Garver, K.A. Piscine orthoreovirus: Biology and distribution in farmed and wild fish. *Journal of fish diseases* **2020**, *43*, 1331-1352.
2. Wessel, Ø.; Braaen, S.; Alarcon, M.; Haatveit, H.; Roos, N.; Markussen, T.; Tengs, T.; Dahle, M.K.; Rimstad, E. Infection with purified piscine orthoreovirus demonstrates a causal relationship with heart and skeletal muscle inflammation in Atlantic salmon. *PLoS One* **2017**, *12*, e0183781, doi:10.1371/journal.pone.0183781.
3. Bjørgen, H.; Wessel, O.; Fjellidal, P.G.; Hansen, T.; Sveier, H.; Saebo, H.R.; Enger, K.B.; Monsen, E.; Kvellestad, A.; Rimstad, E.; et al. Piscine orthoreovirus (PRV) in red and melanised foci in white muscle of Atlantic salmon (*Salmo salar*). *Veterinary research* **2015**, *46*, 89, doi:10.1186/s13567-015-0244-6.
4. Kongtorp, R.; Kjerstad, A.; Taksdal, T.; Guttvik, A.; Falk, K. Heart and skeletal muscle inflammation in Atlantic salmon, *Salmo salar* L.: a new infectious disease. *Journal of fish diseases* **2004**, *27*, 351-358.
5. Svendsen, J.; Fritsvold, C. The health situation in Norwegian aquaculture. *Chapter 4.5 Cardiomyopathy syndrome (CMS). The Norwegian Veterinary Institute report series no 1b-2018. 2018.*
6. Godoy, M.G.; Kibenge, M.J.; Wang, Y.; Suarez, R.; Leiva, C.; Vallejos, F.; Kibenge, F.S. First description of clinical presentation of piscine orthoreovirus (PRV) infections in salmonid aquaculture in Chile and identification of a second genotype (Genotype II) of PRV. *Viral J* **2016**, *13*, 98, doi:10.1186/s12985-016-0554-y.
7. Ferguson, H.W.; Kongtorp, R.T.; Taksdal, T.; Graham, D.; Falk, K. An outbreak of disease resembling heart and skeletal muscle inflammation in Scottish farmed salmon, *Salmo salar* L., with observations on myocardial regeneration. *Journal of fish diseases* **2005**, *28*, 119-123, doi:10.1111/j.1365-2761.2004.00602.x.
8. Di Cicco, E.; Ferguson, H.W.; Schulze, A.D.; Kaukinen, K.H.; Li, S.; Vanderstichel, R.; Wessel, O.; Rimstad, E.; Gardner, I.A.; Hammell, K.L.; et al. Heart and skeletal muscle inflammation (HSMI) disease diagnosed on a British Columbia salmon farm through a longitudinal farm study. *PLoS One* **2017**, *12*, e0171471, doi:10.1371/journal.pone.0171471.
9. Kongtorp, R.; Taksdal, T.; Lyngøy, A. Pathology of heart and skeletal muscle inflammation (HSMI) in farmed Atlantic salmon *Salmo salar*. *Diseases of aquatic organisms* **2004**, *59*, 217-224.
10. Bjørgen, H.; Haldorsen, R.; Oaland, O.; Kvellestad, A.; Kannimuthu, D.; Rimstad, E.; Koppang, E.O. Melanized focal changes in skeletal muscle in farmed Atlantic salmon after natural infection with Piscine orthoreovirus (PRV). *Journal of fish diseases* **2019**, *42*, 935-945, doi:10.1111/jfd.12995.
11. Finstad, O.W.; Dahle, M.; Lindholm, T.; Nyman, I.; Løvoll, M.; Wallace, C.; Olsen, C.; Storset, A.; Rimstad, E. Piscine orthoreovirus (PRV) infects Atlantic salmon erythrocytes. *Veterinary Research* **2014**, *45*, 13.
12. Wessel, Ø.; Olsen, C.M.; Rimstad, E.; Dahle, M.K. Piscine orthoreovirus (PRV) replicates in Atlantic salmon (*Salmo salar* L.) erythrocytes ex vivo. *Veterinary research* **2015**, *46*, 26-26, doi:10.1186/s13567-015-0154-7.
13. Dhamotharan, K.; Bjørgen, H.; Malik, M.S.; Nyman, I.B.; Markussen, T.; Dahle, M.K.; Koppang, E.O.; Wessel, Ø.; Rimstad, E.J.P. Dissemination of Piscine orthoreovirus-1 (PRV-1) in Atlantic Salmon

- (*Salmo salar*) during the Early and Regenerating Phases of Infection. *Pathogens (Basel, Switzerland)* **2020**, *9*, 143.
14. Dahle, M.K.; Wessel, Ø.; Timmerhaus, G.; Nyman, I.B.; Jørgensen, S.M.; Rimstad, E.; Krasnov, A. Transcriptome analyses of Atlantic salmon (*Salmo salar* L.) erythrocytes infected with piscine orthoreovirus (PRV). *Fish & shellfish immunology* **2015**, *45*, 780-790.
 15. Røsæg, M.V.; Lund, M.; Nyman, I.B.; Markussen, T.; Aspehaug, V.; Sindre, H.; Dahle, M.K.; Rimstad, E. Immunological interactions between Piscine orthoreovirus and Salmonid alphavirus infections in Atlantic salmon. *Fish & shellfish immunology* **2017**, *64*, 308-319.
 16. Haatveit, H.M.; Wessel, Ø.; Markussen, T.; Lund, M.; Thiede, B.; Nyman, I.B.; Braaen, S.; Dahle, M.K.; Rimstad, E. Viral protein kinetics of piscine orthoreovirus infection in atlantic salmon blood cells. *Viruses* **2017**, *9*, 49.
 17. Mikalsen, A.B.; Haugland, O.; Rode, M.; Solbakk, I.T.; Evensen, O. Atlantic salmon reovirus infection causes a CD8 T cell myocarditis in Atlantic salmon (*Salmo salar* L.). *PLoS one* **2012**, *7*, e37269.
 18. Takizawa, F.; Dijkstra, J.M.; Kotterba, P.; Korytář, T.; Kock, H.; Köllner, B.; Jaureguiberry, B.; Nakanishi, T.; Fischer, U. The expression of CD8 α discriminates distinct T cell subsets in teleost fish. *Developmental & Comparative Immunology* **2011**, *35*, 752-763.
 19. Nakanishi, T.; Shibasaki, Y.; Matsuura, Y. T cells in fish. *Biology* **2015**, *4*, 640-663.
 20. Johansen, L.-H.; Thim, H.L.; Jørgensen, S.M.; Afanasyev, S.; Strandkog, G.; Taksdal, T.; Fremmerlid, K.; McLoughlin, M.; Jørgensen, J.B.; Krasnov, A. Comparison of transcriptomic responses to pancreas disease (PD) and heart and skeletal muscle inflammation (HSMI) in heart of Atlantic salmon (*Salmo salar* L.). *Fish & shellfish immunology* **2015**, *46*, 612-623.
 21. Di Cicco, E.; Ferguson, H.W.; Kaukinen, K.H.; Schulze, A.D.; Li, S.; Tabata, A.; Günther, O.P.; Mordecai, G.; Suttle, C.A.; Miller, K.M. The same strain of Piscine orthoreovirus (PRV-1) is involved in the development of different, but related, diseases in Atlantic and Pacific Salmon in British Columbia. *Facets* **2018**, *3*, 599-641.
 22. Malik, M.S.; Bjørgen, H.; Dharmotharan, K.; Wessel, Ø.; Koppang, E.O.; Di Cicco, E.; Hansen, E.F.; Dahle, M.K.; Rimstad, E. Erythroid Progenitor Cells in Atlantic Salmon (*Salmo salar*) May Be Persistently and Productively Infected with Piscine Orthoreovirus (PRV). *Viruses* **2019**, *11*, 824.
 23. Malik, M.S.; Bjørgen, H.; Nyman, I.B.; Wessel, Ø.; Koppang, E.O.; Dahle, M.K.; Rimstad, E. PRV-1 Infected Macrophages in Melanized Focal Changes in White Muscle of Atlantic Salmon (*Salmo salar*) Correlates With a Pro-Inflammatory Environment. *Frontiers in Immunology* **2021**, *12*, doi:10.3389/fimmu.2021.664624.
 24. Wentzel, A.S.; Petit, J.; van Veen, W.G.; Fink, I.R.; Scheer, M.H.; Piazzon, M.C.; Forlenza, M.; Spaink, H.P.; Wiegertjes, G.F. Transcriptome sequencing supports a conservation of macrophage polarization in fish. *Scientific reports* **2020**, *10*, 1-15.
 25. Wiegertjes, G.F.; Wentzel, A.S.; Spaink, H.P.; Elks, P.M.; Fink, I.R. Polarization of immune responses in fish: The 'macrophages first' point of view. *Molecular immunology* **2016**, *69*, 146-156.
 26. Zhang, Y.; Zhang, X.; Liang, Z.; Dai, K.; Zhu, M.; Zhang, M.; Pan, J.; Xue, R.; Cao, G.; Tang, J.; et al. Interleukin-17 suppresses grass carp reovirus infection in Ctenopharyngodon idellus kidney cells by activating NF- κ B signaling. *Aquaculture (Amsterdam, Netherlands)* **2020**, *520*, 734969-734969, doi:10.1016/j.aquaculture.2020.734969.

27. González-Fernández, C.; Chaves-Pozo, E.; Cuesta, A. Identification and Regulation of Interleukin-17 (IL-17) Family Ligands in the Teleost Fish European Sea Bass. *Int J Mol Sci* **2020**, *21*, 2439.
28. Marjara, I.S.; Chikwati, E.M.; Valen, E.C.; Krogdahl, Å.; Bakke, A.M. Transcriptional regulation of IL-17A and other inflammatory markers during the development of soybean meal-induced enteropathy in the distal intestine of Atlantic salmon (*Salmo salar* L.). *Cytokine* **2012**, *60*, 186-196.
29. Mutoloki, S.; Cooper, G.A.; Marjara, I.S.; Koop, B.F.; Evensen, Ø. High gene expression of inflammatory markers and IL-17A correlates with severity of injection site reactions of Atlantic salmon vaccinated with oil-adjuvanted vaccines. *BMC Genomics* **2010**, *11*, 336-336, doi:10.1186/1471-2164-11-336.
30. Schulze, P.C.; Lee, R.T. Macrophage-mediated cardiac fibrosis. **2004**.
31. Grayfer, L.; Kerimoglu, B.; Yaparla, A.; Hodgkinson, J.W.; Xie, J.; Belosevic, M. Mechanisms of Fish Macrophage Antimicrobial Immunity. *Frontiers in immunology* **2018**, *9*, 1105-1105, doi:10.3389/fimmu.2018.01105.
32. Viola, A.; Munari, F.; Sánchez-Rodríguez, R.; Scolaro, T.; Castegna, A. The metabolic signature of macrophage responses. *Frontiers in immunology* **2019**, *10*, 1462.
33. Lassalle, M.W.; Igarashi, S.; Sasaki, M.; Wakamatsu, K.; Ito, S.; Horikoshi, T. Effects of melanogenesis-inducing nitric oxide and histamine on the production of eumelanin and pheomelanin in cultured human melanocytes. *Pigment cell research* **2003**, *16*, 81-84.
34. O'Hara, D.; Patrick, M.; Cepica, D.; Coombs, K.M.; Duncan, R. Avian Reovirus Major μ -Class Outer Capsid Protein Influences Efficiency of Productive Macrophage Infection in a Virus Strain-Specific Manner. *Journal of Virology* **2001**, *75*, 5027-5035, doi:10.1128/jvi.75.11.5027-5035.2001.
35. Mikalsen, A.B.; Haugland, O.; Rode, M.; Solbakk, I.T.; Evensen, O. Atlantic salmon reovirus infection causes a CD8 T cell myocarditis in Atlantic salmon (*Salmo salar* L.). *PLoS one* **2012**, *7*.
36. Chaves-Pozo, E.; Valero, Y.; Lozano, M.T.; Rodríguez-Cerezo, P.; Miao, L.; Campo, V.; Esteban, M.A.; Cuesta, A. Fish Granzyme A shows a greater role than Granzyme B in fish innate cell-mediated cytotoxicity. *Frontiers in immunology* **2019**, *10*, 2579.
37. Dahle, M.K.; Wessel, O.; Timmerhaus, G.; Nyman, I.B.; Jørgensen, S.M.; Rimstad, E.; Krasnov, A. Transcriptome analyses of Atlantic salmon (*Salmo salar* L.) erythrocytes infected with piscine orthoreovirus (PRV). *Fish & shellfish immunology* **2015**, *45*, 780-790, doi:10.1016/j.fsi.2015.05.049.
38. Løvoll, M.; Austbø, L.; Jørgensen, J.B.; Rimstad, E.; Frost, P. Transcription of reference genes used for quantitative RT-PCR in Atlantic salmon is affected by viral infection. *Veterinary research* **2011**, *42*, 8.
39. Finstad Øystein Wessel, M.K.D., Tone Hæg Lindholm, Ingvild Berg Nyman, Marie Løvoll, Christian Wallace, Christel Moræus Olsen, Anne K Storset and Rimstad Espen. Piscine orthoreovirus (PRV) infects Atlantic salmon erythrocytes. *Veterinary Research* **2014**, *45*, 13.
40. Jørgensen, S.M.; Lyng-Syvrtsen, B.; Lukacs, M.; Grimholt, U.; Gjøen, T. Expression of MHC class I pathway genes in response to infectious salmon anaemia virus in Atlantic salmon (*Salmo salar* L.) cells. *Fish & Shellfish Immunology* **2006**, *21*, 548-560, doi:<https://doi.org/10.1016/j.fsi.2006.03.004>.
41. Munang'andu, H.M.; Fredriksen, B.N.; Mutoloki, S.; Dalmo, R.A.; Evensen, Ø. The kinetics of CD4+ and CD8+ T-cell gene expression correlate with protection in Atlantic salmon (*Salmo salar* L)

vaccinated against infectious pancreatic necrosis. *Vaccine* **2013**, *31*, 1956-1963, doi:<https://doi.org/10.1016/j.vaccine.2013.02.008>.

Supplementary Figures

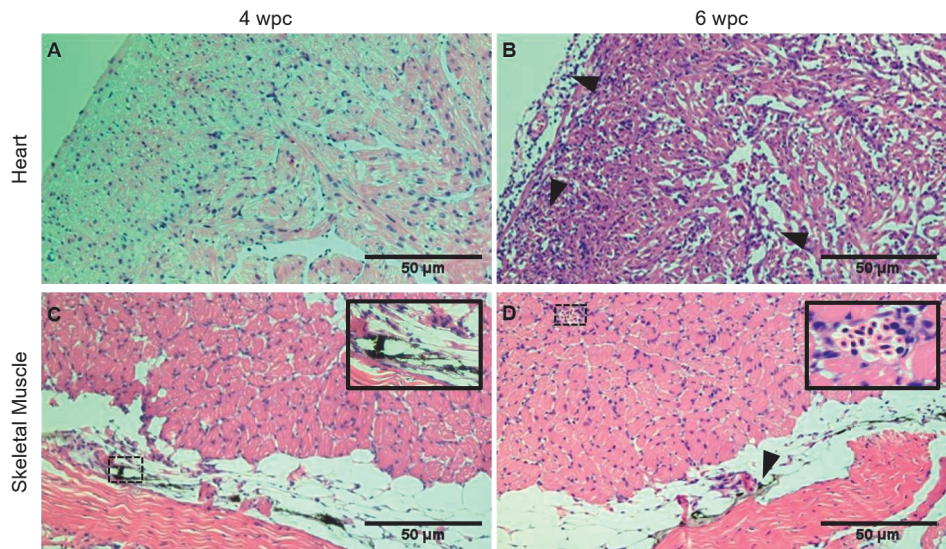


Figure S1. Histopathological overview of heart (A-B) and skeletal muscle (C-D) tissues at 4 and 6 wpc. **(A)** Heart section without any cardiac lesions at 4 wpc. **(B)** Severe cardiac lesions at 6 wpc in all three layers of the heart (arrowheads). **(C)** Intact and conformed myocytes with seldom presence of melanin (shown in inset). **(D)** Overall, mild degeneration with presence of small hemorrhages (shown in inset) with thin melanin deposits (arrowhead). Scale bar = 50 µm

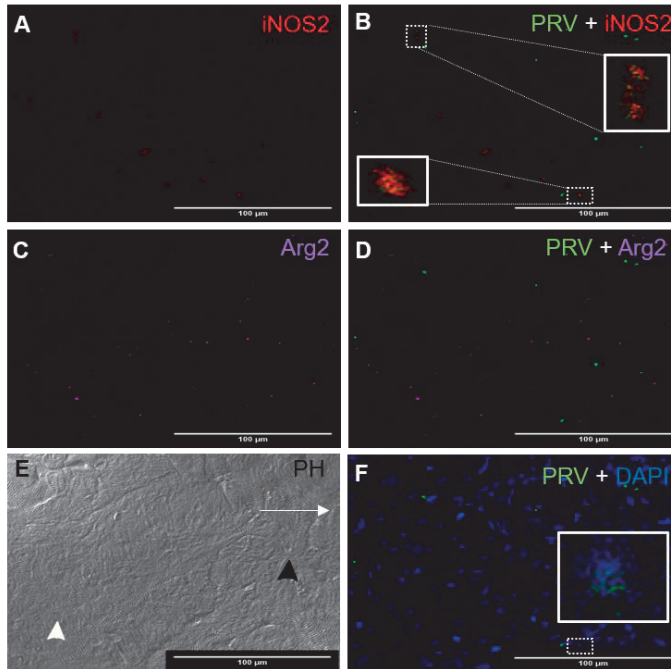


Figure S2. Fluorescent *in situ* hybridization (FISH) of *iNOS2*, *Arg2* and *PRV-1* in HSMI (Heart) at 4 wpc. **(A)** Few *iNOS2* (red) positive M1 macrophages were detected. **(B)** Merged image showing co-localization of some *PRV-1* in M1 macrophages (insets). **(C)** Widely distributed *Arg2* (purple) positive M2 macrophages. **(D)** Merged image showing no co-localization of *PRV-1* in M2 macrophages. **(E)** Phase contrast image showing all different layers of the heart i.e. epicardium (white arrow), compactum (black arrowhead) and spongiosum (white arrowhead). **(F)** *PRV-1* (green) infected cells scattered in all different layers of the heart. Nuclei stained with DAPI (blue). Scale Bar = 100 μ m

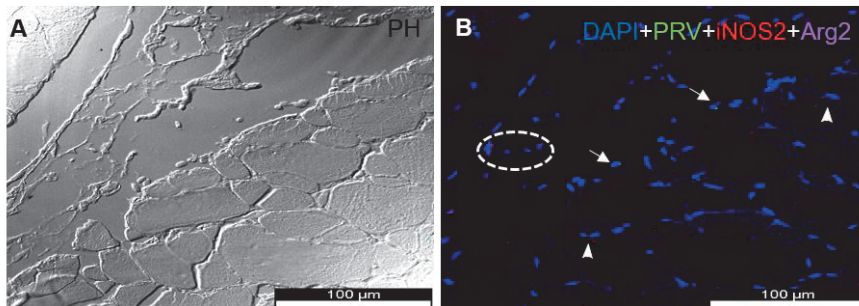


Figure S3. Fluorescent *in situ* hybridization (FISH) of *iNOS2*, *Arg2* and *PRV-1* in HSMI (skeletal muscle) at 4 wpc **(A)** Phase contrast image showing structure of myocytes. **(B)** Merged image showing *PRV-1* infected cells (arrows) surrounded by M1 (arrowheads) and M2 macrophages (dotted circle). No co-localization of *PRV-1* was observed in these cells. Scale bar = 100 μ m

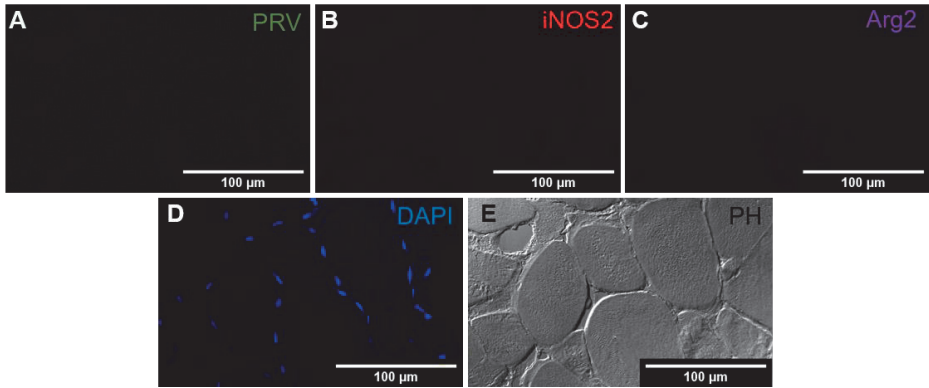


Figure S4. Skeletal muscle tissue from un-infected fish at 4 wpc from the control group of the HSMI experimental challenge trial **(A)** showing no PRV-1 (green) detection. **(B)** no iNOS2 (red) positive cells (M1) were detected. **(C)** No Arg2 (purple) positive cells (M2) were detected. **(D+E)** Nuclei were stained with DAPI (blue) and phase contrast image shows myocytes. Scale bar = 100μm

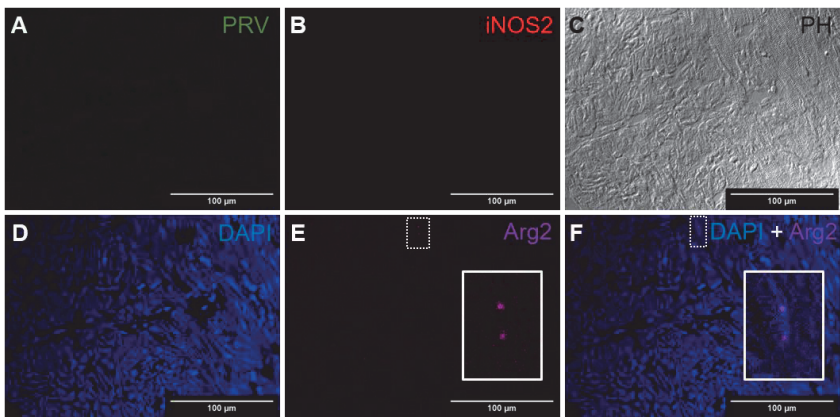


Figure S5. Heart tissue from un-infected fish at 4 wpc from the control, group of the HSMI experimental challenge study **(A)** showing no PRV-1 (green) detection. **(B)** no iNOS2 (red) positive cells (M1). **(C)** showing cellular structures in phase contrast image. **(D)** Cellular nuclei were stained with DAPI (blue). **(E+F)** showing very few Arg2 (purple) positive cells in the heart (insets). Scale bar = 100μm

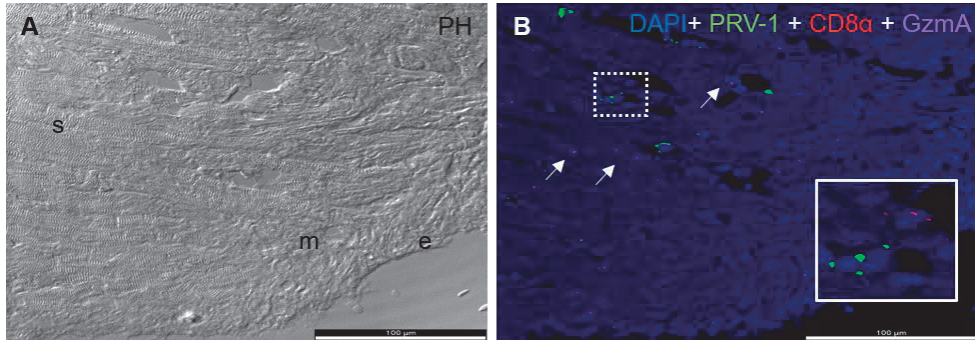


Figure S6. Fluorescent in situ hybridization (FISH) of PRV-1, CD8 α and GzmA in HSMI (Heart) at 4 wpc **(A)** Phase contrast image showing structure of epi- (e), myo- (m) and spongiosum layer. **(B)** Merged image showing no-colocalization of PRV-1 (green) but presence of few CD8 $^+$ (red) cells at the infected site (inset), whereas granzyme A (purple) specific transcripts are distributed in other cell populations as well. Scale bar = 100 μ m

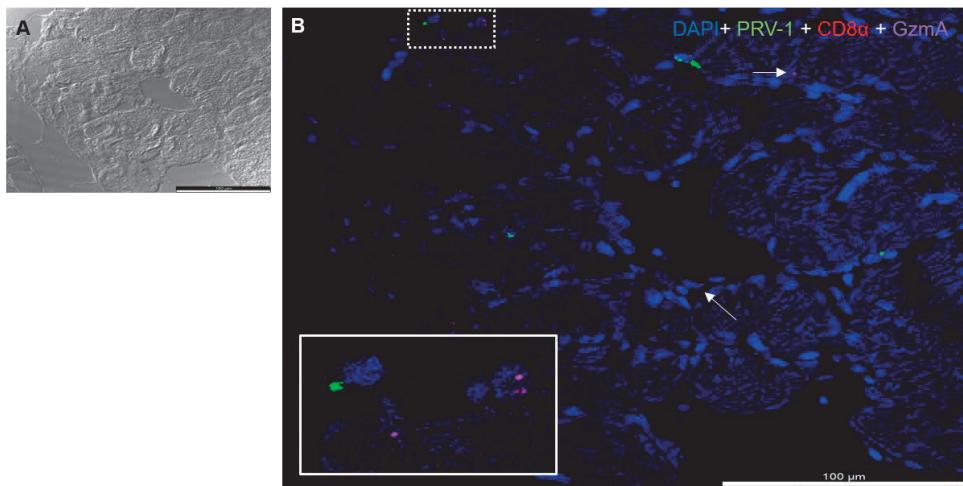


Figure S7. Fluorescent in situ hybridization (FISH) of PRV-1, CD8 α and GzmA in HSMI (skeletal muscle) at 4 wpc **(A)** Phase contrast image showing myocytes structure. **(B)** Merged image showing PRV-1 (green) infected cells (inset) and sporadic presence of granzyme A (purple) specific cells (arrows). No CD8 $^+$ cells (red) were detected in various regions at 4 wpc. Scale bar = 100 μ m

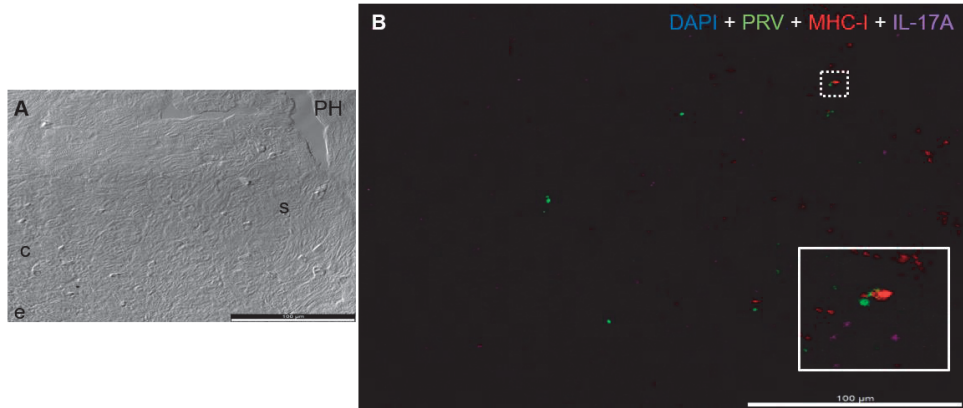


Figure S8. Fluorescent *in situ* hybridization (FISH) of PRV-1, MHC-I and IL-17A in HSMI (Heart) at 4 wpc **(A)** Phase contrast image showing structure of epi- (e), compactum (c) and spongiosum layer. **(B)** Merged image showing partial co-localization of PRV-1 (green) in MHC-I (red) positive cells. Very few IL-17A (purple) specific transcripts were detected (inset). Scale bar = 100 μ m

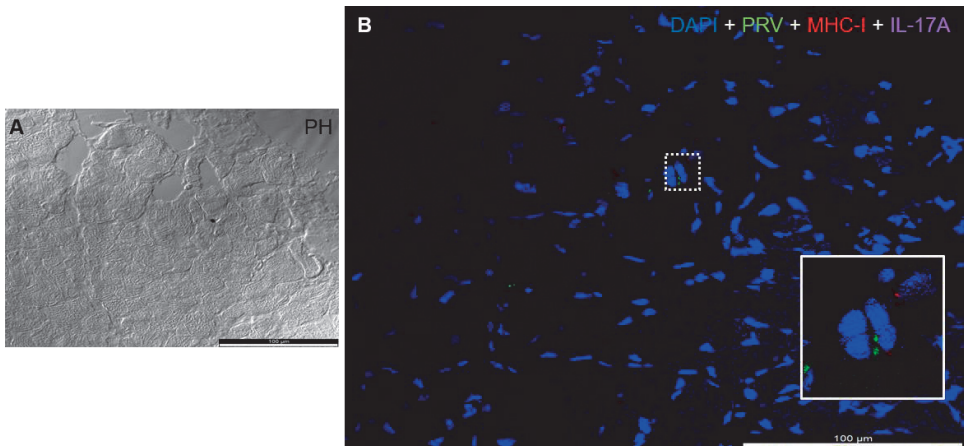


Figure S9. Fluorescent *in situ* hybridization (FISH) of PRV-1, MHC-I and IL-17A in HSMI (skeletal muscle) at 4 wpc. **(A)** Phase contrast image showing myocytes structure. **(B)** Merged image showing PRV-1 (green) infected cells (inset) surrounded by MHC-I (red) cells. Scale bar = 100 μ m

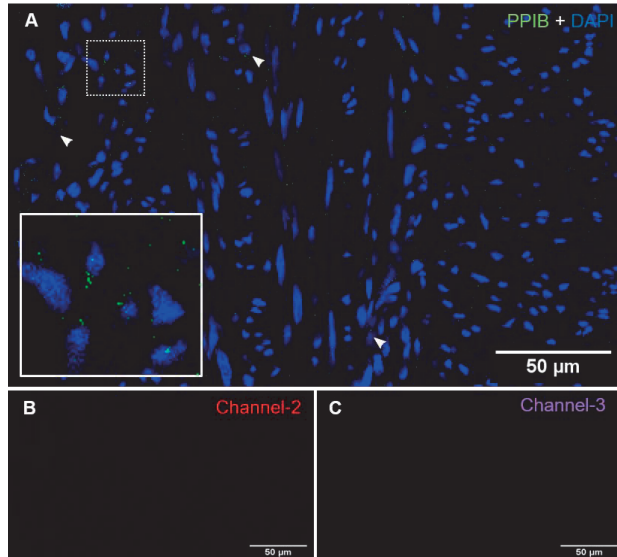


Figure S10. Positive control for Fluorescent *in situ* hybridization (FISH) assay in the heart tissue (4 wpc). (A) PPIB (green) punctuated expression (inset) is detected in various cells (arrowheads). Nuclei stained with DAPI (blue). (B+C) Channel-2 (red) and 3 (purple) were unstained and no signal detected. Scale bar = 50μm

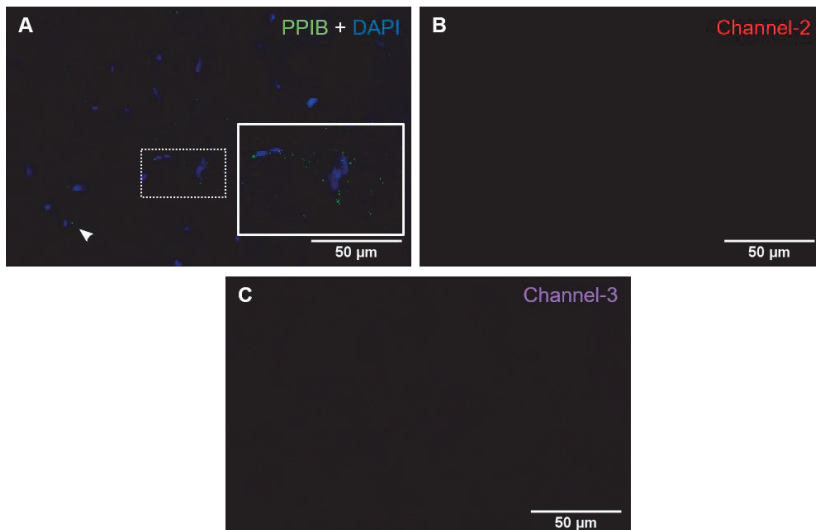


Figure S11. Positive control for Fluorescent *in situ* hybridization (FISH) assay in the skeletal muscle tissue (4 wpc). (A) PPIB (green) punctuated expression (inset) is detected in various cells (arrowheads). Nuclei stained with DAPI (blue). (B+C) Channel-2 (red) and 3 (purple) were unstained and no signal detected. Scale bar = 50μm

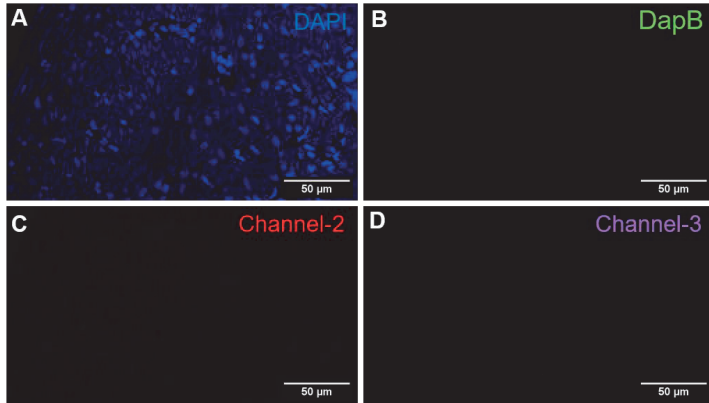


Figure S12. Negative control for Fluorescent *in situ* hybridization (FISH) assay in the heart tissue (4 wpc). (A) Cellular nuclei stained with DAPI (blue). (B) No detection of DapB (green) staining. (C+D) No signal detected in unstained channel-2 (red) and channel-3 (purple). Scale bar = 50 μ m

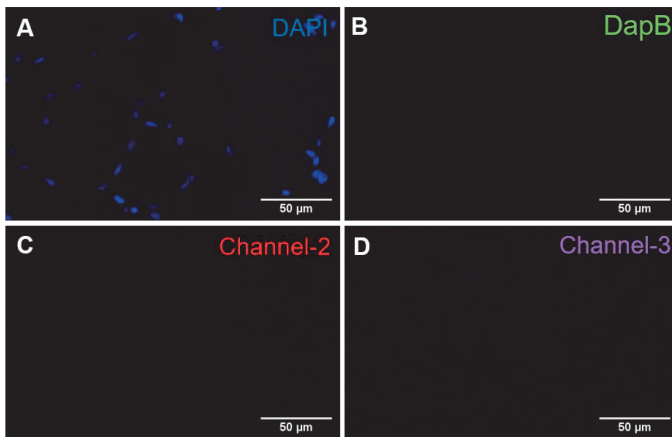


Figure S13. Negative control for Fluorescent *in situ* hybridization (FISH) assay in the skeletal muscle tissue (4 wpc). (A) Cellular nuclei stained with DAPI (blue). (B) No detection of DapB (green) staining. (C+D) No signal detected in unstained channel-2 (red) and channel-3 (purple). Scale bar = 50 μ m

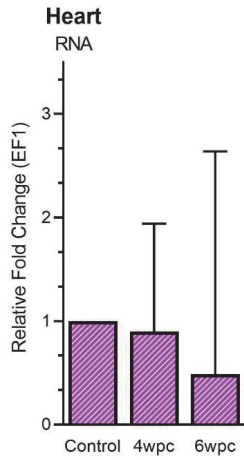


Figure S14. Relative fold change expression (medians) of IL-17A at 4 wpc and 6 wpc in the heart tissue normalized against EF1 α .

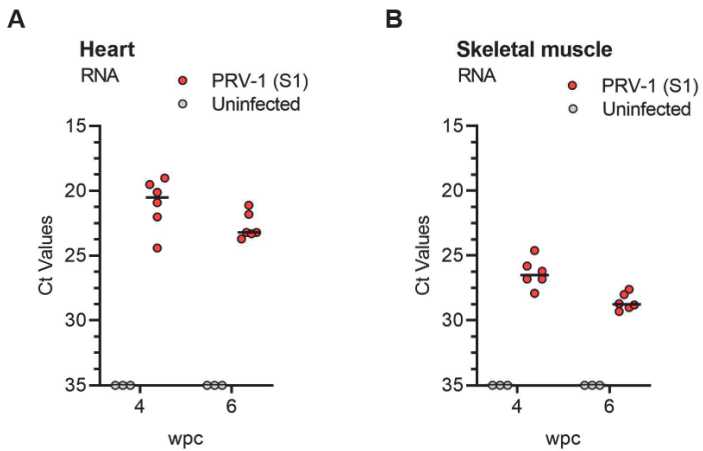


Figure S15. RT-qPCR data of the selected samples showing median (line) PRV-1 level (red) in (A) heart and (B) skeletal muscle tissues at peak viral load (4 wpc) and peak pathological changes (6 wpc). Uninfected fish from each timepoint was included as a control fish.

IV



Article

Piscine Orthoreovirus (PRV)-3, but Not PRV-2, Cross-Protects against PRV-1 and Heart and Skeletal Muscle Inflammation in Atlantic Salmon

Muhammad Salman Malik ^{1,†}, Lena H. Teige ^{1,†}, Stine Braaen ¹, Anne Berit Olsen ², Monica Nordberg ³, Marit M. Amundsen ², Kannimuthu Dhamotharan ¹, Steingrim Svenning ³, Eva Stina Edholm ³, Tomokazu Takano ⁴, Jorunn B. Jørgensen ³, Øystein Wessel ¹, Espen Rimstad ¹ and Maria K. Dahle ^{2,3,*}

- ¹ Faculty of Veterinary Medicine, Norwegian University of Life Sciences, 0454 Oslo, Norway; muhammad.salman.malik@nmbu.no (M.S.M.); l.h.teige@medisin.uio.no (L.H.T.); stine.braaen@nmbu.no (S.B.); dhamotharan.kannimuthu@hi.no (K.D.); oystein.wessel@nmbu.no (Ø.W.); espen.rimstad@nmbu.no (E.R.)
 - ² Department of Fish Health, Norwegian Veterinary Institute, 0454 Oslo, Norway; anne-berit.olsen@vetinst.no (A.B.O.); marit.masoy.Amundsen@vetinst.no (M.M.A.)
 - ³ Norwegian College of Fishery Science, Faculty of Biosciences, Fisheries and Economics, UiT The Arctic University of Norway, 9019 Tromsø, Norway; mno085@post.uit.no (M.N.); steingrim.svenning@uit.no (S.S.); eva-stina.i.edholm@uit.no (E.S.E.); jorunn.jorgensen@uit.no (J.B.J.)
 - ⁴ National Research Institute of Aquaculture, Japan Fisheries Research and Education Agency, Nansei 516-0193, Japan; takanoto@fra.affrc.go.jp
- * Correspondence: maria.dahle@vetinst.no; Tel.: +47-92612718
† Both authors contributed equally.



Citation: Malik, M.S.; Teige, L.H.; Braaen, S.; Olsen, A.B.; Nordberg, M.; Amundsen, M.M.; Dhamotharan, K.; Svenning, S.; Edholm, E.S.; Takano, T.; et al. Piscine Orthoreovirus (PRV)-3, but Not PRV-2, Cross-Protects against PRV-1 and Heart and Skeletal Muscle Inflammation in Atlantic Salmon. *Vaccines* **2021**, *9*, 230. <https://doi.org/10.3390/vaccines9030230>

Received: 25 January 2021

Accepted: 2 March 2021

Published: 6 March 2021

Publisher's Note: MDPI stays neutral with regard to jurisdictional claims in published maps and institutional affiliations.



Copyright: © 2021 by the authors. Licensee MDPI, Basel, Switzerland. This article is an open access article distributed under the terms and conditions of the Creative Commons Attribution (CC BY) license (<https://creativecommons.org/licenses/by/4.0/>).

Abstract: Heart and skeletal muscle inflammation (HSMI), caused by infection with *Piscine orthoreovirus-1* (PRV-1), is a common disease in farmed Atlantic salmon (*Salmo salar*). Both an inactivated whole virus vaccine and a DNA vaccine have previously been tested experimentally against HSMI and demonstrated to give partial but not full protection. To understand the mechanisms involved in protection against HSMI and evaluate the potential of live attenuated vaccine strategies, we set up a cross-protection experiment using PRV genotypes not associated with disease development in Atlantic salmon. The three known genotypes of PRV differ in their preference of salmonid host species. The main target species for PRV-1 is Atlantic salmon. Coho salmon (*Oncorhynchus kisutch*) is the target species for PRV-2, where the infection may induce erythrocytic inclusion body syndrome (EIBS). PRV-3 is associated with heart pathology and anemia in rainbow trout, but brown trout (*S. trutta*) is the likely natural main host species. Here, we tested if primary infection with PRV-2 or PRV-3 in Atlantic salmon could induce protection against secondary PRV-1 infection, in comparison with an adjuvanted, inactivated PRV-1 vaccine. Viral kinetics, production of cross-reactive antibodies, and protection against HSMI were studied. PRV-3, and to a low extent PRV-2, induced antibodies cross-reacting with the PRV-1 $\sigma 1$ protein, whereas no specific antibodies were detected after vaccination with inactivated PRV-1. Ten weeks after immunization, the fish were challenged through cohabitation with PRV-1-infected shedder fish. A primary PRV-3 infection completely blocked PRV-1 infection, while PRV-2 only reduced PRV-1 infection levels and the severity of HSMI pathology in a few individuals. This study indicates that infection with non-pathogenic, replicating PRV could be a future strategy to protect farmed salmon from HSMI.

Keywords: heart and skeletal muscle inflammation; *Piscine orthoreovirus*; vaccine; atlantic salmon; antibodies; immune response

1. Introduction

Infections represent a constant challenge and threat against fish health and welfare in aquaculture. Modern farming of Atlantic salmon (*Salmo salar*) is characterized by high-density populations, rapid growth, short production cycles, and artificial adaptation to

sea water. This life cycle does not ensure natural pathogen exposure in early life or the natural training of the fish innate immune system [1]. When transferred to the sea, the untrained immune system may not be ready to handle the novel repertoire of pathogens. High-density populations increase infection pressure, and transportation and handling procedures increase disease susceptibility due to stress [2]. In Atlantic salmon aquaculture, vaccines have been effective in protecting the fish from many diseases, but several viral diseases remain unsolved challenges [3]. One of the viral diseases of concern in European Atlantic salmon aquaculture is heart and skeletal muscle inflammation (HSMI) caused by *Piscine orthoreovirus* (PRV) [4,5].

PRV particles are non-enveloped with a double-layered protein capsid and a segmented double-stranded RNA genome [6]. PRV is a common virus infection in salmonids, and PRV-1 is the genotype associated with HSMI in farmed Atlantic salmon [5,7]. PRV is ubiquitous in the sea water phase of salmonid aquaculture [8] and is also emerging in fresh water facilities. However, PRV-1 is found to a lower extent in salmonids in the wild [9,10]. PRV-1 was first described in 2010 [4], whereas HSMI emerged in Norway and Scotland a decade earlier [11,12]. The causality between PRV-1 and HSMI was proven experimentally in 2017 using highly purified virus to induce disease [5]. PRV-1 is proposed to infect Atlantic salmon via the intestinal tract [13], followed by a massive infection of red blood cells and high plasma viremia [14,15]. Following the peak infection in red blood cells, the virus infects cardiomyocytes, which may result in an inflammatory response dominated by cytotoxic T-cells in the heart [16,17]. This inflammatory response is a hallmark of HSMI. In Atlantic salmon populations, the disease usually gives a moderate mortality that in severe cases may accumulate to 20% [11]. The relative high frequency of outbreaks makes HSMI a significant problem for the salmon farming industry. The PRV-1 infection becomes persistent in Atlantic salmon, and based on PRV prevalence in farm escapees [10], near 90% of Norwegian farmed salmon are PRV-infected in the marine phase, while near 100% of a small number of escaped Atlantic salmon were reported infected in Washington and British Columbia [18]. The long-term effects of PRV-1 infection are disputed, but the virus has been associated with the worsening of black spots in the skeletal muscle [19], a significant quality problem for the salmon production industry. This association is, however, disputed [20]. PRV-1 is also found in Canadian aquaculture, but few cases of HSMI have been reported [21], and HSMI has not been reproduced experimentally using Canadian isolates [22–24]. Different PRV-1 isolates with genetic variation have been shown to differ in the ability to induce HSMI [7]. PRV-1 has also been reported to infect other salmonid species [25].

Two additional genotypes of PRV, PRV-2 and PRV-3, have been described. They both infect salmonids, but with a different ability to infect and cause disease in the various salmonid species. PRV-2 infects coho salmon (*Oncorhynchus kisutch*) in Japan, causing erythrocytic inclusion body syndrome (EIBS) [26]. The main host species of PRV-3 may be wild brown trout (*S. trutta*) [27], but disease has only been found in farmed rainbow trout (*O. mykiss*), where PRV-3 is associated with heart inflammation and anemia [28–30]. Nucleotide alignment shows 80% (PRV-2) and 89% (PRV-3) identity to PRV-1 [31]. PRV-3 has previously been shown to infect Atlantic salmon experimentally, but without inducing HSMI [29]. Current information on PRV subtypes and distribution was recently reviewed [32].

No vaccines have been marketed against HSMI, but two different experimental vaccination approaches have been published. An inactivated whole virus vaccine, based on purified virus, was shown to give partial protection against HSMI, but less efficient protection against infection and virus replication [33]. Although promising, this approach has been hampered by the problem of producing PRV-1 for vaccine development, as no cell lines efficiently produce viral progeny [34]. A DNA vaccine approach has also been tested, and partial protection against HSMI was reported for a vaccine combining non-structural PRV-1 proteins with outer capsid antigens [35]. Although with some protective effects against HSMI, none of these vaccines have been able to block PRV-1 infection.

PRV-1 infection has been reported to induce strong innate antiviral responses in infected red blood cells [36]. Expression analysis of adaptive immune response genes has indicated that both humoral and cellular responses are induced [37], and it has been shown that infected fish produce specific antibodies against the outer capsid spike protein $\sigma 1$ [38], predicted to be the receptor-binding protein [39]. The cellular immune response initiated by PRV-1 in Atlantic salmon is strongly associated with HSMI development, and the typical HSMI myocarditis is dominated by an influx of cytotoxic T-cells [16,17]. However, this response is also associated with virus eradication from heart tissue, making cellular immunity a two-edged sword in HSMI [16,40].

The purpose of this study was to determine if PRV-2 or PRV-3 infection in Atlantic salmon could provide protection against a consecutive PRV-1 infection and HSMI. We compared the protection induced by PRV-2 and PRV-3 to an inactivated PRV-1 vaccine, and characterized immune responses, including the production of cross-reactive PRV-specific antibodies. The results show that PRV-3 infection in Atlantic salmon, in contrast to PRV-2, blocks a secondary infection with PRV-1, and that cross-protective antibodies may be one of the mechanism involved.

2. Materials and Methods

2.1. Experimental Trial and Sampling

The trial was performed at the Aquaculture Research station at K arvika, Troms, Norway, approved by the Norwegian Animal Research Authority, and performed in accordance with the recommendations of the current animal welfare regulations: FOR-1996-01-15-23 (Norway).

The PRV-1 infection material was prepared from two frozen blood cell pellets ($-80\text{ }^{\circ}\text{C}$) with PRV-1 qPCR ct values of 17.6 and 16.4, harvested from a PRV-1-infected Atlantic salmon from a previous experimental trial [5]. The virus isolate (PRV-1 NOR2012-V3621 [5]) originated from an HSMI outbreak in mid-Norway in 2012 and had been passaged in prior experimental trials, all resulting in HSMI. The PRV-3 infection material was a blood pellet that originated from a Norwegian outbreak in 2014 (PRV-3 NOR2014, [28]) and has been passaged twice experimentally in rainbow trout [30]. The mock-blood cell lysate originated from control fish from an Atlantic salmon experimental trial. The blood cell lysate from PRV-1, PRV-3 and mock was prepared by diluting the blood pellet (plasma removed prior to freezing) 1:10 in L15-medium, sonicating five times at 20 kHz for 10 s with 1 min rest in between and centrifuging at $3000\times g$ for 10 min before the collection of the supernatant. The PRV-2 infection material (PRV-2, [26]) originated from a frozen spleen sample from a Coho salmon. The tissue sample was homogenized in L15 medium as described for the blood pellets. The inactivated PRV-1 material was prepared from a batch of purified PRV-1 particles (PRV-1 NOR2012, 5.35×10^9 copies /mL) by PHARMAQ AS, as described in a previously published trial [33]. In short, the batch was formalin-inactivated and prepared as a water-in-oil formulation where the water phase (containing PRV antigens) was dispersed into a mineral oil continuous phase containing emulsifiers and stabilizers.

At the start of the trial, a total of 630 fish (*Salmo salar* L) were divided into four experimental groups of 75 fish and one mock control group of 125 fish, while 190 na ive fish from the same group were kept for use as transmission controls and future virus shedders. The experimental fish were kept in freshwater ($10\text{ }^{\circ}\text{C}$, 24:0 light:dark cycle, $>90\%$ O_2) and injected intraperitoneally (ip) with 0.2 mL of immunization material described above. Eight fish were sampled prior to Injection Week 0, and from each of the five experimental groups Week 2 and 5. Five weeks after the start of the experiment, 12 na ive fish labelled by tattoo pen were added to each of the tanks containing fish infected with PRV-1, PRV-2 and PRV-3 to monitor transmission of virus. At Weeks 8 and 10, eight experimental fish and six transmission control fish were sampled from each of these groups. At Week 8, 140 na ive fish in a separate tank were injected ip with 0.2 mL of a newly prepared batch of PRV-1 blood cell lysate (PRV-1 NOR2012, same origin and preparation method) and left for two weeks. After Sampling Week 10, 35 fish remained in each of the experimental groups, and

70 fish in the mock-infected control group. The mock group fish were divided into two tanks of 35 fish each, and three experimental tanks (PRV-2, PRV-3, InactPRV-1) and one of the mock-tanks were added to an equal number (35) of tattoo-labelled pre-infected PRV-1 shedder fish. No shedders were added to the original PRV-1 tank, and the other mock group was kept as a negative control. The number of tanks included in the experiment was now 6, and eight fish from each group were sampled on Weeks 12, 15 and 18. No fish died during the experiment.

At each sampling, blood was drawn from the caudal vein on BD Medical Vacutainer heparin-coated tubes (BD Medical, Mississauga, ON, USA). Hearts were sampled on 10% formalin for histology and samples from the heart tip and spleen were sampled on 0.5 mL of RNeasy Lysis Buffer (Qiagen, Hilden, Germany) in separate bar-coded microtubes (FluidX Ltd., Manchester, UK) along with additional organ samples not analyzed here. Blood samples were stored at 4 °C for a maximum of 6 h, centrifuged (3000× *g* for 5 min at 4 °C), and plasma and cell pellets were separated into different microtubes and stored at −80 °C. RNeasy Lysis Buffer samples were stored at 4 °C for 24 h followed by freezing at −20 °C. Formalin samples were stored at RT for 24 h, after which formalin was changed to 70% ethanol, and thereafter stored cold (4 °C).

2.2. RNA Preparation and RT-qPCR for Virus and Host Response Gene Analyses

Tissue samples from the spleen and heart (25 mg) on RNeasy Lysis Buffer (Qiagen) were transferred to 0.65 mL Qiazol lysis reagent (Qiagen) with a 5 mm steel bead and homogenized in a TissueLyzer II (Qiagen) for 2 × 5 min at 25 Hz followed by chloroform inclusion, and the aqueous phase was collected. RNeasy Mini QIAcube Kit (Qiagen) was used as per the manufacturer guidelines for automated RNA isolation. RNA concentrations were quantified using the Nanodrop ND-100 spectrophotometer (Thermo Fisher Scientific, Waltham, MA, USA). RNA was eluted in RNase-free water and stored at −80 °C until further use. For the PRV subtype expression analysis, i.e., PRV-1 and PRV-3, one-step RT-qPCR was performed using an Agilent Brilliant III Ultra Fast kit (Agilent Technologies, Santa Clara, CA, USA) with 100 ng (5 µL of 20 ng/µL) RNA per reaction in duplicates of 15 µL total reaction volume. The template was previously denatured at 95 °C for 5 min. Cycling parameters were set to 10 min for 50 °C, 3 min at 95 °C, and 40 cycles for 5 s at 95 °C and 10 s at 60 °C. The cut-off value was set to 35 and samples were run with positive and no template controls (NTC). For PRV-2 expression analysis, a Quantitect SYBR Green (Qiagen) RT-qPCR kit (catalogue number 204243) was used according to manufacturer instructions. A total of 100 ng RNA with prior denaturation at 95 °C for 5 min was used in duplicates in 15 µL of total reaction volume. Thermal conditions were 50 °C for 30 min, 95 °C for 15 min, and 40 cycles with 94 °C for 15 s, 60 °C for 30 s and 72 °C for 30 s. Specificity of the assay was confirmed by melting curve analysis. The same threshold level and positive controls were used together with NTCs. Probes and primer sequences are given in Supplementary Table S1.

For Immune gene expression, 400 ng total spleen RNA per sample was reverse transcribed to cDNA using the QuantiTect Reverse Transcription Kit with gDNA wipeout buffer (Qiagen). For qPCR, cDNA corresponding to 5 ng RNA was analyzed with Sso Advanced Universal SYBR Green Supermix (Bio-Rad, Hercules, CA, USA) and 10 pmol of forward and reverse target-specific primers in a 10 µL volume in duplicate wells on a 384 well plate. The amplification program (15 s 95 °C, 30 s 60 °C) was run for 40 cycles in a CFX Touch Real-Time PCR Detection System (Bio-Rad), followed by a melt point analysis. The results were analyzed using the software CFX Manager, version 3.1.1621.0826. The expression cycle threshold level was normalized against the elongation factor (EF) 1 α reference gene (Δ Ct). The $\Delta\Delta$ Ct method was used to calculate relative expression levels and fold induction compared to samples from the uninfected control samples.

2.3. Bead-Based Immunoassay

MagPlex[®]-C Microspheres (Luminex Corp., Austin, TX, USA) #12, #21, #27, #29, #34, #36, #44, #62 and #64 were coated with antigens using the Bio-Plex Amine Coupling Kit (Bio-Rad, Hercules, CA, USA) according to the manufacturer's instructions. The N-Hydroxysulfosuccinimide sodium salt and N-(3-Dimethylaminopropyl)-N'-ethylcarbodiimide used for the coupling reaction were from Sigma-Aldrich. For each coupling reaction, 6–24 µg of recombinant protein was used. The proteins used were recombinant PRV µ11 [41], lipid-modified PRV σ1 (LM-PRVσ1), unmodified infectious salmon anemia virus fusion protein (ISAV-FP), and lipid-modified ISAV-FP (LM-ISAV-FP) [39]. The bead concentrations were determined using the Countess automated cell counter (Invitrogen, Carlsbad, CA, USA). Coupled beads were stored in black Eppendorf tubes at 4 °C for up to 10 weeks. Incubations were performed at room temperature and protected from light on a HulaMixer rotator (Thermo Fisher Scientific) at 15 rpm.

The immunoassay was performed as described earlier (8). Briefly, Bio-Plex Pro™ Flat Bottom Plates (Bio-Rad) were used. Beads were diluted in phosphate buffered saline (PBS) containing 0.5% bovine serum albumin (BSA) (Bio-Rad Diagnostics GmbH, Dreieich, Germany) and 0.05% azide (Merck, Darmstadt, Germany) (PBS+) and 2500 beads of each bead number were added to each well. AntiSalmonid-IgH monoclonal antibody (clone IPA5F12, Cedarlane, Burlington, ON, Canada) diluted 1:400 in PBS+ was used as an unconjugated anti-IgM heavy chain monoclonal antibody. Biotinylated goat AntiMouse IgG2a antibody (Southern Biotechnology Association, Birmingham, AL, USA) diluted 1:1000 in PBS+ was used as a secondary antibody, and Streptavidin-PE (Invitrogen) diluted 1:50 in PBS+ was used as the reporter fluorochrome. Plates were read using two different Bio-Plex 200 (Bio-Rad) machines as part of a validation plan. The DD-gate was set to 5000–25,000, and between 20 and 100 beads from each population were read from each well. The reading was carried out using a low (standard) photomultiplier tube (PMT) setting. The results were analyzed using the Bio-Plex Manager 5.0 and 6.1 (Bio-Rad). All samples were analyzed in duplets on each of the two different Bio-Plex 200 (Bio-Rad) machines. The data used originated from one machine, but no differences were observed during validation. The data were given in mean fluorescence intensity (MFI), based on secondary antibody binding to beads, and were corrected for binding to control beads without antigen: $MFI(\text{antigen-containing beads}) - MFI(\text{control beads}) = MFI(\text{sample data})$.

2.4. Histopathology

Formalin-fixed hearts were paraffin embedded and routinely processed. The sections, 3–4 µm, were stained with hematoxylin and eosin (H&E, Merck, Kenilworth, NJ, USA) and studied under microscope. The slides from Experimental Weeks 15 and 18 ($n = 96$) were blinded to the study groups and scored by an experienced fish pathologist using a visual analogue scale from 0 to 3 as previously described [11].

2.5. Statistical Analysis

All statistical analyses were performed within GraphPad Prism 8.1.1 (GraphPad Software Inc., La Jolla, CA, USA). Ct values of the target groups (PRV-2, PRV-3 and Inact. PRV-1-injected fish exposed to PRV-1 shedder fish at 10 weeks post injection) were compared to the PRV-1 control group by using the non-parametric Mann–Whitney test due to the small sample size ($n = 8$) in each group. p -values of $p \leq 0.05$ were considered as significant.

3. Results

3.1. PRV Immunization Trial

The trial was performed as outlined in Figure 1. Initially (Week 0), Atlantic salmon with a mean weight of 41.3 g (± 5.8 g) were grouped and injected intraperitoneally (ip) with cell or tissue lysates containing infective PRV-1, PRV-2 or PRV-3, uninfected blood lysate (mock), or purified, inactivated and adjuvanted PRV-1 [33]. At 10 weeks, the mean weight of the injected fish was 107.6 g (± 18.4 g) with no significant difference

between groups (Supplementary file S2). At this timepoint, PRV-1-infected shedder fish were added to the remaining fish in the groups injected with PRV-2, PRV-3, inactivated PRV and half of the mock group to test the effects of immunization. Neither the initial ip challenge/immunization nor the cohabitant challenge led to mortality in any of the treatment groups, and there was no loss of fish or aberrant clinical observations during the experimental period. At the end of the experiment in Week 18, the fish mean weight was 193.6 g (+/− 29.5 g), with no statistically significant difference between groups.

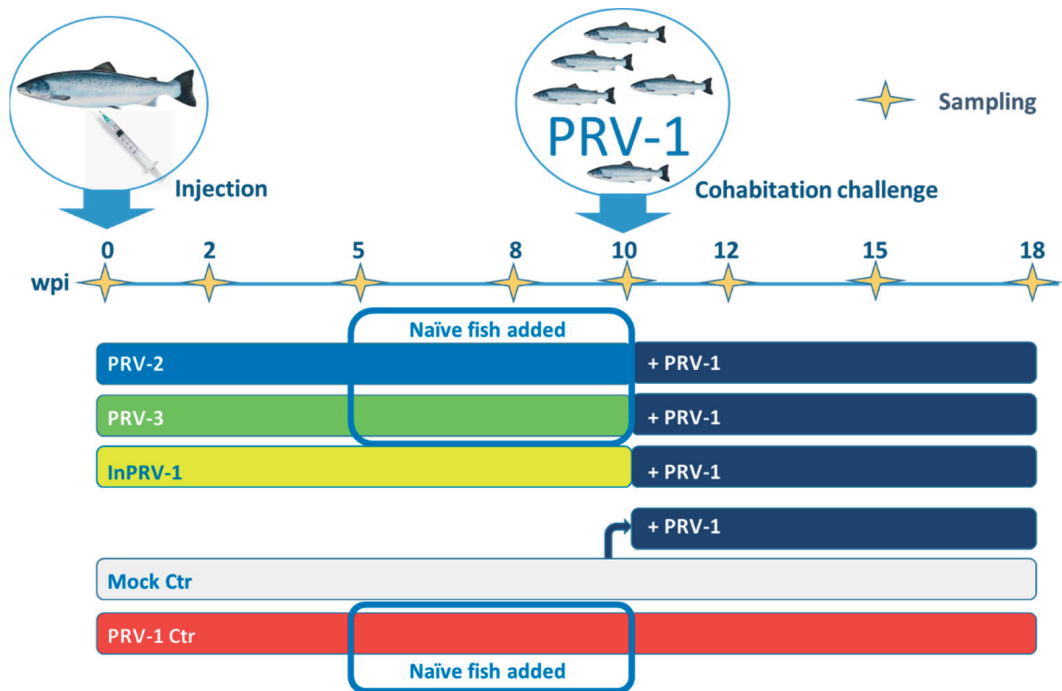


Figure 1. Groups and timeline of the *Piscine orthoreovirus* (PRV) immunization trial. Fish were immunized intraperitoneally (ip) with either spleen homogenate containing PRV-2 (blue group), blood cell lysate containing PRV-3 (green group), or purified, inactivated and adjuvanted PRV-1 (InPRV-1, yellow group). The negative control group (mock, white) was injected with blood cell lysate from uninfected fish. A positive control group was injected with PRV-1 (red). Naïve fish were added to tanks containing fish injected with infective PRV-1, PRV-2 and PRV-3 five weeks post injection (wpi) and sampled Week Eight and Ten to control viral shedding. After 10 weeks, the immunized group and half of the mock group was infected through cohabitation with fish experimentally infected with PRV-1 (shedders, dark blue) and thereafter monitored until Week 18. Yellow stars on the timeline show sampling time points (all groups).

3.2. Replication and Transmission of PRV Genotypes in Atlantic Salmon

The RNA loads of PRV-1, PRV-2 and PRV-3 were monitored by the RT-qPCR of spleen samples through the experimental period (Figure 2, Supplementary file S2). The spleen was chosen for analysis since PRV replicates in red blood cells, and spleen has been shown to reflect the levels of PRV infection in blood [42] better than, e.g., kidney. PRV-1 showed maximum replication during the first 5 weeks, as expected from previous trials (median Ct 14.79, interquartile range (IQR) Ct 14.12–15.37 (Figure 2A)), and persisted in spleen through the 18 weeks of the study with median PRV-1 levels above a Ct level of 20 at all sampling time points. Five weeks after injection, naïve fish were added to tanks of fish injected with PRV-1, PRV-2 and PRV-3 to study the transmission of the injected virus. The

naïve cohabitants added to the PRV-1 group at Week 5 were all infected 3 and 5 weeks later (Experimental Week 8 and 10, not analyzed at later time points). PRV-2 levels were generally low and reached the highest level after 2 weeks (median Ct of 26.7, IQR Ct 25.99–27.08), after which the infection declined. After 18 weeks, PRV-2 was detected in only one out of eight sampled fish. No naïve cohabitants added to the PRV-2 tank Week 5 were infected (Figure 2B). PRV-3 levels increased up to Week 5 (median Ct of 19.19, IQR Ct 18.02–20.75), then declined until Week 18 (Figure 2C). The added naïve cohabitants were not infected. No cross-infection was observed between the tanks, and no replication was observed in the fish injected with inactivated PRV-1, as monitored on Weeks 2, 5 and 10 (Supplementary Figure S1, Supplementary File S2).

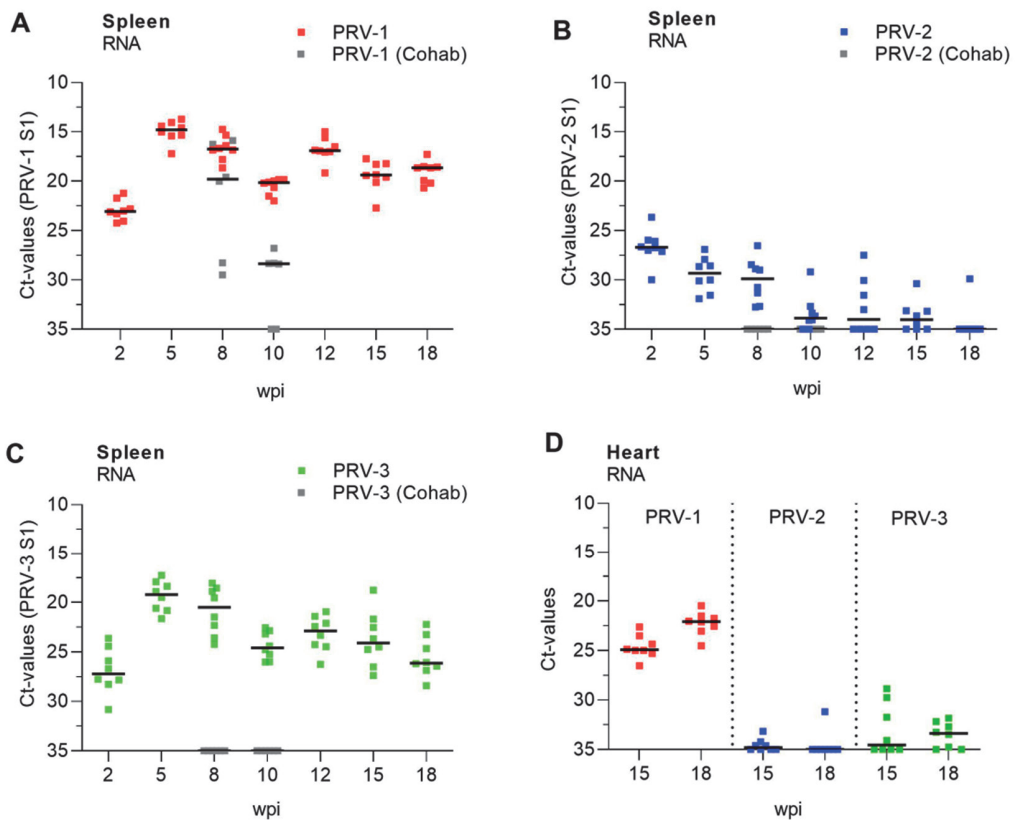


Figure 2. Development of infection with PRV-1, -2 and -3. Levels of PRV-1 (A), PRV-2 (B) and PRV-3 (C) as detected in spleen with specific RT-qPCR assays targeting the S1 genome segment in the respective viruses and trial groups. The figures show individual Ct values and median (line) at each sampling from 2 to 18 weeks post injection (wpi). Gray dots show virus levels in naïve cohabitants added to the tank at 5 wpi and removed at 10 wpi (5 weeks after exposure). Relative levels of PRV-1, -2 and -3 in heart at 15 and 18 weeks post infection (D).

To explore if there was any persistence of PRV2 and PRV3 in hearts at the end of the trial, we compared RNA loads of PRV-1, PRV-2 and PRV-3 in heart samples at 15 and 18 weeks (Figure 2D). Whereas PRV-1 levels in heart were below Ct 25, PRV-2 was only detected (median 34.87, IQR Ct 34.31–37.24) in the heart in two fish at 15 weeks after infection, and one fish at 18 weeks. PRV-3 was detected at low levels in 50% of the fish

hearts at both time points. Except for two fish at 15 weeks, all PRV-3-positive fish had Ct levels above 30 in the heart.

3.3. Production of Anti-PRV Antibodies

Using a bead-based multiplexed immunoassay based on recombinant PRV-1 spike protein σ 1 and outer capsid protein μ 1c [39], the ability of the viruses to induce cross-binding antibodies in plasma (IgM) was explored for the period 2 to 10 weeks after virus injection (Figure 3, Supplementary file S4). PRV-1 infection induced the production of PRV-1-specific antibodies against the viral proteins σ 1 and μ 1 after 8 and 10 weeks (Figure 3A) and induced unspecific antibodies binding to non-PRV antigens. PRV-2 induced low levels of PRV-1 σ 1 binding antibodies as detected at Weeks 5 and 8, declining at Week 10 (Figure 3B), in line with a low PRV-2 replication in the fish. PRV-3 infection induced intermediate levels of PRV-1 σ 1 binding antibodies, with lower background binding to non-PRV antigens (Figure 3C). Inactivated PRV-1 did not induce detectable production of antibodies binding to PRV-1 σ 1 (Figure 3D).

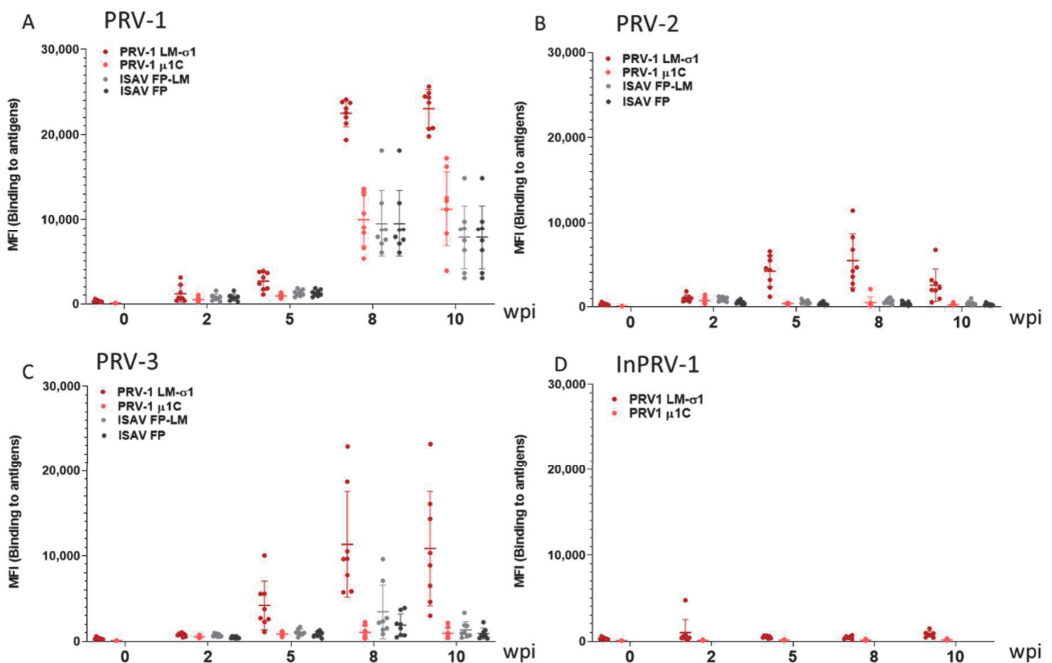


Figure 3. Production of anti-PRV antibodies. Magnetic beads coated with recombinant lipid-modified (LM)-PRV-1- σ 1, PRV-1 μ 1c, infectious salmon anemia virus fusion protein (ISAV-FP) or LM-ISAV-FP in a multiplexed assay were used to measure PRV-specific and unspecific antibodies in blood plasma sampled from fish in the PRV-1 (A), PRV-2 (B), PRV-3 (C) and InactPRV-1 (D) injected groups in the first 10 weeks post injection (wpi). MFI: median fluorescence intensity. The results from beads coated with PRV antigens are shown in red, and beads with non-PRV antigens in gray/black.

3.4. Innate and Cellular Immune Responses

In order to explore which immune responses were activated in the fish at the time of exposure to PRV-1 shedder fish (10wpi), spleen RNA samples were analyzed for transcript markers of cellular cytotoxic immunity (Figure 4, Supplementary file S5): CD8 α , IFN- γ and Granzyme A (Figure 4A), and innate interferon-mediated antiviral responses: viperin, myxovirus resistance gene (Mx), and interferon-stimulated gene (ISG)15 (Figure 4B). These genes have previously been shown to be induced in spleen after infection with PRV-1 [37].

PRV-1 infection induced both cellular and innate immune responses in spleen, whereas infection with PRV-2, PRV-3 or inactivated adjuvanted PRV-1 showed no or minor induction of the cellular and selected innate antiviral response genes.

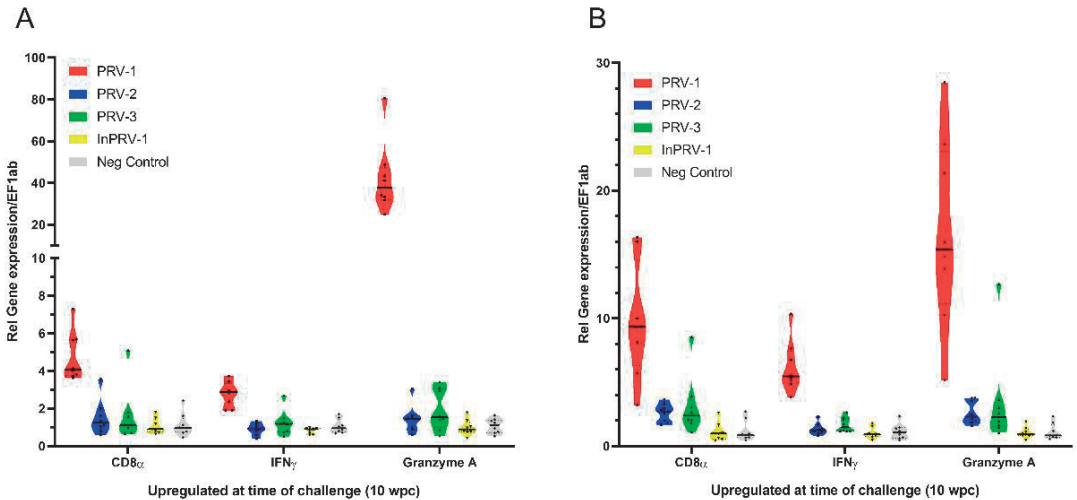


Figure 4. Cellular and innate antiviral immune responses 10 weeks after immunization (wpi). Cellular responses CD8 α , IFN γ and Granzyme A (A) and innate antiviral responses viperin, myxovirus resistance gene (Mx) and interferon-stimulated gene (ISG)15 (B) were analyzed by RT-qPCR in spleen, normalized for the reference gene EF1 α and shown as $2^{-\Delta\Delta Ct}$ levels. Gene expression in spleen samples from fish injected with PRV-1 (red), PRV-2 (blue), PRV-3 (green), inactivated PRV (yellow) and mock lysate (gray) are shown.

3.5. Protection from PRV Infection and HSMI

Infection with PRV-1 was monitored in all groups from 12 to 18 wpi (Figure 5A,B, Supplementary file S2). The mock-injected + PRV-1-exposed group acted as a positive control and was infected with PRV-1 after two weeks, peaking 5 weeks later (Experimental Week 15) at median Ct levels of 15 in the spleen and median Ct levels of 17 in the heart. Fish that had been immunized with PRV-2 showed a delayed and variable PRV-1 infection level at 15 and 18 weeks ranging from Ct 15 to 30 in the heart and Ct 10 to 24 in the spleen. Surprisingly, the highest PRV-1 infection levels in the PRV-2 group ranged beyond the levels in the positive controls, indicating that PRV-2 increased susceptibility to PRV-1 infection in some individuals. A similar partial protection was seen in the fish immunized with inactivated, adjuvanted PRV-1 (InactPRV-1), but without the replication boost seen in some fish in the PRV-2 group. In fish infected with PRV-3, the PRV-1 infection was completely blocked, except for two individuals showing high Ct levels in the spleen, one of which also had detectable PRV-3 in the heart.

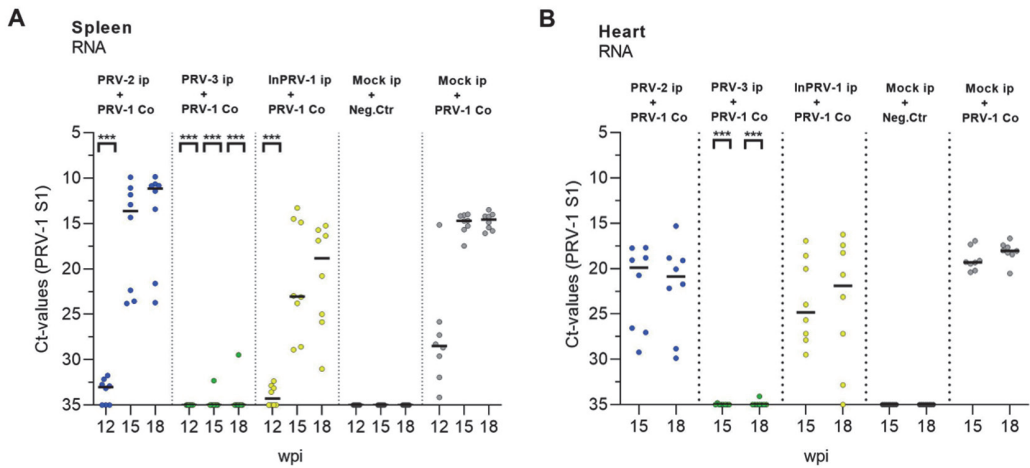


Figure 5. Development of PRV-1-infection after exposure by cohitation. The level of PRV-1 after infection with PRV-1 shedders at 10 weeks was monitored by RT-qPCR at Weeks 12, 15 and 18 in the spleen (A) and Weeks 15 and 18 in the heart (B). Each dot represents an individual Ct value with a line (median) at each sampling. Dot color: Fish pre-injected with PRV-2 (Blue), PRV-3 (green), Inactivated PRV-1 (Yellow), or mock (grey), then secondary infected with PRV-1 where marked. Statistical analyses were performed by comparing each target group with the PRV-1 control group at each time point using the Mann–Whitney test. Asterisk shows significant difference (***) $p < 0.001$); wpi = weeks post immunization.

Hearts from fish sampled at 15 and 18 weeks after PRV-1 infection by shedders, and the corresponding uninfected control group, were prepared for histopathology and scored for tissue changes consistent with HSMI (score system 0–3 [11], Figure 6, Supplementary file S6). At 15 weeks, heart pathology was seen only in the PRV-1 group infected ip at the beginning of the trial (five of eight fish had mild lesions, i.e., a score of 1). HSMI-like lesions were present in all individuals in the mock + PRV-1 control group (positive control) at Week 18, with a median HSMI pathology score of 2.5 (1.5–2.5). For the PRV-2 + PRV-1 group, the median pathology score was reduced to 2 (six out of eight fish had lesions), and for the PRV-3 + PRV-1 group pathology was completely absent in all eight fish (a score of 0). Six out of eight fish from the InactPRV-1 + PRV-1 group were also without heart lesions. The group infected with PRV-1 ip Week 0 showed a median pathology score of 1 (six out of eight fish had mild lesions), 18 weeks after infection.

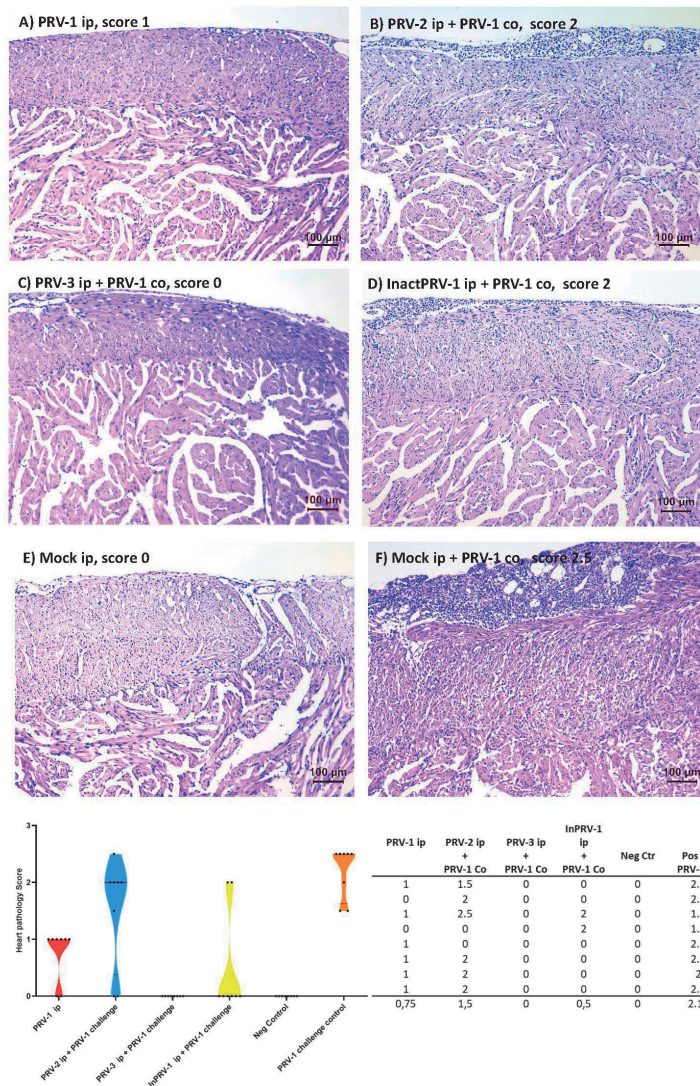


Figure 6. Histopathology and scores of *A. salmon* hearts. The status of Atlantic salmon hearts was scored for heart and skeletal muscle inflammation (HSMI) pathology 18 weeks after immunization and eight weeks after PRV-1 cohabitant challenge. The scoring of pancarditis was performed according to a visual analogue scale from 0 to 3, where 0 represents a healthy heart, scores above 1 represent hearts with increased cellularity due to immune cell recruitment in the outer epicardial layer, and more severe cases (a score of 2,5) also show increased cellularity in the outer compact and inner spongy layers of the heart ventricle. (A) PRV-1 ip injected Week 0, (B) PRV-2 immunized ip + PRV-1, (C) PRV-3 immunized ip + PRV-1, (D) inactivated InPRV-1 immunized ip + PRV-1, (E) negative control, mock-injected ip, (F) positive control, mock-injected ip + PRV-1, and (G) a table and violin plot showing pathology scores of individual fish in each experimental group ($n = 8$) pre-injected with PRV-1 (red), PRV-2 (Blue), PRV-3 (green), Inactivated PRV-1 (Yellow), or mock (grey), then secondary infected with PRV-1 where marked.

3.6. Immune Responses after Challenge of Immunized Salmon

The specific antibody response (Figure 7A, Supplementary file S4) and cellular cytotoxic immune gene activation—Granzyme A, IFN γ (Figure 7B,C, Supplementary file S5)—were monitored after the PRV-1 challenge at Experimental Weeks 12–18 (two to eight weeks after exposure to shedder fish). The positive control group showed specific and unspecific antibody production and induction of Granzyme A and IFN γ levels in the spleen. The PRV-1-induced antibody response tended to be higher in some fish in the PRV-2 immunized group and lower in fish immunized with inactivated PRV-1. Both observations were in line with the PRV-1 levels found in the spleen. Both groups induced Granzyme A and IFN γ transcripts in fish with high PRV-1 loads, but not in individuals with low PRV-1 loads. In the fish immunized with PRV-3, the antibody levels declined from Week 10 to 18, and since the fish were protected against PRV-1 infection, the antibodies observed most likely resulted from the initial immunization with PRV-3. No regulation of cytotoxic T-cell-associated immune genes was seen. The antibody levels in this group can be compared to the group infected with PRV-1 at Week 0, which showed even higher levels of anti PRV-1 σ 1 antibodies during Weeks 12–18. In contrast, whereas fish that were PRV-1 infected Week 0 still had induced levels of Granzyme A in their spleens, the PRV-3-injected group did not.

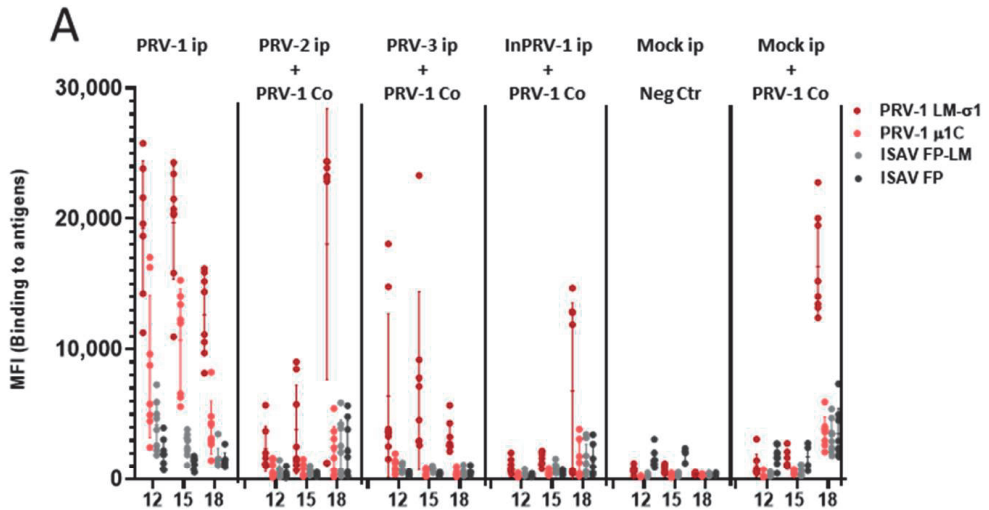


Figure 7. Cont.

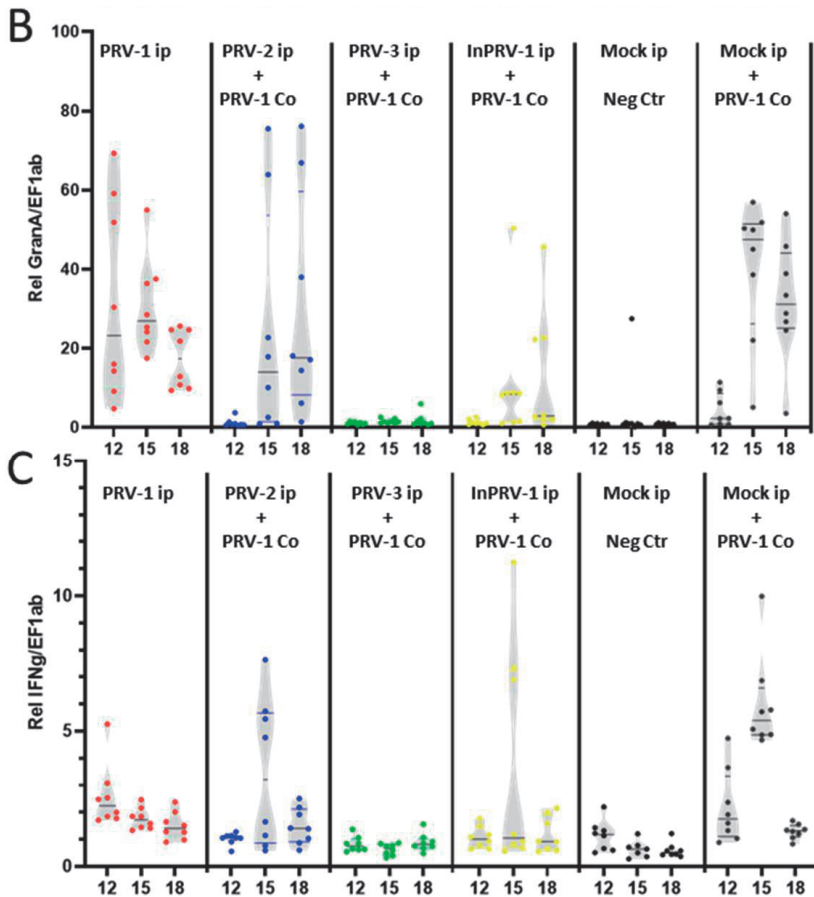


Figure 7. Immune responses in the spleen after PRV-1 challenge of immunized fish. (A) Magnetic beads coated with recombinant lipid-modified PRV antigens (LM-PRV-1 σ 1, PRV-1 μ 1c), and non-PRV antigens (ISAV-FP or LM-ISAV-FP), used in a multiplexed assay to measure antibodies from diluted blood plasma sampled from fish in the trial groups. Levels of fluorescent secondary antibody bound to the beads (median fluorescence units, MFI) carrying PRV-antigens (red) and non-PRV antigens (gray/black) were assayed. (B) Gene expression of Granzyme A. (C) Gene expression of IFN γ in spleen samples from fish injected with PRV-1 (red), PRV-2 + PRV-1 (blue), PRV-3 + PRV-1 (green), InactPRV-1 + PRV-1 (yellow), mock negative control, and mock + PRV-1 positive control groups (black).

4. Discussion

We clarified the potential of the PRV genotypes PRV-2 and PRV-3 to cross-protect against PRV-1 and HSMI, compared them with an inactivated PRV vaccine, and studied some of the possible protective mechanisms involved. Cross-protection induced by related low virulent virus variants was the first successful immunization strategy more than 200 years ago. It was then found that smallpox was prevented by previous exposure to a low virulent pox virus infecting cows [43]. This strategy was used for several years before it was published by Jenner in 1796. A cross-protective approach to immunization introduces many uncertain factors. The theoretical ability of the low virulent virus to cause low-grade disease, develop into virulence over time, or cause disease in other species requires initial mapping and testing. Nevertheless, a replicating mimic of the disease-causing virus itself has the potential of being the ultimate inducer of efficient immune protection, as this will

set off the exact mechanisms used to fight the virus. The rationale for this study is to increase our understanding of cross-protective mechanisms, aiming for the design of more efficient future vaccination approaches.

Although the three PRV genotypes mainly cause disease in different salmonid species, evidence of cross-species infection exists. PRV-1 infect coho salmon, Chinook salmon, and rainbow trout in addition to Atlantic salmon [25], and PRV-3 infects rainbow trout and coho salmon in addition to brown trout [27]. Our observations of experimental infection of Atlantic salmon with PRV-3 confirmed those of a previous study where it was observed that PRV-3 replicated and persisted over a period of 16 weeks and transmitted less efficiently to naïve cohabitants, compared to PRV-1 [29]. Infection with PRV-2, however, is less studied in other species than farmed coho salmon. Here, we show that PRV-2 can infect and replicate in Atlantic salmon after injection, although not as efficiently as PRV-1 and PRV-3. This ability of both PRV-2 and PRV-3 to infect and replicate in Atlantic salmon calls for awareness of all three viruses in aquaculture and breeding.

As previously shown in several previous experimental challenge studies [5,15,44], the PRV-1 genetic variant used in this trial, originating from a Norwegian disease outbreak, induces HSMI in Atlantic salmon. The same ability to cause HSMI experimentally has not been found for Canadian PRV-1 genetic variants [22,23]. The differences in pathogenicity induced by PRV-1 variants was demonstrated experimentally in 2020 [15], and shown to be associated with genetic differences within four out of the ten genetic segments of PRV. Properties of the outer capsid and virus dissemination in the host was suggested as determinants of pathogenicity [15]. Considering the overall similarities between the PRV genotypes at the amino acid level, PRV-1 is more similar to PRV-3 (90% identity) than to PRV-2 (80%) [31]. The most prominent genetic differences were found in the segment S1, encoding the outer clamp protein $\sigma 3$ and the non-structural protein p13, encoded by an internal open reading frame. These proteins have both been suggested to be implicated in the pathogenicity of PRV [6,45,46], $\sigma 3$ for promoting virus replication by dsRNA binding and inhibition of the dsRNA-activated protein kinase PKR [47] and p13 for inducing cytotoxicity [45]. The $\sigma 3$ and p13 proteins are among the least conserved between the PRV genotypes. For PRV2, $\sigma 3$ and p13 aa identities to PRV-1 homologues are 69.7 and 62.9%, and for PRV-3 the identities are 79.1 and 78.2%, respectively [31]. The rather low aa conservation could potentially be of importance for the host-specific pathogenicity differences of these viruses, or their ability to interact with each other during infection.

When focusing specifically on the amino acid sequence of the outer capsid protein $\sigma 1$ (S4) from PRV-1, used as antigen in the bead-based immunoassay [39], the identity is 82% with PRV-3 and only 67% with PRV-2 (NCBI database). Since $\sigma 1$ is considered to be the receptor-binding protein of PRV [6], its sequence variation may explain the species specificity, and the lack of transmission to naïve cohabitants in Atlantic salmon. The higher amino acid identity between PRV-1 and PRV-3, which is in line with their main host species being more closely related, consequently gave a more efficient infection and replication of PRV-3 compared to PRV-2 in Atlantic salmon. A higher rate of virus replication and higher amino acid identity for $\sigma 1$ as well as for other virus proteins could explain the higher level of cross-binding antibodies detected after PRV-3 infection and thus the higher cross-protecting effect. Although the genetic diversity in PRV-1 is generally not associated with the $\sigma 1$ gene, it is possible that cross-protection could be different against the genotypes.

In this trial, histological analyses were performed only in the late phase of the trial, i.e., after 18 weeks. At that time, PRV-2 was eradicated from the heart, and PRV-3 levels were low, with Ct values above 30 in 50% of the fish and the remaining fish virus being negative. Compared to this, 100% of the fish injected with PRV-1 at the start of the trial were still virus positive in the heart after 18 weeks, with Ct-levels around 20. We cannot completely rule out that heart inflammation occurred at some point after injection with PRV-2 and PRV-3. In a former study on PRV-3 in Atlantic salmon, minor inflammatory foci were detected in the PRV-3-infected hearts [29], but these findings were not comparable, neither to the inflammation induced by PRV-3 in rainbow trout hearts nor to HSMI in

Atlantic salmon. Infection and pathological changes in other organs, such as the liver and kidney, earlier shown to be sites for PRV replication [21,48,49], or pathological changes at earlier time points in heart cannot be ruled out either, as this was not explored here.

Based on analyses of spleen and heart, PRV-2 appears to be eradicated a few weeks after infection in Atlantic salmon compared to PRV-1 and PRV-3. PRV-2 loads in spleen were similar to those of PRV-3 two weeks after infection, but after 5 weeks PRV-2 levels declined, whereas PRV-3 and PRV-1 levels increased. PRV-3 is reported to be successfully cleared in rainbow trout after infection, not moving into persistence like PRV-1 in Atlantic salmon [29,30]. However, PRV-3 appeared to persist for at least 18 weeks in Atlantic salmon in our study, and also for 16 weeks in a former study [29]. This may indicate that persistence is related to host factors in farmed Atlantic salmon.

In the magnetic bead-based assay used to detect anti-PRV antibodies, the PRV-1 LM- σ 1 antigen has earlier been found to be the most efficient antigen for antibody detection [39]. PRV-3 triggered the production of antibodies that were able to cross-bind to PRV-1 LM- σ 1. PRV-1 infection has previously been reported to also trigger the production of polyreactive antibodies that bind to non-PRV control antigens [39]. Similarly, we observed high levels of background binding to the ISAV-F-protein control antigens after PRV-1 infection. The production of polyreactive antibodies start at the same time as the more specific antibodies but decrease earlier. The polyreactive antibody response was not seen after PRV-2 or PRV-3 infection. This could be linked to the much higher innate antiviral response triggered by PRV-1, which correlated with the replication efficiency or load of virus for this genotype, compared to the other genotypes. This phenomenon will be subject to further study.

Low levels of antibodies binding to PRV-1 σ 1 was observed in blood from PRV-2-injected individuals as well, but only in a short time frame while the virus was still present. Although this low antibody level did not lead to protection from PRV-1 and HSMI, the specificity against PRV antigens and association with virus eradication is notable.

The inactivated, adjuvanted PRV-1 vaccine did not induce any measurable antibodies against PRV-1 σ 1. Still, the inactivated PRV-1 vaccine lowered PRV-1 infection levels after secondary challenge, and protected six out of eight individuals from HSMI, in line with previous findings [33]. The mechanism behind this effect is not clear, as neither innate immune activation nor cellular immune activation was revealed through the analyses performed here. We cannot rule out if an early immune activation was triggered by the adjuvant or if antibody-based protection targeting PRV-1 antigens other than PRV-1 σ 1 is involved [6]. It is also possible that the inactivation procedure may have changed the structure of the σ 1 protein in the inactivated viral particle, as it is in an exposed position in the outer capsid.

The PRV-3 pre-exposure totally blocked PRV-1 infection. Cross-protective antibodies are likely to be one explanation but are most likely not the only one. Several fish had very low levels of detectable antibodies in plasma after 10 weeks, but PRV-1 infection was still completely blocked in these fish. The analysis of expressed antiviral immunity genes and indicators of cellular adaptive immunity (cytotoxic cell markers) did not indicate that these mechanisms were triggered by PRV-3 beyond 10 weeks, at least not in spleen, which was tested. The almost total infection block may lead us to think that protective mechanisms have been induced also at mucosal surfaces, although PRV-3 was given ip and not as a bath exposure. In general, orthoreoviruses enter through respiratory and gastrointestinal mucosal surfaces. Although PRV-1 is reported to infect via the intestinal wall [13], it may use other ports of entry as well. The infection route of PRV-3 has not been studied but could be assumed similar to that of PRV-1. This could point to a mucosal protection mechanism involved in the blockage of PRV-1 infection by PRV-3, which would be a highly desired effect of a future vaccine. Such a PRV-1-blocking effect was not obtained with previous PRV-2 exposure or the inactivated PRV-1 vaccine. It should be noted that PRV-3, but not PRV-2, persisted in the spleen of all fish when they were exposed to PRV-1, and further until the end of the study (18 weeks). It may be that the almost full protection and blocking of PRV-1 infection is dependent on the presence of PRV-3.

All PRV isoforms infect red blood cells, and PRV-1 is shown to strongly induce interferon-regulated antiviral genes in these cells [50]. Thus, the blocking of secondary PRV-1 infection could be a result of red blood cells in an antiviral state. This would be reflected in analysis of spleen antiviral responses. However, very little innate antiviral immune response was induced by PRV-3 in Atlantic salmon although fish were still infected with the virus after 10 weeks. This is remarkably different to a PRV-1 infection, which induces long-lasting antiviral responses. PRV-3 is also reported earlier to induce antiviral responses in rainbow trout [29,30], but not in Atlantic salmon [29]. This difference could be linked to the observed differences in pathogenicity in the two species, but this is still not confirmed and will be further explored.

For PRV-2, 50–80% of the fish had cleared the virus between 10 and 18 weeks after infection. In this group, we found a contradictory effect on PRV-1 infection and HSMI. As two out of eight fish did not develop HSMI, there was no effect on the remaining six. In addition, PRV-1 levels were lower in some fish, but strongly boosted in others. It appeared that PRV-1 may have replicated more efficiently in some of the individuals that had eradicated PRV-2, compared to individuals that had not. Like for PRV-3, we did not detect innate antiviral immune responses to PRV-2 infection 10 weeks after infection.

PRV-1 induces cytotoxic T-cell (CTL) activity in Atlantic salmon [17,37], which is strongly associated with HSMI pathology [16], and also heart inflammation in rainbow trout infected with PRV-3 [30]. Here, there is clear evidence that PRV-1 induces a strong regulation of innate antiviral and cytotoxic immune response genes 10 weeks after infection, which is not induced by PRV-2 or PRV-3, and which is likely to be decisive for HSMI pathology. The role of CTL activity in vaccine effects and long-term protection against viruses in salmonids is not much studied, but specific cytotoxicity against the salmonid alphavirus (SAV) has recently been explored after vaccination with an adjuvanted inactivated SAV vaccine, in comparison with SAV infection [51]. There, it was clearly demonstrated that while SAV infection induced specific cytotoxicity, only unspecific cytotoxic activity was induced by the vaccine [51]. It would, in a follow-up study, be interesting to compare specific CTL activity in the period after PRV-2 and PRV-3 infection to explore any correlation with the ability to cross-protect against PRV-1.

This study illustrates some potential pitfalls in using replicating viruses for vaccine purposes. They may be very efficient, like PRV-3, which completely blocks PRV-1 infection. However, PRV-3 itself persists in the fish, which may have unknown long-term consequences.

This study also indicates that antibodies against the putative receptor-binding protein $\sigma 1$ may be an important protective measure. PRV-3, but not PRV-2, induced the production of anti- $\sigma 1$ antibodies. This could be due to the higher replication rate of PRV-3 to PRV-2 in Atlantic salmon and the higher identity between the $\sigma 1$ protein of PRV-1 and -3. A protective effect could eventually be verified in a passive immunization test by administration of purified serum immunoglobulin from PRV-3-infected fish to PRV-1 experimentally infected fish. The long-term protective effects of these antibodies will be subject to follow-up experiments, as we could observe a decline after > 15 weeks of PRV-3 infection. If plasma antibodies are also involved in blocking infection at mucosal surfaces is an open question.

PRV-2 replicates at low levels in Atlantic salmon and is eventually cleared, which normally could be considered beneficial properties of a “live” replicating vaccine. However, the replication must be at a level sufficient to induce an effective immune response. Here, only minor innate and cellular responses were found at the transcript level. However, there may be effects at the post-transcriptional or post-translational levels that we did not monitor. PRV-2 caused contradictory results by protecting some fish from HSMI but causing even higher susceptibility to PRV-1 infection in others. The large individual differences could possibly be due to host genetics, leading to a different ability to present antigen. This study also confirms the partial efficiency of the inactivated PRV-1 vaccine published earlier; although, it is still without a clear answer to the main mechanism of protection.

Besides the obvious pitfalls in immunizing Atlantic salmon against HSMI with PRV-3, a virus pathogenic to rainbow trout [28], there are also additional concerns associated with a live attenuated vaccination approach. Segmented RNA viruses may reassort or recombine if two related genotypes infect the same cell [52], creating new viruses with unpredictable properties, potentially pathogenic.

Future vaccine production can provide us with reverse genetic approaches and viruses tailored by synthesis and gene editing. Combined with thorough long-term studies of risks and effects of the different vaccine approaches and a higher repertoire of ways to measure vaccine effect, this will hopefully ensure safe and effective attenuated vaccines in the future.

5. Conclusions

This work shows that PRV-1, PRV-2 and PRV-3 replicate in Atlantic salmon, and can induce production of antibodies that bind to the PRV-1 $\sigma 1$ antigen. Only PRV-1 infection induces unspecific antibodies, long-lasting expression of antiviral response genes and cytotoxic genes in spleen in Atlantic salmon, which could be associated with the ability to cause HSMI. When compared to vaccination with an inactivated PRV-1 vaccine, PRV-3 infection provides full protection from PRV-1 introduced ten weeks later, and development of HSMI. In comparison, inactivated PRV-1 vaccine and PRV-2 infection does not prevent PRV-1 infection and only partially protects against HSMI. This work indicates that a replicating attenuated vaccine approach could protect against HSMI.

Supplementary Materials: The data are available online at <https://www.mdpi.com/2076-393X/9/3/230/s1>, Table S1: Primer and probe sequences (5'-3') for PRV genotypes and immune genes, Supplementary File S2: PRV Ct values and weight data from the PRV immunization trial, Figure S1: Infection level of PRV genetic variants in all groups 2, 5 and 10 weeks post injection (wpi), control of cross-infection. Supplementary File S4: Antibody binding to PRV antigens given as mean fluorescence intensity (MFI) corrected for binding to control beads, Supplementary File S5: Immune gene expression data, Supplementary File S6: Histopathology scores of heart samples.

Author Contributions: Conceptualization, J.B.J., Ø.W., E.R. and M.K.D.; Data curation, M.S.M., L.H.T., M.N., M.M.A. and M.K.D.; Formal analysis, M.S.M., L.H.T., S.B., A.B.O., M.N., M.M.A., K.D. and M.K.D.; Funding acquisition, J.B.J., Ø.W., E.R. and M.K.D.; Investigation, M.S.M., L.H.T., S.B., A.B.O., K.D., S.S., E.S.E., T.T., E.R. and M.K.D.; Methodology, L.H.T., A.B.O., M.M.A., K.D., S.S., E.S.E., T.T., Ø.W. and M.K.D.; Project administration, J.B.J., E.R. and M.K.D.; Resources, E.S.E., T.T., J.B.J., Ø.W., E.R. and M.K.D.; Software, L.H.T.; Supervision, L.H.T., J.B.J., Ø.W., E.R. and M.K.D.; Validation, M.S.M., L.H.T., S.B., A.B.O., M.N., E.S.E., Ø.W., E.R. and M.K.D.; Visualization, M.S.M., M.N., Ø.W. and M.K.D.; Writing—original draft, M.S.M., L.H.T. and M.K.D.; Writing—review and editing, M.S.M., L.H.T., S.B., A.B.O., M.N., M.M.A., K.D., S.S., E.S.E., T.T., J.B.J., Ø.W., E.R. and M.K.D. All authors have read and agreed to the published version of the manuscript.

Funding: The research was funded by the Research Council of Norway, grant number 280847/E40 (ViVaAct), and UiT the Arctic University of Norway.

Institutional Review Board Statement: The study was conducted according to the guidelines of the Declaration of Helsinki, and approved by the Norwegian Animal Research Authority, and performed in accordance with the recommendations of the current animal welfare regulations: FOR-1996-01-15-23 (Norway), protocol code 19119 (FOTS), date of approval Jan 8. 2019.

Data Availability Statement: The supplementary data files presented in this study are openly available in Zenodo, at <https://doi.org/10.5281/zenodo.4450287> (accessed on 6 March 2021).

Acknowledgments: We thank Astrid-Elisabeth Christiansen Hanssen and Morten Marienborg for planning and practical assistance at the aquaculture research station in Kårvik, Tromsø, Øyvind Haugland at PHARMAQ AS, Oslo, for the Inactivated PRV vaccine preparation, Agata Teresa Wyrozemska at the institute of Biosciences, Fisheries and Economy at UiT, Arctic University of Norway, for sampling assistance, Kumar Subramaniam at Centre for Biotechnology, Anna University, Chennai, 600,025, India, for producing the lipid-modified antigens used in the immunoassays, Karen B Soleim at the NVI Fish Health research group for immunoassay assistance, Ingvild B Nyman from

the Department of food safety and infection biology at NMBU for sample handling, and Turhan Markussen, NMBU, for sharing the PRV-2-specific primer set. Additional thanks to several people at the NVI section of Media production for the preparation of sampling equipment and the NVI section of Pathology for tissue slide preparation.

Conflicts of Interest: The authors declare no conflict of interest.

References

- Byrne, K.A.; Loving, C.L.; McGill, J.L. Innate Immunomodulation in Food Animals: Evidence for Trained Immunity? *Front. Immunol.* **2020**, *11*, 1099. [[CrossRef](#)]
- Segner, H.; Sundh, H.; Buchmann, K.; Douxfils, J.; Sundell, K.S.; Mathieu, C.; Ruane, N.; Jutfelt, F.; Toften, H.; Vaughan, L. Health of farmed fish: Its relation to fish welfare and its utility as welfare indicator. *Fish Physiol. Biochem.* **2011**, *38*, 85–105. [[CrossRef](#)] [[PubMed](#)]
- Adams, A. Progress, challenges and opportunities in fish vaccine development. *Fish Shellfish Immunol.* **2019**, *90*, 210–214. [[CrossRef](#)]
- Palacios, G.; Lovoll, M.; Tengs, T.; Hornig, M.; Hutchison, S.; Hui, J.; Kongtorp, R.-T.; Savji, N.; Bussetti, A.V.; Solovyov, A.; et al. Heart and Skeletal Muscle Inflammation of Farmed Salmon Is Associated with Infection with a Novel Reovirus. *PLoS ONE* **2010**, *5*, e11487. [[CrossRef](#)]
- Wessel, Ø.; Braaen, S.; Alarcón, M.; Haatveit, H.; Roos, N.; Markussen, T.; Tengs, T.; Dahle, M.K.; Rimstad, E. Infection with purified Piscine orthoreovirus demonstrates a causal relationship with heart and skeletal muscle inflammation in Atlantic salmon. *PLoS ONE* **2017**, *12*, e0183781. [[CrossRef](#)]
- Markussen, T.; Dahle, M.K.; Tengs, T.; Lovoll, M.; Finstad, O.W.; Wiik-Nielsen, C.R.; Grove, S.; Lauksund, S.; Robertsen, B.; Rimstad, E. Sequence analysis of the genome of piscine orthoreovirus (PRV) associated with heart and skeletal muscle inflammation (HSMI) in Atlantic salmon (*Salmo salar*). *PLoS ONE* **2013**, *8*, e70075. [[CrossRef](#)]
- Dhamotharan, K.; Tengs, T.; Wessel, Ø.; Braaen, S.; Nyman, I.B.; Hansen, E.F.; Christiansen, D.H.; Dahle, M.K.; Rimstad, E.; Markussen, T. Evolution of the Piscine orthoreovirus Genome Linked to Emergence of Heart and Skeletal Muscle Inflammation in Farmed Atlantic Salmon (*Salmo salar*). *Viruses* **2019**, *11*, 465. [[CrossRef](#)]
- Løvoll, M.; Alarcón, M.; Jensen, B.B.; Taksdal, T.; Kristoffersen, A.B.; Tengs, T. Quantification of piscine reovirus (PRV) at different stages of Atlantic salmon *Salmo salar* production. *Dis. Aquat. Org.* **2012**, *99*, 7–12. [[CrossRef](#)]
- Garseth, A.H.; Fritsvold, C.; Opheim, M.; Skjerve, E.; Biering, E. Piscine reovirus (PRV) in wild Atlantic salmon, *Salmo salar* L., and sea-trout, *Salmo trutta* L., in Norway. *J. Fish Dis.* **2013**, *36*, 483–493. [[CrossRef](#)]
- Madhun, A.S.; Isachsen, C.H.; Omdal, L.M.; Einen, A.C.B.; Maehle, S.; Wennevik, V.; Niemela, E.; Svasand, T.; Karlsbakk, E. Prevalence of piscine orthoreovirus and salmonid alphavirus in sea-caught returning adult Atlantic salmon (*Salmo salar* L.) in northern Norway. *J. Fish Dis.* **2018**, *41*, 797–803. [[CrossRef](#)] [[PubMed](#)]
- Kongtorp, R.T.; Taksdal, T.; Lyngøy, A. Pathology of heart and skeletal muscle inflammation (HSMI) in farmed Atlantic salmon *Salmo salar*. *Dis. Aquat. Org.* **2004**, *59*, 217–224. [[CrossRef](#)] [[PubMed](#)]
- Ferguson, H.W.; Kongtorp, R.T.; Taksdal, T.; Graham, D.; Falk, K. An outbreak of disease resembling heart and skeletal muscle inflammation in Scottish farmed salmon, *Salmo salar* L., with observations on myocardial regeneration. *J. Fish Dis.* **2005**, *28*, 119–123. [[CrossRef](#)]
- Hauge, H.; Dahle, M.; Moldal, T.; Thoen, E.; Gjevre, A.-G.; Weli, S.; Alarcón, M.; Grove, S. Piscine orthoreovirus can infect and shed through the intestine in experimentally challenged Atlantic salmon (*Salmo salar* L.). *Vet. Res.* **2016**, *47*, 1–12. [[CrossRef](#)]
- Wessel, O.; Olsen, C.M.; Rimstad, E.; Dahle, M.K. Piscine orthoreovirus (PRV) replicates in Atlantic salmon (*Salmo salar* L.) erythrocytes ex vivo. *Vet. Res.* **2015**, *46*, 26. [[CrossRef](#)] [[PubMed](#)]
- Wessel, Ø.; Hansen, E.F.; Dahle, M.K.; Alarcon, M.; Vatne, N.A.; Nyman, I.B.; Soleim, K.B.; Dhamotharan, K.; Timmerhaus, G.; Markussen, T.; et al. Piscine Orthoreovirus-1 Isolates Differ in Their Ability to Induce Heart and Skeletal Muscle Inflammation in Atlantic Salmon (*Salmo salar*). *Pathogens* **2020**, *9*, 1050. [[CrossRef](#)]
- Mikalsen, A.B.; Haugland, O.; Rode, M.; Solbakk, I.T.; Evensen, O. Atlantic Salmon Reovirus Infection Causes a CD8 T Cell Myocarditis in Atlantic Salmon (*Salmo salar* L.). *PLoS ONE* **2012**, *7*, e37269. [[CrossRef](#)]
- Johansen, L.-H.; Thim, H.L.; Jørgensen, S.M.; Afanasyev, S.; Strandskog, G.; Taksdal, T.; Fremmerlid, K.; McLoughlin, M.; Jørgensen, J.B.; Krasnov, A. Comparison of transcriptomic responses to pancreas disease (PD) and heart and skeletal muscle inflammation (HSMI) in heart of Atlantic salmon (*Salmo salar* L.). *Fish Shellfish Immunol.* **2015**, *46*, 612–623. [[CrossRef](#)] [[PubMed](#)]
- Kibenge, M.J.T.; Wang, Y.; Gayeski, N.; Morton, A.; Beardslee, K.; McMillan, B.; Kibenge, F.S.B. Piscine orthoreovirus sequences in escaped farmed Atlantic salmon in Washington and British Columbia. *Viol. J.* **2019**, *16*, 41. [[CrossRef](#)]
- Björgen, H.; Wessel, Ø.; Fjellidal, P.G.; Hansen, T.; Sveier, H.; Sæbø, H.R.; Enger, K.B.; Monsen, E.; Kvellestad, A.; Rimstad, E.; et al. Piscine orthoreovirus (PRV) in red and melanised foci in white muscle of Atlantic salmon (*Salmo salar*). *Vet. Res.* **2015**, *46*, 1–12. [[CrossRef](#)]
- Krasnov, A.; Moghadam, H.; Larsson, T.; Afanasyev, S.; Morkore, T. Gene expression profiling in melanised sites of Atlantic salmon filets. *Fish Shellfish Immunol.* **2016**, *55*, 56–63. [[CrossRef](#)]

21. Di Cicco, E.; Ferguson, H.W.; Kaukinen, K.H.; Schultze, A.D.; Li, S.; Tabata, A.; Günther, O.P.; Mordecai, G.; Suttle, C.A.; Miller, K.M. The same strain of Piscine orthoreovirus (PRV-1) is involved in the development of different, but related, diseases in Atlantic and Pacific Salmon in British Columbia. *FACETS* **2018**, *3*. [[CrossRef](#)]
22. Polinski, M.P.; Marty, G.D.; Snyman, H.N.; Garver, K.A. Piscine orthoreovirus demonstrates high infectivity but low virulence in Atlantic salmon of Pacific Canada. *Sci. Rep.* **2019**, *9*, 3297. [[CrossRef](#)] [[PubMed](#)]
23. Garver, K.A.; Johnson, S.C.; Polinski, M.P.; Bradshaw, J.C.; Marty, G.D.; Snyman, H.N.; Morrison, D.B.; Richard, J. Piscine Orthoreovirus from Western North America Is Transmissible to Atlantic Salmon and Sockeye Salmon but Fails to Cause Heart and Skeletal Muscle Inflammation. *PLoS ONE* **2016**, *11*, e0146229. [[CrossRef](#)]
24. Di Cicco, E.; Ferguson, H.W.; Schultze, A.D.; Kaukinen, K.H.; Li, S.; Vanderstichel, R.; Wessel, O.; Rimstad, E.; Gardner, I.A.; Hammell, K.L.; et al. Heart and skeletal muscle inflammation (HSMI) disease diagnosed on a British Columbia salmon farm through a longitudinal farm study. *PLoS ONE* **2017**, *12*, e0171471. [[CrossRef](#)]
25. Purcell, M.K.; Powers, R.L.; Taksdal, T.; McKenney, D.; Conway, C.M.; Elliott, D.G.; Polinski, M.; Garver, K.; Winton, J. Consequences of Piscine orthoreovirus genotype 1 (PRV-1) infections in Chinook salmon (*Oncorhynchus tshawytscha*), coho salmon (*O. kisutch*) and rainbow trout (*O. mykiss*). *J. Fish Dis.* **2020**, *43*, 719–728. [[CrossRef](#)]
26. Takano, T.; Nawata, A.; Sakai, T.; Matsuyama, T.; Ito, T.; Kurita, J.; Terashima, S.; Yasuike, M.; Nakamura, Y.; Fujiwara, A.; et al. Full-Genome Sequencing and Confirmation of the Causative Agent of Erythrocytic Inclusion Body Syndrome in Coho Salmon Identifies a New Type of Piscine Orthoreovirus. *PLoS ONE* **2016**, *11*, e0165424. [[CrossRef](#)]
27. Garseth, Å.H.; Moldal, T.; Gåsnes, S.K.; Hjortaas, M.J.; Sollien, V.P.; Gjevne, A.-G. Piscine orthoreovirus-3 is prevalent in wild sea trout (*Salmo trutta* L.) in Norway. *J. Fish Dis.* **2019**, *42*, 391–396. [[CrossRef](#)] [[PubMed](#)]
28. Olsen, A.B.; Hjortaas, M.; Tengs, T.; Hellberg, H.; Johansen, R. First Description of a New Disease in Rainbow Trout (*Oncorhynchus mykiss* (Walbaum)) Similar to Heart and Skeletal Muscle Inflammation (HSMI) and Detection of a Gene Sequence Related to Piscine Orthoreovirus (PRV). *PLoS ONE* **2015**, *10*, e0131638. [[CrossRef](#)]
29. Hauge, H.; Vendramin, N.; Taksdal, T.; Olsen, A.B.; Wessel, O.; Mikkelsen, S.S.; Alencar, A.L.F.; Olesen, N.J.; Dahle, M.K. Infection experiments with novel Piscine orthoreovirus from rainbow trout (*Oncorhynchus mykiss*) in salmonids. *PLoS ONE* **2017**, *12*, e0180293. [[CrossRef](#)] [[PubMed](#)]
30. Vendramin, N.; Kannimuthu, D.; Olsen, A.B.; Cuenca, A.; Teige, L.H.; Wessel, Ø.; Iburg, T.M.; Dahle, M.K.; Rimstad, E.; Olesen, N.J. Piscine orthoreovirus subtype 3 (PRV-3) causes heart inflammation in rainbow trout (*Oncorhynchus mykiss*). *Vet. Res.* **2019**, *50*, 1–13. [[CrossRef](#)] [[PubMed](#)]
31. Dhamotharan, K.; Vendramin, N.; Markussen, T.; Wessel, Ø.; Cuenca, A.; Nyman, I.B.; Olsen, A.B.; Tengs, T.; Dahle, M.K.; Rimstad, E. Molecular and Antigenic Characterization of Piscine orthoreovirus (PRV) from Rainbow Trout (*Oncorhynchus mykiss*). *Viruses* **2018**, *10*, 170. [[CrossRef](#)] [[PubMed](#)]
32. Polinski, M.P.; Vendramin, N.; Cuenca, A.; Garver, K.A. Piscine orthoreovirus: Biology and distribution in farmed and wild fish. *J. Fish Dis.* **2020**, *43*, 43. [[CrossRef](#)]
33. Wessel, Ø.; Haugland, Ø.; Rode, M.; Fredriksen, B.N.; Dahle, M.K.; Rimstad, E. Inactivated Piscine orthoreovirus vaccine protects against heart and skeletal muscle inflammation in Atlantic salmon. *J. Fish Dis.* **2018**, *41*, 1411–1419. [[CrossRef](#)] [[PubMed](#)]
34. Pham, P.H.; Misk, E.; Papazotos, F.; Jones, G.; Polinski, M.P.; Contador, E.; Russell, S.; Garver, K.A.; Lumsden, J.S.; Bols, N.C. Screening of Fish Cell Lines for Piscine Orthoreovirus-1 (PRV-1) Amplification: Identification of the Non-Supportive PRV-1 Invitrome. *Pathogens* **2020**, *9*, 833. [[CrossRef](#)] [[PubMed](#)]
35. Haatveit, H.M.; Hodneland, K.; Braaen, S.; Hansen, E.F.; Nyman, I.B.; Dahle, M.K.; Frost, P.; Rimstad, E. DNA vaccine expressing the non-structural proteins of Piscine orthoreovirus delay the kinetics of PRV infection and induces moderate protection against heart -and skeletal muscle inflammation in Atlantic salmon (*Salmo salar*). *Vaccine* **2018**, *36*, 7599–7608. [[CrossRef](#)] [[PubMed](#)]
36. Dahle, M.K.; Wessel, Ø.; Timmerhaus, G.; Nyman, I.B.; Jørgensen, S.M.; Rimstad, E.; Krasnov, A. Transcriptome analyses of Atlantic salmon (*Salmo salar* L.) erythrocytes infected with piscine orthoreovirus (PRV). *Fish Shellfish Immunol.* **2015**, *45*, 780–790. [[CrossRef](#)]
37. Johansen, L.-H.; Dahle, M.K.; Wessel, Ø.; Timmerhaus, G.; Løvoll, M.; Røsæg, M.; Jørgensen, S.M.; Rimstad, E.; Krasnov, A. Differences in gene expression in Atlantic salmon parr and smolt after challenge with Piscine orthoreovirus (PRV). *Mol. Immunol.* **2016**, *73*, 138–150. [[CrossRef](#)]
38. Teige, L.H.; Lund, M.; Haatveit, H.M.; Rosaeg, M.V.; Wessel, O.; Dahle, M.K.; Storset, A.K. A bead based multiplex immunoassay detects Piscine orthoreovirus specific antibodies in Atlantic salmon (*Salmo salar*). *Fish Shellfish Immunol.* **2017**, *63*, 491–499. [[CrossRef](#)] [[PubMed](#)]
39. Teige, L.H.; Kumar, S.; Johansen, G.M.; Wessel, Ø.; Vendramin, N.; Lund, M.; Rimstad, E.; Boysen, P.; Dahle, M.K. Detection of Salmonid IgM Specific to the Piscine Orthoreovirus Outer Capsid Spike Protein Sigma 1 Using Lipid-Modified Antigens in a Bead-Based Antibody Detection Assay. *Front. Immunol.* **2019**, *10*, 2119. [[CrossRef](#)] [[PubMed](#)]
40. Dahle, M.K.; Jørgensen, J.B. Antiviral defense in salmonids—Mission made possible? *Fish Shellfish Immunol.* **2019**, *87*, 421–437. [[CrossRef](#)]
41. Finstad, Ø.W.; Falk, K.; Løvoll, M.; Evensen, Ø.; Rimstad, E. Immunohistochemical detection of piscine reovirus (PRV) in hearts of Atlantic salmon coincide with the course of heart and skeletal muscle inflammation (HSMI). *Vet. Res.* **2012**, *43*, 27. [[CrossRef](#)] [[PubMed](#)]

42. Finstad, O.W.; Dahle, M.K.; Lindholm, T.H.; Nyman, I.B.; Lovoll, M.; Wallace, C.; Olsen, C.M.; Storset, A.K.; Rimstad, E. Piscine orthoreovirus (PRV) infects Atlantic salmon erythrocytes. *Vet. Res.* **2014**, *45*, 35. [[CrossRef](#)] [[PubMed](#)]
43. Sánchez-Sampedro, L.; Perdiguero, B.; Mejías-Pérez, E.; García-Arriaza, J.; Di Pilato, M.; Esteban, M. The Evolution of Poxvirus Vaccines. *Viruses* **2015**, *7*, 1726–1803. [[CrossRef](#)] [[PubMed](#)]
44. Lund, M.; Dahle, M.K.; Timmerhaus, G.; Alarcon, M.; Powell, M.; Aspehaug, V.; Rimstad, E.; Jørgensen, S.M. Hypoxia tolerance and responses to hypoxic stress during heart and skeletal muscle inflammation in Atlantic salmon (*Salmo salar*). *PLoS ONE* **2017**, *12*, e0181109. [[CrossRef](#)] [[PubMed](#)]
45. Key, T.; Read, J.; Nibert, M.L.; Duncan, R. Piscine reovirus encodes a cytotoxic, non-fusogenic, integral membrane protein and previously unrecognized virion outer-capsid proteins. *J. Gen. Virol.* **2013**, *94*, 1039–1050. [[CrossRef](#)] [[PubMed](#)]
46. Wessel, O.; Nyman, I.B.; Markussen, T.; Dahle, M.K.; Rimstad, E. Piscine orthoreovirus (PRV) o3 protein binds dsRNA. *Virus Res.* **2015**, *198*, 22–29. [[CrossRef](#)] [[PubMed](#)]
47. Yue, Z.; Shatkin, A.J. Double-Stranded RNA-Dependent Protein Kinase (PKR) Is Regulated by Reovirus Structural Proteins. *Virology* **1997**, *234*, 364–371. [[CrossRef](#)] [[PubMed](#)]
48. Malik, M.S.; Bjørgen, H.; Dhamotharan, K.; Wessel, Ø.; Koppang, E.O.; Di Cicco, E.; Hansen, E.F.; Dahle, M.K.; Rimstad, E. Erythroid Progenitor Cells in Atlantic Salmon (*Salmo salar*) May Be Persistently and Productively Infected with Piscine Orthoreovirus (PRV). *Viruses* **2019**, *11*, 824. [[CrossRef](#)] [[PubMed](#)]
49. Dhamotharan, K.; Bjørgen, H.; Malik, M.S.; Nyman, I.B.; Markussen, T.; Dahle, M.K.; Koppang, E.O.; Wessel, Ø.; Rimstad, E. Dissemination of Piscine orthoreovirus-1 (PRV-1) in Atlantic Salmon (*Salmo salar*) during the Early and Regenerating Phases of Infection. *Pathogens* **2020**, *9*, 143. [[CrossRef](#)] [[PubMed](#)]
50. Wessel, Ø.; Krasnov, A.; Timmerhaus, G.; Rimstad, E.; Dahle, M.K. Antiviral Responses and Biological Consequences of Piscine orthoreovirus Infection in Salmonid Erythrocytes. *Front. Immunol.* **2019**, *9*, 3182. [[CrossRef](#)] [[PubMed](#)]
51. Veenstra, K.A.; Hodneland, K.; Fischer, S.; Takehana, K.; Belmonte, R.; Fischer, U. Cellular Immune Responses in Rainbow Trout (*Onchorhynchus mykiss*) Following Vaccination and Challenge Against Salmonid Alphavirus (SAV). *Vaccines* **2020**, *8*, 725. [[CrossRef](#)] [[PubMed](#)]
52. McDonald, S.M.; Nelson, M.I.; Turner, P.E.; Patton, J.T. Reassortment in segmented RNA viruses: Mechanisms and outcomes. *Nat. Rev. Genet.* **2016**, *14*, 448–460. [[CrossRef](#)] [[PubMed](#)]

ISBN: 978-82-575-1820-2

ISSN: 1894-6402



Norwegian University
of Life Sciences

Postboks 5003
NO-1432 Ås, Norway
+47 67 23 00 00
www.nmbu.no